Pediatric Imaging

A Core Review

Steven L. Blumer
David M. Biko
Safwan S. Halabi

Pediatric Imaging

A Core Review

Pediatric Imaging

A Core Review

E D I T O R S

Steven L. Blumer, MD
Clinical Assistant Professor of Radiology and Pediatrics
Sidney Kimmel Medical College of Thomas Jefferson University
Philadelphia, Pennsylvania
Attending Pediatric Radiologist and Pediatric Radiology Fellowship Program Director
Nemours Associate Medical Director of Imaging Informatics
Nemours/A.I. duPont Hospital for Children
Wilimington, Delaware

David M. Biko, MD
Assistant Professor of Radiology
University of Pennsylvania Perelman School of Medicine
Director, Section of Cardiovascular and Lymphatic Imaging
Division of Body Imaging, Department of Radiology
Children's Hospital of Philadelphia
Philadelphia, Pennsylvania

Safwan S. Halabi, MD
Clinical Assistant Professor
Department of Radiology
Stanford University School of Medicine
Lucile Packard Children's Hospital
Stanford, California

Wolters Kluwer
Philadelphia • Baltimore • New York • London
Buenos Aires • Hong Kong • Sydney • Tokyo

Senior Acquisitions Editor: Sharon Zinner
Editorial Coordinator: Lauren Pecarich
Senior Production Project Manager: Alicia Jackson
Design Coordinator: Stephen Druding
Manufacturing Coordinator: Beth Welsh
Marketing Manager: Dan Dressler
Prepress Vendor: SPi Global

9 8 7 6 5 4 3 2 1
Printed in China

Library of Congress Cataloging-in-Publication Data
Names: Blumer, Steven L., editor. | Biko, David M., editor. | Halabi, Safwan, editor.
Title: Pediatric imaging : a core review / editors, Steven L. Blumer, David M. Biko, Safwan Halabi.
Other titles: Pediatric imaging (Blumer) | Core review series.
Description: Philadelphia : Wolters Kluwer, [2018] | Series: Core review series | Includes bibliographical references and index.
Identifiers: LCCN 2017034938 | ISBN 9781496309808
Subjects: | MESH: Diagnostic Imaging | Child | Infant | Examination Questions
Classification: LCC RJ51.D5 | NLM WN 18.2 | DDC 618.92/00754—dc23 LC record available at https://lccn.loc.gov/2017034938

CONTRIBUTORS

Paul Clark, DO
Assistant Professor
Department of Radiology
F. Edward Hebert School of Medicine
Uniformed Services University of the Health Sciences
Bethesda, Maryland
Chief of Pediatric Imaging
Department of Radiology
Fort Belvoir Community Hospital
Fort Belvoir, Virginia

Kathleen Schenker, MD
Attending Pediatric Radiologist
Nemours/A.I duPont Hospital for Children
Wilimington, Delaware

SERIES FOREWORD

Pediatric Imaging: A Core Review covers the vast field of pediatric radiology in a manner that I am confident this will serve as a useful guide for residents to assess their knowledge and review the material in a question style format that is similar to the core examination.

Dr. Steven L. Blumer, Dr. David M. Biko, and Dr. Safwan S. Halabi have succeeded in producing a book that exemplifies the philosophy and goals of the *Core Review Series*. They have done a magnificent job in covering essential facts and concepts of pediatric radiology. The multiple-choice questions have been divided logically into chapters, so as to make it easy for learners to work on particular topics as needed. Each question has a corresponding answer with an explanation of not only why a particular option is correct but also why the other options are incorrect. There are also references provided for each question for those who want to delve more deeply into a specific subject.

The intent of the *Core Review Series* is to provide the resident, fellow, or practicing physician a review of the important conceptual, factual, and practical aspects of a subject by providing approximately 300 multiple-choice questions in a format similar to the core examination. The *Core Review Series* is not intended to be exhaustive but to provide material likely to be tested on the core exam and that would be required in clinical practice.

As Series Editor of the *Core Review Series*, it has been rewarding to not only be an author of one of the books but also to be able to work with many outstanding individuals in the profession of radiology across the country who contributed to the series. This series represents countless hours of work and involvement by so many that it could not have come together without their participation. It has been very gratifying to see the growing popularity and positive feedback the authors of the *Core Review Series* have received from many reviews.

Dr. Steven L. Blumer, Dr. David M. Biko, Dr. Safwan S. Halabi, and their contributors (Dr. Kathleen Schenker and Dr. Paul Clark) are to be commended on doing an outstanding job. I believe *Pediatric Imaging: A Core Review* will serve as an excellent resource for residents during their board preparation and a valuable reference for fellows and practicing radiologists.

Biren A. Shah, MD, FACR
Director, Breast Imaging
Director, Breast Imaging Fellowship
Associate Professor of Radiology
School of Medicine
Virginia Commonwealth University
Richmond, Virginia

PREFACE

When the American Board of Radiology changed the radiology board certification process from the three exam format to the current two exam format, it not only changed the number of exams administered to radiology trainees but it also fundamentally changed the way that the content was tested. The current examinations are image-rich exams that test higher-order reasoning instead of simple rote memorization of facts. In addition, the testing of practical day-to-day practice scenarios is now emphasized instead of random and obscure conditions.

In preparing this book, we tried to keep the above guidelines in mind. We, along with our contributors Dr. Paul Clark and Dr. Kathleen Schenker, believe that we have written a book that is full of high-quality image-rich questions about conditions commonly encountered in the daily practice of pediatric radiology. The questions are mainly based on scenarios commonly encountered in the day-to-day practice of pediatric radiology. In addition, the questions are also designed to be thought-provoking and designed to test higher-order reasoning. It is our hope that this format will be more interesting than the old-style review books, which often tested rote memorization.

All of us have enjoyed learning about pediatric radiology from the many outstanding attending pediatric radiologists we have worked with during our training. We have also been blessed to work with many wonderful colleagues as junior faculty, which have served as mentors and continued to help us grow as pediatric radiologists. We would like to take the time to thank all of these individuals.

In writing this book, we hope to be able to share our knowledge imparted to us with the next generation of radiology trainees. It is extremely gratifying for us to be able to help our trainees learn about pediatric radiology and to watch them succeed and progress in their careers. We hope that our trainees will use the knowledge gained in this book to provide high-quality care for the pediatric patients and their respective families that they will encounter in their training and professional career. Furthermore, this book should serve as a useful resource for radiologists at more advanced stages of their career, including practicing radiologists.

Finally, this book would not be possible without the understanding of our families. Writing this book obviously represents a significant time commitment, and we would like to thank you for your support.

Steven L. Blumer, MD
David M. Biko, MD
Safwan S. Halabi, MD

ACKNOWLEDGMENTS

We would like to extend our thanks to Dr. Biren Shah, the series editor, as well as Ms. Lauren Pecarich and the rest of the staff at LWW for their guidance and support in preparing this book.

CONTENTS

1 Pediatric Gastrointestinal Tract

Questions

1. A radiograph of a 2-day-old patient with bilious vomiting is shown below. What is the next appropriate step in management?

A. Contrast enema.
B. Emergent upper GI series.
C. Abdominal ultrasound.
D. No further workup is needed.

2. An image from an upper GI series that was subsequently performed on the same patient in Question 1 is shown below. Which of the following would be the next most appropriate step in management?

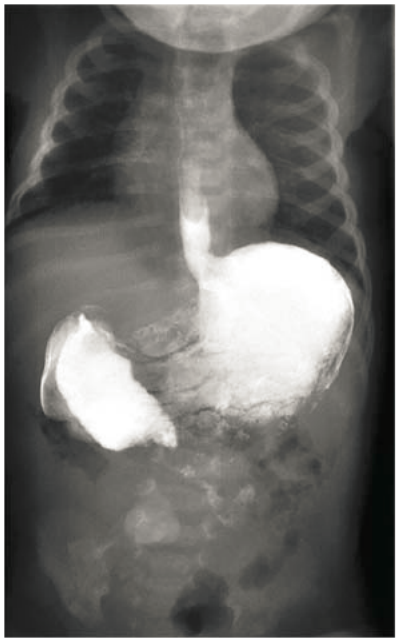

A. Abdominal ultrasound
B. Contrast enema
C. Stat surgical consult
D. CT scan of the abdomen and pelvis

3. Regarding malrotation, which of the following is true?
A. This entity is usually diagnosed after the first year of life.
B. Malrotation is a predisposing risk factor for the development of midgut volvulus.
C. The cecum is usually normally located in the right lower quadrant in patients who are malrotated.
D. The anatomic relationship between the SMA and SMV is usually normal in patients who are malrotated.

4. A 6-week-old male presents to the emergency department with nonbilious projectile vomiting. Plain abdominal radiographs were obtained and are shown below. What is the next appropriate step in management?

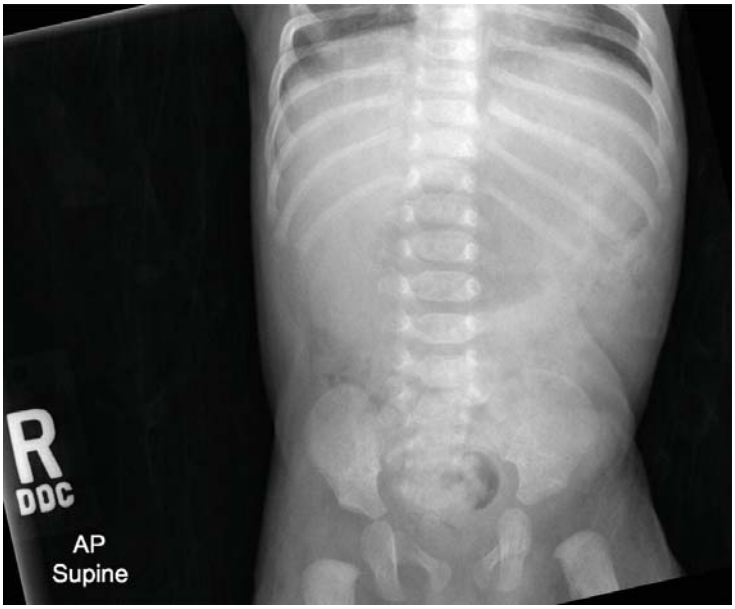

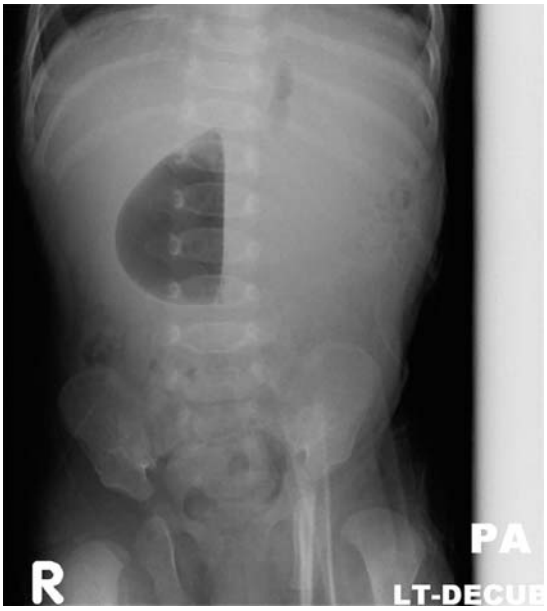

A. Stat surgical consultation
B. Nonemergent abdominal sonogram
C. Contrast enema
D. CT scan of the abdomen and pelvis

5. A nonemergent abdominal sonogram was subsequently performed on the same patient in Question 4, and images from the study are shown below. These images did not change over time. Regarding the entity demonstrated, which of the following is true?

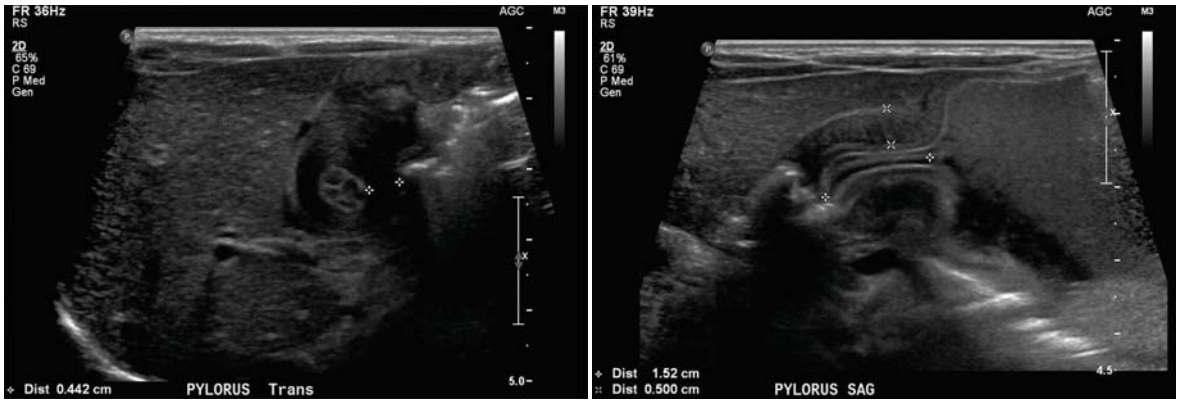

A. This condition often occurs in firstborn females.
B. The treatment of choice is medical.
C. The "double-track sign" and mucosal heaping may be seen in ultrasound exams performed for this condition.
D. Gastric contents often readily empty into the pylorus during exams performed on patients with this condition.

6. A patient presents for an MR exam of the abdomen and pelvis. Representative images from the study are shown below. Concerning the images, which of the following are true?

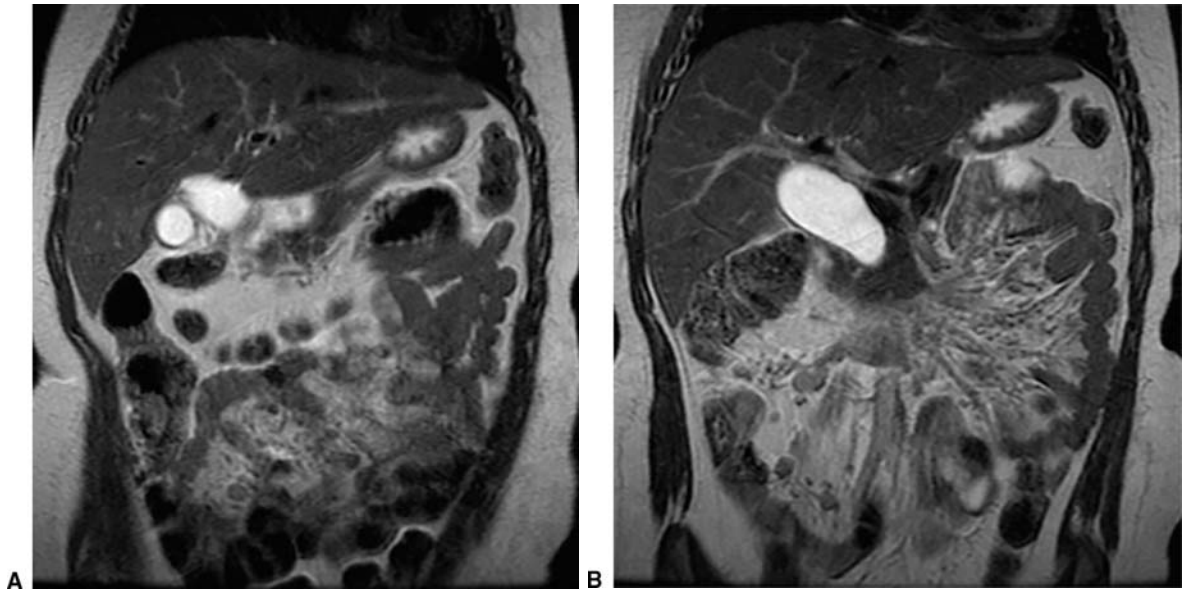

A. This lesion is the most common type of choledochal cyst.
B. This lesion is consistent with a choldeochocele.
C. This lesion is consistent with Caroli disease.
D. This lesion is consistent with a type IVA choledochal cyst.

7. A radiograph from a well-appearing neonate with a distended abdomen and failure to pass meconium is shown below. Which of the following is the next most appropriate step in management?

A. Upper GI series
B. Abdominal ultrasound
C. CT scan
D. Contrast enema

8. A contrast enema was subsequently performed on the patient described in Question 7. Images from the study are shown below (A & B). Which of the following is the most likely diagnosis?

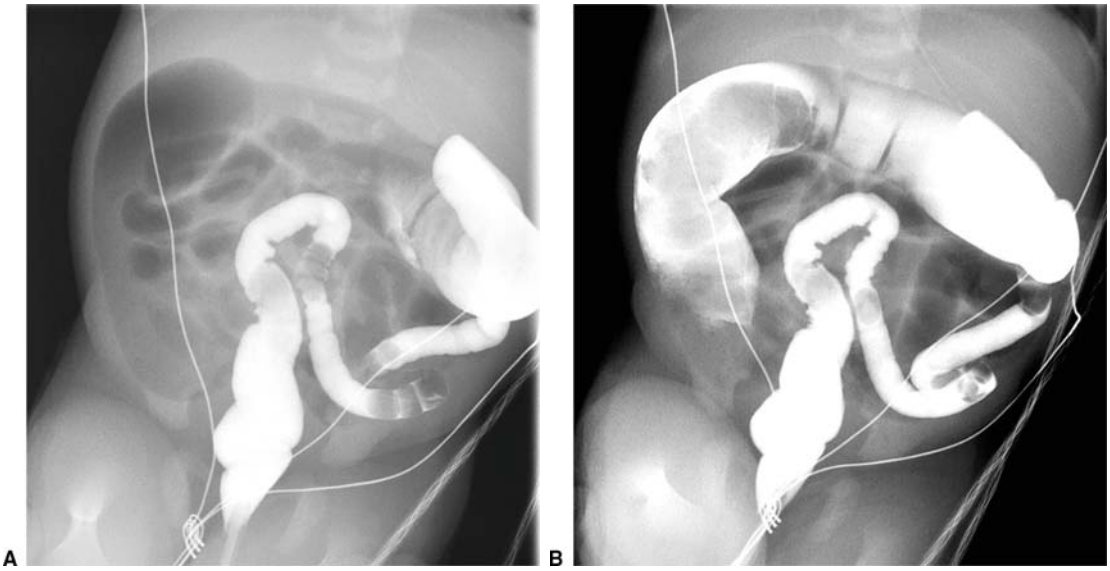

A. Hirschsprung disease
B. Functional immaturity of the colon
C. High ileal atresia
D. Low ileal atresia

9. Regarding the most likely diagnosis of the patient in Question 8, which of the following is true?
A. The initial treatment of choice is surgical.
B. Repeated enemas with water-soluble contrast do not alleviate this condition.
C. This entity is often seen in the offspring of diabetic mothers or mothers treated with magnesium sulfate.
D. This entity is caused by a jejunal atresia.

10. Which of the following entities only occurs in patients with cystic fibrosis?
A. Functional immaturity of the colon
B. Meconium ileus
C. Ileal atresia
D. Jejunal atresia

11. Regarding microcolons, which of the following is true?
A. They are commonly seen in cases of jejunal atresia.
B. They are not seen in patients with low ileal atresia.
C. They are not often seen in meconium ileus.
D. They are seen in conditions in which there is an unused colon.

12. A CT scan is performed on a 5-year-old patient with no known medical history, and an image is shown below. Concerning the finding, which of the following is true?

A. Nonaccidental trauma should be suspected as an etiology.
B. This is a rare complication of pediatric pancreatitis.
C. This is a known early complication of pediatric pancreatitis.
D. There are no more than two known causes of pediatric pancreatitis.

13. A babygram obtained from a neonate is shown below. Concerning the findings, which of the following is true?

A. There is an association with oligohydramnios.
B. The prognosis is generally poor.
C. The findings are the result of an antenatal bowel perforation.
D. The findings are likely secondary to bowel obstruction after birth.

14. An abdominal ultrasound examination is performed in a patient who presents with neonatal jaundice and conjugated hyperbilirubinemia. A representative figure is shown below. Which of the following is the next appropriate step in management?

A. Upper GI series.
B. Tc-99m HIDA scan.
C. CT scan of the abdomen and pelvis.
D. No further imaging is indicated.

15. Static images from a Tc-99m HIDA scan that was subsequently performed on the patient described in Question 14 are shown below. These images were obtained after 6 hours of imaging. Which of the following is the next appropriate step in management?

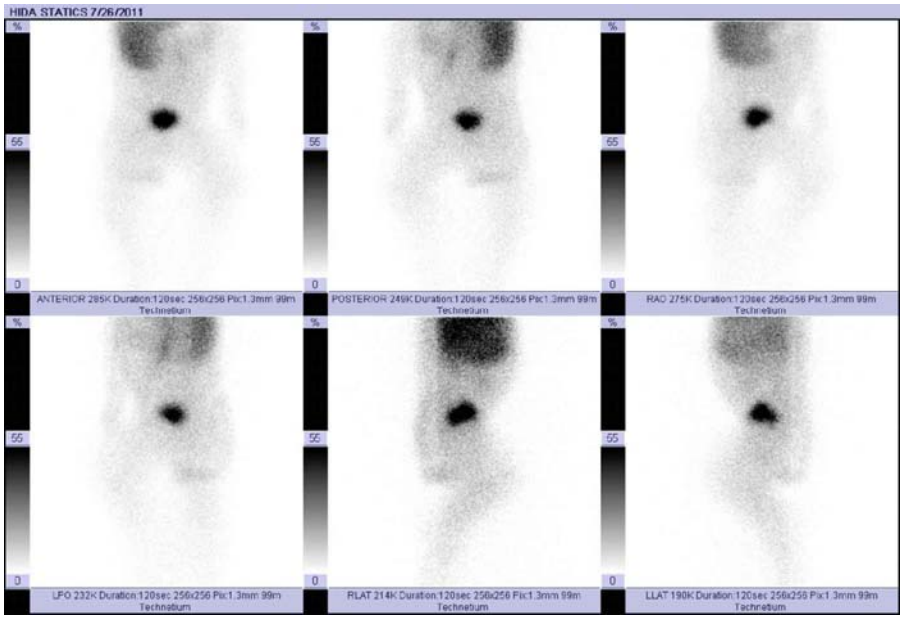

A. The study is normal and should be ended.
B. Surgery should be immediately consulted as the findings are consistent with chronic cholecystitis.
C. Delayed 24-hour images should be obtained.
D. SPECT imaging should be performed to better delineate the focus of radiotracer activity in the pelvis.

16. The decision was then made to obtain a delayed image at 24 hours after radiotracer injection on the patient described in Questions 14 and 15. The delayed image is shown below. Concerning the findings, which of the following is true?

A. Neonatal hepatitis has been excluded.
B. A Kasai procedure is the treatment of choice.
C. The findings are not consistent with biliary atresia.
D. It is unlikely that this patient will need a liver transplant.

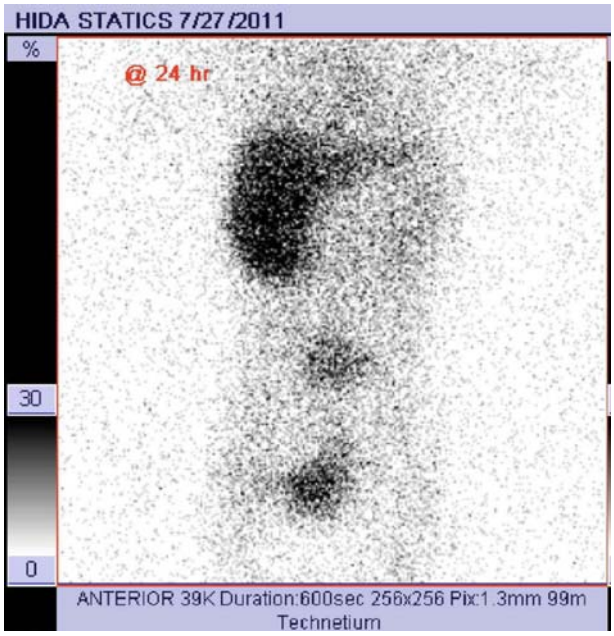

17. Before performing the exam depicted in Questions 15 and 16, pretreatment with which of the following agents can be used to enhance the specificity of the test?
A. Phenobarbital
B. CCK
C. Cimetidine
D. Morphine

18. Images from an ultrasound and CT scan performed in an infant with a history of GI bleeding are shown below. Regarding the findings, which of the following is true?

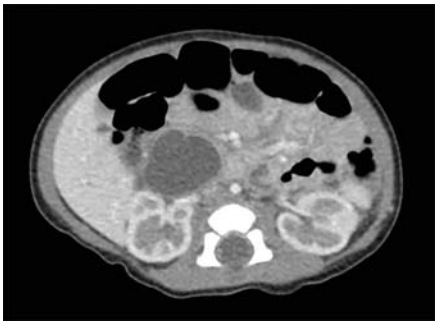

A. A Meckel (Tc-99m Pertechnetate) scan can be helpful in making the diagnosis.
B. The lesion is likely pancreatic in origin.
C. These findings represent the most common type of choledochal cyst.
D. The findings are suggestive of an exophytic cystic Wilms tumor.

19. An incidental abnormality is noted in the visualized portions of the abdomen on a portable chest radiograph obtained from a 3-year-old patient shown below. Which of the following would be the next appropriate step in management?

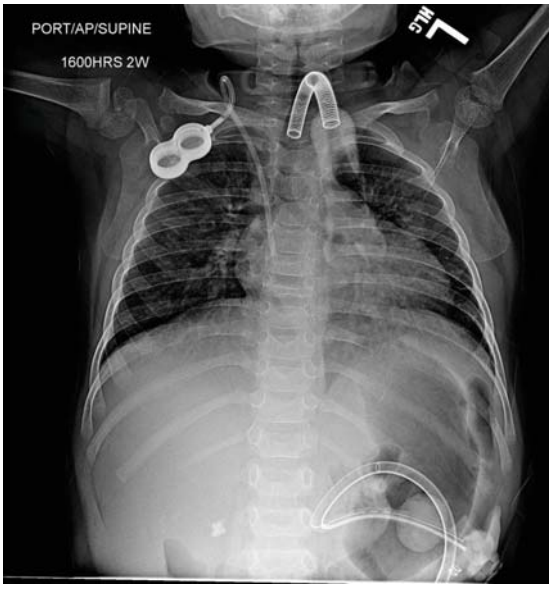

A. Notify the referring clinician of the unexpected finding, and recommend an abdominal ultrasound.
B. No further workup is needed.
C. Notify the referring clinician of the unexpected finding, and recommend a stat upper GI series.
D. Notify the referring clinician of the unexpected finding, and recommend an IR consult to check appropriate positioning of the gastrojejunostomy tube.

20. Instead of an abdominal ultrasound, further evaluation of the patient in Question 19 was performed with a CT scan (Figure A) and MR examination (Figure B). Images from those studies are shown below. Which of the following is the most likely diagnosis?

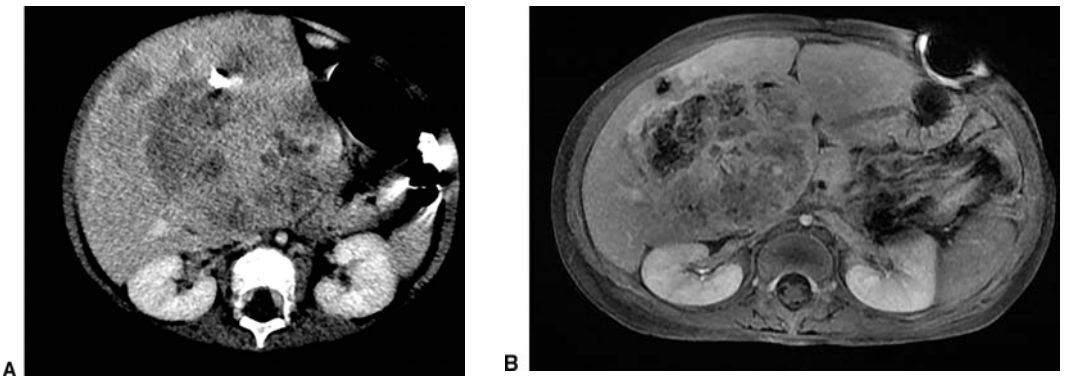

A. Mesenchymal hamartoma of the liver
B. Hepatocellular carcinoma
C. Hepatoblastoma
D. Focal nodular hyperplasia

21. Concerning hepatoblastoma, which of the following is true?
A. AFP is not typically elevated in affected patients.
B. There is a known association with Beckwith-Wiedemann syndrome.
C. There is no known association with other congenital abnormalities.
D. Most tumors are unresectable at diagnosis even with neoadjuvant chemotherapy.

22. An adolescent patient who is status post recent motor vehicle accident (MVA) is noted to have recurrent vomiting. An upper GI series is subsequently performed and images obtained after waiting a significant amount of time after administration of oral contrast are shown below. Which of the following would be the next most appropriate step in management?

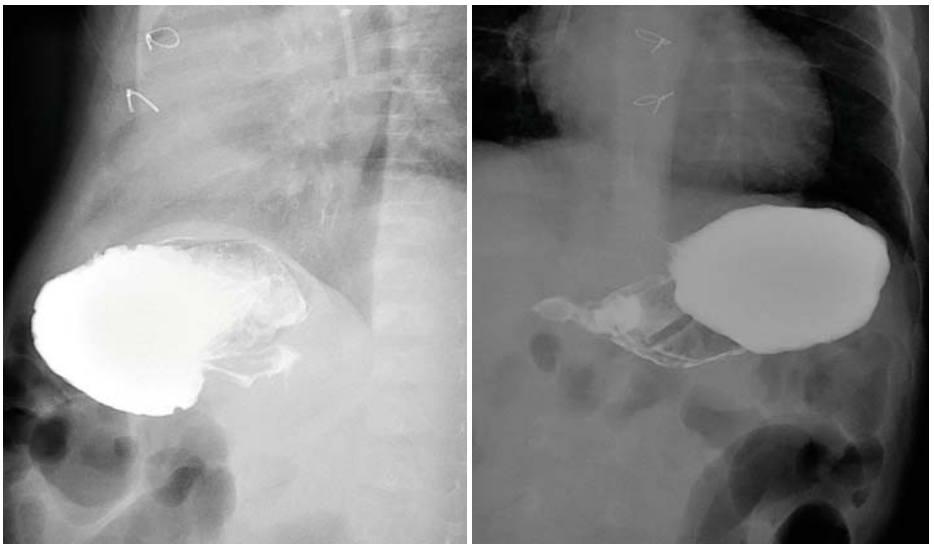

A. Abdominal plain films
B. Small bowel follow-through
C. Gastric emptying study
D. Cross-sectional imaging

23. A CT scan with intravenous contrast but without oral contrast was subsequently performed on the patient in Question 22. Representative images are shown below. Intravenous contrast was administered but oral contrast was not administered. Regarding the findings, which of the following is true?

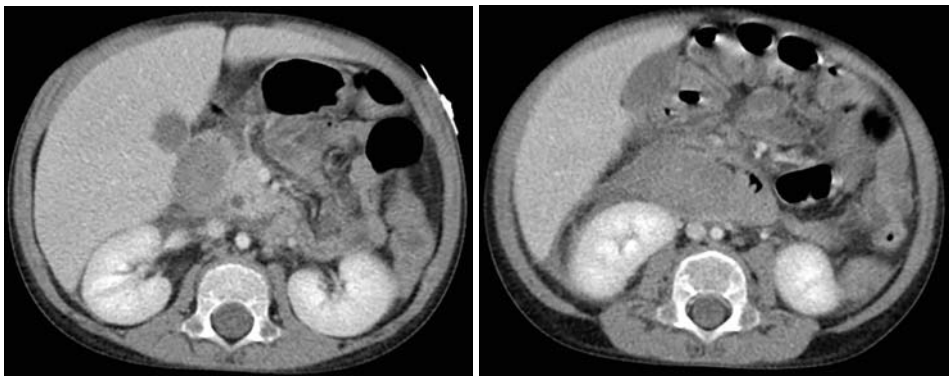

A. These lesions are often the result of penetrating abdominal trauma.
B. In small children, these lesions are not commonly associated with nonaccidental trauma.
C. Anticoagulation can often prevent these lesions from occurring.
D. These lesions can sometimes be caused by endoscopic biopsies.

24. An axial image from a CT scan is shown below. What is the most likely etiology of the appearance of the pancreas?

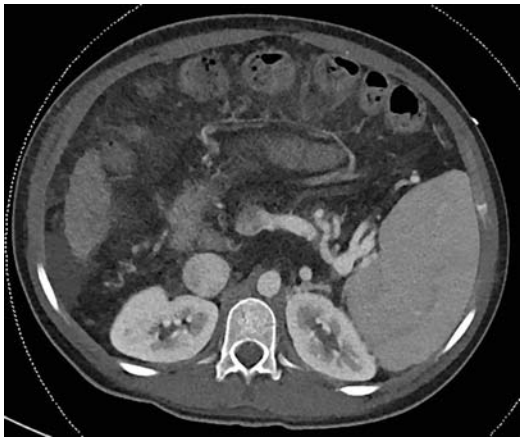

A. Tuberous sclerosis
B. von-Hippel–Lindau syndrome
C. Sturge-Weber syndrome
D. Cystic fibrosis

25. Regarding the most likely etiology of the appearance of the pancreas in the patient described in Question 24, which of the following is true?
A. This entity is often suspected with the presence of echogenic bowel seen on fetal ultrasounds.
B. A sweat test is not helpful in making the diagnosis.
C. Bronchiectasis is rare in these patients.
D. Diagnosis usually occurs in adulthood.

26. An image from an ultrasound exam performed on a young child with a history of cervical lymphadenopathy, fever, a red-colored "strawberry-"appearing tongue, rash, and conjunctival injection is shown below. Regarding the most likely etiology, which of the following is true?

A. EKG patterns of affected patients are almost always normal.
B. Myocarditis in these patients is extremely rare.
C. There is no known therapy for this entity.
D. There is an association with coronary artery aneurysms.

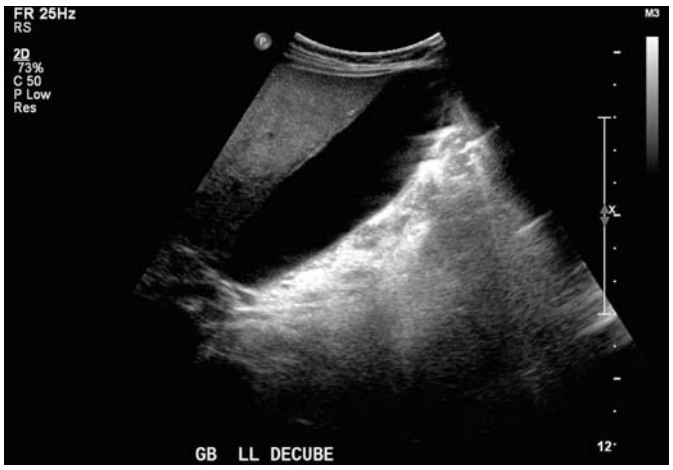

27. Images obtained after a patient's nasogastric tube was injected with 10 cc of air are shown below. Regarding the findings, which of the following is true?

A. Further evaluation with an upper GI series is recommended.
B. The treatment of choice for this condition is medical.
C. The findings are caused by extrinsic and intrinsic conditions that lead to duodenal obstruction.
D. These findings are only seen on plain film radiographs.

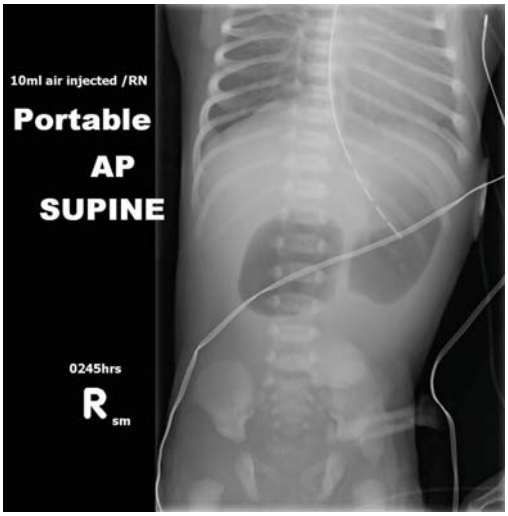

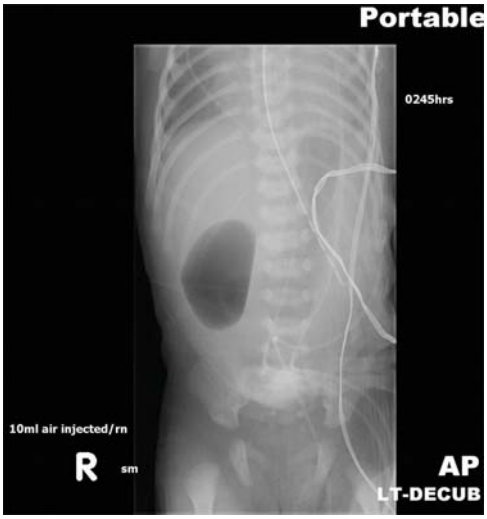

28. Regarding duodenal atresia, which of the following is true?
A. The "double-bubble" sign is pathognomonic for this entity.
B. This entity usually presents with nonbilious vomiting.
C. There is a strong association with Down syndrome.
D. The atretic segment is usually just proximal to the ampulla of Vater.

29. Images from a fetal MRI are shown below. Regarding the most likely diagnosis, which of the following is true?

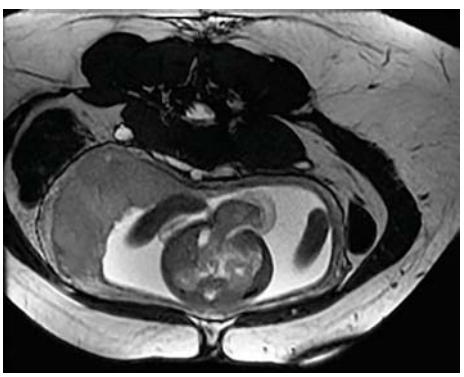

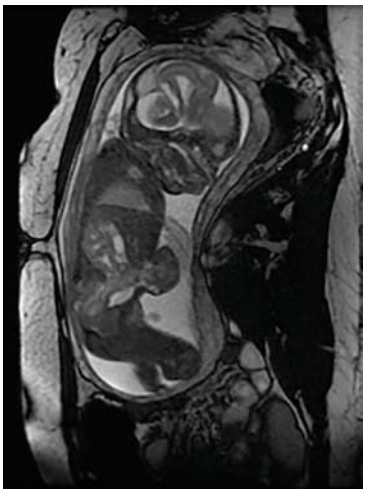

A. Other associated anomalies are uncommon.
B. The defect is not usually covered by a membrane.
C. The mortality rates of this condition are low even with associated defects.
D. The umbilical cord usually inserts into the defect.

30. Regarding gastroschisis, which of the following is true?
A. There is usually a midline defect.
B. There is a high association with associated anomalies.
C. The umbilical cord usually inserts into the defect.
D. The intrauterine mortality rate is low.

31. An abdominal radiograph from a 3-day-old premature infant with bloody stools is shown below. Which of the following would be the next most appropriate step in management?

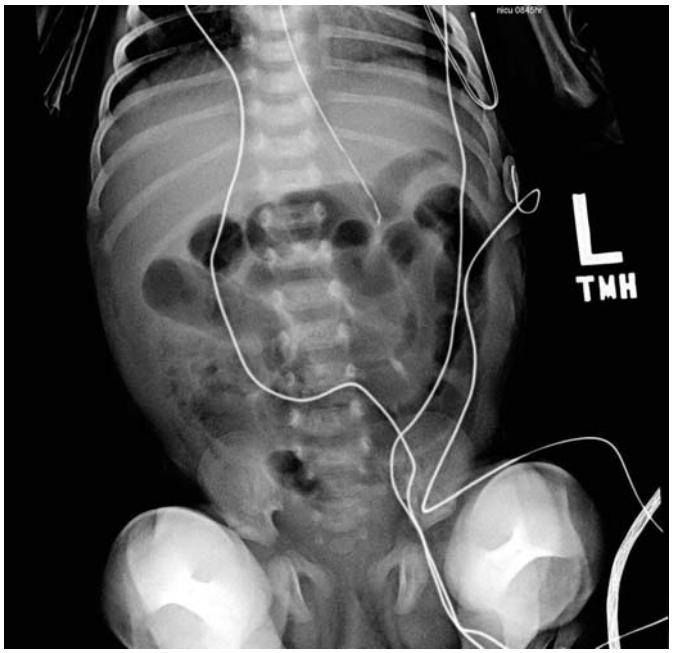

A. Stat upper GI series
B. Contrast enema
C. Emergent surgical consult
D. Bowel rest, antibiotics, and serial abdominal radiographs

32. Regarding necrotizing enterocolitis (NEC), which of the following is true?
A. The development of large bowel strictures is a known complication.
B. The disease is only treated medically.
C. It affects only premature patients.
D. Pneumatosis is an indication for surgical management.

33. Images from a study performed on a child with recurrent gastrointestinal bleeding are shown below. Regarding the abnormality, which of the following is true?

A. The finding represents a false diverticulum.
B. The abnormality is most commonly found in the right side of the colon.
C. These structures are most often lined by heterotopic gastric and pancreatic mucosa.
D. No known complications of this entity have been reported.

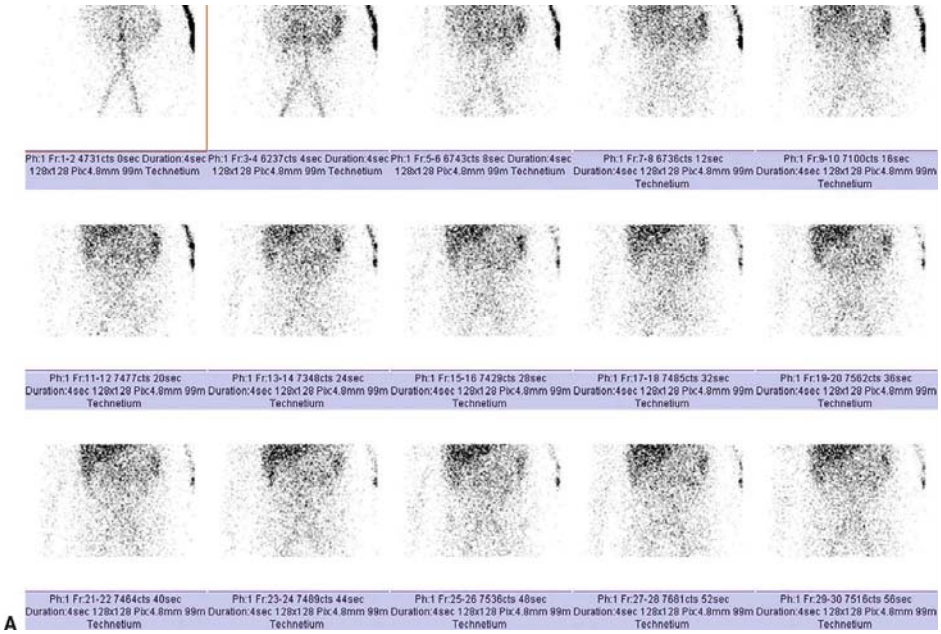

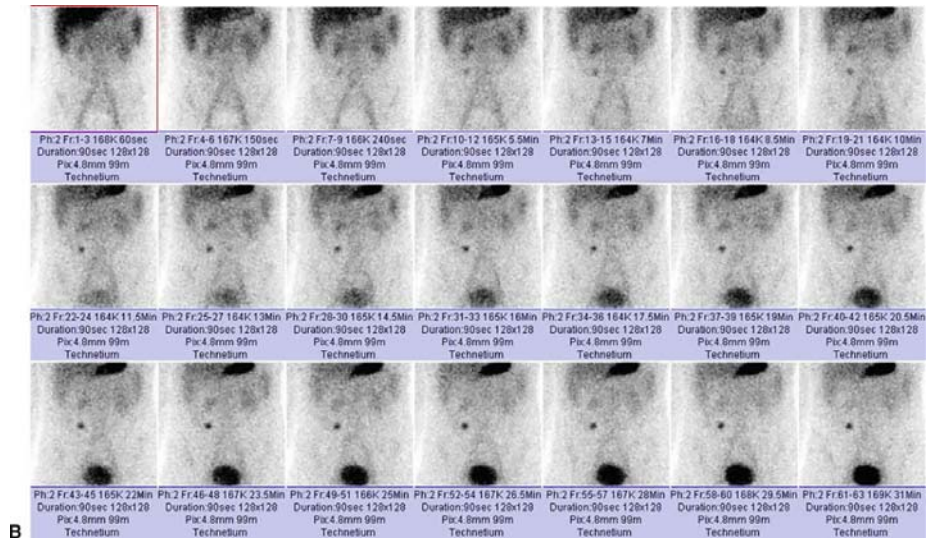

34. Pretreating the patient before the examination performed in Question 33 with which of the following medications may help improve the sensitivity of the exam?
A. Cimetidine
B. Phenobarbital
C. CCK
D. Morphine

35. An abdominal radiograph obtained from a neonate in the NICU is shown below. Which of the following lines is not in correct position?

A. UA line
B. UV line
C. Bladder catheter
D. NG tube

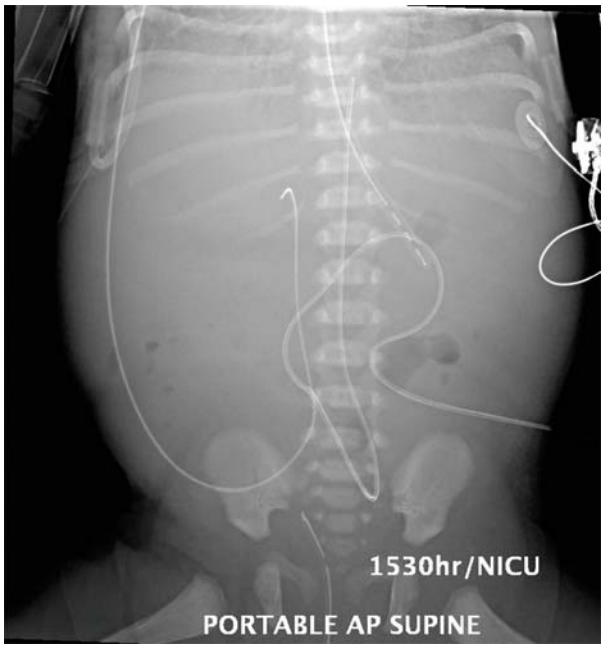

36. Which of the following is the correct position for the tip of an umbilical venous catheter?
A. Superior cavoatrial junction
B. Inferior cavoatrial junction
C. L3 or below
D. Over the sacrum

37. An otherwise healthy 10-year-old thin patient presents with a recent onset of fever and right lower quadrant abdominal pain with guarding and rebound on physical examination. Lab results reveal an elevated white blood cell count with a left shift. A plain film of the abdomen was ordered and was unremarkable. Which of the following would be the next most appropriate step in management?
A. Contrast enema
B. Upper GI series and small bowel follow-through
C. Ultrasound of the right lower quadrant
D. CT scan of the abdomen and pelvis with IV contrast

38. A right lower quadrant ultrasound was performed on the patient from Question 37, and a representative image is shown below. Despite the findings, the clinical staff is still highly suspicious for appendicitis. Which of the following would be the next most appropriate step in management?

A. Meckel (Tc-99m Pertechnetate) scan
B. MRI of the abdomen and pelvis
C. Upper GI and small bowel follow-through
D. CT scan of the abdomen and pelvis with intravenous contrast

39. Regarding the abnormality demonstrated in the images below from an MR of the abdomen and pelvis performed on the same patient in Questions 37 and 38, which of the following is true?

A. CT is more sensitive than MR in detecting this abnormality.
B. MR is more sensitive than CT in detecting this abnormality.
C. CT is as sensitive as MR in detecting this abnormality.
D. Ultrasound is more sensitive than CT in detecting this abnormality.

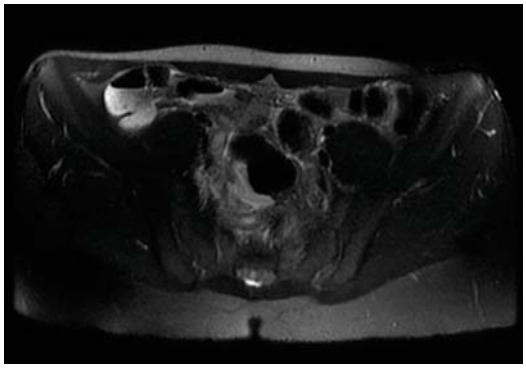

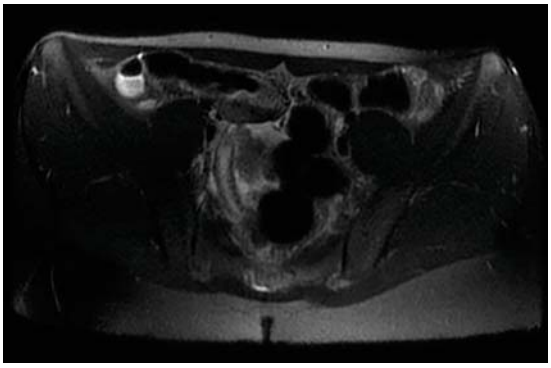

40. Images are shown below from a study performed on a 6-month-old child who has a history of wheezing. Regarding the study shown below, which is the most likely diagnosis?

A. Normal study
B. Gastroesophageal reflux
C. Malrotation with midgut volvulus
D. Duodenal atresia

		Parameter	99m Technetium
Bkgd Correction	On	Emptying	1 %
Decay Correction	On	Emptying begin (T0)	0 mins
Geometric Mean	Off	Emptying end	62 mins
		T 1/2	2942 mins
		T0 -> T 1/2	2942 mins

41. Regarding the exam performed on the patient in Question 40, which of the following is true?
A. The patient has rapid gastric emptying.
B. The patient has delayed gastric emptying.
C. The gastric emptying rate is normal.
D. The patient likely has bilious vomiting.

42. A plain abdominal radiograph obtained from a 16-year-old patient is shown below. Regarding the patient, which of the following is true?

A. The radiograph is normal.
B. A pelvic ultrasound should be ordered for further evaluation.
C. The patient likely presented with abdominal pain and diarrhea.
D. An emergent upper GI should be performed.

43. A young child presents to the emergency room with abdominal pain. Abdominal radiographs obtained with the patient placed in the supine and left lateral decubitus position are shown below. What is the next most appropriate step in management?

A. Emergent upper GI series
B. Abdominal ultrasound
C. Stat surgical consult
D. Treatment for pneumonia

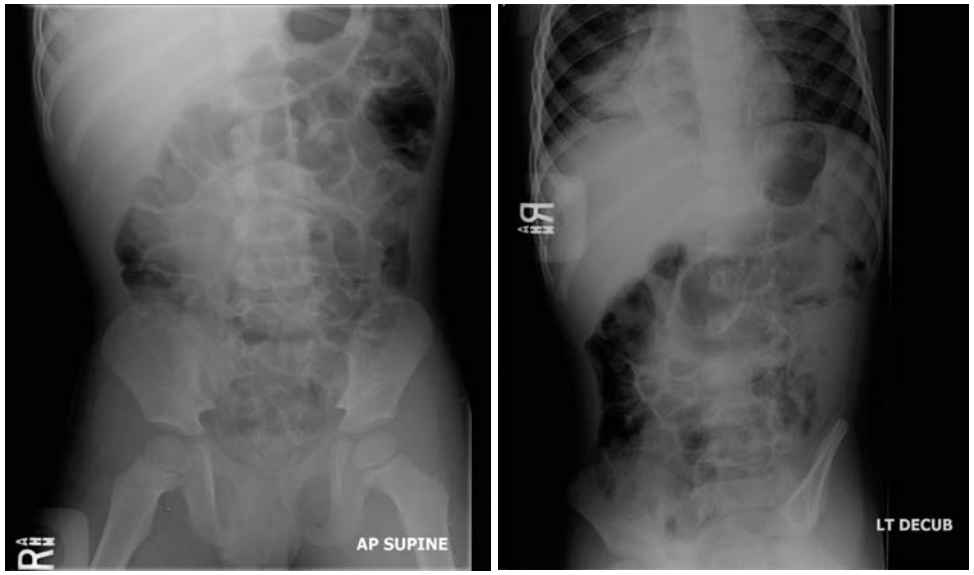

44. An MR examination was performed on a teenage patient with a long-standing history of abdominal pain and diarrhea. Images are shown below. Which of the following is the most likely diagnosis?

A. Crohn disease
B. Ulcerative colitis
C. Typhlitis
D. Pseudomembranous colitis

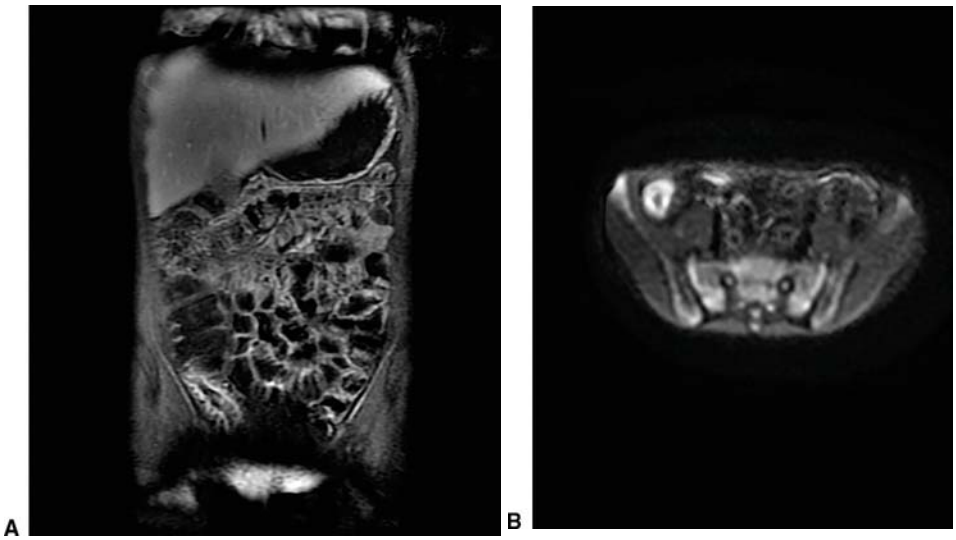

45. A 1-day-old patient presents for a CT scan of an abdominal mass and images are shown below. What is the most likely diagnosis?

A. Focal nodular hyperplasia
B. Hepatocellular carcinoma
C. Focal fatty infiltration
D. Infantile hemangioendothelioma

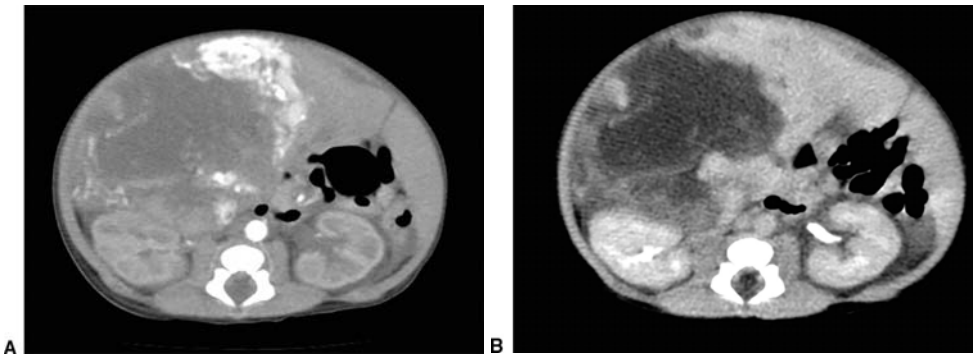

46. Prior to the CT scan performed on the patient in Question 45, a babygram was obtained. Regarding the study, which of the following is true?

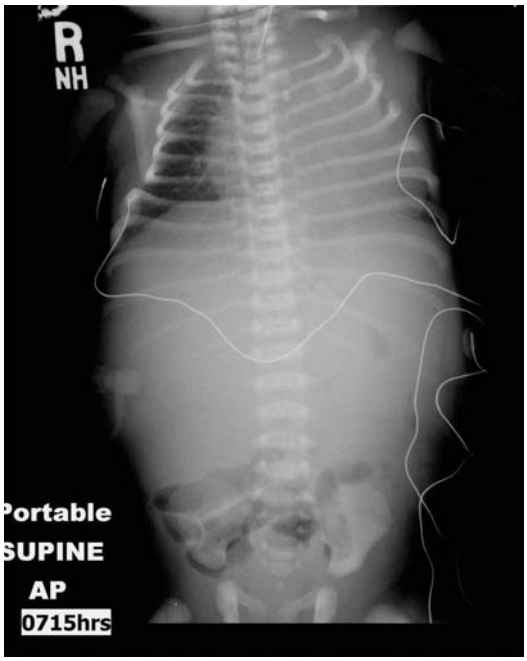

A. There is autoinfarction of the spleen.
B. There is a bowel obstruction.
C. The nasogastric tube is malpositioned.
D. There is evidence of vascular shunting.

Gastrointestinal: Answers and Explanations

1 Answer B. Bilious vomiting in a neonate is an emergency as it raises concern for malrotation of the bowel along with midgut volvulus. A delay in diagnosis and treatment of this entity may result in small bowel necrosis, short gut syndrome, and dependence on total parenteral nutrition (TPN). Mortality in affected newborns with malrotation and midgut volvulus ranges between 3% to 5%.
Abdominal radiographs may be normal in appearance or show distention of the stomach and proximal duodenum by air, with little distal bowel gas. The radiograph of the patient in this case does not demonstrate the abnormal findings which have been associated with volvulus or evidence of an obstruction. However, malrotation and midgut volvulus still must be excluded. The most sensitive test for the diagnosis of malrotation is an upper GI series with sensitivities ranging from 93% to 100%. However, the sensitivity of this exam for midgut volvulus has been reported at 54%.
A contrast enema is often used to evaluate for the cause of a distal bowel obstruction but is not the most sensitive test to evaluate for malrotation and midgut volvulus which can cause a proximal bowel obstruction. This exam can be helpful in assessing the location of the cecum, which is normally located in the right lower quadrant. Eighty percent of patients with malrotation have an abnormal cecal position, which a contrast enema can help demonstrate.
An abdominal ultrasound is also not the most sensitive test to evaluate for malrotation or midgut volvulus. However, in cases of malrotation with midgut volvulus, the "whirlpool sign" can be seen when the bowel wraps around the superior mesenteric artery (SMA), and the intestinal tract and the mesenteric vessels become twisted, resulting in secondary venous engorgement.
References: Applegate KE, Anderson JM, Klatte EC. Intestinal malrotation in children: a problem-solving approach to the upper gastrointestinal series. *Radiographics* 2006;26(5):1485–1500.
Epelman M. The whirlpool sign. *Radiology* 2006;241(1):83–94.

2 Answer C. The study demonstrates a "beaked" appearance of the third portion of the duodenum and only a small amount of contrast distal to the location of the beaking or obstruction (arrow). This appearance is consistent with malrotation with midgut volvulus.

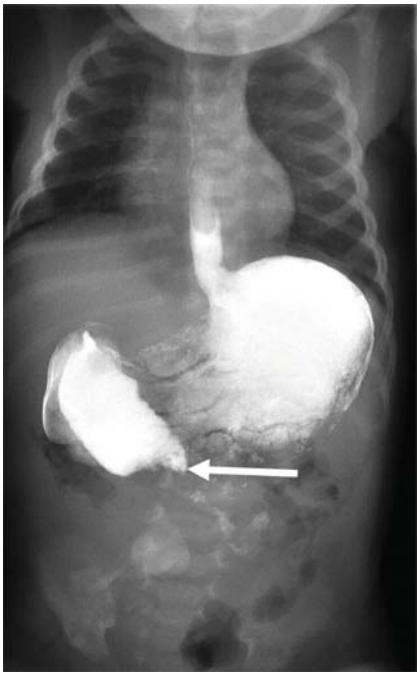

Other appearances of volvulus include the "corkscrew sign," which describes the spiral appearance of the distal duodenum and proximal jejunum seen in midgut volvulus. In patients with malrotation with midgut volvulus who exhibit these findings, the duodenum and proximal jejunum do not cross the midline and instead take an inferior direction. The loops twist on a shortened small bowel mesentery resulting in a corkscrew appearance.
The normal position of the duodenojejunal junction is to the left of the left-sided pedicle of the vertebral body at the level of the duodenal bulb on frontal views. If the duodenojejunal junction is located inferior or to the right of this level, malrotation should be considered. Note however that inferior displacement of the duodenojejunal junction is a common variant seen on frontal views in infants. This finding may be due to displacement of the relatively mobile ligament of Treitz by the adjacent distended stomach or bowel.
In cases where malrotation is in question, a posterior location of the duodenojejunal junction on a true lateral view, as expected for a retropritoneal structure, is reassuring. In children with malrotation, the

distal course of the duodenum on the lateral view often does not reach the level of the duodenal bulb an instead turns in an anterior direction into the peritoneal cavity.
Given that the study performed in the question demonstrates findings consistent with malrotation with midgut volvulus, the patient needs to go to the operating room for further treatment. Therefore, none of the other choices are correct.

References: Applegate KE, Anderson JM, Klatte EC. Intestinal malrotation in children: a problem-solving approach to the upper gastrointestinal series. *Radiographics* 2006;26(5):1485–1500.
Ortiz-neira CL. The corkscrew sign: midgut volvulus. *Radiology* 2007;242(1):315–316.

3 Answer B. Malrotation of the bowel is a predisposing risk factor for midgut volvulus. In individuals with malrotation, the mesenteric attachment of the midgut, particularly the portion from the duodenojejunal junction to the cecum, is abnormally short. The gut is therefore prone to twist counterclockwise around the superior mesenteric artery and vein creating a volvulus. As stated above, 80% of patients with malrotation have an abnormal cecal position, which a contrast enema can help demonstrate. The superior mesenteric vein is normally located to the right of and anterior to the superior mesenteric artery on axial imaging studies, but the relative positions of the vein and artery are reversed in 60% of individuals with malrotation. Malrotation is usually diagnosed in newborns and young infants; up to 75% of symptomatic cases occur in newborns, and up to 90% of symptomatic cases occur within the first year of life. The classic clinical manifestation of malrotation in newborns is bilious vomiting with or without abdominal distention associated with either duodenal obstructive bands or midgut volvulus. However, malrotation with midgut volvulus can occur at any age.
Reference: Applegate KE, Anderson JM, Klatte EC. Intestinal malrotation in children: a problem-solving approach to the upper gastrointestinal series. *Radiographics* 2006;26(5):1485–1500.

4 Answer B. The clinical history and imaging findings presented in this case are concerning for hypertrophic pyloric stenosis, a common entity in young infants characterized by hypertrophy of the circular muscle and narrowing of the antropyloric canal (channel), partially caused by crowded and edematous mucosa within the lumen. This leads to a gastric outlet obstruction, which causes intractable nonbilious projectile vomiting. The age of the child at diagnosis is usually 3 weeks to 3 months of age. The male-to-female ratio is approximately 4:1, and firstborn children are more often affected than their younger siblings. Other causes of nonbilious vomiting in children are pylorospasm and gastroesophageal reflux.
The radiographs of the patient demonstrate gaseous distention of the stomach with an air–fluid level on the left lateral decubitus view. There is a paucity of bowel gas beyond the stomach. These findings are suggestive of a gastric outlet obstruction as can be seen in pyloric stenosis.
The next best step in management would be to perform a nonemergent abdominal ultrasound to confirm the diagnosis of pyloric stenosis which is not a true medical emergency. Therefore, an emergent surgical consultation is not required. Ultrasound allows direct visualization of the pyloric muscle. A contrast enema of the colon would not be helpful in making the diagnosis. A CT scan of the abdomen and pelvis would also not be helpful in making the diagnosis as real-time visualization of the pylorus over an extended period is required to make the diagnosis and would expose the child unnecessarily to ionizing radiation.
References: Donnelly LF. *Pediatric imaging the fundamentals*. Philadelphia, PA: Elsevier/Saunders, 2009.
Hernanz-Schulman M. Infantile hypertrophic stenosis. *Radiology* 2003;227(2):319–331.

5 Answer C. The ultrasound images shown demonstrate a thickened pyloric muscle and elongated pyloric channel, which did not change over time. These findings are consistent with hypertrophic pyloric stenosis (HPS). As stated above, this condition often occurs in firstborn males. The treatment for this condition is a surgical pyloromyotomy. It is important to distinguish HPS from pylorospasm as the latter is treated medically.

On ultrasound examinations, the pyloric wall thickness should normally be <3 mm and the length of the pyloric channel should not exceed 15 mm. In the images from this case, the pyloric wall thickness measures up to 5 mm on the transverse view and the pyloric channel length measures up to 15.2 mm on the long-axis view. However, the published criteria for both of these measurements have varied. Most importantly, the pylorus should not open during the ultrasound examination. In pylorospasm, there is transient thickening of the pyloric muscle and elongation of the channel length.

However, the pylorus does eventually open in cases of pylorospasm. If the ultrasound examination demonstrates a closed pylorus with abnormal measurements of muscular thickness and channel length, it is important to extend the length of the examination by an extra 3 to 5 minutes to confirm that the pylorus remains closed and exclude pylorospasm.

In addition to the findings above, there are ancillary or secondary signs of pyloric stenosis on ultrasound including the "double-track sign." This sign is created by the abnormally thickened muscle mass that compresses the pyloric channel into two smaller channels or tracks. In addition, thickened pyloric mucosa may indent into the antrum consistent with antral or mucosal heaping.

References: Blumer SL, Zucconi WB, Cohen HL, et al. The vomiting neonate: a review of the ACR appropriateness criteria and ultrasound's role in the work-up of such patients. *Ultrasound Q* 2004;20(3):79–89.

Cohen HL, Blumer SL, Zucconi WB. The sonographic double-track sign: not pathognomonic for hypertrophic pyloric stenosis; can be seen in pylorospasm. *J Ultrasound Med* 2004;23(5):641–646.

Donnelly LF. *Pediatric imaging the fundamentals.* Philadelphia, PA: Elsevier/Saunders, 2009.

6 Answer A. The images demonstrate fusiform dilatation of the common bile duct. This is best visualized on the second image to the right of the first image. The Todani classification system has been used to classify choledochal cysts. The imaging findings depicted on the MRI are consistent with a type I choledochal cyst. Note that on Figure A, the gallbladder (short arrow) is seen to the left (patient's right) of the common bile duct (long arrow). Type I choledochal cysts are seen in 80% to 90% of patients with choledochal cysts. Note that type I cysts can be further divided into type IA, IB, and IC cysts depending upon their morphologic characteristics. A choledochocele is a type III cyst and involves only the intraduodenal portion of the common bile duct. Caroli disease or a type V cyst involves dilatation of one or several segments of the intrahepatic bile ducts. A type IVA cyst involves dilatation of the intrahepatic and extrahepatic biliary ducts.

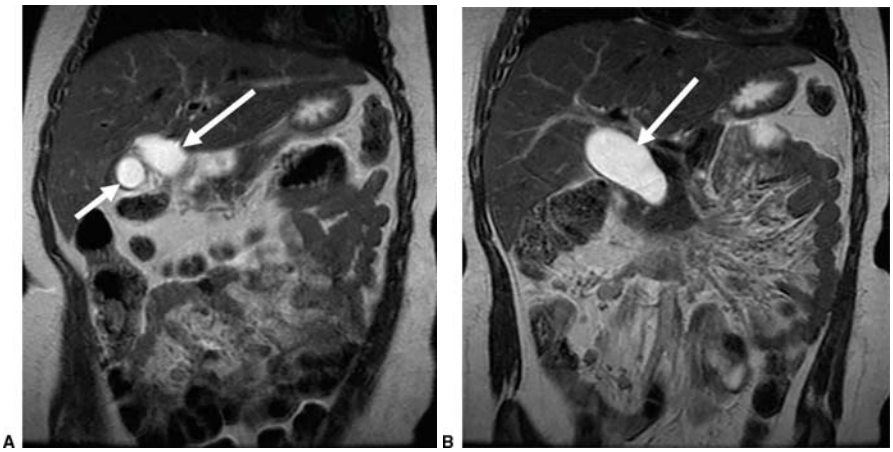

Todani Classification of Choledochal Cysts

Todani Classification	Imaging Characteristics
TYPE I—MOST COMMON	Confined to the extrahepatic biliary ducts (EBD). They can be further subdivided into type Ia (diffuse) cysts, which involve the entire EBD; type Ib (focal) cysts, which involve only a focal segment of the EBD; and type Ic (fusiform) cysts, which involve only the common bile duct (CBD)
TYPE II	True diverticula of the EBD
TYPE III	Choledochoceles, represent ectasia of an intramural CBD segment
TYPE IV	Multiple and can have both intrahepatic and extrahepatic components. They can be further subdivided into type IVa cysts, which involve both the EBD and the IBD, and type IVb cysts, which involve only the EBD with multiple saccular dilatations
TYPE V	Caroli disease, which is a rare congenital cystic dilatation of the intrahepatic biliary ducts

References: Kim OH, Chung HJ, Choi BG. Imaging of the choledochal cyst. *Radiographics* 1995;15(1):69–88.
Mortelé KJ, Rocha TC, Streeter JL, et al. Multimodality imaging of pancreatic and biliary congenital anomalies. *Radiographics* 2006;26(3):715–31.

7 **Answer D.** The image shown in the figure demonstrates diffusely dilated loops of bowel without definite rectal bowel gas. These findings along with the patient's clinical history are concerning for an obstruction of the distal or lower GI tract. The best way to evaluate for the etiology of such lower GI tract obstructions is to perform a contrast enema. Common causes of lower tract obstructions include Hirschprung disease, meconium plug syndrome (small left colon syndrome) (functional immaturity of the colon), ileal atresia, meconium ileus and anal atresia or anorectal malformations. An upper GI series is the test of choice to evaluate for a suspected upper or high obstruction in neonates. Common causes of upper tract obstructions include midgut volvulus/malrotation, duodenal atresia/stenosis, duodenal web, annular pancreas and jejunal atresia. A CT scan is not the appropriate initial method to evaluate suspected distal obstructions and would needlessly expose the child to ionizing radiation. An abdominal ultrasound is not an appropriate way to evaluate a neonate with a suspected distal bowel obstruction.

Reference: Donnelly LF. *Pediatric imaging the fundamentals*. Philadelphia, PA: Elsevier/Saunders, 2009.

8 **Answer B.** Figures A and B demonstrate a contrast enema examination. In contrast enemas, it is important to evaluate the rectosigmoid ratio. The rectum should have a diameter equal to or larger than the sigmoid, which is a normal rectosigmoid ratio. Patients who have Hirschsprung disease have an abnormal rectosigmoid ratio in which the sigmoid has a larger diameter than the rectum.
The study in this case demonstrates a normal rectosigmoid ratio. In addition, the left side of the colon appears small and ahaustral. The transverse and ascending colon are dilated. There are scattered filling defects seen throughout the colon likely due to meconium plugs. These findings are consistent with functional immaturity of the colon.
Patients who have a high intestinal obstruction, or an obstruction that occurs proximal to the midileum, such as a high ileal atresia, will have a normal caliber colon. This is because there is ample proximal bowel to produce secretions that migrate distally and nourish the colon. Patients who have a low intestinal obstruction or an obstruction that occurs in the distal ileum or colon will have a microcolon or unused colon because there is not enough proximal small bowel to produce secretions to nourish the colon.
Reference: Berrocal T, Lamas M, Gutieerrez J, et al. Congenital anomalies of the small intestine, colon and rectum. *Radiographics* 1999;19(5):1219–1236.

9 **Answer C.** The initial treatment of choice for patients with functional immaturity of the colon is a contrast enema with water-soluble contrast. Sometimes, repeated enemas are needed to flush out the meconium plugs. This condition is often seen in offspring of diabetic mothers or mothers treated with magnesium sulfate for preeclampsia. Patients who have a jejunal atresia will have a normal-appearing colon as explained in the explanation for Question 8.
Reference: Berrocal T, Lamas M, Gutieerrez J, et al. Congenital anomalies of the small intestine, colon and rectum. *Radiographics* 1999;19(5):1219–1236.

10 **Answer B.** Meconium ileus occurs secondary to obstruction of the distal ileum due to the accumulation of abnormally tenacious meconium. It occurs exclusively in patients with cystic fibrosis and is the earliest clinical presentation of the disease.
Reference: Donnelly LF. *Pediatric imaging the fundamentals*. Philadelphia, PA: Elsevier/Saunders, 2009.

11 **Answer D.** Microcolons are seen in conditions in which there is an unused colon such as distal bowel obstructions including low ileal atresia and meconium ileus. Jejunal atresias are high bowel obstructions, and there is enough proximal bowel to produce secretions to nourish the colon. Thus, a normal-caliber colon would be seen in contrast enemas performed in patients with a jejunal atresia or other proximal bowel obstructions.
References: Berrocal T, Lamas M, Gutieerrez J et al. Congenital anomalies of the small intestine, colon and rectum. *Radiographics* 1999;19(5):1219–1236.
Donnelly LF. *Pediatric imaging the fundamentals*. Philadelphia, PA: Elsevier/Saunders, 2009.

12 **Answer A.** The CT scan demonstrates a pancreatic pseudocyst, which is a known common late complication of acute pancreatitis, typically occurring 4 weeks after the development of a peripancreatic fluid collection. Pancreatic pseudocysts are the most common complication of pediatric pancreatitis. Pancreatitis in a young child should be suspected to be abuse related. However, there are other known causes of pediatric pancreatitis including pancreatitis secondary to trauma, biliary anomalies, and medication-related and autoimmune etiologies.
Reference: Restrepo R, Hegerott HE, Kulkarni S, et al. Acute pancreatitis in pediatric patients: demographics, etiology and diagnostic imaging. *Am J Roentgenol* 2016;206(3):632–644.

13 Answer C. The radiograph demonstrates a nonspecific bowel gas pattern with multiple calcifications throughout the abdomen (arrows). These findings are most consistent with meconium peritonitis. This entity is a result of a sterile chemical peritonitis that occurs after antenatal bowel perforation, which usually occurs after the 3rd month of gestation. The bowel perforation is a result of a bowel atresia, in utero volvulus, or meconium ileus. There is an association with polyhydramnios and not oligohydramnios. The prognosis is generally good.

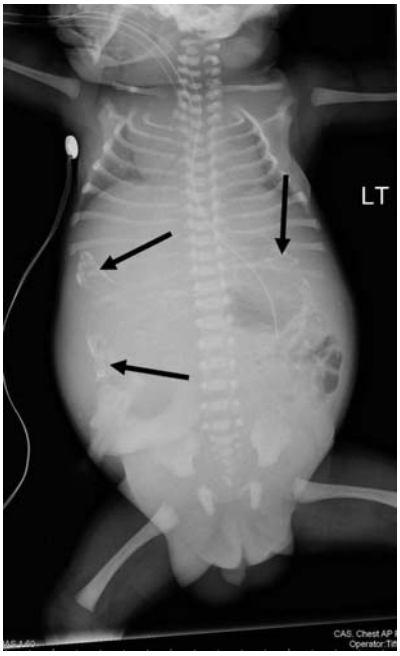

References: Dähnert W. *Radiology review manual*, 6th ed. Philadelphia, PA: Wolters Kluwer Health/Lippincott Williams & Wilkins, 2007.
Donnelly LF. *Pediatric imaging the fundamentals*. Philadelphia, PA: Saunders Elsevier, 2009.

14 Answer B. The ultrasound image of the patient in the region of the gallbladder fossa fails to demonstrate the gallbladder. The clinical presentation of neonatal jaundice and absence of the gallbladder raises concern for biliary atresia. The best way to demonstrate biliary atresia is with a Tc-99m HIDA scan. None of the other tests are helpful to make the diagnosis of biliary atresia and in the case of an upper GI series and CT scan, will needlessly expose the patient to ionizing radiation.
Reference: Kirks DR, Coleman RE, et al. An imaging approach to persistent neonatal jaundice. *Am J Roentgenol* 1984;142(3):461–465.

15 Answer C. The images fail to demonstrate bowel activity after 6 hours. A delayed image should then be obtained after 24 hours to evaluate for possible radiotracer excretion into bowel as biliary atresia cannot be excluded at this point in the study. This patient did not appear to have a gallbladder on the ultrasound exam as can be seen in the setting of biliary atresia. Note, however, that while some patients with biliary atresia do not have a gallbladder, some affected patients have a small gallbladder and other affected patients have a normal gallbladder. This patient, however, did not have a gallbladder and therefore could not have cholecystitis. The focus of radiotracer in the pelvis is excreted radiotracer within the urinary bladder, an expected finding.
Reference: Dähnert W. *Radiology review manual*, 6th ed. Philadelphia, PA: Wolters Kluwer Health/Lippincott Williams & Wilkins, 2007.

16 Answer B. The image fails to demonstrate radiotracer excretion into bowel after 24 hours. Radiotracer activity is again seen in the urinary bladder, and the activity inferior to the bladder is excreted radiotracer within the diaper. Given the clinical history, the imaging findings are consistent with biliary atresia. However, these findings can also be seen in the setting of severe hepatocellular dysfunction from neonatal hepatitis, and a liver biopsy is sometimes necessary to distinguish between these two entities. The Kasai procedure (portoenterostomy) is performed in a majority of the patients with biliary atresia and has a greater success rate when performed in children <60 days old. This is why it is imperative to make the diagnosis of biliary atresia as early as possible. Note that the Kasai procedure is often a palliative procedure as most patients will eventually need a liver transplant.
References: Bijl EJ, Bharwani KD, Houwen RHJ, et al. The long-term outcome of the Kasai operation in patients with biliary atresia: a systematic review. *Neth J Med* 2013;71(4):170–173.
Dähnert W. *Radiology review manual*, 6th ed. Philadelphia, PA: Wolters Kluwer Health/Lippincott Williams & Wilkins, 2007.

17 Answer A. In jaundiced infants in whom biliary atresia is suspected, pretreatment with phenobarbital, 5 mg/kg/d, may be given orally in two divided doses daily for a minimum of 3 to 5 days before a Tc-99m HIDA scan to enhance biliary excretion of the radiotracer and increase the specificity of the test. Phenobarbital stimulates biliary secretion by inducing hepatic enzymes, which increases conjugation and excretion of bilirubin. Morphine is given during HIDA scans to shorten the study time if there is nonvisualization of the gallbladder. This is typically injected 45 to 60 minutes after injection of radiotracer if activity is seen in the bowel. It causes contraction of the sphincter of Oddi, which raises intrabiliary pressure and can cause retrograde filling of the gallbladder. Cimetidine can be given before Meckel scans to decrease gastric secretions. CCK is a synthetic hormone that causes gallbladder contraction, but many patients with biliary atresia do not have a gallbladder.

References: Dähnert W. *Radiology review manual*, 6th ed. Philadelphia, PA: Wolters Kluwer Health/Lippincott Williams & Wilkins, 2007.
Majd M, Reba RC, Altman RP. Hepatobiliary scintigraphy with 99mTc-PIPIDA in the evaluation of neonatal jaundice. *Pediatrics* 1981;67:140–145.

18 Answer A. The lesion depicted on the ultrasound images demonstrates an anechoic cystic lesion with a wall composed of multiple layers resembling a normal bowel wall. This is characteristic of enteric duplication cysts where the cyst wall "reduplicates" the normal enteric wall. These lesions are usually attached to normal bowel but occasionally migrate into the mesentery and become a type of mesenteric cyst. Thus, these lesions are not pancreatic or renal in origin. In addition, this lesion also appears separate from the kidney and pancreas on the CT scan as there is no claw sign. Because enteric duplication cysts can contain ectopic gastric mucosa, a Meckel (Tc-99m pertechnetate) scan can be helpful in making the diagnosis.

References: Kumar R, Tripathi M, Chandrashekar N, et al. Diagnosis of ectopic gastric mucosa using 99Tcm-pertechnetate: spectrum of scintigraphic findings. *Br J Radiol* 2005;78(932):714–720.
Stoupis C, Ros PR, Abbit PL, et al. Bubbles in the belly: imaging of cystic mesenteric or omental masses. *Radiographics* 1994;14(4):729–737.

19 Answer A. Although the image presented below is a chest radiograph, there is a coarse calcification seen in the right upper quadrant (arrow). Although this calcification can be caused by multiple etiologies, a liver mass remains on the differential, and further evaluation with an ultrasound examination is indicated. An upper GI examination would not help to elucidate the etiology of a suspected hepatic calcification. Although there is a gastrojejunostomy tube seen on the radiograph, the tip has been excluded from the film, and therefore, it cannot be determined whether or not the tube is in its appropriate position. The next most appropriate step to determine whether or not the tube is in appropriate position would be to get an abdominal plain radiograph. Furthermore, the etiology of the suspected hepatic calcification cannot be determined with either an IR consult or abdominal radiograph.

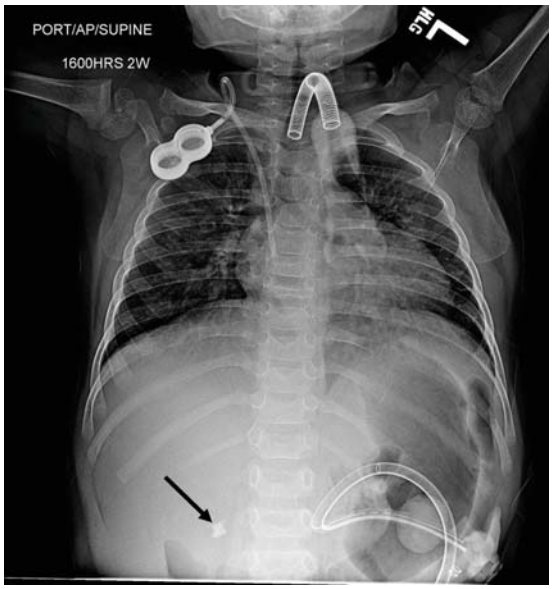

References: Blickman JG, Parker BR, Barnes PD. *Pediatric radiology: the requisites*, 3rd ed. Philadelphia, PA: Elsevier/Saunders, 2009.
Chung EM, Lattin GE Jr, Cube R, et al. From the archives of the AFIP: Pediatric liver masses: radiologic-pathologic correlation part 2. Malignant tumors. *Radiographics* 2011;31(2):483–507.

20 Answer C. Figure A is an axial image from a contrast-enhanced CT scan of the abdomen demonstrating a large heterogeneous solid mass in the liver with a large calcification (long arrow), which may represent the calcification seen on the plain film of the abdomen seen in Question 19. There are smaller satellite lesions in the periphery of the liver (short arrows). Figure B is an axial T1 fat-saturated image after contrast enhancement, which also demonstrates a heterogeneous solid enhancing mass with smaller satellite lesions in the periphery of the liver. Given the age group and constellation of imaging findings, the most likely diagnosis is hepatoblastoma, a malignant liver mass. Ninety percent of cases of hepatoblastoma occur in children younger than 5 years of age. Hepatocellular carcinoma, which is also a malignant solid tumor, rarely occurs in children under 5 years of age. Mesenchymal hamartoma of the liver is a benign liver lesion, which often appears as a complex cystic mass and primarily affects children under 5 years of age. Focal nodular hyperplasia (FNH) is most often seen in adult women but uncommonly occurs in young children and adolescents. Because FNH is composed predominantly of hepatocytes, it appears similar to normal liver, and the lesion may be difficult to visualize. Sometimes the only clue of the presence of this lesion is its mass effect on adjacent structures. The presence of a central scar may aid identification of this lesion.

References: Chung EM, Cube R, Hall GJ, et al. From the archives of the AFIP: Pediatric liver masses: radiologic-pathologic correlation part 1. Benign tumors. *Radiographics* 2010;30(3):801–826.
Chung EM, Lattin GE Jr, Cube R, et al. From the archives of the AFIP: Pediatric liver masses: radiologic-pathologic correlation part 2. Malignant tumors. *Radiographics* 2011;31(2):483–507.
Donnelly LF. *Pediatric imaging the fundamentals*. Philadelphia, PA: Elsevier/Saunders, 2009.

21 Answer B. Hepatoblastoma has been associated with several syndromes, including Beckwith-Wiedemann syndrome, Gardner syndrome, familial adenomatous polyposis, type 1A glycogen storage disease, and trisomy 18. Approximately 5% of cases occur in conjunction with other congenital anomalies, commonly of the genitourinary and gastrointestinal systems. The most useful laboratory marker for hepatoblastoma is AFP. At least 90% of patients with hepatoblastoma show abnormal elevation of AFP levels. Surgical resection is the mainstay of treatment for hepatoblastoma, and the prognosis depends on the resectability of the tumor. About 40% to 60% of hepatoblastomas are unresectable at diagnosis; however, with the use of neoadjuvant chemotherapy, up to 85% of these become resectable.

Reference: Chung EM, Lattin GE Jr, Cube R, et al. From the archives of the AFIP: Pediatric liver masses: radiologic-pathologic correlation part 2. Malignant tumors. *Radiographics* 2011;31(2):483–507.

22 Answer D. The images provided from an upper GI series demonstrate obstruction of the proximal duodenum. In a patient, involved in recent blunt trauma, a duodenal hematoma should be suspected. The next best step in management would be an additional cross-sectional imaging study to see if the cause of the duodenal obstruction is due to a duodenal hematoma or other lesion. Abdominal radiographs would not yield any further information about the cause of the obstruction. A small bowel follow-through would not help if there is a duodenal obstruction. A gastric emptying study is used to evaluate the rate of gastric emptying into the duodenum. It would not help elucidate the cause of a duodenal obstruction.

References: Donnelly LF. *Pediatric imaging the fundamentals*. Philadelphia, PA: Elsevier/Saunders, 2009.
Swischuk LE. *Emergency imaging of the acutely ill or injured child*, 4th ed. Philadelphia, PA: Lippincott, Williams and Wilkins, 2000.

23 Answer D. The axial images from a contrast-enhanced CT examination demonstrate an intramural lesion of heterogeneous fluid attenuation, which is likely secondary to a hematoma within the duodenum (arrows). The hematoma causes luminal narrowing. Intramural duodenal hematomas are often the result of blunt trauma that can be caused by accidental trauma as well as nonaccidental trauma. Anticoagulation can also be a cause of spontaneous intramural duodenal hematomas. These lesions are also known to occur after endoscopic biopsy.

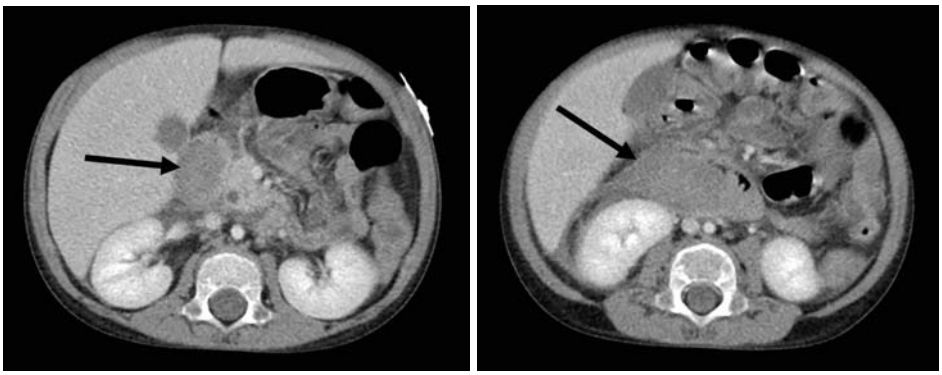

References: Donnelly LF. *Pediatric imaging the fundamentals*. Philadelphia, PA: Elsevier/Saunders, 2009.
Ghersin E, Gaitini D, Willis O, et al. Intramural duodenal hematoma mimicking an intestinal mass on sonography. *J Ultrasound Med* 2002;21(6):693–695.

24 Answer D. The axial CT image demonstrates extensive low attenuation in the region of the pancreas so much so that it is difficult to see normal pancreatic parenchyma. These findings are compatible with fatty infiltration of the pancreas. In children, cystic fibrosis is the most common etiology of fatty replacement of the pancreas. None of the other answer choices are known causes of fatty replacement of the pancreas.

Reference: Vaughn DD, Jabra AA, Fishman EK. Pancreatic disease in children and young adults: evaluation with CT. *Radiographics* 1998;18(5):1171–1187.

25 Answer A. Echogenic bowel is seen in up to 60% to 70% of patients affected with cystic fibrosis. A sweat test is used to help make the diagnosis of cystic fibrosis, and affected patients have elevated concentrations of sodium and chloride in their sweat. There is progressive cystic and cylindrical bronchiectasis in these patients, which affects up to 100% of patients after 6 months of age. The mean age of diagnosis of cystic fibrosis is 2.9 years of age, and 90% of patients are diagnosed by 12 years of age.

Reference: Dähnert W. *Radiology review manual*, 6th ed. Philadelphia, PA: Lippincott Williams & Wilkins, 2007.

26 Answer D. The image from the ultrasound examination demonstrates hydropic distension of the gallbladder, which along with the patient's symptoms suggests Kawasaki syndrome. This entity often leads to the development of coronary artery aneurysms. Myocarditis occurs in 25% of these patients and when severe can cause congestive heart failure. Atrioventricular conduction disturbances have been reported, which can cause abnormal EKG tracings. Treatment with gamma globulins can decrease the severity of the illness and can decrease the likelihood of delayed complications such as coronary aneurysms.

References: Dähnert W. *Radiology review manual*, 6th ed. Philadelphia, PA: Wolters Kluwer Health/Lippincott Williams & Wilkins, 2007.
Donnelly LF. *Pediatric imaging the fundamentals*. Philadelphia, PA: Elsevier/Saunders, 2009.

27 Answer C. The radiographs demonstrate the "double-bubble" sign, which is seen in cases of duodenal obstruction caused by intrinsic as well as extrinsic causes. The intrinsic causes are duodenal atresia, duodenal stenosis, and duodenal webs; the extrinsic causes include annular pancreas, malrotation of the gut with obstruction produced by midgut volvulus or by Ladd bands, and preduodenal position of the portal vein. The two air-filled bubbles represent the stomach and proximal duodenum. The most common cause of this finding among the causes of duodenal obstruction is duodenal atresia, which is reproducible with a variety of other imaging modalities, including upper gastrointestinal studies and sonography. For the neonate with the classic appearance of a double bubble, additional radiologic investigation is unnecessary, and the surgeon is alerted to plan for surgery, because all congenital causes of duodenal obstruction require surgery.

Reference: Traubici J. The double bubble sign. *Radiology* 2001;220(2):463–464.

28 Answer C. Duodenal atresia is associated with many congenital syndromes, the foremost being Down syndrome. Approximately 30% of children with duodenal atresia have trisomy 21. There is also an association with anomalies of the VACTERL (vertebral, anorectal, cardiac, tracheoesophageal, renal, and limb anomalies) spectrum. The atretic segment is most often just beyond or distal to the ampulla of Vater. Therefore, patients usually present with bilious vomiting. However, the atretic segment can sometimes be proximal to the ampulla of Vater, and therefore, some patients can present with nonbilious vomiting. As stated above, the "double-bubble" sign is seen in cases of duodenal obstruction, which can be caused by a variety of intrinsic and extrinsic causes, and therefore, this sign is not only seen in duodenal atresia.

Reference: Traubici J. The double bubble sign. *Radiology* 2001;220(2):463–464.

29 Answer D. The fetal MR images demonstrate a midline anterior abdominal wall defect. There is herniation of the liver and bowel through the defect. The umbilical cord can be seen inserting in the defect (arrow). These are hallmarks of an omphalocele. Omphaloceles are also usually covered by a membrane. Omphaloceles are commonly (54.2%) found to be associated with other anomalies, which determines prognosis. The mortality rate is 80% when any associated defect is present and increases to near 100% when chromosomal or cardiovascular anomalies exist.

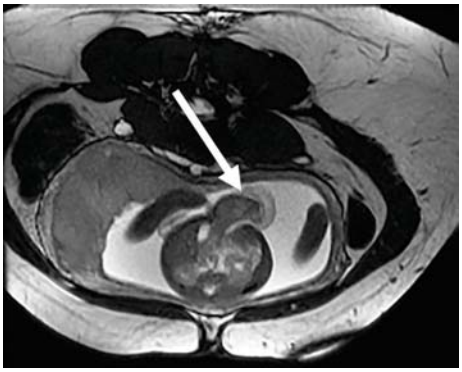

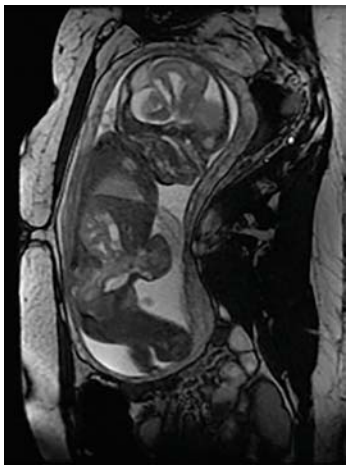

Reference: Daltro P, Fricke BL, Kline-Ath BM, et al. Prenatal MRI of congenital abdominal and chest wall defects. *Am J Roentgenol* 2005;184(3):1010–1016.

30 **Answer D.** Gastroschisis is the herniation of fetal bowel loops into the amniotic cavity usually through a right-sided paraumbilical abdominal wall defect. A midline defect is seen in cases of omphalocele. This anomaly does not have a surrounding membrane as is seen in cases of omphalocele. Associated anomalies are rare in gastroschisis. This is in contrast to cases of omphalocele, which is commonly associated with other defects. The intrauterine mortality rate of gastroschisis is 10% to 15%, which is relatively low.

Comparing Gastroschisis and Omphalocele

Gastroschisis	Omphalocele
Anterior wall defect that is lateral to midline	Midline anterior wall defect
Herniated contents (usually just bowel) are not covered by a peritoneal membrane, which allows exposure to amniotic fluid that is toxic to bowel	Herniated contents (usually bowel and liver) are covered by a peritoneal membrane
Associated anomalies are rare	Up to 66% of patients have associated congenital defects (usually cardiac)

References: Daltro P, Fricke BL, Kline-Ath BM, et al. Prenatal MRI of congenital abdominal and chest wall defects. *AJR Am J Roentgenol* 2005;184(3):1010–1016. Donnelly LF. *Pediatric imaging the fundamentals*. Philadelphia, PA: Elsevier/Saunders, 2009.

31 **Answer D.** The clinical history of a premature infant who is in the first week of life presenting with bloody stools is suggestive of necrotizing enterocolitis (NEC). The abdominal radiograph demonstrates an abnormal bowel gas pattern with gaseous distension of the bowel and right lower quadrant pneumatosis intestinalis (arrow), which are findings consistent with the clinical history of NEC. On the radiographs, there is no evidence of free peritoneal air or bowel perforation to indicate an emergent surgical consult. Bowel perforation is the main indication for surgical intervention in patients with NEC. A stat upper GI series would not be indicated in this situation as the history is not consistent with an upper gastrointestinal obstruction. A contrast enema may eventually be performed in this patient later on to evaluate for colonic strictures, which can develop from NEC. However, it is not indicated at this time. The next best appropriate step in management is for the patient to be made n.p.o. and for antibiotics to be initiated along with serial abdominal radiographs to monitor disease progression.

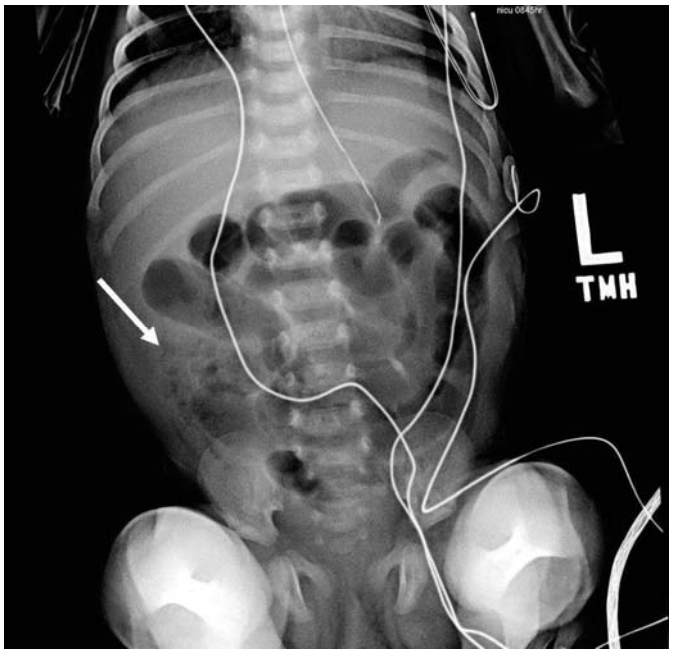

Reference: Epelman M, Daneman A, Navarro OM, et al. Necrotizing enterocolitis: review of state-of-the-art imaging findings with pathologic correlation. *Radiographics* 2007;27(2):285–305.

32 Answer A. Approximately 10% of neonates with NEC are born at term, and congenital heart disease is the main risk factor in this group. However, the incidence of NEC is inversely proportional to the gestational age. Infants of 28 weeks or less gestational age and those of extremely low birth weight (<1,000 g) are at a greater risk for NEC.
NEC is treated surgically as well as medically. Bowel perforation and free air is the main indication for surgical instead of medical therapy for NEC. Pneumatosis is not an indication for surgical treatment. In the clinical setting of NEC, the presence of intramural gas confirms the diagnosis of NEC—if not present, the patient may still have NEC, and treatment should be commenced if the clinical findings are suggestive of NEC. The amount of intramural gas present does not always relate to the clinical severity of NEC in any particular patient, and disappearance of intramural gas does not always correlate with clinical improvement. Portal venous gas has also been reported on plain abdominal radiographs in up to 30% of neonates with NEC, and these are usually, but not always, the more severely affected cases. Portal venous gas is not always associated with a fatal outcome. As stated above, colonic strictures can develop from NEC, and contrast enemas are often performed to evaluate the colon in patients with a history of NEC.
References: Donnelly LF. *Pediatric imaging the fundamentals*. Philadelphia, PA: Elsevier/Saunders, 2009.
Epelman M, Daneman A, Navarro OM, et al. Necrotizing enterocolitis: review of state-of-the-art imaging findings with pathologic correlation. *Radiographics* 2007;27(2):285–305.

33 Answer C. The images shown are from a Meckel (Tc-99m pertechnetate) scan. The study demonstrates a tiny focus of increased radiotracer uptake in the right lower quadrant with activity in the stomach appearing at the same time which is best seen on Figure B. After intravenous injection of Tc-99m pertechnetate, a Meckel diverticulum containing gastric mucosa will manifest as a small rounded area of increased activity in the right lower quadrant. A Meckel diverticulum is a true diverticulum, composed of all layers of the intestinal wall, and is lined by normal small intestinal mucosa. It frequently contains heterotopic gastric and pancreatic mucosa and less commonly, duodenal, colonic, or biliary mucosa. They commonly occur in the distal ileum. Clinical symptoms arise from complications of the diverticulum such as peptic ulceration with hemorrhage; diverticulitis; intestinal obstruction from diverticular inversion, intussusception, volvulus, torsion, or inclusion of the diverticulum in a hernia; formation of enteroliths; and development of neoplasia within the diverticulum.

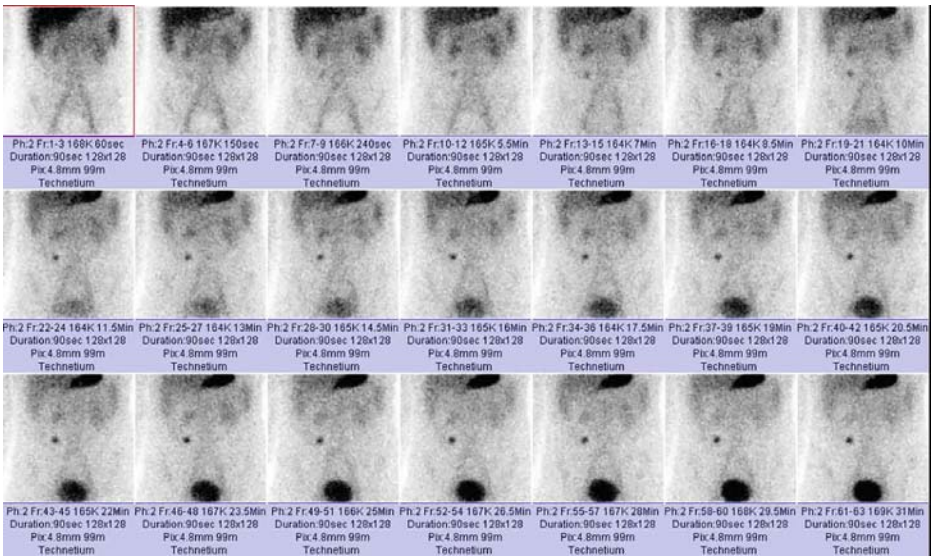

Reference: Levy AD, Hobbs CM. From the archives of the AFIP. Meckel diverticulum: radiologic features with pathologic correlation. *Radiographics* 2004;24(2):565–587.

34 **Answer A.** Histamine H_2 blockers (cimetidine, ranitidine, famotidine) inhibit acid secretion by the parietal cells, thus limiting release of Tc-99m pertechnetate by the mucosal cells and improving the sensitivity of the Meckel scan. Phenobarbital stimulates biliary secretion by inducing hepatic enzymes, which increases conjugation and excretion of bilirubin. It is given prior to HIDA scans to evaluate for biliary atresia to increase the specificity of the test. Morphine is given during HIDA scans to shorten the study time if there is nonvisualization of the gallbladder. Morphine is typically injected 45 to 60 minutes after injection of radiotracer if activity is seen in the bowel. It causes contraction of the sphincter of Oddi, which raises intrabiliary pressure and can cause retrograde filling of the gallbladder. CCK is a synthetic hormone that causes gallbladder contraction and can be used to pretreat patients who have been fasting >24 hours prior to Tc-99m HIDA scans.

References: Dähnert W. *Radiology review manual*, 6th edition. Philadelphia, PA: Wolters Kluwer Health/Lippincott Williams & Wilkins, 2007.

Majd M, Reba RC, Altman RP. Hepatobiliary scintigraphy with 99mTc-PIPIDA in the evaluation of neonatal jaundice. *Pediatrics* 1981;67:140–145.

Spottswood SE, Pfluger T, Bartold SP, et al. SNMMI and EANM practice guideline for meckel diverticulum scintigraphy 2.0. *J Nucl Med Technol* 2014;42(3):163–169.

35 **Answer B.** Note that on a single AP radiograph, it is difficult to say with certainty whether lines and tubes are actually within certain anatomical structures, and therefore, it is preferable to say that lines and tubes project over or within anatomical structures. The tip of the UV line projects in the right upper quadrant presumably within the portal venous system (long arrow) and is clearly in an inferior position to the inferior cavoatrial junction, which is its proper position. The UV line should not be placed within the right atrium to prevent the development of cardiac arrhythmias. The tip of the UA line projects over the T8/T9 intervertebral disc space (short arrow), which is an acceptable position. The UA line should be placed in the abdominal aorta either in a high position at the T6 to T10 level or in a low position at the L3 to L5 level. If placed in either of these positions, it should avoid the mesenteric branches of the abdominal aorta where it could potentially cause end-organ damage secondary to dissections or thrombus formation. The distal tip and side ports of the nasogastric tube project over the stomach. The side port and tip of the bladder catheter are in normal position and project over the urinary bladder.

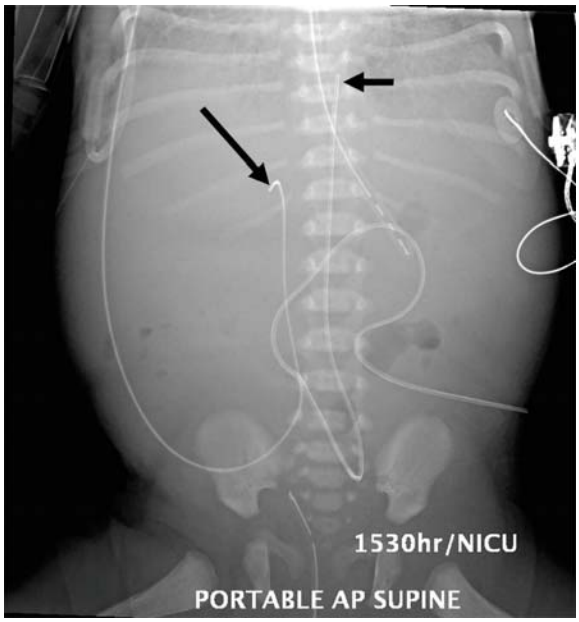

Reference: Hunter TB, Taljanovic MS. Medical devices of the abdomen and pelvis. *Radiographics* 2005;25(2):503–523.

36 **Answer B.** As stated above, the correct placement for an umbilical venous catheter is over the inferior cavoatrial junction. The correct placement for the other major lines and tubes often used in neonates can be found in the explanation for Question 35.

Reference: Hunter TB, Taljanovic MS. Medical devices of the abdomen and pelvis. *Radiographics* 2005;25(2):503–523.

37 **Answer C.** The clinical picture is concerning for appendicitis. Of the exams listed, an ultrasound of the right lower quadrant would be the next most appropriate test to evaluate for appendicitis in this clinical setting. Ultrasound is the initial imaging modality of choice for diagnosing acute appendicitis in children primarily because of its lack of ionizing radiation.

Reference: Larson DB, Trout AT, Fierke SR, et al. Improvement in diagnostic accuracy of ultrasound of the pediatric appendix through the use of equivocal interpretive categories. *Am J Roentgenol* 2015;204(4):849–856.

38 **Answer B.** The ultrasound exam fails to visualize the appendix. In addition, there are no secondary signs of appendicitis such as echogenic fat, abscesses, or abnormal-appearing loops of bowel. However, appendicitis is still clinically suspected. Of the exams listed, an MR examination of the abdomen and pelvis is the most appropriate next test in this clinical scenario. MRI has a sensitivity of 100% and specificity of 96% for appendicitis in pediatric patients after inconclusive appendix sonography. These results are similar to published sensitivity and specificity rates of CT for appendicitis, which historically has been the preferred way to evaluate for appendicitis after an inconclusive ultrasound. However, unlike MR, CT utilizes ionizing radiation. CT is still often the preferred way to evaluate for appendicitis in younger patients or those patients who would need sedation to complete an MR examination, which is significantly longer than a CT examination and requires greater patient cooperation.

References: Dillman JR, Gadepalli S, Sroufe NS, et al. Equivocal pediatric appendicitis: unenhanced MR imaging protocol for nonsedated children—a clinical effectiveness study. *Radiology* 2016;279(1):216–225.
Herliczek TW, Swenson DW, Mayo-Smith WW. Utility of MRI after inconclusive ultrasound in pediatric patients with suspected appendicitis: retrospective review of 60 consecutive patients. *Am J Roentgenol* 2013;200(5):969–973.

39 **Answer C.** The images shown are two axial ultrafast spin echo fat-saturated sequences images from an MR of the abdomen and pelvis. They demonstrate a fluid-filled, tubular structure (arrows) with surrounding edema and inflammatory changes of the adjacent fat planes. These findings are consistent with acute appendicitis.

The reported sensitivities of MR and CT for the detection of appendicitis in children has been found to be similar in multiple publications and is preferred to CT in patients who do not require sedation due to its lack of ionizing radiation. CT is more sensitive than ultrasound for the detection of appendicitis in children. However, ultrasound is often utilized prior to CT or MR because it is cheaper and does not utilize ionizing radiation as in the case of CT.

References: Dillman JR, Gadepalli S, Sroufe NS, et al. Equivocal pediatric appendicitis: unenhanced MR imaging protocol for nonsedated children—a clinical effectiveness study. *Radiology* 2016;279(1):216–225.
Herliczek TW, Swenson DW, Mayo-Smith WW. Utility of MRI after inconclusive ultrasound in pediatric patients with suspected appendicitis: retrospective review of 60 consecutive patients. *Am J Roentgenol* 2013;200(5):969–973.
Strouse PJ. Pediatric appendicitis: an argument for US. *Radiology* 2010;255(1):8–13.

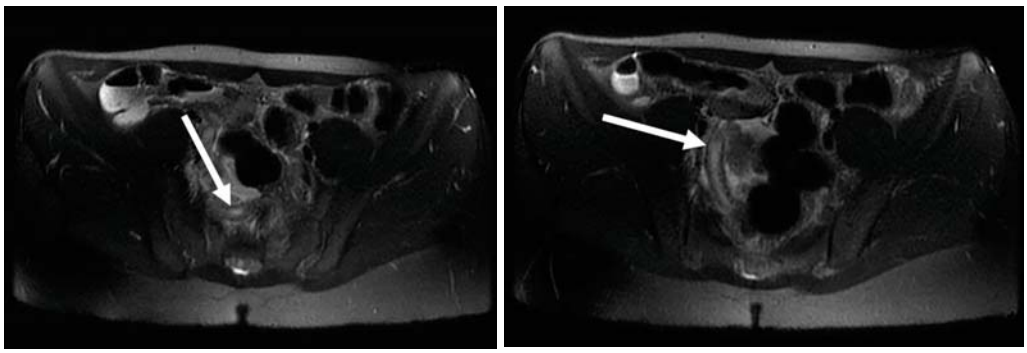

40 Answer B. Figure A shows sequential images from a liquid gastric emptying exam, which demonstrates reflux of radiotracer from the stomach to the esophagus on several images (arrows). Therefore, the study is not normal. In these studies, Tc-99m sulfur colloid is mixed with milk or formula. Duodenal atresia is best diagnosed on a plain film with the "double-bubble" sign. Malrotation and midgut volvulus is best diagnosed on an upper GI series.

References: Applegate KE, Anderson JM, Klatte EC. Intestinal malrotation in children: a problem-solving approach to the upper gastrointestinal series. *Radiographics* 2006;26(5): 1485–1500.
Reyhan M, Yapar AF, Aydin M, et al. Gastroesophageal scintigraphy in children: a comparison of posterior and anterior imaging. *Ann Nucl Med* 2005;19(1):17–21.
Traubici J. The double bubble sign. *Radiology* 2001;220(2):463–464.

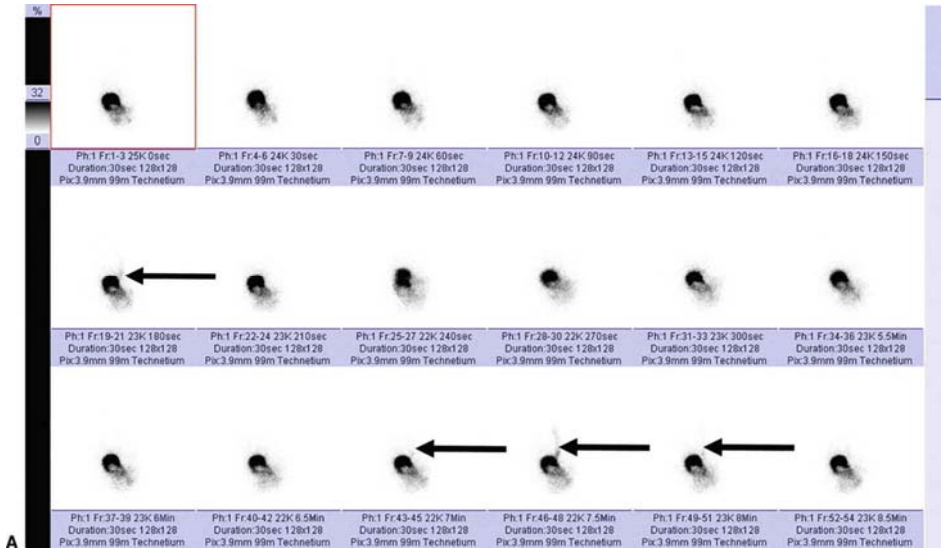

41 Answer B. Figure B reports the percent of gastric emptying after 62 minutes is 1%. Although the published normative values for gastric emptying of liquids vary by age, 1% is definitely delayed based on published studies. In small children <2 years of age, the published normal gastric emptying rate is 32% or greater. In children older than 2 years of age, the normal reported range is 44% or higher. Memorizing these numbers is not as important as realizing that 1% would be markedly low by these standards. Based on these standards, the gastric emptying rate is not normal, and the patient has markedly delayed gastric emptying, not rapid gastric emptying. Delayed gastric emptying is not a cause of bilious vomiting. Note that nonbilious vomiting as opposed to bilious vomiting is associated with gastroesophageal reflux.
Reference: Heyman S. Gastric emptying in children. *J Nucl Med* 1998;39(5):865–869.

42 Answer C. The plain abdominal radiograph demonstrates thickening of the haustral folds consistent with colonic "thumbprinting" (arrows). This sign is usually indicative of submucosal edema. Classically described with ischemic colitis, it is also noted in other forms of colitis, including ulcerative and infectious colitis. Thus, the radiograph is abnormal. Abdominal pain and diarrhea are often signs of a colitis. Both an upper GI series and pelvic ultrasound would not be helpful in evaluating the colon.

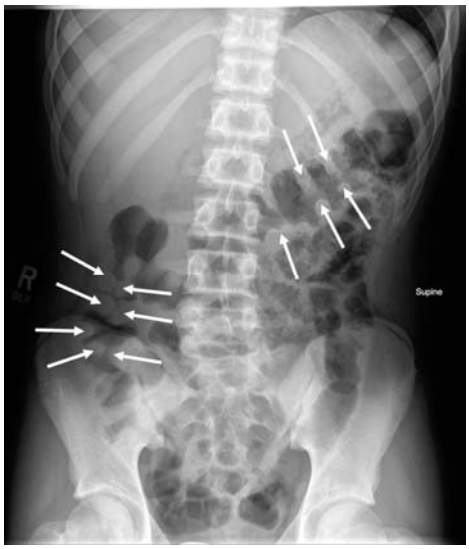

Reference: Cutinha AH, De Nazareth AG, Alla VM, et al. Clues to colitis: tracking the prints. *West J Emerg Med* 2011;11 (1):112–113.

43 Answer D. There is a nonobstructive bowel gas pattern seen on the abdominal radiographs. However, there is extensive air-space opacity at the right lung base on the left lateral decubitus view, which likely represents pneumonia. Therefore, this patient should be treated for pneumonia. Abdominal pain can be a presentation of an occult pneumonia in children and that is why it is important to always look at the lung bases on pediatric abdominal radiographs. Once the diagnosis of pneumonia is made, an upper GI series, surgical consult, or abdominal ultrasound is not necessary.
Reference: Kanegaye JT, Harley JR. Pneumonia in unexpected locations: an occult cause of pediatric abdominal pain. *J Emerg Med* 1995;13(6):773–779.

44 Answer A. Figure A is a coronal T1 fat-saturated contrast-enhanced MRI image, which demonstrates contrast enhancement of the terminal ileum (arrow). Figure B is an axial DWI image that shows restricted diffusion of the terminal ileum (arrow). Although high signal on a DWI image should correspond with low signal on an ADC map if there is true restricted diffusion, the combination of the contrast enhancement and high signal on the DWI sequence in the terminal ileum is suggestive of a terminal ileitis. Note that the remainder of the bowel including the colon appears normal on both images. Therefore, typhlitis or neutropenic colitis, which usually affects the right colon, is unlikely as is pseudomembranous colitis, which usually manifests as a pancolitis. Although there can be a "backwash ileitis" in ulcerative colitis, this usually occurs when the entire colon is affected.

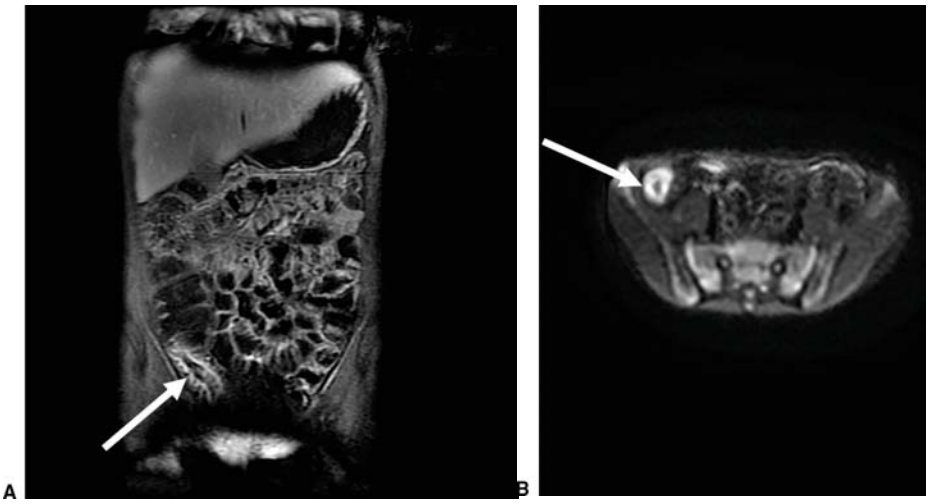

References: Donnelly LF. *Pediatric imaging the fundamentals*. Philadelphia, PA: Elsevier/Saunders, 2009.
Mollard BJ, Smith EA, Dillman JR. Pediatric MR enterography: technique and approach to interpretation-how we do it. *Radiology* 2015;274(1):29–43.
Roggeveen MJ, Tismenetsky M, Shapiro R. Best cases from the AFIP: ulcerative colitis. *Radiographics* 2006;26(3):947–951.
Towbin AJ, Sullivan J, Denson LA, et al. CT and MR enterography in children and adolescents with inflammatory bowel disease. *Radiographics* 2013;33(7):1843–1860.

45 **Answer D.** Figure A and B are axial images from a contrast-enhanced CT scan of the abdomen and pelvis in the early arterial (Figure A) and delayed excretory (Figure B) phases of contrast enhancement. Figure A demonstrates a heterogeneous mass with central low attenuation and early peripheral puddling of contrast (arrow). Figure B demonstrates later peripheral pooling of contrast (arrow). These findings are most consistent with an infantile hemangioendothelioma. Focal nodular hyperplasia is a solid lesion that usually has a central scar, which fills in on delayed imaging. Although hepatocellular carcinoma can have a varied appearance, this is not the right age group for this diagnosis. Finally, the heterogeneity of the lesion and the presence of contrast enhancement argue against focal fatty infiltration.

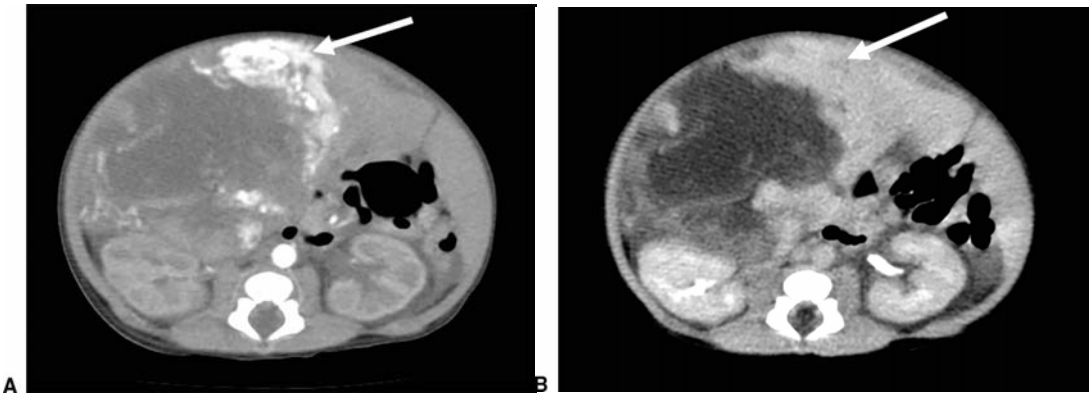

References: Chung EM, Cube R, Hall GJ, et al. From the archives of the AFIP: Pediatric liver masses: radiologic-pathologic correlation part 1. Benign tumors. *Radiographics* 2010;30(3):801–826.
Chung EM, Lattin GE Jr, Cube R, et al. From the archives of the AFIP: Pediatric liver masses: radiologic-pathologic correlation part 2. Malignant tumors. *Radiographics* 2011;31(2):483–507.
Roos JE, Pfiffner R, Stallmach T, et al. Infantile hemangioendothelioma. *Radiographics* 2003;23(6):1649–1655.

46 **Answer D.** Both the liver and spleen appear enlarged on this study, and thus, there is no evidence of splenic autoinfarction. Infantile hemangioendotheliomas are often large tumors and affected patients often have enlarged livers, abdominal distention, or a palpable upper abdominal mass. Note that the bowel loops are inferiorly displaced on this study because of mass effect from the liver and spleen. There may be extensive arteriovenous shunting within infantile hemangioendotheliomas, resulting in decreased peripheral vascular resistance. Thus, increased blood volume and cardiac output are required to maintain vascular bed perfusion, which may lead to high cardiac output and congestive heart failure in up to 50% to 60% of patients. This explains why the cardiothymic silhouette appears enlarged on this study. The nasogastric tube is properly positioned with its tip and distal side port projecting in the stomach. Although the bowel loops appear inferiorly displaced, they do not appear obstructed. Note that the bladder is distended on this study, which likely accounts for the lack of rectal bowel gas.

Reference: Roos JE, Pfiffner R, Stallmach T, et al. Infantile hemangioendothelioma. *Radiographics* 2003;23(6):1649–1655.

2 Pediatric Genitourinary Tract

Questions

1. A 1-month-old male neonate with an abdominal mass presents for an abdominal ultrasound. Images from the examination are shown below. What is the next appropriate step in management?

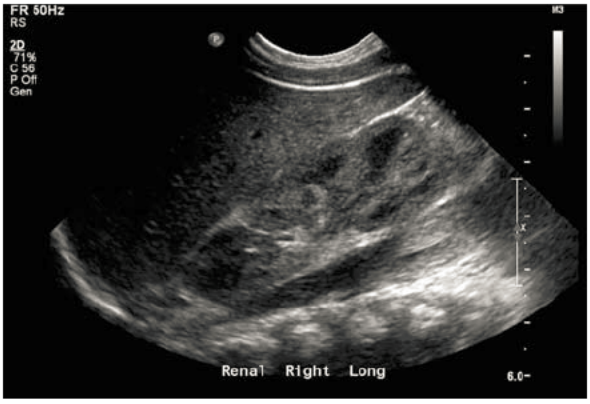

A. Plain radiographs of the abdomen
B. Voiding cystourethrogram (VCUG)
C. CT scan of the abdomen and pelvis
D. Testicular ultrasound

2. A representative image obtained from a VCUG examination subsequently performed on the same patient in Question 1 is shown below. What would be the next appropriate step in management?

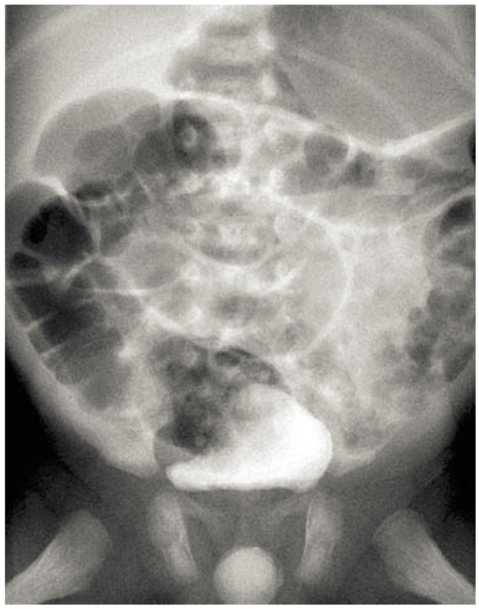

A. Tc-99m MAG-3 scan
B. Tc-99m DMSA scan
C. CT scan of the abdomen and pelvis
D. Right upper quadrant ultrasound

3. A Tc-99m MAG-3 scan was subsequently performed on the same patient in Questions 1 and 2. The pre-Lasix renogram for the right kidney was normal. The pre-Lasix renogram for the left kidney was abnormal. The post-Lasix renogram for the left kidney is shown below. Which of the following is TRUE?

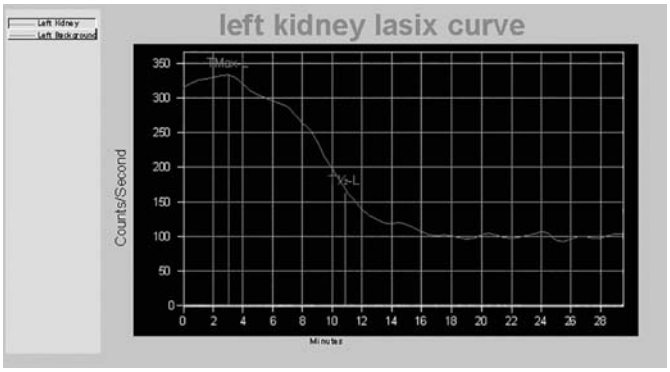

A. There is a definite obstruction.
B. The patient will require surgical intervention.
C. The patient will likely not require surgical intervention.
D. The time from max to half max is 15 minutes.

4. Images from a renal ultrasound are demonstrated below with the patient imaged in the left lateral decubitus (LLD) position. Regarding the entity demonstrated in the images of the right kidney, which of the following is TRUE?

A. These lesions almost always develop into a Wilms tumor.
B. There is an association with contralateral UPJ obstructions.
C. The kidney often maintains this appearance for the rest of the patient's life.
D. There would be extensive radiotracer uptake by the right kidney on a MAG-3 scan.

5. Coronal images from a contrast-enhanced CT scan of the abdomen and pelvis are demonstrated below in a 16-year-old patient who has new-onset hypertension. Concerning the entity demonstrated, which of the following is TRUE?

A. The inheritance pattern of the disease is likely autosomal recessive.
B. There is often an onset of disease in early childhood.
C. There is an association with berry aneurysms.
D. There is an association of this entity with hepatic fibrosis.

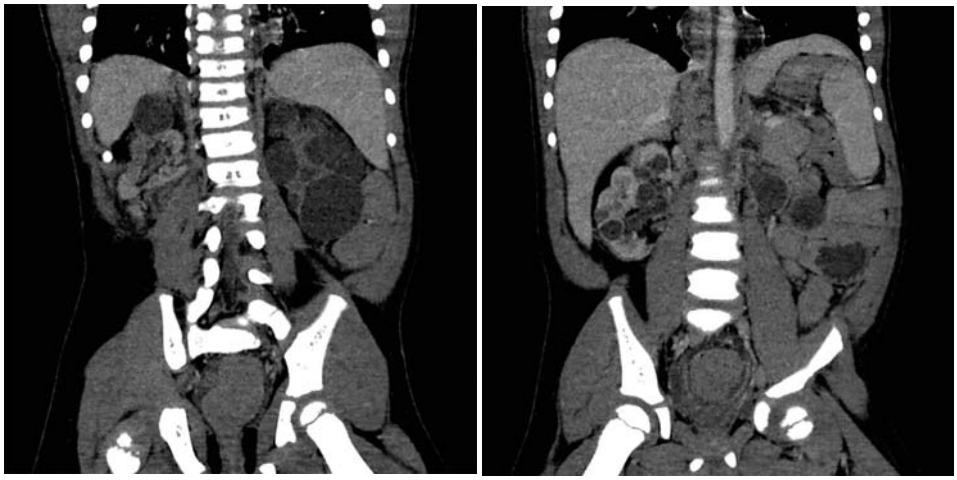

6. A 3-year-old presents with left upper quadrant pain and vomiting. A supine abdominal radiograph was subsequently obtained and is shown below. What is the next most appropriate step in management?

A. Tc-99m MAG-3 scan
B. I-123 MIBG scan
C. Abdominal ultrasound
D. Tc-99m DMSA scan

7. An abdominal ultrasound of the patient in Question 6 was subsequently performed. Representative images are shown below. What is the next most appropriate step in management?

A. I-123 MIBG scan
B. Tc-99m MAG-3 scan
C. VCUG
D. MRI of the abdomen

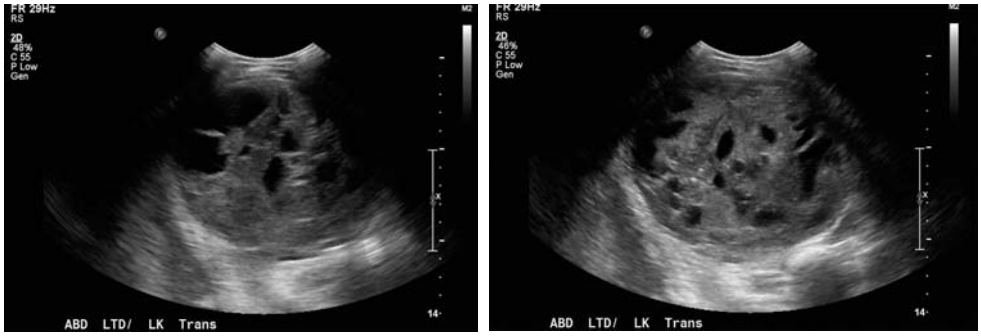

8. An MRI of the abdomen was subsequently performed on the same patient in Questions 6 and 7. Representative images are shown below. What is the most likely diagnosis?

A. Neuroblastoma
B. Mesoblastic nephroma
C. Wilms tumor
D. Renal cell carcinoma

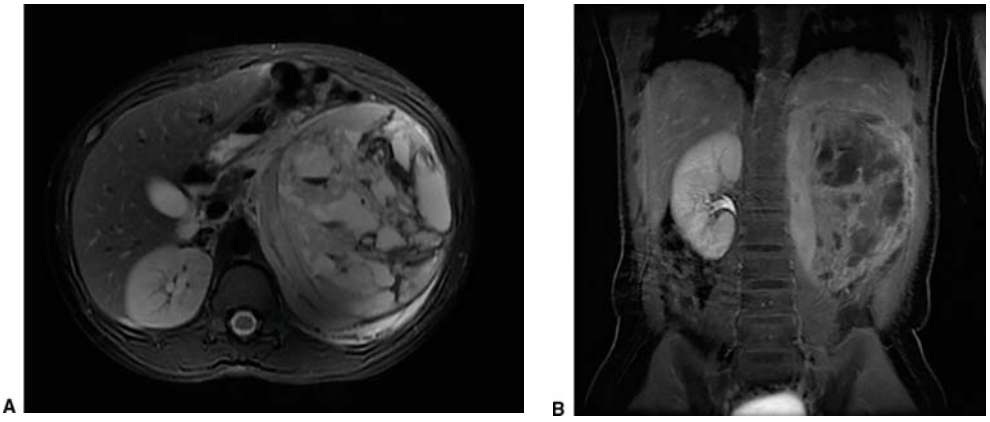

9. Which of the following additional tests would be indicated on the patient in questions 6, 7 and 8?
A. CT scan of the chest
B. Bone scan
C. I-123 MIBG scan
D. VCUG

10. Regarding Wilms tumor, which of the following is TRUE?
A. There is only one histology.
B. The overall survival is >90%.
C. The tumor does not commonly invade the renal veins.
D. There is no known association with nephroblastomatosis.

11. Which of the following renal tumors is associated with sickle cell trait?
A. Renal cell carcinoma
B. Multilocular cystic renal tumor
C. Mesoblastic nephroma
D. Medullary carcinoma

12. A 10-year-old male presents with right testicular pain. A testicular ultrasound was performed, and representative images are shown below. Regarding the images, which of the following is TRUE?

A. These findings constitute a urologic emergency and require emergent surgical exploration.
B. These findings demonstrate a testicular mass, and the patient should be referred to oncology.
C. These findings are likely secondary to infection, and the patient will need to be started on antibiotics.
D. Only supportive care is indicated.

13. A teenage female presents to the emergency department with intermittent pelvic pain. Representative images of the pelvic ultrasound that was performed are shown below. Which of the following would be the next most appropriate step in management?

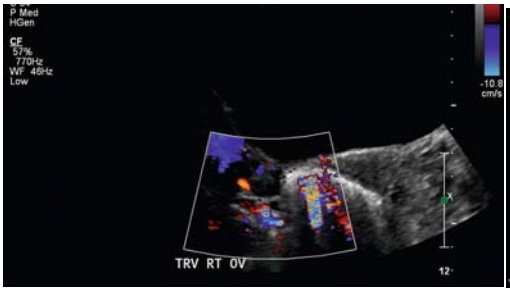

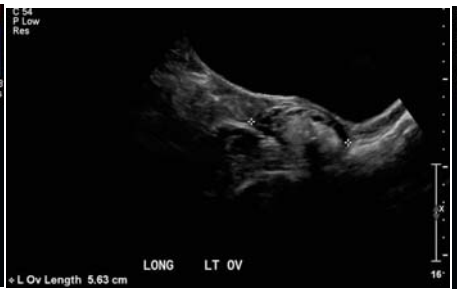

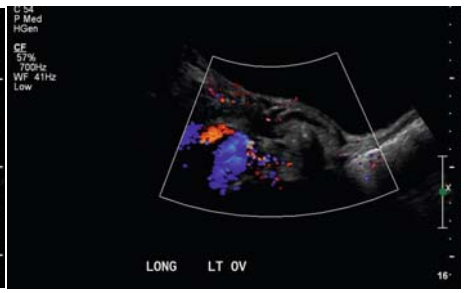

A. MRI of the pelvis
B. Repeat ultrasound in 6 to 8 weeks.
C. I-123 MIBG scan
D. No further imaging is needed.

14. Because of the inability of the patient in Question 13 to tolerate an MR examination and problems with sedating the patient, a CT scan of the pelvis was performed instead of an MR study. A representative image of the study is shown below. Regarding the abnormality, which of the following is TRUE?

A. Approximately 90% of these lesions rupture.
B. Torsion of the affected ovary occurs in approximately 95% of cases.
C. A Rokitansky nodule is commonly seen in mature cystic teratomas.
D. There is no risk of malignant transformation.

15. A 1-day-old male with a history of prenatal hydronephrosis presents for a renal ultrasound. Images from the examination are shown below. Which of the following would be the next most appropriate step in management?

A. Emergent surgical intervention
B. VCUG
C. Tc-99m MAG-3 scan
D. Tc-99m DMSA scan

16. A VCUG study was subsequently performed on the patient described in Question 15. An image from the study is shown below. Regarding the entity shown, which of the following is TRUE?

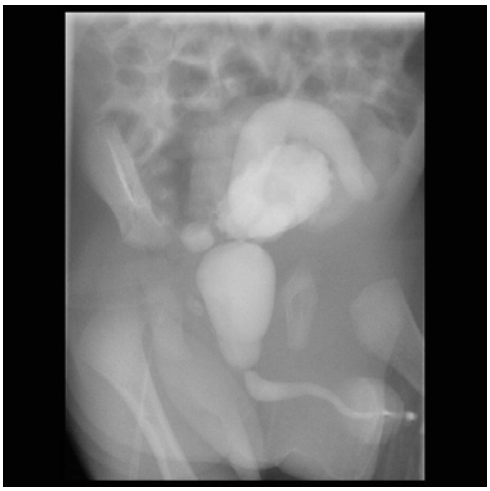

A. There is marked dilatation of the anterior urethra.
B. Urinary ascites is a good prognostic indicator.
C. They are not commonly found in males.
D. The definitive treatment is medical.

17. An image from a testicular ultrasound is shown below. Which of the following would be the next most appropriate step in management?

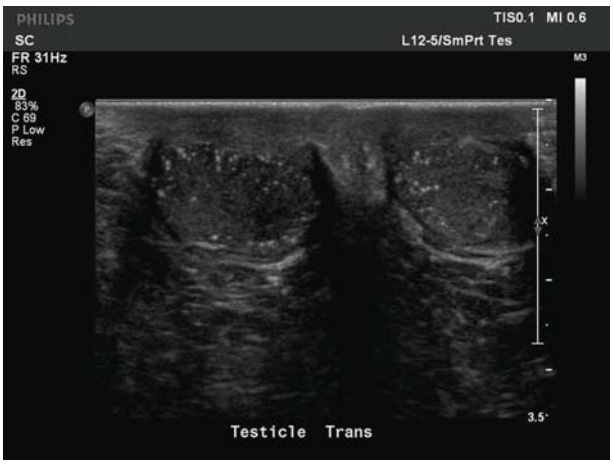

A. Stat urology consult
B. CT scan of the chest, abdomen, and pelvis to look for metastatic disease
C. MRI of the pelvis to look for a source of infection
D. Routine urology follow-up along with surveillance ultrasounds in younger patients and testicular self-examination in older patients

18. A patient presents for a VCUG examination for a history of urinary tract infections. A representative image from the study is shown below. Regarding the findings, which of the following is TRUE?

A. There is a single collecting system on the right.
B. There is a duplex collecting system on the right.
C. There is a duplex collecting system on the left.
D. There is no vesicoureteral reflux.

19. According to the Weigert-Meyer rule, which of the following is TRUE?
A. The upper pole moiety is more prone to reflux.
B. The upper pole moiety is more prone to a UPJ obstruction.
C. The ureter for the lower pole moiety frequently ends in a ureterocele.
D. The ureter for the upper pole moiety has an ectopic insertion, which inserts inferomedially to the insertion of the upper pole moiety.

20. A 5-year-old male presents for a CT scan and MR exam to better evaluate abnormal findings on an abdominal ultrasound. Images from the CT scan (Figure A) and MRI exam (Figure B) are shown below. Which of the following would be the next most appropriate step?

A. I-123 MIBG scan
B. Gallium 67 scan
C. Tc-99m MAG-3 scan
D. Tc-99m DMSA scan

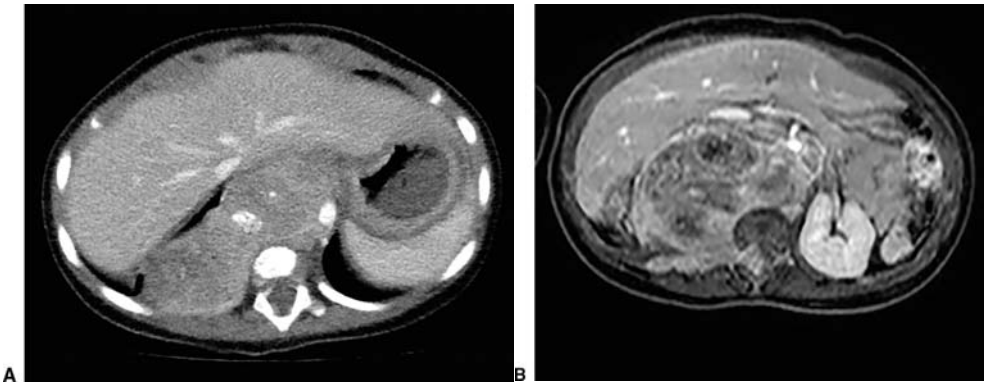

21. An I-123 MIBG scan was performed on the patient described in Question 20 and images from the examination are shown below. Which of the following features of this tumor are associated with a better prognosis?

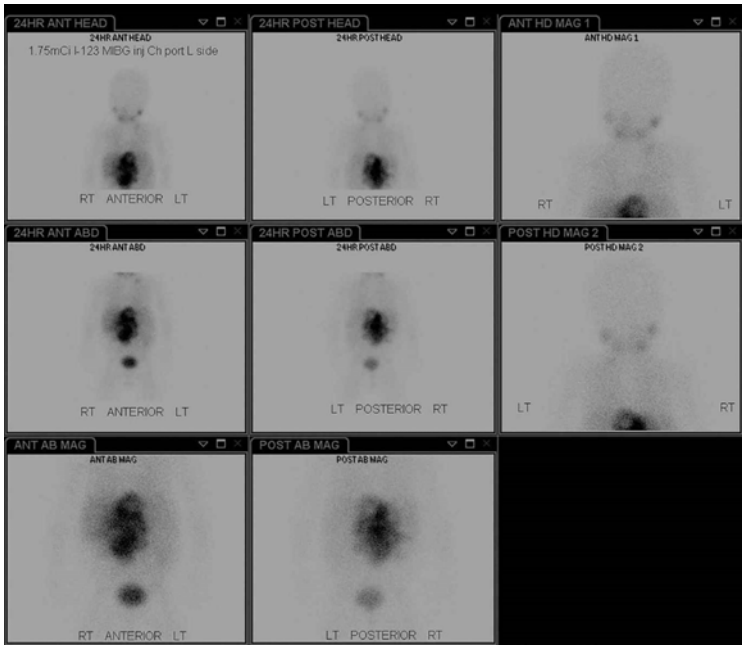

A. Elevated N-Myc amplification
B. Age of diagnosis of <1 year
C. Decreased levels of CD44
D. Elevated levels of ferritin

22. When performing an I-123 MIBG nuclear medicine examination for evaluation of this tumor, which of the following drugs should be discontinued if possible prior to the examination?
A. Imipramine
B. Potassium chloride
C. Omeprazole
D. Furosemide

23. Regarding neuroblastoma stage IV-S, which of the following is TRUE?
A. It is associated with a poor prognosis.
B. It affects the skin, liver, and bone marrow.
C. It is seen in children older than 2 years of age.
D. There is no metastatic disease.

24. A CT scan performed on a 2-month-old patient is shown below. What is the most likely diagnosis?

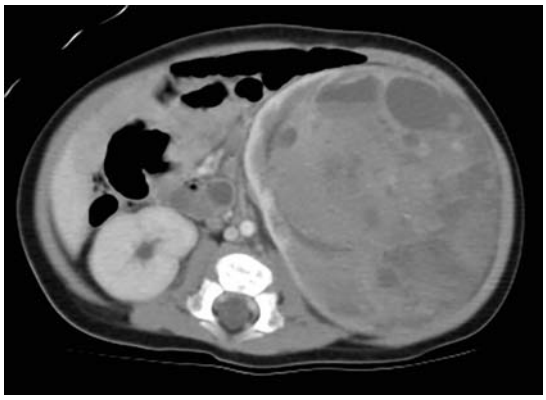

A. Congenital neuroblastoma
B. Wilms tumor
C. Renal cell carcinoma
D. Congenital mesoblastic nephroma

25. Regarding congenital mesoblastic nephroma, which of the following is TRUE?
A. There is more than one subtype.
B. The tumor is never aggressive.
C. It is easy to differentiate this tumor from other lesions based on imaging.
D. It is a rare tumor in neonates.

26. An ultrasound exam was performed on a 4-year-old patient, and an image is shown below. What is the most likely diagnosis?

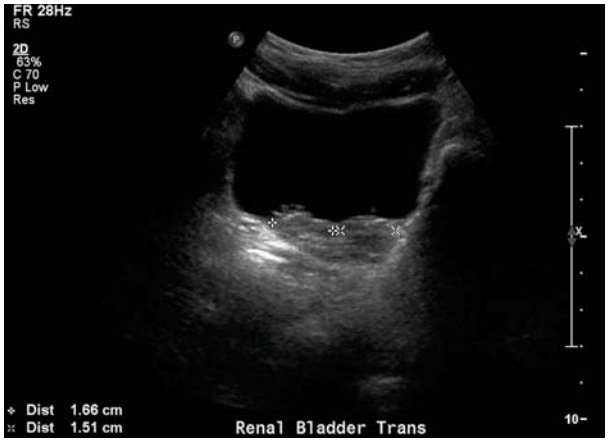

A. Rhabdomyosarcoma of the bladder
B. Distal ureteral calculi
C. Treatment of vesicoureteral reflux
D. Neurogenic bladder

27. An ultrasound examination was performed on a 1-month-old patient. Images are shown below. No kidney on the right side was able to be demonstrated after further imaging. Regarding the entity demonstrated, which of the following is TRUE?

A. Seminal vesicle cysts are associated with this condition in males.
B. The solitary kidney is usually smaller in size for age in a majority of cases.
C. Only a small percentage of women with this condition have uterine anomalies.
D. This condition is more common in females.

28. A CT scan from a patient is shown below. Which is the most likely diagnosis?

A. Tuberous sclerosis
B. Sturge-Weber syndrome
C. Prune belly syndrome
D. Multifocal pyelonephritis

29. Regarding angiomyolipomas (AMLs), which of the following is TRUE?
A. They are pathognomonic of tuberous sclerosis.
B. There is an increased risk of hemorrhage with lesions greater in size than 4 cm.
C. They are malignant lesions.
D. They occur more commonly in males.

30. Concerning crossed fused renal ectopia, which of the following is TRUE?
A. It occurs more commonly in females.
B. The risk of complications such as nephrolithiasis, infection, and hydronephrosis is low and approaches 5%.
C. Although the kidneys are fused to each other on the same side, the ureters insert in their normal location at both the right and left ureterovesical junctions.
D. Right-to-left ectopy is more common than left-to-right ectopy.

31. A pelvic ultrasound exam is performed on a 15-year-old female patient who has yet to have her first menstrual cycle. An image from the exam is shown below. Which of the following is TRUE?

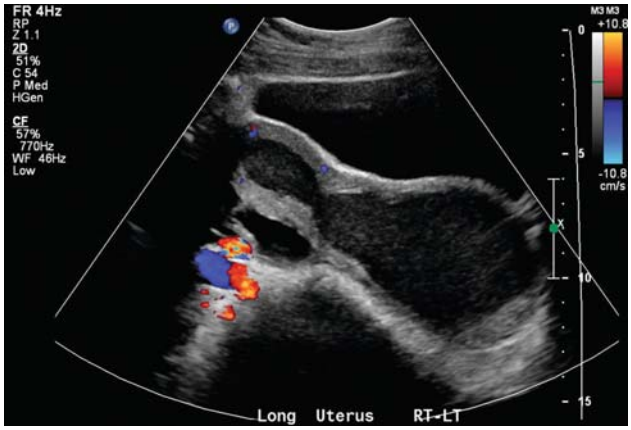

A. The findings may be secondary to an imperforate hymen.
B. There are no known presenting symptoms.
C. There is no known cure for this condition.
D. The uterus usually expands to a greater degree than does the vagina.

32. Regarding multilocular cystic renal tumors, which of the following is TRUE?
A. They usually occur in young girls and older males.
B. Surgery is required for diagnostic and therapeutic purposes.
C. These tumors are usually bilateral.
D. There are three subtypes of this tumor.

33. An image from a VCUG examination performed on a 4-year-old female is shown below. Which of the following is TRUE?

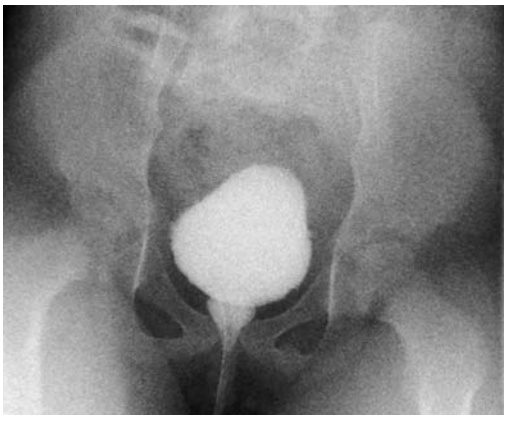

A. There are posterior urethral valves.
B. There is vesicoureteral reflux.
C. This condition is associated with dysfunctional voiding.
D. There is a ureterocele.

34. A 1-year-old female presents with vaginal discharge. An ultrasound exam is performed, and representative images are shown below. Which of the following is the next best step in management?

A. VCUG
B. Renal ultrasound
C. MRI of the pelvis
D. Tc-99m MAG-3 scan

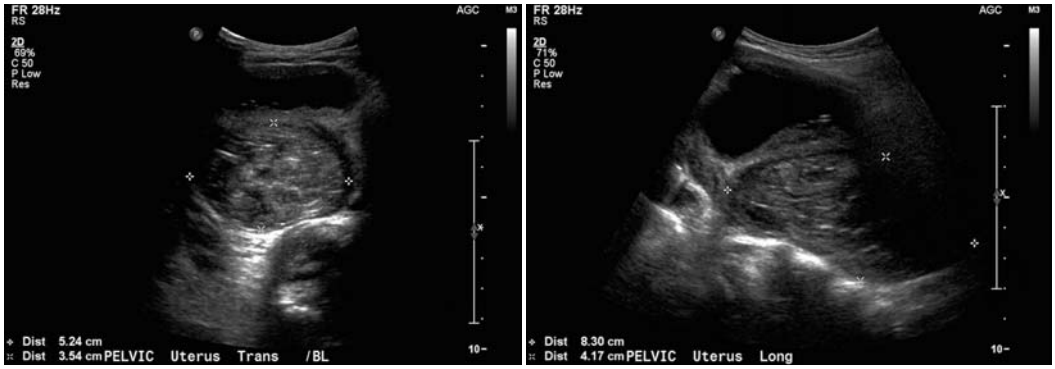

35. An MRI of the pelvis was subsequently performed on the patient described in Question 34, and representative images are shown below. Concerning the most likely diagnosis, which of the following is TRUE?

A. This tumor is a subtype of adenocarcinoma.
B. This tumor has a "grape-like" appearance.
C. The survival rate for nonmetastatic disease is approximately 5% to 10%.
D. Recurrence is uncommon after surgery.

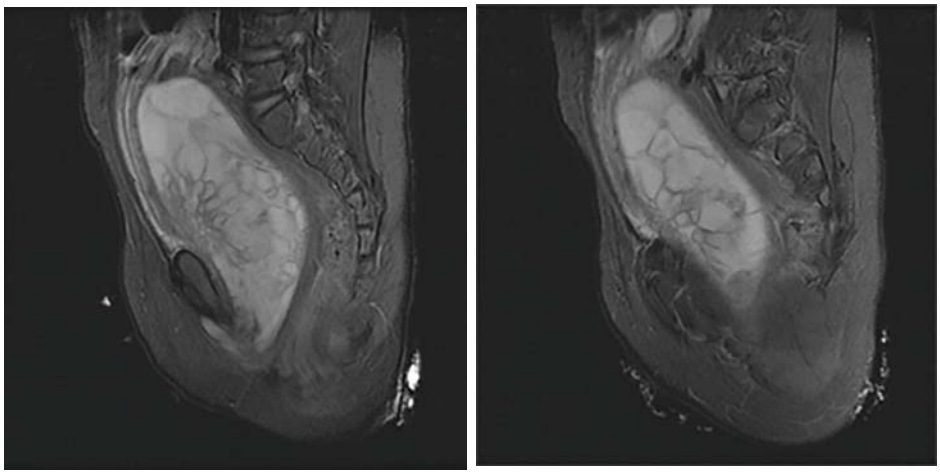

36. Which of the following renal tumors is most likely to demonstrate osseous metastasis?
A. Mesoblastic nephroma
B. Wilms tumor
C. Clear cell sarcoma
D. Atypical rhabdoid tumor

37. Regarding nephroblastomatosis, which of the following is TRUE?
A. There is an association with the development of Wilms tumor.
B. There are only two histologic subtypes.
C. There are no known associations with other diseases.
D. Once detected, there is no need for follow-up imaging.

38. A young child presents with bacteriuria and vague abdominal pain prompting concern for pyelonephritis. Which of the following studies would be the most sensitive test for the detection of acute pyelonephritis?
A. CT scan of the abdomen and pelvis without contrast
B. Renal ultrasound
C. Tc-99m DMSA scan
D. Abdominal plain film

39. Images from a Tc-99m DMSA scan obtained on the patient described in Question 38 are shown below. Given the findings on the images, what is the likely diagnosis?

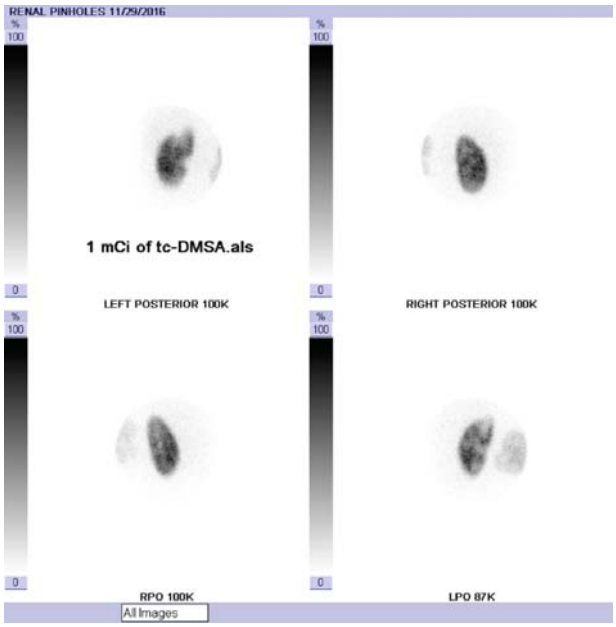

A. Left-sided pyelonephritis in the mid-upper pole
B. Right-sided pyelonephritis in the upper pole
C. Normal study
D. Right-sided pyelonephritis in the lower pole

40. A 16-year-old stable female presents with a 2-hour history of acute sharp right lower quadrant pain. The patient had a negative pregnancy test. A pelvic ultrasound was performed, which was equivocal for the diagnosis of right ovarian torsion. The appendix was normal. What other examination would be the next most appropriate step in imaging?
A. Abdominal plain film
B. Emergent MRI of the pelvis with and without IV contrast
C. Repeat ultrasound in 4 hours.
D. No other imaging studies would be helpful.

41. An MRI of the pelvis was performed on the patient described in Question 40. Representative images are shown below. Which of the following is TRUE?

A. The right ovary is torsed and likely viable.
B. The left ovary is torsed and likely nonviable.
C. The right ovary is torsed and likely nonviable.
D. The left ovary is torsed and likely viable.

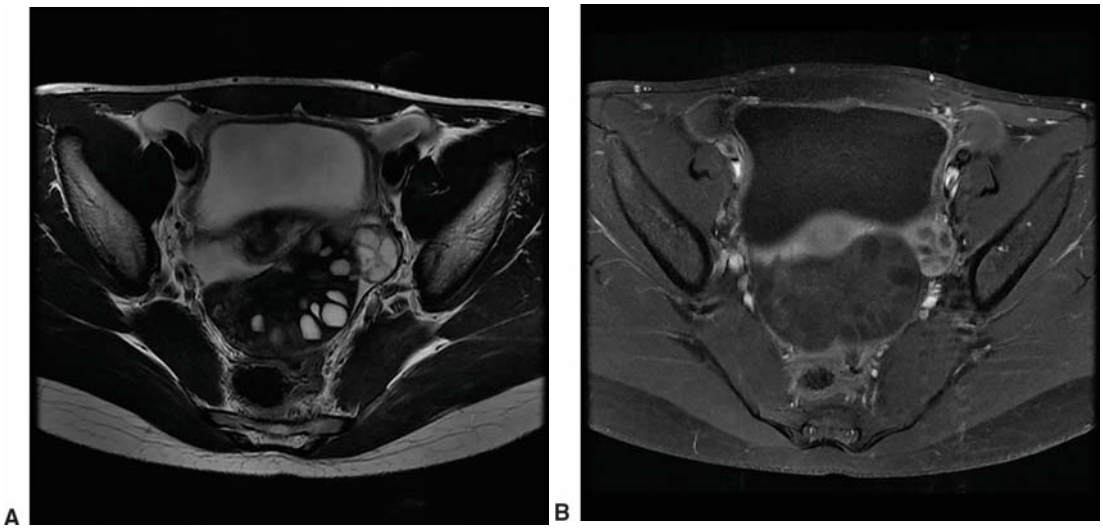

42. In ovarian torsion, what is the proper order of vascular compromise from the first affected vascular supply to the last?
A. Venous, lymphatic, arterial
B. Lymphatic, venous, arterial
C. Arterial, venous, lymphatic
D. Venous, arterial, lymphatic

43. A renal ultrasound examination was performed on a 10-year-old patient, and representative images are shown below. Concerning the study, which of the following is TRUE?

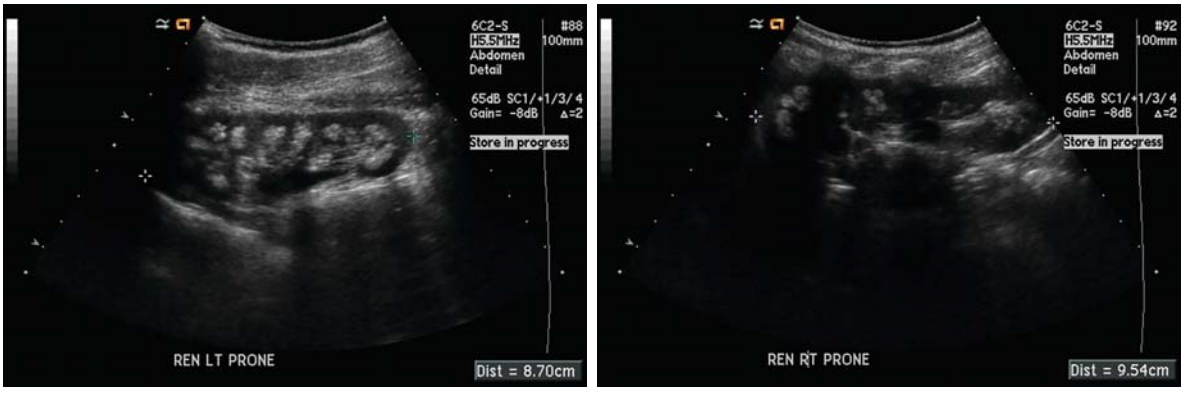

A. This condition is usually associated with proximal renal tubular acidosis.
B. This entity is uncommon among immobilized patients.
C. Most causes of this condition are associated with hypercalciuria.
D. The renal pyramids are normal appearing for the patient's age group.

44. Concerning the differences in size between the kidneys in the exam performed on the patient in Question 43, which of the following is TRUE?
A. The difference in sizes of the kidneys is too large.
B. The difference in sizes of the kidneys is too small.
C. The difference in size of the kidneys is within normal limits.
D. There is compensatory hypertrophy of the left kidney.

45. A teenage male presents with acute right-side testicular pain. A scrotal ultrasound was performed, and a representative image is shown below. What is the next appropriate step in management?

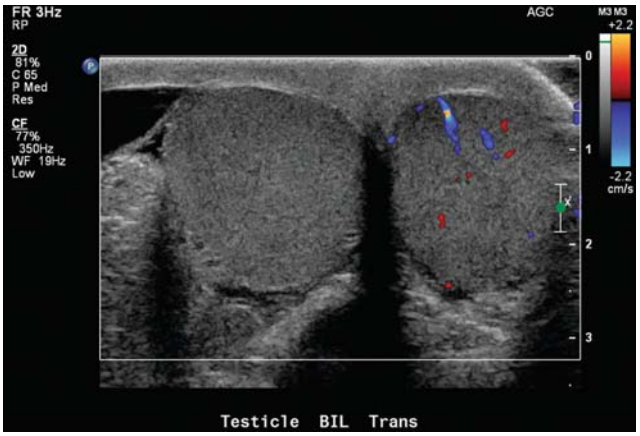

A. Antibiotics
B. Conservative treatment
C. Stat urologic consult
D. No further treatment is indicated.

46. A 1-month-old male with fluid draining from his umbilicus presents for a renal and bladder ultrasound, and a representative image is shown below. Concerning the entity demonstrated, which of the following is TRUE?

A. This entity is more common in women.
B. The majority of patients with this entity are symptomatic.
C. Later on in life, these lesions can give rise to adenocarcinoma.
D. There are only two types of this entity.

Genitourinary: Answers and Explanations

1 Answer B. The images demonstrate dilatation of the left renal pelvis and calyces without ureterectasis. The right kidney is normal. These findings are often seen in a UPJ obstruction. However, vesicoureteral reflux should be excluded as the cause of the left-sided pelvicaliectasis, which is why a VCUG would be the next best step in management. Note that in a male, a VCUG would also help exclude a posterior urethral valve, which can cause bladder outlet obstruction and pelvicaliectasis. Plain radiographs of the abdomen will not be helpful in determining the cause of the pelvicaliectasis, and a CT scan of the abdomen and pelvis will also not be helpful in determining whether vesicoureteral reflux is the cause of the pelvicaliectasis. Both of these exams would needlessly expose the child to ionizing radiation. Although a testicular ultrasound does not utilize ionizing information, it would not give us any information about the cause for the pelvicaliectasis.

References: Blickman JG, Parker BR, Barnes PD. *Pediatric radiology: the requisites*, 3rd ed. Philadelphia, PA: Elsevier/Saunders, 2009.
Donnelly LF. *Pediatric imaging the fundamentals*. Philadelphia, PA: Elsevier/Saunders, 2009.

2 Answer A. The image from the VCUG examination fails to demonstrate vesicoureteral reflux, which can now be excluded as a cause for the left-sided pelvicaliectasis. So, there is now a suspected left-sided UPJ obstruction and a functional and dynamic imaging study should be ordered to determine whether surgical intervention will be necessary. A Tc-99m MAG-3 study should provide that information as it is a dynamic test that evaluates uptake and clearance of radiotracer by the kidneys as well as drainage of radiotracer into the ureters and bladder. None of the other tests will yield this information as they are not functional exams. A Tc-99m DMSA scan is a functional but not a dynamic study used to evaluate for cortical scarring and/or pyelonephritis. This exam might be helpful if the patient had vesicoureteral reflux, especially if it was accompanied by a UTI, but the VCUG was negative for reflux. A CT scan is not a dynamic exam. A right upper quadrant ultrasound also would not be helpful but could evaluate the gray-scale appearance of the right kidney. However, the right kidney was normal on the initial ultrasound exam.

References: Blickman JG, Parker BR, Barnes PD. *Pediatric radiology: the requisites*, 3rd ed. Philadelphia, PA: Elsevier/Saunders, 2009.
Donnelly LF. *Pediatric imaging the fundamentals*. Philadelphia, PA: Elsevier/Saunders, 2009.
Fernbach SK, Feinstein KA, Schmidt MB. Pediatric voiding cystourethrography: a pictorial guide. *Radiographics* 2000;20(1):155–168; discussion 168–171.

3 Answer C. The image demonstrated is a renogram of the left kidney obtained after Lasix administration. The time of maximum activity (Tmax) is approximately 2.5 minutes, and the time of ½ maximum activity (T1/2max) is around 10.5 minutes. Therefore, the time from max to half max is about 8 minutes. In addition, there is significant downsloping of the curve consistent with a good response to Lasix.

Dilated collecting systems secondary to fixed or functional obstruction may produce continuously rising renogram curves before Lasix administration with little to no evidence of excretion or downsloping. After Lasix administration, the curve should be inspected for change. In dilated, nonobstructed systems, Lasix causes increased urine flow through the collecting system, which washes out the initial increase in activity and causes a decline of the excretion similar to this case. In the case of significant mechanical obstruction, there is very little decrease in the renal collecting system activity after administration of Lasix because of the narrowed and fixed lumen of the ureter. The rising renogram curve is changed little or is unaffected. These patients are often treated with a surgical pyeloplasty.

Reference: Mettler FA, Guiberteau MJ. *Essentials of nuclear medicine*, 6th ed. Philadelphia PA: Saunders Elsevier, 2012.

4 Answer B. The images demonstrate multiple noncommunicating cysts throughout the right kidney without a dilated renal pelvis. These findings are consistent with a multicystic dysplastic kidney. These lesions are associated with a contralateral UPJ obstruction in 7% to 27% of cases. There is some controversy whether or not these lesions have a risk of malignant transformation and because of this are usually followed by serial ultrasound exams. These lesions usually slowly decrease in size over time, and often, the remaining residual dysplastic kidney will no longer be visualized by imaging techniques. There is typically no radiotracer uptake by the affected kidney on a MAG-3 scan as there is no function. Because of this, the contralateral kidney will often be enlarged in size because of compensatory hypertrophy.

References: Dähnert W. *Radiology review manual*, 6th ed. Philadelphia, PA: Wolters Kluwer Health/Lippincott Williams & Wilkins, 2007. Donnelly LF. *Pediatric imaging the fundamentals*. Philadelphia, PA: Elsevier/Saunders, 2009.

5 Answer C. The images are coronal images from a contrast-enhanced CT scan of the abdomen and pelvis, which demonstrate multiple round foci of low attenuation compatible with renal cysts. The cysts appear to be a few centimeters in size. These findings are most compatible with autosomal dominant polycystic kidney disease (ADPKD). This can be distinguished by the age of the patient as well as the size of the cysts. Although autosomal recessive polycystic kidney disease (ARPKD) can give renal macrocysts, most cysts are usually small and in the range of 1 to 2 mm. There is an association of ARPKD with congenital hepatic fibrosis. In addition, ARPKD usually affects children in the first decade of life, whereas ADPKD usually affects patients during the teenage to adult years. ADPKD is associated with berry aneurysms in approximately 10% of cases.

References: Dähnert W. *Radiology review manual*, 6th ed. Philadelphia, PA: Wolters Kluwer Health/Lippincott Williams & Wilkins, 2007. Donnelly LF. *Pediatric imaging the fundamentals*. Philadelphia, PA: Elsevier/Saunders, 2009.

6 Answer C. The abdominal plain film demonstrates a soft tissue density in the left hemiabdomen, which is concerning for a mass lesion (arrows). The next best test would be a cross-sectional imaging study to try and identify the mass and its origin. An abdominal ultrasound would be the best way to accomplish this in an inexpensive way without the use of ionizing radiation. A Tc-99m MAG-3 scan may show some renal abnormality, but it would not be the best way to visualize the suspected tumor. An I-123 MIBG scan would be helpful to see if the tumor is MIBG avid as in cases of tumors of neural crest origin such as neuroblastomas, which often originate in the adrenal region. However, at this point, we do not know the origin of the tumor. A VCUG would not be helpful to visualize the tumor as this test is usually performed to look for vesicoureteral reflux.

References: Dähnert W. *Radiology review manual*, 6th ed. Philadelphia, PA: Wolters Kluwer Health/Lippincott Williams & Wilkins, 2007. Donnelly LF. *Pediatric imaging the fundamentals*. Philadelphia, PA: Elsevier/Saunders, 2009.

7 Answer D. The ultrasound images demonstrate a heterogeneous mass in the region of the left kidney labeled as "LK" on the ultrasound images. It is still difficult to determine the origin of the tumor. Therefore, an alternative cross-sectional imaging modality is needed to define the origin and extent of the mass lesion. An MRI of the abdomen and pelvis with and without intravenous contrast would be a good way to further image the tumor without the use of ionizing radiation although the child would likely need to be sedated for the exam. For similar reasons explained in the explanation to Question 6, neither an I-123 MIBG scan, Tc-99m MAG-3 scan, nor a VCUG scan would be helpful. A CT scan of the abdomen would also be appropriate to further image the tumor but would require the use of ionizing radiation.

References: Donnelly LF. *Pediatric imaging the fundamentals*. Philadelphia, PA: Elsevier/Saunders, 2009.
Son J, Lee EY, Restrepo R, et al. Focal renal lesions in pediatric patients. *Am J Roentgenol* 2012;199(6):W668–W682.

8 Answer C. Figure A is an axial T2-weighted image with fat saturation from an MR exam, which demonstrates a heterogeneous mass arising from the left kidney. A "claw sign" of renal tissue is seen medially (arrows). Figure B is a coronal image from a T1-weighted image with fat saturation and after contrast administration, which again demonstrates a heterogeneous lesion arising from the left kidney with a medial "claw sign" of renal parenchyma (arrows). Given the patient's age group, a Wilms tumor would be the most likely tumor. Renal cell carcinoma occurs in older children and the adult population, and mesoblastic nephroma, a generally benign tumor, usually occurs in neonates. Neuroblastomas often arise from the adrenals.

References: Donnelly LF. *Pediatric imaging the fundamentals*. Philadelphia, PA: Elsevier/Saunders, 2009.
Son J, Lee EY, Restrepo R, et al. Focal renal lesions in pediatric patients. *Am J Roentgenol* 2012;199(6):W668–W682.

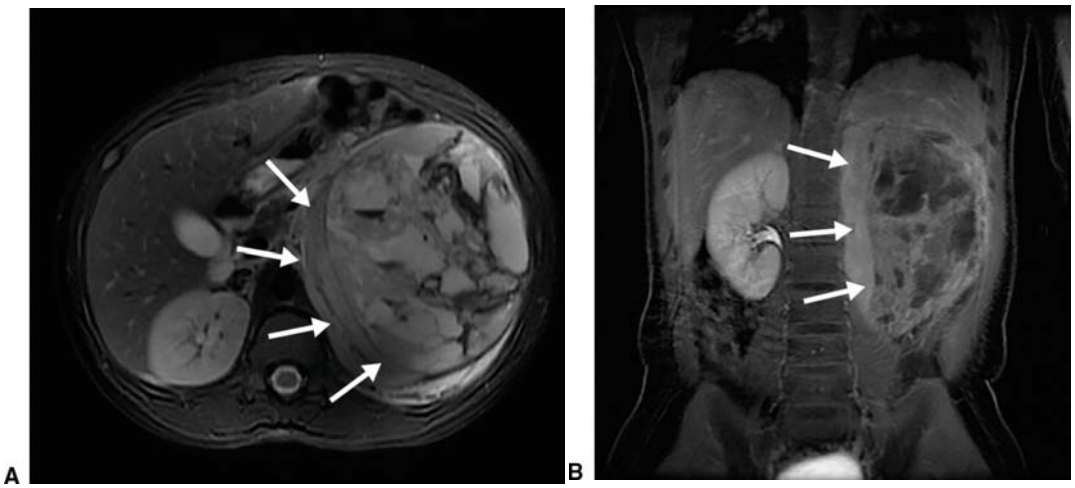

9 Answer A. When evaluating a suspected Wilms tumor, it is important to document the following features: lymph node involvement, liver and lung metastasis, involvement of the contralateral tumor by a synchronous tumor, the anatomic distribution of the intrarenal tumor, involvement of the renal vein or inferior vena cava, and the path of the ureters in relation to the mass. Therefore, a CT scan of the chest would be indicated. A VCUG would not be helpful to evaluate any of the above features. An I-123 MIBG scan would be helpful to evaluate the extent of a neuroblastoma but is not indicated for a Wilms tumor. Because osseous metastatic disease is rare in Wilms tumor, bone scans are not required as part of the workup.

Reference: Carroll WL, Finlay JL. *Cancer in children and adolescents*. Boston, MA: Jones and Bartlett Publishers, 2010.

10 **Answer B.** The current overall survival for Wilms tumor is slightly >90%, but this does vary with extent of disease and histology. There are both favorable and unfavorable histologic subtypes. Invasion of the renal vein and inferior vena cava occurs commonly in Wilms tumor. Nephroblastomatosis is a rare entity that is related to the persistence of nephrogenic rests within the renal parenchyma. These nephrogenic rests are the precursors of Wilms tumors.

References: Dähnert W. *Radiology review manual*, 6th ed. Philadelphia, PA: Wolters Kluwer Health/Lippincott Williams & Wilkins, 2007. Donnelly LF. *Pediatric imaging the fundamentals*. Philadelphia, PA: Elsevier/Saunders, 2009.

11 **Answer D.** Renal medullary carcinoma is a rare aggressive renal malignancy that is strongly associated with sickle cell (SC) trait or hemoglobin SC disease. With a peak age of presentation at 20 years, this neoplasm arises predominantly from the renal medulla. None of the other tumors listed are associated with sickle cell trait.

Reference: Son J, Lee EY, Restrepo R, et al. Focal renal lesions in pediatric patients. *Am J Roentgenol* 2012;199(6):W668–W682.

12 **Answer D.** The ultrasound images demonstrate a hypoechoic oval avascular mass located between the right testicle and epididymis (arrows). This is consistent with a torsed appendix testis. Note that torsed testicular appendages can be of varying echogenicity. Testicular appendageal torsion is a common cause of an acute scrotum in prepubertal boys. The appendages are normal remnants of embryonic tissue and are usually located adjacent to the superior testicle or epididymal head. Testicular appendages are more prevalent than epididymal appendages; however, the distinction is often difficult to make and is not important clinically. Additional findings may include scrotal edema and reactive hydroceles. Color Doppler may show hyperemia surrounding the torsed appendage. Treatment involves conservative management.

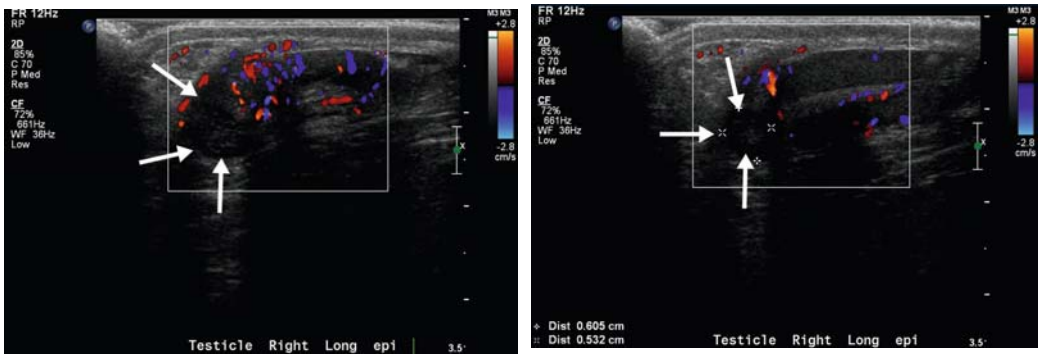

Reference: Sung EK, Setty BN, Castro-Aragon I. Sonography of the pediatric scrotum: emphasis on the Ts–torsion, trauma, and tumors. *Am J Roentgenol* 2012;198(5):996–1003.

13 **Answer A.** The ultrasound images demonstrate a lesion within the left ovary that contains hyperechoic foci, some of which appear to shadow. Thus, this lesion may contain fat and/or calcium. The lesion itself appears avascular, but there does appear to be flow in the surrounding left ovarian parenchyma. A cross-sectional imaging modality is necessary to better define and characterize the lesion. An MRI would be preferred over CT because of the lack of ionizing radiation and its ability to characterize sonographically indeterminate adnexal masses of uncertain origin and solid or complex cystic content. Although this lesion may contain calcium, it appears to arise from the left ovary and therefore is extremely unlikely to be a neuroblastoma, so an MIBG scan would not be indicated.

Reference: Adusumilli S, Hussain HK, Caoili EM, et al. MRI of sonographically indeterminate adnexal masses. *Am J Roentgenol* 2006;187(3):732–740.

14 **Answer C.** The CT scan demonstrates a lesion arising from the left ovary, which contains fat and calcium as well as solid components. These findings are consistent with an ovarian teratoma. These lesions lead to torsion of the involved ovary in approximately 16% of cases. Approximately 1% to 4% of ovarian teratomas rupture, and approximately 1% to 2% undergo malignant transformation. It is common to see a soft tissue protuberance in a mature cystic teratoma; this is known as a Rokitansky nodule or dermoid plug. Although this protuberance may be partly solid and consist of diverse tissues, benign teratomas never show transmural growth of the protuberance. Contrast enhancement of a Rokitansky nodule raises the possibility of malignant transformation, although this finding does not always necessarily indicate malignancy.

Reference: Park SB, Kim JK, Kim KR, et al. Imaging findings of complications and unusual manifestations of ovarian teratomas. *Radiographics* 2008;28(4):969–983.

15 **Answer B.** The images demonstrate bilateral pelvicaliectasis. In addition, the bladder wall appears irregularly thickened and trabeculated even for a partially contracted bladder. In a male, these findings raise the possibility of bladder outlet obstruction from a posterior urethral valve. A VCUG exam will evaluate the urethra as well as test for vesicoureteral reflux. None of the other tests will be able to determine if there is a posterior urethral valve. Although the patient will require surgery if there is a posterior urethral valve, it is necessary to determine if the patient has a posterior urethral valve prior to surgical intervention.

Reference: Donnelly LF. *Pediatric imaging the fundamentals*. Philadelphia, PA: Elsevier/Saunders, 2009.

16 **Answer B.** The images demonstrate marked dilatation of the posterior urethra (long arrows) with a normal appearance of the anterior urethra (short arrows). These findings are consistent with a posterior urethral valve, which is found exclusively in males. These lesions are treated surgically. In patients with posterior urethral valves (PUV), severe unilateral vesicoureteral reflux (VUR) is one of the three conditions associated with preservation of renal function. Others are urinary ascites or urinoma in newborns and large congenital bladder diverticula. These conditions most likely provide a pop-off mechanism preventing the development of high intravesical pressure. Only 5% of patients with PUV and an associated pop-off mechanism will develop renal failure as opposed to 40% of patients with PUV without a protective factor.

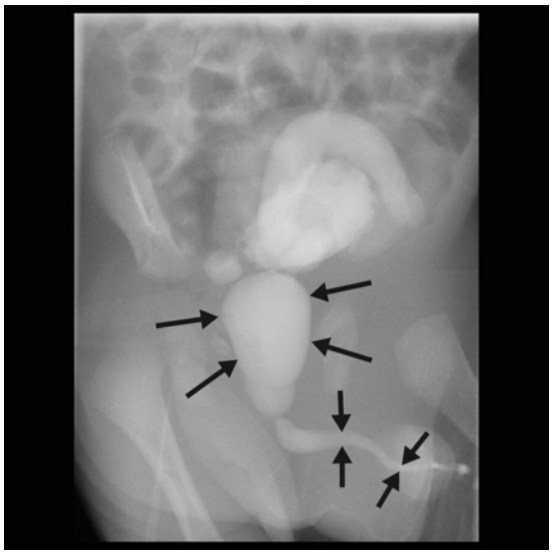

References: Donnelly LF. *Pediatric imaging the fundamentals*. Philadelphia, PA: Elsevier/Saunders, 2009.
Goodwin OI, Ayotunde OO. Posterior urethral valves with severe unilateral vesicoureteral reflux in a 3-year-old boy. *Ann Ib Postgrad Med* 2007;5(2):73–76.

17 **Answer D.** The ultrasound image demonstrates multiple bright echogenic nonshadowing foci throughout the testes. These findings are consistent with testicular microlithiasis. There is often no posterior acoustic shadowing because of the small size of the calcifications. It was initially reported that the risk of development of testicular neoplasms of those with this condition is between 18% and 75%. This led to recommendations for serial screening ultrasounds in patients with testicular microlithiasis to exclude development of neoplasm. However, more recent reports have shown that testicular microlithiasis is much more common than suspected, occurring in about 6% of males between 17 and 35 years of age and that the overwhelming majority of these patients will not develop malignancies. Some now advocate following these patients with physical examination rather than ultrasound. One recent paper stated that recommended follow-up depends on the ability of the child to cooperate and may include periodic US, periodic physical examination by the physician, and/or education of the patients to perform self-examination of the scrotum.
Because this condition is not a urologic emergency, a stat urology consult would not be indicated. This condition is not associated with active infection, and therefore an MRI of the pelvis to look for a site of infection is not indicated. As stated earlier, this condition is more common than anticipated in the young male population and a metastatic workup is not indicated in the absence of other findings of neoplasm.
References: Cooper ML, Kaefer M, Fan R, et al. Testicular microlithiasis in children and associated testicular cancer. *Radiology* 2014;270(3):857–863.
Donnelly LF. *Pediatric imaging the fundamentals*. Philadelphia, PA: Elsevier/Saunders, 2009.

18 **Answer B.** The image is taken from a voiding cystourethrogram, which demonstrates bilateral vesicoureteral reflux. A "drooping lily" sign is seen on the right (arrows). This sign is identified in patients with a duplex collecting system. The drooping lily sign is due to inferior and lateral displacement of the lower pole moiety of a duplex kidney, rather than displacement of an entire kidney. An obstructed, poorly functioning upper pole moiety exerts a mass effect on the lower pole collecting system, which is responsible for the abnormal axis of the lower pole calices and which causes the droop of the lily. Because only the lower pole collecting system is opacified with contrast material, a decreased number of calices are depicted, as no calices extend cephalad from the renal pelvis. No drooping lily sign is seen in the left kidney, which has a single collecting system.

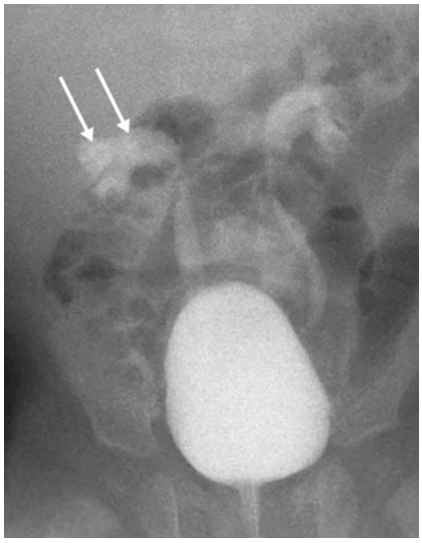

Reference: Callahan MJ. The drooping lily sign. *Radiology* 2001;219(1):226–228.

19 **Answer D.** In patients with complete ureteropelvic duplication, the ureteral orifice of the upper pole moiety inserts more medially and inferiorly than does the orifice of the lower pole ureter. The lower pole system is more prone to vesicoureteral reflux and UPJ obstruction. The upper pole moiety is more prone to obstruction secondary to a ureterocele. This is known as the Weigert-Meyer rule.
Reference: Donnelly LF. *Pediatric imaging the fundamentals*. Philadelphia, PA: Elsevier/Saunders, 2009.

20 Answer A. The images demonstrate a large paravertebral mass, which is seen in the right lower portions of the thorax and upper retroperitoneum. There are internal calcifications seen on the CT scan (arrows in Figure A). On the MR image, there is extension of the tumor into the right spinal canal (arrow in Figure B). In a child of this age group, the most likely etiology of the lesion is a neurogenic tumor such as neuroblastoma (NB) or a ganglioneuroblastoma (GNB). In an older child, a ganglioneuroma (GN) could also be considered. I-123 MIBG is taken up by catecholamine-producing tumors such as NB, GNB, and GN. Although 90% to 95% of NB and GNB secrete catecholamines, only about 70% of NB and GNB are MIBG positive; one of the drawbacks of I-123 MIBG imaging is that a considerable minority of tumors (30%) are not MIBG avid.
Tc-99m MAG-3 scans are used to determine renal function and evaluate for possible obstruction. Tc-99m DMSA scans are used to evaluate for pyelonephritis or renal cortical scarring. There is no evidence of the tumor involving the kidneys. Gallium 67 scans are used to evaluate for sources of chronic infection. In addition, this radiotracer is also taken up by certain neoplasms such as non-Hodgkin lymphoma, Hodgkin disease, hepatoma, and melanoma. Gallium 67 scans are not useful to evaluate neuroblastoma.

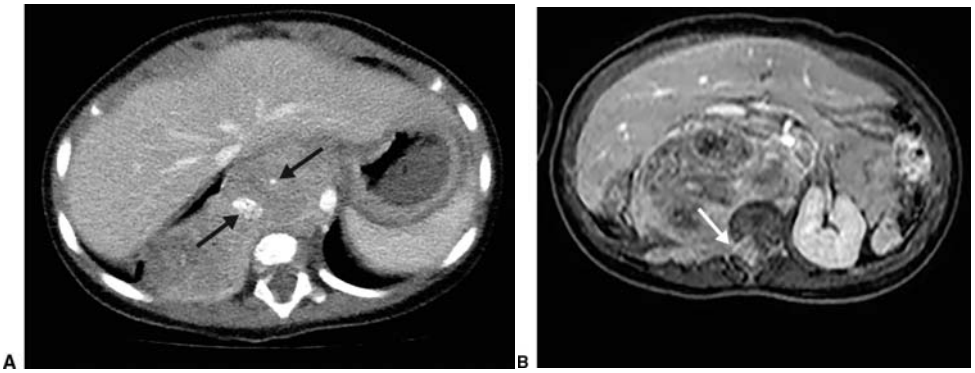

References: Dähnert W. *Radiology review manual*, 6th ed. Philadelphia, PA: Wolters Kluwer Health/Lippincott Williams & Wilkins, 2007.
Lonergan GJ, Schwab CM, Suarez ES, et al. Neuroblastoma, ganglioneuroblastoma, and ganglioneuroma: radiologic-pathologic correlation. *Radiographics* 2002;22(4):911–934.

21 Answer B. The tumor seen on the CT and MR images is MIBG avid and therefore likely represents a neuroblastoma. Children who are diagnosed with these tumors at <1 year of age usually have a good prognosis. In these patients, the disease tends to spread to the liver and skin. Children who are diagnosed with neuroblastoma older than 1 year of age usually have a poor prognosis. In these patients, the disease tends to spread to the bone. Note that there is a special stage in the staging of neuroblastoma known as IV-S, which is given to patients who are diagnosed at less than a year of age with metastatic disease that is confined to the skin, liver, and bone marrow. Cortical bone involvement is not considered to be part of IV-S.
Expression of the N-Myc protein has been found to correlate with poor prognosis and aggressive tumor behavior in children older than 1 year. Other tumor features that influence prognosis include CD44, a glycoprotein on the surface of NB cells. Increased levels of CD44 correlate with a better prognosis. Elevated serum levels of ferritin indicate a worse prognosis.
References: Donnelly LF. *Pediatric imaging the fundamentals*. Philadelphia, PA: Elsevier/Saunders, 2009.
Lonergan GJ, Schwab CM, Suarez ES, et al. Neuroblastoma, ganglioneuroblastoma, and ganglioneuroma: radiologic-pathologic correlation. *Radiographics* 2002;22(4):911–934.

22 Answer A. Imipramine is a tricyclic antidepressant that may inhibit localization of radioiodinated MIBG. Therefore, this drug should be discontinued before imaging when practical. Other drugs that may similarly inhibit localization of radioiodinated MIBG and that should be withheld if possible prior to imaging include insulin, reserpine, other tricyclic antidepressants, and amphetamine-like drugs. None of the other drugs listed need to be withheld prior to imaging.

Reference: Mettler FA, Guiberteau MJ. *Essentials of nuclear medicine*, 6th ed. Philadelphia, PA: Elsevier/Saunders, 2012.

23 Answer B. There is a special stage in the staging of neuroblastoma known as IV-S, which is given to patients who are diagnosed at less than a year of age with metastatic disease that is confined to the skin, liver, and bone marrow. Cortical bone involvement is not considered to be part of IV-S. Children diagnosed with IV-S tumors have a good prognosis and a 3-year event-free survival rate of 75% to 90%.

References: Donnelly LF. *Pediatric imaging the fundamentals*. Philadelphia, PA: Elsevier/Saunders, 2009.
Lonergan GJ, Schwab CM, Suarez ES, et al. Neuroblastoma, ganglioneuroblastoma, and ganglioneuroma: radiologic-pathologic correlation. *Radiographic* 2002;22(4):911–934.

24 Answer D. The CT image demonstrates a heterogeneous solid mass arising from the left kidney as evidenced by a rim of renal tissue medially (arrows) consistent with a "claw sign." In a 2-month-old patient, this lesion most likely represents a congenital mesoblastic nephroma (CMN). Congenital mesoblastic nephroma is the most common solid renal tumor in the neonate. It is usually identified within the first 3 months of life, with 90% of cases discovered within the first year of life. Imaging studies demonstrate a large solid intrarenal mass that typically involves the renal sinus. The mass replaces a large portion of renal parenchyma and may contain cystic, hemorrhagic, and necrotic regions. CMN was first described in 1967 as a benign leiomyoma-like tumor. Current research now suggests that a spectrum of disease exists, ranging from the classic benign CMN to a more aggressive cellular CMN variant, which accounts for 42% to 63% of cases.

The peak age of Wilms tumor is at 3 to 4 years of age. It is rare in neonates, with <0.16% of cases manifesting in this age group. Renal cell carcinoma has been reported in patients <6 months of age. However, the tumor is rare in children, accounting for <7% of all primary renal tumors presenting in the first two decades of life. Less than 2% of all cases of renal cell carcinoma occur in pediatric patients, with a peak incidence in the sixth decade of life. Renal medullary carcinoma is a highly aggressive malignant tumor that occurs almost exclusively in adolescent and young adult blacks with sickle cell trait or hemoglobin SC disease. The age range is 10 to 39 years with a mean age of 20 years.

References: Lowe LH, Isuani BH, Heller RM, et al. Pediatric renal masses: Wilms tumor and beyond. *Radiographics* 2000;20(6):1585–1603.
Sheth MM, Cai G, Goodman TR. AIRP best cases in radiologic-pathologic correlation: congenital mesoblastic nephroma. *Radiographics* 2012;32(1):99–103.

25 **Answer A.** Congenital mesoblastic nephroma (CMN) is the most common renal tumor in neonates and in infants under 1 year of age. CMN was first described in 1967 as a benign leiomyoma-like tumor. Current research now suggests that a spectrum of disease exists, ranging from the classic benign CMN to a more aggressive cellular CMN variant, which accounts for 42% to 63% of cases. The imaging appearances of CMN vary depending on tumor composition, because classic variants are predominantly solid, whereas cellular variants are largely cystic. Unfortunately, many diverse disease processes may present as a solid, cystic, or mixed renal mass within the first year of life. The differential diagnosis is broad and includes renal and nonrenal tumors such as Wilms tumor, clear cell sarcoma, rhabdoid tumors, neuroblastoma, and multilocular cystic renal tumor. Although patient history, presentation, and associated findings can suggest a particular diagnosis, in many cases, a definitive diagnosis can be made only on the basis of histopathologic findings.
Reference: Sheth MM, Cai G, Goodman TR. AIRP best cases in radiologic-pathologic correlation: congenital mesoblastic nephroma. *Radiographics* 2012;32(1):99–103.

26 **Answer C.** Minimally invasive endoscopic treatment or periureteral injection is considered for the treatment of vesicoureteral reflux (VUR) when the degree of VUR is severe, if there is evidence of renal scarring, if the reflux has not resolved over a reasonable time, or if breakthrough infections occur frequently. After periureteral injection, ultrasound will show iso- or hyperechoic mounds in the bladder wall in the region of the ureteral orifices without posterior acoustic shadowing. A dextranomer–hyaluronic acid copolymer (Deflux) has been used as an injectable material in pediatric urology for 15 years. Dextranomer–hyaluronic acid copolymer is currently the most commonly used agent and will consequently be most frequently encountered on imaging studies. Deflux mounds should not be mistaken for distal ureteral calculi. They should not be mistaken for rhabdomyosarcomas or other bladder masses based on their characteristic location and imaging features. They should also not be mistaken for bladder wall trabeculations which are often seen in neurogenic bladders.
References: Cerwinka WH, Kaye JD, Scherz HC, et al. Radiologic features of implants after endoscopic treatment of vesicoureteral reflux in children. *Am J Roentgenol* 2010;195(1):234–240.
Donnelly LF. *Pediatric imaging the fundamentals*. Philadelphia, PA: Elsevier/Saunders, 2009.

27 **Answer A.** The ultrasound images fail to demonstrate a kidney on the right. The findings are consistent with right-sided renal agenesis. This condition is more common in males than females. Associated genitourinary anomalies in males include hypoplasia or agenesis of the testes and vas deferens as well as seminal vesicle cysts. Ninety percent of females with renal agenesis have uterine anomalies. There is compensatory hypertrophy of the contralateral kidney in 50% of cases.
Reference: Dähnert W. *Radiology review manual*, 6th ed. Philadelphia, PA: Wolters Kluwer Health/Lippincott Williams & Wilkins, 2007.

28 **Answer A.** The image demonstrates multiple small foci of low attenuation fat-containing lesions in both kidneys that likely represent angiomyolipomas. Angiomyolipomas are an uncommon tumor that consists of a disordered arrangement of vascular, smooth muscle, and fatty elements. Its histologic composition suggests a hamartoma, but it is currently believed to represent a benign neoplasm. These tumors most often occur sporadically. However, they may occur in 40% to 80% of patients with tuberous sclerosis. Angiomyolipomas are also associated with neurofibromatosis and von Hippel-Lindau syndrome. In children, angiomyolipomas are rare in the absence of tuberous sclerosis. Eighty percent of children with tuberous sclerosis may be expected to develop lesions by the age of 10 years. Multifocal pyelonephritis typically demonstrates multiple peripheral and triangular regions of decreased contrast enhancement as well as a striated nephrogram on contrast-enhanced CT scans. Angiomyolipomas are not found in patients with Prune belly or Sturge-Weber syndrome.

References: Donnelly LF. *Pediatric imaging the fundamentals*. Philadelphia, PA: Elsevier/Saunders, 2009.
Lowe LH, Isuani BH, Heller RM, et al. Pediatric renal masses: Wilms tumor and beyond. *Radiographics* 2000;20(6):1585–1603.

29 Answer B. Angiomyolipomas most often occur sporadically. However, they may occur in 40% to 80% of patients with tuberous sclerosis. Angiomyolipomas are also associated with neurofibromatosis and von Hippel-Lindau syndrome. In children, angiomyolipomas are rare in the absence of tuberous sclerosis. Angiomyolipomas larger than 4 cm in diameter are more likely to spontaneously hemorrhage, leading to flank or abdominal pain, hematuria, or even severe life-threatening hemorrhage. There is a 4:1 female predominance of angiomyolipomas. Angiomyolipomas are believed to represent a benign neoplasm.
Reference: Lowe LH, Isuani BH, Heller RM, et al. Pediatric renal masses: Wilms tumor and beyond. *Radiographics* 2000;20(6):1585–1603.

30 Answer C. In cross-fused renal ectopia, both kidneys lie on the same side of the abdomen and are fused. The ureter from the ectopic kidney crosses the midline and enters the bladder in the expected location of the contralateral ureterovesical junction. There is a 3:2 male predominance. Approximately half of the patients manifest with complications such as hydronephrosis, infections, and nephrolithiasis. Left-to-right crossover occurs more frequently, and the upper pole of the crossed ectopic kidney is fused to the lower pole of the normally located kidney in most instances.
References: Donnelly LF. *Pediatric imaging the fundamentals*. Philadelphia, PA: Elsevier/Saunders, 2009.
Solanki S, Bhatnagar V, Gupta AK, et al. Crossed fused renal ectopia: challenges in diagnosis and management. *J Indian Assoc Pediatr Surg* 2013;18(1):7–10.

31 Answer A. The long-axis ultrasound image demonstrates distention of the vagina and uterine cavity with fluid containing echoes that are likely secondary to blood products. Note that the vagina (long arrow) is distended to a greater degree than the uterine cavity (short arrow). In a 15-year-old patient who has not begun her menstrual cycle, these findings are most likely secondary to hematometrocolpos. This entity is often caused by an imperforate hymen that obstructs flow from the vagina. This entity is cured by relieving the obstruction. Patients with this condition often present with cyclic abdominal pain as well as a midline abdominal mass. Because the vagina is more elastic, it becomes markedly dilated and composes the bulk of the mass.

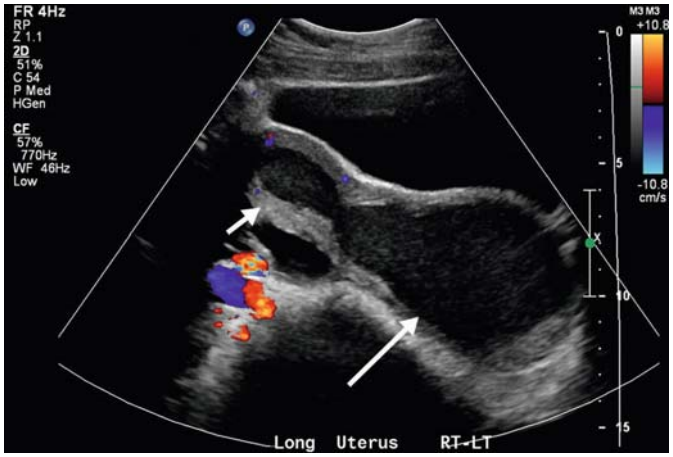

References: Donnelly LF. *Pediatric imaging the fundamentals*. Philadelphia, PA: Elsevier/Saunders, 2009.
Garel L, Dubois J, Grignon A, et al. US of the pediatric female pelvis: a clinical perspective. *Radiographics* 2001;21(6):1393–1407.

32 Answer B. Multilocular cystic renal cell tumor is a term that encompasses two types of tumors that are on opposite sides of a spectrum. On one end of the spectrum is cystic nephroma (CN), which is a rare, nonhereditary benign renal neoplasm that is purely cystic and is lined by epithelium and fibrous septa that contain mature tubules. At the other end of the spectrum is cystic partially differentiated nephroblastoma (CPDN), which can show aggressive behavior and in which the septa contain foci of blastemal cells. Cystic nephroma and CPDN are indistinguishable from one another based on their gross and radiographic appearances and are therefore lumped under the term multilocular cystic renal tumor (MCRT). MCRT has a bimodal age and sex distribution and tends to occur in children (mostly boys with CPDN) between 3 months and 4 years of age and in adults (mostly women with cystic nephroma) between 40 and 60 years of age.
MCRT is usually solitary, but bilateral tumors have been described. At CT, cystic nephroma typically appears as a well-circumscribed, encapsulated multicystic mass with variably enhancing septa and no excretion of contrast agent into the loculi. Extension into the renal pelvis and ureter may also be easily seen at CT. On MR, the lesion is a multicystic mass with a capsule and septa that are hypointense regardless of pulse sequence presumably because of the fibrous tissue present in these structures. Contents of the cyst are hyperintense on T2-weighted images, but their signal intensity varies on T1-weighted images, possibly because of the different concentrations of old hemorrhage or protein. The septa have also been shown to enhance on MR images following administration of gadolinium. Because neither the clinical nor the imaging features of MCRT can predict its histologic characteristics, surgery is required for both diagnosis and treatment.
Reference: Silver IM, Boag AH, Soboleski DA. Best cases from the AFIP: multilocular cystic renal tumor: cystic nephroma. *Radiographics* 2008;28(4):1221–1225.

33 Answer C. The image provided from a VCUG examination performed on a young female demonstrates dilatation of the posterior urethra (arrow) in the shape of a "spinning top." This configuration of the urethra is known as a "spinning top urethra." The most common mechanism for this entity is unstable bladder contractions that are resisted by a voluntary increase in distal sphincter tension so as to prevent leakage of urine. This entity is associated with dysfunctional voiding. Posterior urethral valves are only found in males and not in females. There is no evidence of vesicoureteral reflux or a ureterocele on the image provided.

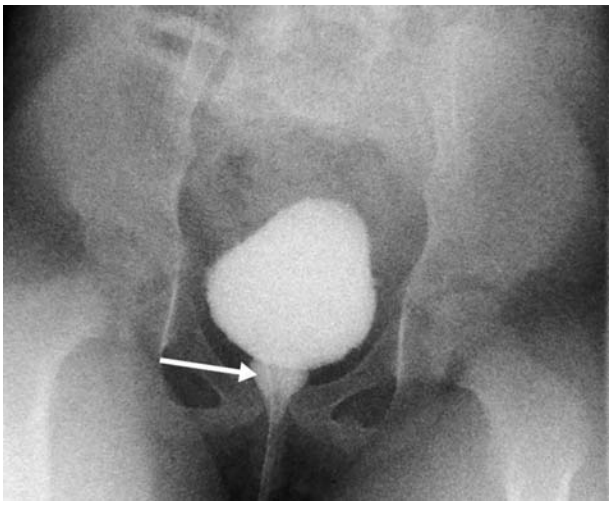

References: Dähnert W. *Radiology review manual sixth edition*. Philadelphia, PA: Wolters Kluwer Health/Lippincott Williams & Wilkins, 2007.
Ichim G, Fufezan O, Farcău M, et al. Clinical, imaging and cystometric findings of voiding dysfunction in children. *Med Ultrason* 2011;13(4):277–282.
Saxton HM, Borzyskowski M, Mundy AR, et al. Spinning top urethra: not a normal variant. *Radiology* 1988;168(1):147–150.

34 **Answer C.** The ultrasound images demonstrate a mass that is incompletely evaluated and that appears to involve or displace the uterus and is located posterior to the urinary bladder. Magnetic resonance imaging provides precise demonstration of anatomic features in multiple planes in cases of complex anomalies when US findings are incomplete or inconclusive. A voiding cystourethrogram is used to evaluate for vesicoureteral reflux and is not indicated in this particular case. A Tc-99m MAG-3 scan is used to evaluate renal function and potential obstruction and would not be indicated in this instance. Finally, a renal ultrasound would also not help localize or determine the etiology of the tumor.

References: Dähnert W. *Radiology review manual*, 6th ed. Philadelphia, PA: Wolters Kluwer Health/Lippincott Williams & Wilkins, 2007.
Donnelly LF. *Pediatric imaging the fundamentals*. Philadelphia, PA: Elsevier/Saunders, 2009.
Garel L, Dubois J, Grignon A, et al. US of the pediatric female pelvis: a clinical perspective. *Radiographics* 2001;21(6):1393–1407.

35 **Answer B.** The sagittal T2 fat-saturated images demonstrate a large heterogeneous lesion, which arises from and markedly distends the vagina. The uterus is displaced superiorly toward the superior extent of the image as can be discerned from the linear appearing and T2 hyperintense endometrial canal (arrows). The tumor appears as a septated high T2 signal cystic mass. Given the clinical history and imaging findings, this lesion likely represents a sarcoma botryoides, a variant of embryonal rhabdomyosarcoma. This tumor is the most common malignancy arising in the genitourinary (GU) tract of the pediatric population prior to 15 years of age. In children, rhabdomyosarcoma has a bimodal distribution pattern, the first peak occurring between 2 and 6 years and the second peak between 14 and 18 years of age. Gross pathology examination of sarcoma botryoides typically reveals an exophytic multinodular polyploid mass caused by cellular tumor growth pushing outward upon the overlying mucosal surface; hence the term “botryoid,” meaning “grape-like.” In general, local recurrence of rhabdomyosarcoma is common with or without metastatic disease. Children presenting with nonmetastatic rhabdomyosarcoma have been shown to have an excellent survival rate. If the primary tumor completely arises from a favorable site such as the vagina and is completely excised, the overall 3-year survival rate is >90%.

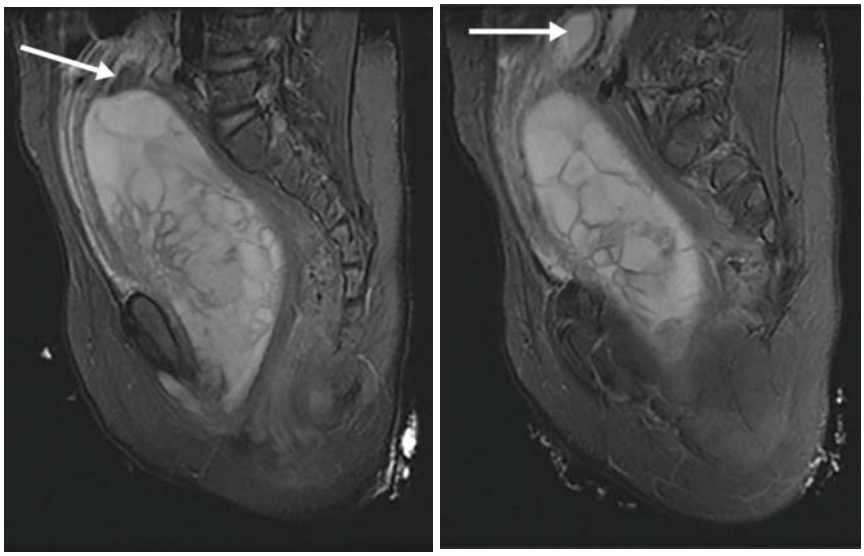

References: Agrons GA, Wagner BJ, Lonergan GJ, et al. From the archives of the AFIP. Genitourinary rhabdomyosarcoma in children: radiologic-pathologic correlation. *Radiographics* 1997;17(4):919–937.
Kobi M, Khatri G, Edelman M, et al. Sarcoma botryoides: MRI findings in two patients. *J Magn Reson Imaging* 2009;29(3):708–712.

36 **Answer C.** Clear cell renal sarcoma is a rare tumor and constitutes 4% of primary pediatric malignant renal tumors. It is known as an aggressive tumor with a poor prognosis. Clinically and radiographically, it resembles Wilms tumor. Clear cell sarcoma is seen mainly in young children with a peak incidence between 2 and 3 years of age with a male predominance. The most common site of metastasis at the time of presentation in patients with this tumor is the ipsilateral renal hilar lymph nodes. Treatment consists of nephrectomy and chemotherapy with current long-term survival rate of 60% to 70%. One important distinguishing feature of this tumor is its 40% to 60% incidence of bone metastasis, which is much higher than the 2% incidence of bone metastasis found in Wilms patients. The bone metastasis can be both lytic and sclerotic. Bone is the most common site of distant metastases followed by the lung, retroperitoneum, brain, and liver.

Mesoblastic nephroma is usually a benign tumor with some exceptions as detailed in the explanations for Questions 24 and 25. Rarely, this lesion may recur locally if incompletely resected or metastasize to the lungs, brain or bones.

Rhabdoid tumor is a rare highly aggressive renal neoplasm seen exclusively in the pediatric calcification. Peak incidence of rhabdoid tumor occurs at 11 months of age with a slight male predominance. On imaging, a rhabdoid tumor may present as an enhancing soft tissue renal mass with a similar imaging appearance to a Wilms tumor. As a result, a rhabdoid tumor often cannot be differentiated from a Wilms tumor. More specific imaging characteristics include subcapsular fluid collections with a mildly enhancing intrarenal tumor. Because brain malignancy, often midline and in the posterior fossa, may present concurrently, an MRI examination of the head is recommended at the time of diagnosis to assess for concomitant malignancy in this region. Rhabdoid tumor is the renal neoplasm with the worst prognosis, with metastatic disease most commonly involving the lungs. Surgical resection followed by chemotherapy is the current standard of care in pediatric patients with rhabdoid tumor. The survival rate is <15%.

References: Franco A, Dao TV, Lewis KN, et al. A case of clear cell sarcoma of the kidney. *J Radiol Case Rep* 2011;5(2):8–12.
Lowe LH, Isuani BH, Heller RM, et al. Pediatric renal masses: Wilms tumor and beyond. *Radiographics* 2000;20(6):1585–1603.
Son J, Lee EY, Restrepo R, et al. Focal renal lesions in pediatric patients. *AJR Am J Roentgenol* 2012;199(6):W668–W682.

37 **Answer A.** Nephroblastomatosis refers to diffuse or multifocal areas of nephrogenic rests. Although nephrogenic rests can be classified histologically as dormant, sclerosing, hyperplastic, or neoplastic, these types cannot be differentiated by imaging. Anatomically, nephroblastomatosis can be separated into perilobar and intralobar types. Perilobar nephroblastomatosis presents as soft tissue nodules with mild contrast enhancement located at the peripheral portion of the kidney. Most cases of nephroblastomatosis occur sporadically. However, perilobar nephroblastomatosis is associated with Beckwith-Wiedemann syndrome, hemihypertrophy, and Perlman syndrome. Intralobar nephroblastomatosis usually occurs as a single poorly marginated mass that can be found anywhere in the kidney. It is associated with Drash syndrome, sporadic aniridia, and WAGR (Wilms tumor, aniridia, genitourinary anomalies, and mental retardation) syndrome.

Most children with nephroblastomatosis do not develop Wilms tumor. However, 30% to 40% of Wilms tumors are thought to arise from nephrogenic rests. With bilateral Wilms tumors, nephrogenic rests are thought to be involved in as many as 99% of patients. Treatment of nephroblastomatosis is currently controversial, with some advocating chemotherapy, whereas others recommend close surveillance, preferably with MRI, which is more sensitive than ultrasound for detecting residual or recurrent nephroblastomatosis.

Reference: Son J, Lee EY, Restrepo R, et al. Focal renal lesions in pediatric patients. *AJR Am J Roentgenol* 2012;199(6):W668–W682.

38 Answer C. The definition of a urinary tract infection (UTI) is the presence of bacteria in the urine, but the term typically refers to infections of the lower urinary tract. Acute pyelonephritis is defined as urinary tract infection that involves the kidney. Young children with pyelonephritis often present with nonspecific symptoms such as fever, irritability, and vague abdominal pain. In older children, the findings may be more specific and include fever and associated flank pain. In patients in whom the diagnosis is straightforward, no imaging is needed in the acute phase, but patients are imaged later as part of the standard workup for a UTI to look for renal scarring. In patients in whom there is clinical difficulty in distinguishing an upper from a lower UTI, cortical scintigraphy with Tc-99m dimercaptosuccinic acid (DMSA) has been advocated as the most sensitive test. In cases of pyelonephritis, this study demonstrates single or multiple areas of lack of renal uptake of the radiotracer. These areas tend to be triangular and peripheral.

As an initial screening study, abdominal radiography is a rapid, inexpensive examination. Abdominal radiographs were routinely obtained as the first component of an excretory urographic study; however, use of CT has overtaken that of radiography in nearly all institutions. The scout radiographs were used to detect urinary tract gas and calcifications, but pitfalls included unreliable differentiation of abdominal bowel gas from urinary tract gas and nonvisualization of small urinary tract calcifications overlying normally ossified structures such as a transverse process.

Ultrasonography (US) is occasionally used as a first-line diagnostic tool to evaluate the urinary tract in patients with symptoms of pyelonephritis. Unfortunately, pyelonephritis is often not well characterized on routine gray-scale images. Therefore, most patients with clinically suspected acute pyelonephritis have negative ultrasound exams. When positive findings of pyelonephritis are found at US, they can include congenital anomalies and a variety of changes in the renal parenchyma such as hydronephrosis, renal enlargement, loss of renal sinus fat because of edema, changes in echogenicity due to both edema (hypoechoic) and hemorrhage (hyperechoic), loss of corticomedullary differentiation, abscess formation, and areas of hypoperfusion (visible with power Doppler interrogation).

Occasionally, areas of abnormal echogenicity can have a mass-like appearance. Unenhanced CT is excellent for identifying urinary tract gas, calculi, hemorrhage, renal enlargement, inflammatory masses, and obstruction. Involved regions occasionally appear with lower attenuation related to edema; less frequently, they have pockets of higher attenuation that are thought to represent hemorrhage. The above findings are frequently absent, however, and unenhanced CT images may appear normal.

It is only after contrast material is administered that the diagnostic features of acute bacterial nephritis are revealed. These features are better described in the explanation for Question 28.

References: Craig WD, Wagner BJ, Travis MD. Pyelonephritis: radiologic-pathologic review. *Radiographics* 2008;28(1):255–277.
Donnelly LF. *Pediatric imaging the fundamentals*. Philadelphia, PA: Elsevier/Saunders, 2009.

39 Answer A. The images shown were obtained using a pinhole collimator during a Tc-99m DMSA scan. There is a photopenic defect in the cortex of the mid to upper pole of the left kidney (long arrows). Given the clinical history of the patient, these findings are consistent with acute pyelonephritis although similar findings could be seen with chronic renal scarring. There is also some irregularity of the cortex of the lower pole of the left kidney (short arrow). The right kidney is normal.

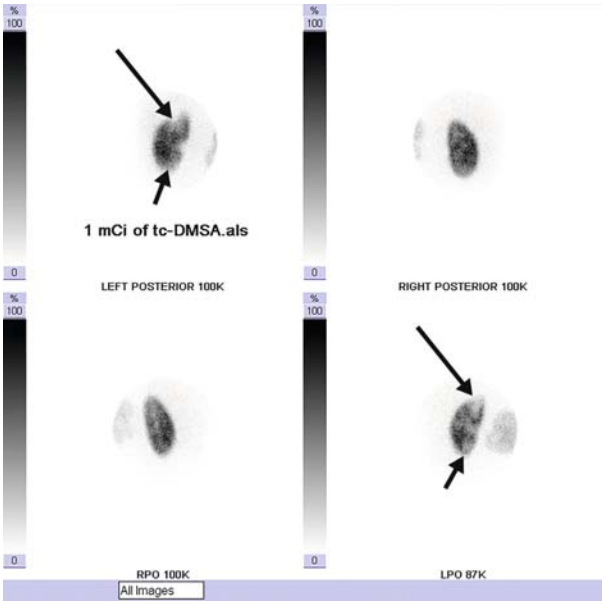

Reference: Donnelly LF. *Pediatric imaging the fundamentals*. Philadelphia, PA: Elsevier/Saunders, 2009.

40 Answer B. Ultrasound sensitivities for the diagnosis of adnexal torsion range from 46% to 74%. Investigators have evaluated the value of CT in the diagnosis of ovarian torsion because of its accessibility in emergent situations. However, exposure to pelvic irradiation makes this a less favorable imaging method in young women. MR has been found to be accurate in the diagnosis of adnexal torsion in the context of acute pelvic pain that presents rapidly over <4 hours with accuracies higher than 80%. A repeat ultrasound in 4 hours would not be indicated because this would cause a potential delay in the diagnosis of ovarian torsion, which is a surgical emergency. An abdominal radiograph would not be helpful in the diagnosis of ovarian torsion and would expose the patient to needless radiation.

Reference: Béranger-Gibert S, Sakly H, Ballester M, et al. Diagnostic value of MR imaging in the diagnosis of adnexal torsion. *Radiology* 2016;279(2):461–470.

41 Answer C. Figure A is an axial T2-weighted image and Figure B is an axial T1 fat-saturated image obtained after the administration of intravenous contrast. The right ovary is asymmetrically enlarged when compared to the left ovary on both images. There is a lack of internal T2-weighted signal within the right ovary on the T2-weighted image and lack of internal contrast enhancement on the second image. The follicles within the right ovary are in a peripheral distribution. These features can be compared with the normal size, internal T2 signal, uniform follicle distribution, and internal contrast enhancement of the normal left ovary. The most common but fairly nonspecific finding of a torsed ovary is an enlarged ovary (>4.0 cm in maximal dimension), which is reliably seen both on CT and MRI. An enlarged ovary with a central afollicular stroma (resulting from hemorrhage and edema) and peripherally displaced follicles is a more specific feature of ovarian torsion and can sometimes be identified on contrast-enhanced CT or on fast spin-echo T2-weighted MRI. The torsed ovary is characterized by disrupted blood flow, which is seen as abnormal enhancement after IV contrast agent administration. Heterogeneous minimal or absent enhancement indicates the evolution of ovarian torsion from ischemia to infarction. However, the presence of enhancement does not exclude torsion because a twisted ovary, with its redundant blood supply, can appear to enhance normally, presumably because the torsion is intermittent or of recent onset.

Reference: Duigenan S, Oliva E, Lee SI. Ovarian torsion: diagnostic features on CT and MRI with pathologic correlation. *Am J Roentgenol* 2012;198(2):W122–W131.

42 **Answer B.** Twisting of the adnexal pedicle as occurs in ovarian torsion obstructs the lymphatic drainage causing enlargement of the ovary. This is followed by obstruction of the venous drainage resulting in hemorrhagic infarction. Finally, the arterial supply is obstructed resulting in necrosis. This order of vascular compromise explains why vascular flow, especially arterial flow, may be present and detected by pelvic Doppler ultrasound examinations in torsed ovaries if the torsion is intermittent or early or partial torsion.
Reference: Reid JR, Paladin A, Davros W, et al. *Rotations in radiology pediatric radiology*. New York, NY: Oxford University Press, 2013.

43 **Answer C.** The ultrasound images of the kidneys demonstrate diffusely increased echogenicity of the medullary pyramids bilaterally consistent with medullary nephrocalcinosis. The most common metabolic abnormality responsible for histologic changes in the pyramids that may be depicted as increased echogenicity at sonography is nephrocalcinosis. Nephrocalcinosis primarily affects the renal pyramids, but it can occasionally be appreciated in the cortex as well. Although nephrocalcinosis may eventually progress to involve most of the pyramid, acoustic shadowing is rarely seen. The lack of shadowing may reflect the way in which the calcium is laid down within the pyramid. Acoustic shadowing may be appreciated only in rare cases of extreme involvement of the pyramids or if there is development of associated calculi in the adjacent calices.
There are numerous causes for medullary nephrocalcinosis in children. The majority of these conditions are associated with hypercalciuria and include distal renal tubular acidosis and prolonged immobilization.
References: Dähnert W. *Radiology review manual*, 6th ed. Philadelphia, PA: Wolters Kluwer Health/Lippincott Williams & Wilkins, 2007.
Daneman A, Navarro OM, Somers GR, et al. Renal pyramids: focused sonography of normal and pathologic processes. *Radiographics* 2010;30(5):1287–1307.

44 **Answer C.** In children, the left and right kidney should generally measure within 1 cm of each other. If there is a discrepancy of more than 1 cm, an underlying abnormality should be suspected. Such discrepancies may result from a disorder that causes one of the kidneys to be too small, such as global scarring, or from a process that causes one of the kidneys to be too large, such as renal duplication or acute pyelonephritis. In every case, it is important to compare the patient's renal length with tables that plot normal renal length against age.
Reference: Donnelly LF. *Pediatric imaging the fundamentals*. Philadelphia, PA: Elsevier/Saunders, 2009.

45 **Answer C.** The transverse ultrasound image shown demonstrates a normal echotexture of both testes, but there is a lack of color Doppler flow in the right testis. These findings are consistent with acute right-sided testicular torsion, and the patient will require prompt diagnosis and treatment. In the early phases of torsion (1 to 3 hours), testicular echogenicity appears normal. With progression, enlargement of the affected testis and increased or heterogeneous echogenicity are common findings. Testicular viability can be suggested from gray-scale and color Doppler findings. Normal echogenicity with mild testicular enlargement is a good sign of viability, whereas marked enlargement, heterogeneous echotexture, and scrotal wall hypervascularity are signs of testicular infarction and necrosis.
Note that demonstration of flow within a normal testis is more difficult in children <2 years of age. Gray-scale ultrasound may demonstrate asymmetric enlargement and slightly decreased echogenicity of the affected testis. Advanced findings in young children that occur with progressive ischemia and infarction are similar to those for older patients. These include hemorrhage and necrosis, which may cause increasing asymmetric heterogeneity
References: Aso C, Enríquez G, Fité M, et al. Gray-scale and color Doppler sonography of scrotal disorders in children: an update. *Radiographics* 2005;25(5):1197–1214.
Donnelly LF. *Pediatric imaging the fundamentals*. Philadelphia, PA: Elsevier/Saunders, 2009.

46 Answer C. The ultrasound image demonstrates an anechoic fluid tract extending from the anterosuperior aspect of the urinary bladder (arrow). This is consistent with a urachal remnant. The urachus, or median umbilical ligament, is a midline tubular structure that extends upward from the anterior dome of the bladder toward the umbilicus. It is a vestigial remnant of at least two embryonic structures: the cloaca, which is the cephalic extension of the urogenital sinus (a precursor of the fetal bladder), and the allantois, which is a derivative of the yolk sac. The tubular urachus normally involutes before birth, remaining as a fibrous band with no known function. However, persistence of an embryonic urachal remnant can give rise to various clinical problems, not only in infants and children but also in adults.

Congenital urachal anomalies are twice as common in men as in women. There are four types of congenital urachal anomalies: patent urachus, umbilical–urachal sinus, vesicourachal diverticulum, and urachal cyst. A patent urachus is purely congenital and accounts for about 50% of all cases of congenital anomalies. An umbilical–urachal sinus (15% of cases), vesicourachal diverticulum (3% to 5% of cases), or urachal cyst (about 30% of cases) may close normally after birth but then reopen in association with pathologic conditions that are often categorized as acquired diseases.

The majority of patients with urachal abnormalities (except those with a patent urachus) are asymptomatic. However, they may become symptomatic if these abnormalities are associated with infection. If a persistent communication exists between the bladder lumen and the umbilicus, urine leakage is usually noted during the neonatal period.

Although the normal urachus is most commonly lined by the transitional epithelium, urachal carcinoma predominantly manifests as adenocarcinoma (90% of cases), probably because of the metaplasia of the urachal mucosa into columnar epithelium followed by malignant transformation; conversely, 34% of bladder adenocarcinomas are of urachal origin. These tumors are most commonly seen in patients 40 to 70 years of age, two-thirds of whom are men.

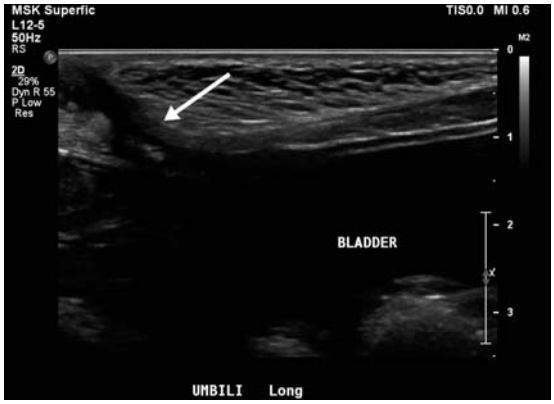

Reference: Yu JS, Kim KW, Lee HJ, et al. Urachal remnant diseases: spectrum of CT and US findings. *Radiographics* 2001;21(2):451–461.

3 Pediatric Musculoskeletal System

Questions

1. An 8-year-old male with a history of hip pain presents with a frontal radiograph of the pelvis.

What is the most likely diagnosis?
A. Developmental dysplasia of the hip
B. Slipped capital femoral epiphysis
C. Legg-Calvé-Perthes Disease
D. Osteomyelitis

2. What is the stage of the disease in Question 1?
A. Stage 1
B. Stage 2
C. Stage 3
D. Stage 4

3. A 7-year-old male with knee pain presents with an AP radiograph and a coronal image from an MRI of the same knee.

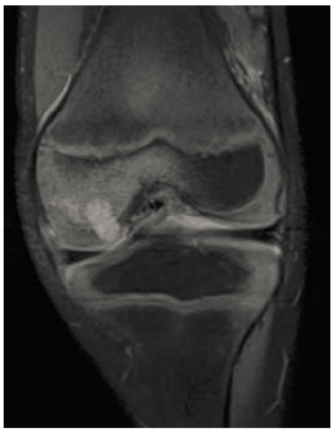

What is the most likely diagnosis?
A. Chondroblastoma
B. Osteomyelitis
C. Osteoid osteoma
D. OCD

4. In what location does osteomyelitis occur most often in children?
A. Metaphysis
B. Diaphysis
C. Epiphysis
D. Intra-articular

5. Osteoarticular osteomyelitis in young children (<4 years of age) involving the epiphyseal cartilage is suggestive of which causative organism?
A. *Staphylococcus aureus*
B. *Streptococcus*
C. *Kingella kingae*
D. *Pseudomonas*

6. A child presents with a radiograph of the elbow following trauma.

What is the diagnosis?
A. Lateral condylar fracture
B. Supracondylar fracture
C. Medial condylar fracture
D. Lateral epicondylar fracture
E. Medical epicondylar fracture

7. What is the most common age at which the fracture seen in Question 6 occurs?
A. 0 to 3 years
B. 3 to 6 years
C. 5 to 10 years
D. 10 to 15 years

8. The fracture in Question 6 most commonly represents which Salter-Harris fracture type?
A. Salter-Harris II
B. Salter-Harris III
C. Salter-Harris IV
D. Salter-Harris V

9. A 2-year-old with history of abnormal knee alignment presents with the following radiograph of the knee.

What is the diagnosis?
A. Genu varum
B. Blount disease
C. Rickets
D. Epiphyseal dysplasia

10. Which of the following is an imaging characteristic of the disorder in Question 9?
A. Fracture of the distal femoral metaphysis
B. Absence of the cruciate ligaments
C. Tibial hemimelia
D. Hypertrophy of the medial meniscus

11. A 13-year-old boy with subacute hip pain and joint stiffness presents with an MRI of the pelvis and hip.

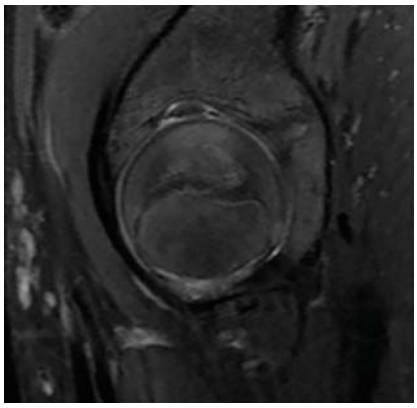

What is the diagnosis?
A. Avascular necrosis
B. Osteomyelitis
C. Idiopathic chondrolysis
D. Bone contusion

12. A 12-year-old male with knee pain presents for a whole-body MRI.

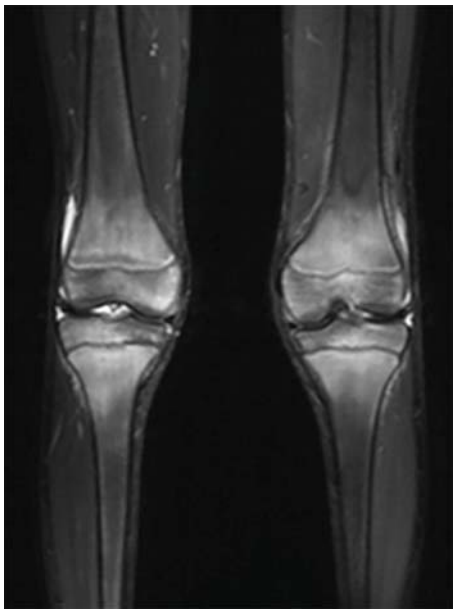

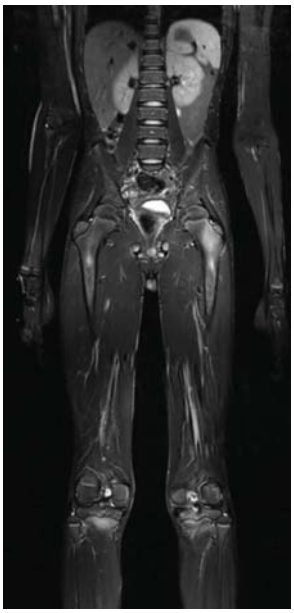

What is the most likely diagnosis?
A. Leukemia
B. Rickets
C. Metastasis
D. Chronic recurrent multifocal osteomyelitis

13. What is the most common location of the bone in the disorder in Question 12?
A. Epiphysis
B. Metaphysis
C. Diaphysis

14. Which of the following conditions is associated with the disorder in Question 12?
A. Autosomal recessive polycystic kidney disease (ARPKD)
B. Wegener granulomatosis
C. Truncus arteriosus
D. Chondroblastoma

15. A child with history of a congenital foot abnormality presents with the following radiograph.

What is the diagnosis?
A. Proteus syndrome
B. Macrodystrophia lipomatosa
C. Neurofibromatosis
D. Hemihypertrophy

16. The following babygram was performed on a stillborn neonate.

What is the diagnosis?
A. Achondroplasia
B. Jeune syndrome
C. Thanatophoric dysplasia
D. Osteogenesis imperfecta

17. A central nervous system abnormality associated with the disorder in Question 16 is which of the following?
A. Tethered cord
B. Ocular nerve enlargement
C. Megalencephaly
D. Basal ganglia calcification

18. An adolescent with elbow pain presents with a frontal radiograph of the elbow and sagittal MR image from a fluid-sensitive sequence of the elbow.

What is the diagnosis?
A. Osteomyelitis
B. Avascular necrosis
C. Osteoid osteoma
D. Osteochondritis dissecans

19. The disorder in Question 18 has a high prevalence of which of the following?
A. Radial head subluxation
B. Supracondylar fracture
C. Olecranon bursitis
D. Lateral epicondylitis

20. In the diagnosis in Question 18, which of the following is a criterion on MRI to diagnose an unstable lesion?
A. Focal defect of 5 mm or more in the meniscus adjacent to the lesion
B. Thin line of hyperintensity within the metaphysis of the bone
C. Small cystic focus of 5 mm or greater in the articular surface of the lesion
D. Low signal extending through the articular cartilage

21. An 8-year-old presents with left hip pain. The following radiograph of the pelvis was performed.

What is the diagnosis?
A. Avulsion of the anterior inferior iliac spine
B. Avulsion of the anterior superior iliac spine
C. Nondisplaced fracture of the femoral neck
D. Fracture of the anterior column of the acetabulum
E. Fracture of the posterior column of the acetabulum

22. Which of the following is TRUE?
A. Avulsion from the anterior superior iliac spine is related to the adductor muscles.
B. Avulsion of the anterior inferior iliac spine is related to the hamstrings.
C. Avulsion of the greater trochanter is related to the rectus femoris.
D. Avulsion of the lesser trochanter is related to the iliopsoas muscle.

23. Frontal and lateral radiographs of the tibia/fibula were performed in an infant who presents with skull fracture.

What is the diagnosis?
A. Toddler's fracture
B. Metaphyseal corner fracture
C. Buckle fracture
D. Triplane fracture

24. The mechanism of the fracture in Question 23 is which of the following?
A. Direct trauma to the bone
B. Shearing injury
C. Insufficiency fracture
D. Bending injury

25. Which of the following imaging findings is commonly associated with nonaccidental injury (child abuse)?
A. Buckle fracture of the distal radius
B. Toddler's fracture of the tibia
C. Medial epicondyle avulsion fracture
D. Posterior rib fractures

26. The preferred initial imaging evaluation of infants with suspected nonaccidental injury (child abuse) is:
A. Radiographical skeletal survey
B. Radiographs at site of suspected injury only
C. Whole-body MRI examination
D. Sonographic skeletal survey

27. The following radiograph of the forearm was performed in a patient with a history of an arm deformity.

Which of the following is TRUE concerning radial dysplasia?
A. It is associated with hypoplasia of the thumb.
B. On physical examination, there is ulnar and palmar deviation of the hand.
C. Development of the radius occurs between the 10th and 12th week of gestation.
D. Bilateral radial dysplasia occurs in <10% of affected children.

28. Which of the following syndromes is associated with radial dysplasia?
A. Holt-Oram syndrome
B. Trisomy 21
C. Achondroplasia
D. Ehlers-Danlos syndrome

29. A teenager presents with right shoulder pain. The following radiograph was obtained.

What is the most likely diagnosis?
A. Chondroblastoma
B. Osteoid osteoma
C. Fibrous dysplasia
D. Rhabdomyosarcoma
E. Osteosarcoma

30. When imaging the lesion in Question 29, it is important to image the complete long bone from the proximal joint to the distal joint because:
A. A malignant joint effusion is common and should be evaluated.
B. Skip metastases can be seen in this lesion and should be evaluated.
C. Articular dislocations are common and should be evaluated.
D. Invasion of the ligaments of the joint are common and should be evaluated.

31. Where is the most common site of relapse of the lesion in Question 29?
A. Locally within the bone
B. Lung parenchyma
C. Liver
D. Lymph nodes

32. An 8-week-old infant presents with an abnormal hip click on physical examination. What imaging examination is recommended for further evaluation of this infant?
A. Radiograph of the hips
B. MRI of the hips
C. Ultrasound of the hips
E. CT of the hips

33. The following sonographic image of the hip was obtained in an infant.

What is the diagnosis?
A. Avascular necrosis
B. Developmental hip dysplasia
C. Traumatic dislocation
D. Transient synovitis

34. Which of the following is a risk factor for developing the condition in Question 33?
A. Congenital heart disease
B. Surfactant deficiency disorder
C. Posterior urethral valves
D. Foot deformity

35. The following frontal radiograph of the thoracolumbar spine was obtained.

What is the diagnosis?
A. Levoscoliosis of the thoracolumbar spine WITHOUT a vertebral anomaly
B. Levoscoliosis of the thoracolumbar spine WITH a vertebral anomaly
C. Dextroscoliosis of the thoracolumbar spine WITHOUT a vertebral anomaly
D. Dextroscoliosis of the thoracolumbar spine WITH a vertebral anomaly

36. Which of the following concerning structural and nonstructural scoliotic curves is TRUE?
A. A structural curve is correctable with ipsilateral bending.
B. A structural curve has vertebral morphologic changes such as wedging and rotation.
C. A nonstructural curve never progresses to a structural curve.
D. A Cobb angle of 15 degrees or more on ipsilateral side-bending views differentiates a structural curve from a nonstructural curve.

37. At what Cobb angle is bracing recommended for treatment of adolescent scoliosis?
A. 10 to 35 degrees
B. 20 to 45 degrees
C. 30 to 55 degrees
D. 40 to 65 degrees

38. A 3-year-old child presents with a limp. The following frontal and lateral radiographs were performed.

What is the diagnosis?
A. Toddler's fracture of the tibia
B. Buckle fracture of the proximal tibia
C. Buckle fracture of the distal tibia
D. Avulsion fracture of the medial malleolus of the distal tibia

39. A child presents with a short leg. The following radiograph was performed.

What is the diagnosis?
A. Achondroplasia
B. Osteonecrosis
C. Rhabdomyosarcoma
D. Proximal focal femoral deficiency disorder

40. Which of the following is associated with the disorder in Question 39?
A. Congenital syringomyelia
B. Neuroblastoma
C. Coxa valgus deformity
D. Absent cruciate ligaments

41. Frontal and oblique radiographs of the left foot were obtained in a teenager with chronic foot pain.

What is the diagnosis?
A. Cuboid fracture
B. Tarsal coalition
C. Equinovarus foot
D. Plantar fasciitis
E. Septic arthritis

42. The condition in Question 41 is bilateral in approximately what percentage of affected individuals?
A. 20%
B. 50%
C. 70%
D. 90%

43. A child with history of multiple fractures presents with the following radiograph.

What is the most likely diagnosis?
A. Rickets
B. Scurvy
C. Chronic recurrent multifocal osteomyelitis
D. Osteogenesis imperfecta

44. Which of the following in regard to the diagnosis in Question 43 is the lethal form of the disease due to respiratory insufficiency?
A. Type I
B. Type II
C. Type III
D. Type IV
E. Type V

45. Following treatment, this patient developed dense metaphyseal lines (arrow) within the long bones and a "bone within a bone pattern" within the spine and flat bones. What treatment did this patient receive?

A. NSAID therapy
B. Metronidazole therapy
C. Calcium therapy
D. Bisphosphonate therapy

46. What is the most likely diagnosis?

A. Ewing sarcoma
B. Osteosarcoma
C. Fibrous dysplasia
D. Chondroblastoma

47. What is the treatment of the lesion seen in Question 46?
A. Chemotherapy followed by above-the-knee amputation (AKA)
B. Chemotherapy followed by local resection
C. Curettage and bone grafting
D. Chemotherapy only

48. The following sonographic examination was performed of both the right and left hip in an 8-year-old child with hip pain.

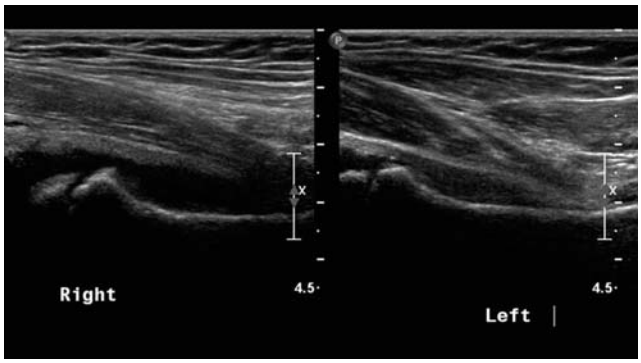

What is the most likely diagnosis?
A. Transient synovitis
B. Fracture of the radial neck
C. Slipped capital femoral epiphysis (SCFE)
D. Osteoid osteoma

49. A child presents with chronic pain in the left knee. Frontal and lateral radiographs of the left knee were performed.

What is the most likely diagnosis?
A. Sinding-Larsen-Johansson syndrome
B. Osgood-Schlatter disease
C. Patellar sleeve avulsion fracture
D. Bipartite patella

50. Which of the following is TRUE regarding the diagnosis in Question 49?
A. It is an osteochondrosis due to traction of the quadriceps tendon.
B. It most commonly occurs between the ages of 14 and 18 years.
C. On MRI evaluation, bone marrow edema may be seen in the anterior tibial tubercle.
D. Initial treatment is rest and nonsteroidal anti-inflammatory drugs (NSAIDs).

Musculoskeletal: Answers and Explanations

1 Answer C. Legg-Calvé-Perthes (LCP) disease is the result of idiopathic, avascular necrosis of the developing proximal femoral epiphysis that often presents between 4 and 8 years of age. There are four stages of pathogenesis with radiographic correlation: avascularity, revascularization, healing, and residual deformity.

The radiographic pattern of a dense, flattened femoral epiphysis (arrow) with normal acetabular morphology are the imaging hallmarks of LCP, thus excluding hip dysplasia as a diagnosis. Slipped capital femoral epiphysis typically occurs in older children (mean age of 13 years), and radiographs reveal an irregularity of the physis, versus the epiphysis, that is more pronounced on frog-leg lateral projections. Osteomyelitis of the hip may result in a dense irregular epiphysis. However, there is typically an aggressive, osteolytic appearance to the proximal femur with involvement of the entire hip joint and rapid destruction if not treated urgently.

References: Dillman JR, Hernandez RJ. MRI of Legg-Calvé-Perthes disease. *AJR Am J Roentgenol* 2009;193(5):1394–1407.
Resnick D. *Osteochondroses in diagnosis of bone and joint disorders*, 4th ed. New York, NY: WB Saunders and Company, 2002:3686–3741.
Salter RB. In: *Textbook of disorders and injuries of the musculoskeletal system*, 3rd ed. Baltimore, MD: Williams & Wilkins, 1999:339–350.

2 Answer C. This case represents a late healing stage of Perthes disease with dense bone replacing trabecular bone at the middle pillar of the epiphysis. The initial, stage 1 of avascularity is radiographically occult. A symptomatic child with normal radiographs may be further evaluated by MRI with a high sensitivity for detecting osteonecrosis, marrow edema, and hip effusion. The figure below represents the different stages of Perthes disease. The earliest radiographic finding of a relatively dense epiphysis represents stage 2, revascularization. At this time, children are often asymptomatic. The "crescent sign" that is sometimes seen at stage 2 results from a pathologic, subchondral fracture of the anterosuperior epiphysis (see arrow in **A**). Stage 4 reveals a chronic, residual deformity of the femoral head, often with collapse, fragmentation, and lateral subluxation. Additional findings during disease progression may include a cystic lucency of the subphyseal, femoral neck (see arrow in **B**) and coxa magna with a short and widened femoral metaphysis.

Stages of Legg-Calvé-Perthes (LCP) disease on radiograph. **A:** 2 months; **B:** 4 months; **C:** 7 months; **D:** 10 months.

References: Dillman JR, Hernandez RJ. MRI of Legg-Calvé-Perthes disease. *AJR Am J Roentgenol* 2009;193(5):1394–1407.
Resnick D. *Osteochondroses in diagnosis of bone and joint disorders*, 4th ed. New York, NY: WB Saunders and Company, 2002:3686–3741.
Salter RB. In: *Textbook of disorders and injuries of the musculoskeletal system*, 3rd ed. Baltimore, MD: Williams & Wilkins, 1999:339–350.

3 Answer B. The radiograph reveals a geographic, lytic lesion without sclerotic margins (arrows) involving the epiphysis of the knee, the differential diagnosis of which includes both chondroblastoma and osteomyelitis. However, most chondroblastomas demonstrate a thin sclerotic margin radiographically.

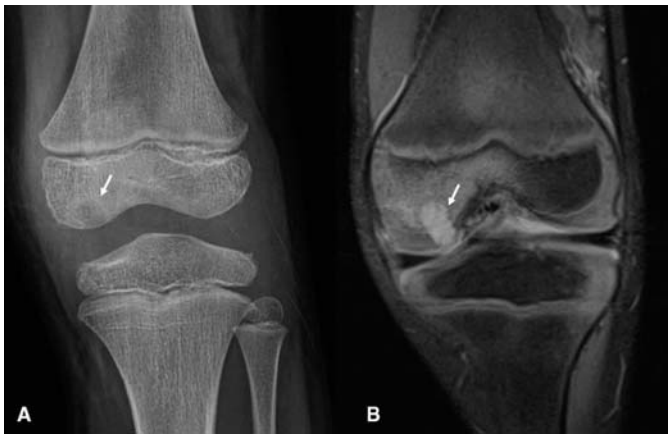

Osteoid osteomas classically appear as a central, lucent lesion or nidus that is often cortically based but can occur in subchondral, intra-articular locations. Nonetheless, absent any surrounding cortical hyperostosis, an osteoid osteoma is unlikely. An osteochondral defect (OCD) should have an irregular fracture lucency, often with sclerotic margins abutting a fragment of subchondral bone, all of which are not present in this case.
The MRI appearance of a fluid signal, solitary lytic lesion centered at the distal epiphysis and cartilage (arrow) with surrounding reactive marrow signal is highly suggestive of osteomyelitis. Rim enhancement of the lytic lesion (not shown) would then suggest an associated abscess. Chondroblastomas also have surrounding T2 hyperintense marrow signal. However, the lesion itself is characteristically lobular with internal matrix that is T2 isointense/hypointense, not present in this case.
Understanding the imaging findings of osteomyelitis is important as the classic clinical history of fever, elevated white blood cell count, and inflammatory markers are not always present.
References: Guillerman RP. Osteomyelitis and beyond. *Pediatr Radiol* 2013;43(1):S193–S203.
Lyer RS, Chapman T, Chew FS. Pediatric bone imaging: diagnostic imaging of osteoid osteoma. *AJR Am J Roentgenol* 2012;198:1039–1052.
Weatherall PT, Maale GE, Mendelsohn DB, et al. Chondroblastoma: classic and confusing appearance at MR imaging. *Radiology* 1994;190:467–474.

4 Answer A. The metaphyses of long bones are the most common sites of hematogenous osteomyelitis in children owing to the unique changes in metaphyseal and epiphyseal vascularity with age. In neonates, the epiphysis is at an increased risk of infection as nutrient vessels cross the physis. However, transphyseal extension of metaphyseal osteomyelitis may still occur in children older than 2 years of age despite the theoretic protection of an avascular physis.
References: Gilbertson-Dahdal D, Wright JE, Krupinski E, et al. Transphyseal involvement of pyogenic osteomyelitis is considerably more common than classically taught. *AJR Am J Roentgenol* 2014;203:190–195.
Guillerman RP. Osteomyelitis and beyond. *Pediatr Radiol* 2013;43(1):S193–S203.

5 Answer C. The gram-positive cocci (GPC), *S. aureus* followed by *Streptococcus*, are considered the most common pathogens for acute hematogenous osteomyelitis. However, the gram-negative bacillus, *K. kingae*, has an increased prevalence in children younger than 4 years of age.
MRI is highly sensitive for distinguishing *K. kingae* from GPC in young children when there is focal epiphyseal (and equivalent) cartilage involvement. There is also a diminished inflammatory response and bone marrow/soft tissue reaction with *K. kingae* compared to GPC. *Pseudomonas* and *Escherichia coli* are often associated with osteomyelitis from penetrating trauma, typically within the foot, but this is rare in the intra-articular epiphysis.
References: Gilbertson-Dahdal D, Wright JE, Krupinski E, et al. Transphyseal involvement of pyogenic osteomyelitis is considerably more common than classically taught. *AJR Am J Roentgenol* 2014;203:190–195.
Guillerman RP. Osteomyelitis and beyond. *Pediatr Radiol* 2013;43(1):S193–S203.
Kanavaki A, Ceroni D, Tchernin D, et al. Can early MRI distinguish between *Kingella kingae* and Gram-positive cocci in osteoarticular infections in young children? *Pediatr Radiol* 2012;42:57–62.

6 Answer A. The crescentic fracture fragment (arrow) arising from the lateral condyle is the typical location of a lateral condylar fracture. This often results from a varus injury to an extended supinated forearm. The more common supracondylar fracture is a horizontal fracture located at the distal humeral metaphysis, often involving the coronoid fossa without involvement of the physis.

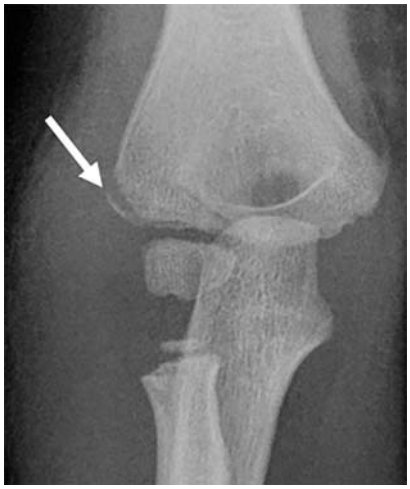

Reference: Green NE. Fractures and dislocations about the elbow. In: Green NE, Swiontkowski MF. (eds). *Skeletal trauma in children*, 3rd ed. Philadelphia, PA: WB Saunders, 2003:257.

7 Answer C. Lateral condylar fractures most commonly occur between the ages of 5 and 10 years.
Reference: Green NE. Fractures and dislocations about the elbow. In: Green NE, Swiontkowski MF (eds). *Skeletal trauma in children*, 3rd ed. Philadelphia, PA: WB Saunders, 2003:257.

8 Answer C. Lateral condylar fractures of the elbow are most commonly Salter-Harris IV fractures. The Milch classification groups lateral condylar fractures into types I and II based on fracture involvement lateral or medial to the capitello-trochlear groove, respectively. A Milch I fracture is lateral to the trochlea and extends through the capitellum. As the capitellum is usually ossified in this age group, it clearly represents a Salter-Harris IV fracture on elbow radiographs. However, the elbow remains stable as the humeroulnar joint is spared.
The Milch II fracture spares the capitellum and extends medial to the capitello-trochlear groove. There has been controversy classifying this fracture type as Salter-Harris IV when the involved trochlear epiphysis is not yet ossified and it appears radiographically as a Salter-Harris II fracture. However, the consensus is that the Milch II fracture pattern is also a Salter-Harris IV fracture as it involves the metaphysis, physis, and unossified trochlear epiphysis. Therefore, nearly all lateral condylar fractures are considered Salter-Harris IV fractures. However, the Milch classification is more important than the Salter-Harris classification for management because Milch II fractures are unstable and require surgical fixation.
This case highlights the more common Milch type II lateral condylar fracture as the metaphyseal fragment (arrow) extends medial to the capitellum. Radiographic evaluation is limited in this age group because of incomplete ossification of the trochlea. As a result, surgical management may rely on the degree of displacement of the metaphyseal fragment (>2 mm).
References: Bache E. Elbow injuries. In: Johnson KJ, Bache E (eds). *Imaging in pediatric skeletal trauma*. Berlin: Springer, 2008:257–270.
Green NE. Fractures and dislocations about the elbow. In: Green NE, Swiontkowski MF (eds). *Skeletal trauma in children*, 3rd ed. Philadelphia, PA: WB Saunders, 2003:257.
Letts M, Davidson D. Fractures of the lateral condyle of the humerus in children. *Orthopaedic Knowledge Online Journal* 2002;1(6). http://orthoportal.aaos.org/oko/article.aspx?article=OKO_PED007

9 **Answer B.** Blount disease (tibia vara) is secondary to pathologic stress upon the posteromedial physis of the proximal tibia that results in medial growth suppression and associated tibia vara. As the name tibia vara implies, the lower extremity bowing (varus) is centered at the proximal tibia. The metaphyseal–diaphyseal angle is >11 degrees (~20 degrees in this case). This angle is drawn from the metaphyseal beak to a line at the physis that is perpendicular to the lateral cortex of the tibial diaphysis (see angle). Although bilateral in this case, Blount disease is often unilateral or asymmetric and has infantile, juvenile, and adolescent presentations. The Langenskiold classification describes six stages of progressive metaphyseal depression, beaking, and fragmentation.

Developmental (physiologic) genu varus (bowing) normally resolves within 6 months of walking or by the age two. Congenital bowing classically presents as convex posterior and medial bowing of the tibial diaphysis and may be due to intrauterine positioning or skeletal dysplasia. In both cases, there is a normal medial metaphysis of the tibia. As rickets represents deficient mineralization of the growing physis, radiographs should display symmetric widening, cupping, and fraying of the growth plates of the distal femur and proximal and distal tibia (not present in this case).

References: Biko DM, Miller AL, Ho-Fung V, et al. MRI of congenital and developmental abnormalities of the knee. *Clin Radiol* 2012;67:1198–1206.
Cheema FI, Grissom LE, Harcke T. Radiographic characteristics of lower-extremity bowing in children. *Radiographics* 2003;23:871–880.

10 **Answer D.** Imaging findings of Blount disease include radiographical findings of depression of the medial tibial metaphysis. Additional MRI can better evaluate the growth plate demonstrating bony bridging, delayed ossification of the medial tibial epiphysis, widening of the tibial growth plate, and hypertrophy of the medial meniscus. The hypertrophy of the medial meniscus is likely compensatory hypertrophy due to abnormal forces within the knee.

Reference: Biko DM, Miller AL, Ho-Fung V, et al. MRI of congenital and developmental abnormalities of the knee. *Clin Radiol* 2012;67:1198–1206.

11 **Answer C.** Idiopathic chondrolysis (ICH) is a disease of unknown etiology that results in progressive articular cartilage destruction. ICH is often unilateral and presents with spontaneous hip or knee pain with worsening joint stiffness. There are neither systemic symptoms nor abnormal inflammatory biomarkers present. Early radiographs are often normal and performed to exclude more common acute causes of hip pain such as slipped capital femoral epiphysis. Later radiographs 10 to 12 months from symptom onset often reveal degenerative changes of concentric joint space loss, protrusio acetabuli, subchondral cysts, and sclerosis. It is important to distinguish ICH from secondary causes of cartilage loss from JIA or infection. The MRI findings in this case reveal a geographic pattern of T1/T2 signal prolongation confined to the middle third of the subchondral femoral head to the physis (arrows). This pattern is characteristic of early MRI findings of ICH. Synovial enhancement is less commonly reported with ICH compared to JIA. However, this negative finding is not specific. Additional findings of muscle wasting and atrophy are reported with follow-up imaging usually with associated joint contractures. Synovial biopsy is often performed for pathologic confirmation and to exclude infection. The prognosis is variable from spontaneous resolution to significant joint contracture and ankylosis.

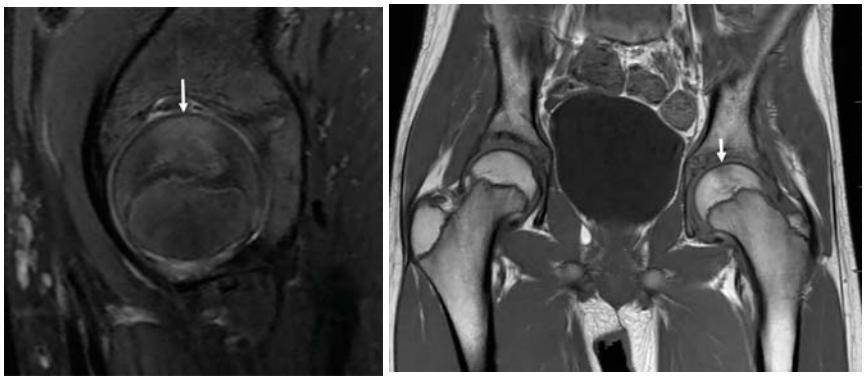

References: Johnson K, Haigh SF, Ehtisham S, et al. Childhood idiopathic chondrolysis of the hip: MRI features. *Pediatr Radiol* 2003;33:194–199.
Laor T, Crawford AH. Idiopathic chondrolysis of the hip in children: early MRI findings. *AJR Am J Roentgenol* 2009;192:526–531.

12 **Answer D.** The imaging findings are most suggestive of chronic recurrent multifocal osteomyelitis (CRMO). CRMO is an idiopathic inflammatory disorder most commonly seen in children and adolescents. This disorder is characterized by multiple inflammatory bone lesions that demonstrate a relapsing/remitting pattern. On imaging, these lesions are most often lytic on plain radiographs initially followed by sclerosis in the chronic course. On MR imaging, the lesions demonstrate bone marrow edema and periostitis. CRMO commonly occurs in the long tubular bone and clavicle but can occur anywhere throughout the skeleton.

Reference: Khanna G, Sato TS, Ferguson P. Imaging of chronic recurrent multifocal osteomyelitis. *Radiographics* 2009;29:1159–1177.

13 **Answer B.** Chronic recurrent multifocal osteomyelitis (CRMO) most commonly involves the metaphysis and metaphyseal equivalents. This is similar to the distribution of hematogenous spread of osteomyelitis, but CRMO may involve the clavicle.

References: Khanna G, Sato TS, Ferguson P. Imaging of chronic recurrent multifocal osteomyelitis. *Radiographics* 2009;29:1159–1177.
Mandell GA, Contreras SJ, Conrad K, et al. Bone scintigraphy in the detection of chronic recurrent multifocal osteomyelitis. *J Nucl Med* 1998;39:1778–1783.

14 Answer B. Multiple conditions are associated with chronic recurrent multifocal osteomyelitis (CRMO). These include dermatologic conditions such as psoriasis and pyoderma gangrenosum, autoinflammatory disorders such as Takayasu arteritis and Wegener granulomatosis, gastrointestinal syndromes such as inflammatory bowel disease, and genetic syndromes such as Majeed syndrome. CRMO is also associated with SAPHO syndrome (synovitis, acne, pustulosis, hyperostosis, osteitis) and spondyloarthropathies.

Reference: Khanna G, Sato TS, Ferguson P. Imaging of chronic recurrent multifocal osteomyelitis. *Radiographics* 2009;29:1159–1177.

15 Answer B. Lipomatosis of a nerve with macrodactyly is referred to as macrodystrophia lipomatosa. In this disorder, the affected nerve is enlarged by fibrofatty tissue. This can occur without macrodactyly or with macrodactyly (macrodystrophia lipomatosa). Clinically, this disorder is characterized by a slow-growing mass most frequently within the upper extremity. Most cases involve the median nerve in the upper extremity and the medial plantar nerve in the lower extremity. Radiographs of this disorder demonstrate both soft tissue and bony overgrowth in the distribution of a sclerotome (arrows). MRI demonstrates a diffusely enlarged thickened nerve surrounded by adipose tissue.

References: Murphey MD, Carroll JF, Flemming DJ, et al. From the archive of the AFIP: benign musculoskeletal lipomatous lesions. *Radiographics* 2004;24:1433–1466.
Tripathi SK, Nanda SN, Kumar S, et al. Macrodystrophia lipomatosa—a rare congenital anomaly: a case report and review of literature. *Ann Int Med Dent Res* 2016;2(5):1–3.

16 Answer C. Thanatophoric dysplasia is a short-limbed dwarfism caused by a mutation of fibroblast growth factor receptor 3 gene (FGFR3). It is the most common lethal neonatal skeletal dysplasia. In this disorder, the long bones are short and may have a curved "telephone receiver" appearance (arrowheads). The ribs are shortened. Additionally, the vertebral bodies are flattened and may appear H shaped (arrows). This feature can be used to differentiate thanatophoric dysplasia from the short rib polydactyly syndromes such as Jeune syndrome.

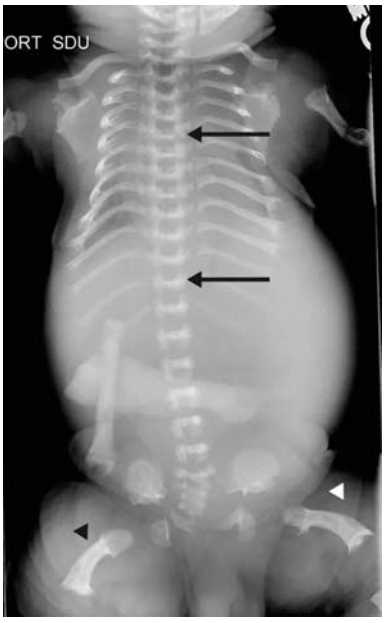

Reference: Miller E, Blaser S, Shannon P, et al. Brain and bone abnormalities of thanatophoric dwarfism. *AJR Am J Roentgenol* 2009;192:48–51.

17 **Answer C.** The most common central nervous system manifestations of thanatophoric dysplasia are the cloverleaf skull deformity and megalencephaly. Additional central nervous system abnormalities are deep fissures and abnormal sulcation of the temporal lobes, a dysplastic hippocampus, and polymicrogyria.
Reference: Miller E, Blaser S, Shannon P, et al. Brain and bone abnormalities of thanatophoric dwarfism. *AJR Am J Roentgenol* 2009;192:48–51.

18 **Answer D.** Osteochondritis dissecans (OCD) of the capitellum is a focal injury of the articular cartilage and subchondral bone within the humeral capitellum. It is most commonly seen in this location in throwing athletes and is typically seen in patients between 12 and 17 years old. The suggested etiology of this lesion is repetitive microtrauma. OCD is most commonly seen within the knee.
On plain radiographs, there is most often a subchondral lucent focus (arrow), but there may be fragmentation or sclerosis. MRI best depicts the OCD where the subchondral abnormality is readily visible (arrowhead).

References: Cruz AI, Shea KG, Ganley TJ. Pediatric knee osteochondritis dissecans lesions. *Orthop Clin N Am* 2016;47:763–775.
Itsubo T, Murakami N, Uemura K, et al. Magnetic resonance imaging staging to evaluate stability of capitella osteochondritis dissecans lesions. *Am J Sports Med* 2014;42:1972–1977.
Jarret DY, Walters MM, Kleinman PK. Prevalence of capitellar osteochondritis dissecans in children with chronic radial head subluxation and dislocation. *AJR Am J Roentgenol* 2016;206:1329–1334.

19 **Answer A.** The prevalence of capitellar osteochondritis dissecans (OCD) is increased in children with radial head subluxation. Capitellar OCD is seen in 32% to 33% of children with chronic radial head subluxation likely because of abnormal radiocapitellar mechanics.
Reference: Jarret DY, Walters MM, Kleinman PK. Prevalence of capitellar osteochondritis dissecans in children with chronic radial head subluxation and dislocation. *AJR Am J Roentgenol* 2016;206:1329–1334.

20 **Answer C.** The criteria for unstable osteochondritis dissecans (OCD) on MRI are the following:
a. Thin line of high signal intensity 5 mm or greater between the OCD and bone
b. Discrete cystic focus 5 mm or greater in diameter beneath the OCD
c. Focal defect with a width of 5 mm or greater in the articular surface of the OCD
d. High signal intensity line extending through the articular cartilage and subchondral bone into the OCD
Reference: Cruz AI, Shea KG, Ganley TJ. Pediatric knee osteochondritis dissecans lesions. *Orthop Clin N Am* 2016;47:763–775.

21 Answer B. The image demonstrates a small osseous fragment adjacent to the pelvis consistent with an avulsion fracture of the anterior superior iliac spine (arrow). The anterior superior iliac spine is the attachment point of the sartorius muscle and tensor muscle of the fascia lata. This injury occurs during forceful extension of the hip and is commonly seen in sprinters. Treatment is activity restriction.

Reference: Stevens MA, El-Khoury GY, Kathol MH, et al. Imaging features of avulsion injuries. *Radiographics* 1999;19:655–672.

22 Answer D. The table below lists the common sites for avulsion injuries of the pelvis and the associated muscular attachments.

Avulsion fracture	Muscle attachment
Iliac crest	Abdominal muscles
Anterior superior iliac spine (ASIS)	Sartorius, tensor fasciae latae
Anterior inferior iliac spine (AIIS)	Rectus femoris
Greater trochanter	Hip rotators
Lesser trochanter	Iliopsoas
Ischial tuberosity	Hamstrings
Body/inferior pubic ramus	Adductors, gracilis

Reference: Stevens MA, El-Khoury GY, Kathol MH, et al. Imaging features of avulsion injuries. *Radiographics* 1999;19:655–672.

23 Answer B. The image demonstrates a metaphyseal corner fracture of the proximal tibia (arrow). This is a disc-shaped fracture though the metaphysis where the fracture line is nearly parallel to the physis. The fracture has been described a corner fracture or bucket handle fracture depending on the orientation of the radiographic projection. This fracture has been called a classic metaphyseal lesion (CML) and is common in abused infants particularly <18 months of age. CMLs are considered highly specific for infant child abuse.

References: Kleinman PK. Diagnostic imaging in infant abuse. *AJR Am J Roentgenol* 1990;155:703–712.
Lonergan GJ, Baker AM, Morey MK, et al. Child abuse: radiologic-pathologic correlation. *Radiographics* 2003;23:811–845.
Thackeray JD, Wannemacher J, Adler BH, et al. The classic metaphyseal lesion and traumatic injury. *Pediatr Radiol* 2016;46:1128–1133.

24 Answer B. A metaphyseal corner fracture or classic metaphyseal lesion (CML) occurs because of shearing injury, which causes differential horizontal motion across the metaphysis. This shearing force is caused by to-and-fro movement such as seen in shaking an infant by holding the infant from the feet or hands or shaking an infant while holding the chest and whiplashing their extremities.

References: Lonergan GJ, Baker AM, Morey MK, et al. Child abuse: radiologic-pathologic correlation. *Radiographics* 2003;23:811–845.
Thackeray JD, Wannemacher J, Adler BH, et al. The classic metaphyseal lesion and traumatic injury. *Pediatr Radiol* 2016;46:1128–1133.

25 Answer D. Although skeletal injuries without an explanation may be concerning for abuse, skeletal imaging findings that are associated with infant nonaccidental injury are metaphyseal corner fractures, rib fractures, sternal fractures, vertebral spinous process fractures, and acromion fractures of the scapula. Metaphyseal corner fractures or classic metaphyseal lesions (CML) are due to shear injury that can be seen with shaking. Rib fractures in infants are rare injuries given the plasticity of the bones. Given this, rib fractures require substantial force but can be seen with squeezing of the chest. Given the rarity of sternal fractures, vertebral spinous fractures, and acromion fractures of the scapula in infants, these fractures are also concerning for abuse. Skull fracture patterns such as multiple fractures, fractures crossing sutures, and bilateral fractures have also been associated with abusive injury.

References: Kleinman PK. Diagnostic imaging in infant abuse. *AJR Am J Roentgenol* 1990;155:703–712.
Lonergan GJ, Baker AM, Morey MK, et al. Child abuse: radiologic-pathologic correlation. *Radiographics* 2003;23:811–845.

26 Answer A. All infants with suspected abusive injury should undergo a skeletal survey. Additionally, a repeat skeletal survey 10 to 14 days following may identify additional injuries that could not be seen on the initial skeletal survey. The recommended views for a skeletal survey of suspected infant abuse are the following:

Axial Skeleton	Appendicular Skeleton
Thorax (AP, lateral, optional right and left Oblique)	Humerus (AP)
Abdomen (AP to include pelvis)	Forearms (AP)
Lumbosacral spine (lateral)	Hands (PA)
Skull (frontal and lateral to include cervical spine)	Femora (AP)
	Tibiae (AP)
	Feet (AP)

References: Kleinman PK. Diagnostic imaging in infant abuse. *AJR Am J Roentgenol* 1990;155:703–712.
Lonergan GJ, Baker AM, Morey MK, et al. Child abuse: radiologic-pathologic correlation. *Radiographics* 2003;23:811–845.

27 Answer A. Radial deficiency or dysplasia is also referred to as clubhand due to failure of development of the radius occurring between the 5th and 6th week of gestation. In this disorder, there are varying degrees of dysplasia, but complete absence of the radius is most common. The trapezium, scaphoid, and thumb are usually absent or deformed. The remainder of the carpal bones and the 2nd through 5th ray are most often normal. Radial dysplasia occurs bilaterally in 50% of affected children.
On physical examination, there is commonly radial and ulnar deviation of the hand due to the unopposed flexor carpi ulnaris and brachioradialis.

Reference: Laor T. Congenital malformations of bone. In: Slovis TS (ed). *Caffey's pediatric diagnostic imaging*. Philadelphia, PA: Elsevier, 2008:2594–2612.

28 Answer A. The table below lists syndromes associated with radial dysplasia.

Syndrome	Other associations
Trisomy 13 Trisomy 18	Chromosomal abnormalities
Holt-Oram syndrome	Congenital heart disease
Cornelia de Lange syndrome Seckel syndrome	Mental delay
Thalidomide embryopathy Varicella embryopathy	Teratogens
Fanconi anemia Thrombocytopenia absent radius	Blood dyscrasias
VACTERL	

Reference: Laor T. Congenital malformations of bone. In: Slovis TS (ed). *Caffey's pediatric diagnostic imaging*. Philadelphia, PA: Elsevier, 2008:2594–2612.

29 Answer E. Osteosarcoma is the most common primary malignant bone tumor of childhood. Osteoblastic osteosarcomas are intramedullary and most commonly occur adjacent to the metaphysis of the long bone. Given that there is osteoid, the osteoblastic osteosarcoma is most often sclerotic on plain radiographs (arrow). If the osteosarcoma invades the cortex, it can produce periosteal reaction along with Codman triangles and a "sunburst" appearance of the cortex.

References: Clayer M. Many faces of osteosarcoma on plain radiographs. *ANZ J Surg* 2015;85:22–26.
Murphey MD, Robbin MR, McRae GA, et al. The many faces of osteosarcoma. *Radiographics* 1997;17:1205–1231.

30 **Answer B.** In osteosarcoma, skip metastases, which are foci of tumor separate from the primary lesion, can be seen. Because of this, when imaging osteosarcomas, it is important to define the extent of the disease by imaging from the proximal to the distal joint.
Although the physis is sometimes considered a barrier to extension of tumors, 75% to 88% of metaphyseal osteosarcomas extend across the physis to the epiphysis. Joint involvement is seen in nearly 25% of osteosarcomas, but the synovium is not often infiltrated. Malignant joint effusions do occur when the joint is invaded, but this is not the reason that both the proximal and distal joints need to be imaged.
Reference: Murphey MD, Robbin MR, McRae GA, et al. The many faces of osteosarcoma. *Radiographics* 1997;17:1205–1231.

31 **Answer B.** Approximately 30% to 40% of patients with localized osteosarcoma will develop recurrence. The most common location for recurrence is within the lung (90%), usually occurring within the first 2 to 3 years. After 5 years, relapse of osteosarcoma is rare, occurring in about 2%. Lung metastases may be calcified.
Reference: Luetke A, Meyers PA, Lewis I, et al. Osteosarcoma treatment—Where do we stand? A state of the art review. *Cancer Treat Rev* 2014;40:523–532.

32 **Answer C.** For the evaluation of the hip in patients up to at least 4 months of age, sonographic examination is recommended. After 4 months, an ultrasound may be attempted, but some advocate a radiograph.
Additionally, sonographic evaluation of an infant with risk factor for hip dysplasia should be delayed until 4 to 6 weeks of life to avoid normal instability of the hip present during the first 2 weeks of life.
References: Gerscovich EO. Infant hip in developmental dysplasia: facts to consider for a successful diagnostic ultrasound examination. *Appl Radiol* 1999;28:18–25.
Harcke HT. Screening newborns for developmental dysplasia of the hip: the role of sonography. *AJR Am J Roentgenol* 1994;162:395–397.

33 **Answer B.** In this infant, the femoral head (*) is subluxed and the acetabulum is shallow consistent with developmental dysplasia of the hip. The slope of the acetabulum with respect to the ilium can be evaluated sonographically (lines). The angle (arrow) formed by these two lines is the alpha angle. An alpha angle of >60 degrees is normal. An alpha angle between 50 and 60 degrees may be physiologic during the first 3 months of age and should be followed up. An alpha angle <50 degrees is abnormal.

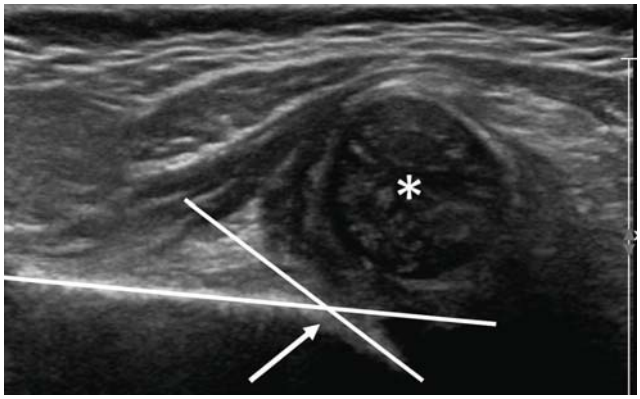

References: Gerscovich EO. Infant hip in developmental dysplasia: facts to consider for a successful diagnostic ultrasound examination. *Appl Radiol* 1999;28:18–25.
Harcke HT. Screening newborns for developmental dysplasia of the hip: the role of sonography. *AJR Am J Roentgenol* 1994;162:395–397.

34 **Answer D.** The main risk factors for developmental dysplasia of the hip are breech presentation at birth, family history of hip dysplasia, and postural deformities such as torticollis or a foot deformity. Additionally, physical examination findings of hip instability, limited range of motion, or a hip click may indicate underlying hip dysplasia.
References: Gerscovich EO. Infant hip in developmental dysplasia: facts to consider for a successful diagnostic ultrasound examination. *Appl Radiol* 1999;28:18–25.
Harcke HT. Screening newborns for developmental dysplasia of the hip: the role of sonography. *AJR Am J Roentgenol* 1994;162:395–397.

35 Answer D. This frontal radiograph of the thoracolumbar spine demonstrates a dextroscoliosis centered at the level of T12–L1. In a dextroscoliosis, there is a rightward curvature of the spine. In a levoscoliosis, there is a leftward curvature of the spine. Additionally, there is a vertebral segmentation anomaly at L1 (arrow). This bifid vertebral body should be identified with this curve and would be an indication for further imaging with MRI.

Reference: Kim H, Kim HS, Moon ES, et al. Scoliosis imaging: what radiologists should know. *Radiographics* 2010;30:1823–1842.

36 Answer B. In a structural scoliotic curve, there are vertebral morphologic changes such as wedging and rotation. The structural curve is not correctable with ipsilateral bending. In a nonstructural curve, there are no vertebral morphologic changes. Given this, a nonstructural curve is correctable with ipsilateral bending. Although a nonstructural curve does not usually progress, it can progress to a structural curve because of ligament shortening from decreased growth on the concave side of the curve. Differentiation of a structural from nonstructural scoliotic curvature is a Cobb angle of 25 degrees or more on ipsilateral side-bending.
Reference: Kim H, Kim HS, Moon ES, et al. Scoliosis imaging: what radiologists should know. *Radiographics* 2010;30:1823–1842.

37 Answer B. The Cobb angle is the measurement of the angle between two lines, one of which is at the superior end plate of the superior end vertebral body and the other at the inferior end plate of the inferior end vertebral body. In adolescent idiopathic scoliosis, observation is recommended for a Cobb angle <20 degrees, bracing is recommended when the Cobb angle is between 20 and 45 degrees, and surgery is recommended when the Cobb angle is >45 degrees. The greatest factors suggesting the probability of progression of an adolescent idiopathic scoliosis are spinal growth velocity and the degree of curvature at presentation.
Reference: Kim H, Kim HS, Moon ES, et al. Scoliosis imaging: what radiologists should know. *Radiographics* 2010;30:1823–1842.

38 **Answer A.** The radiograph demonstrates a lucency extending through the tibial diaphysis (arrow) consistent with a toddler's fracture. This is a nondisplaced fracture of the tibia, which can be radiographically occult. The fracture typical occurs between 9 months and 3 years of age. The most common presenting symptom is refusal to walk or refusal to bear weight on the affected leg. These fractures most often heal without treatment.

Reference: Donnelly L. Toddler's fracture of the fibula. *AJR Am J Roentgenol* 2000;175:922.

39 **Answer D.** In the provided image, there is shortening of the femur with tapering of the proximal femur (arrow) and absence of the femoral head. There is also associated dysplasia of the acetabulum. These findings are consistent with the diagnosis of proximal focal femoral deficiency disorder (PFFD). PFFD is a rare disorder, which is characterized by failure of development of the proximal femur. In this disorder, there is deficiency of the iliofemoral articulation, limb malrotation, and a leg length discrepancy.
The Aitken classification (table) is the most common classification scheme for this disorder.

Class	Femoral head	Femoral segment	Acetabulum
A	Present	Short	Normal
B	Present	Short, usually proximal bony tuft	Developed or moderately dysplastic
C	Absent or very small	Short, usually proximally tapered	Severely dysplastic
D	Absent	Short, deformed	Absent

Reference: Biko DM, Davidson R, Pena A, Jaramillo D. Proximal focal femoral deficiency: evaluation by MR imaging. *Pediatr Radiol* 2012;42:50–56.

40 **Answer D.** In proximal focal femoral deficiency disorder (PFFD), there is maldevelopment of the proximal femur. The femoral head may be present or absent. A coxa vara deformity is often present. The acetabulum may be normal, dysplastic, or absent. In the knee, there may be flattening of the distal femoral epiphysis, underdevelopment of the intercondylar notch, and absent cruciates.
References: Biko DM, Davidson R, Pena A, et al. Proximal focal femoral deficiency: evaluation by MR imaging. *Pediatr Radiol* 2012;42:50–56.
Biko DM, Mill AL, Ho-Fung V, et al. MRI of congenital and developmental abnormalities of the knee. *Clin Radiol* 2012;67:1198–1206.

41 **Answer B.** A tarsal coalition is an abnormality of the foot where two or more tarsal bones are joined by bone, cartilage, or fibrous tissue. In this case, there is irregular sclerosis at the calcaneonavicular joint with decrease in the calcaneonavicular gap (arrow) consistent with a calcaneonavicular tarsal coalition. In approximately 10% of cases, there is an osseous bridge between the calcaneus and the navicular. Additional findings of this disorder are an elongated lateral navicular as it approaches the anterior calcaneus on the lateral view and hypoplasia of the lateral talar head.

References: Newman JS, Newberg AH. Congenital tarsal coalition: multimodality evaluation with emphasis on CT and MR imaging. *Radiographics* 2000;20:321–332.
Zaw H, Calder JDF. Tarsal coalitions. *Foot Ankle Clin N Am* 2010;15:349–364.

42 **Answer B.** Tarsal coalitions are bilateral in approximately 50% of affected individuals. The prevalence of tarsal coalitions is approximately 1% to 2% of the population. Ninety percent of tarsal coalitions involve the talocalcaneal or calcaneonavicular joints.

Reference: Newman JS, Newberg AH. Congenital tarsal coalition: multimodality evaluation with emphasis on CT and MR imaging. *Radiographics* 2000;20:321–332.

43 **Answer D.** Osteogenesis imperfecta (OI) is a genetic disorder commonly referred to as brittle bone disease. In this autosomal dominant inherited disorder, there are abnormalities in type 1 collagen, which leads to fragile, and osteopenic bones.

The severity of this disorder is variable depending on the classification (see answer to Question 44 below). The disorder is suspected clinically in children who present with repeated or unexplained fractures or fractures with minor trauma.

On imaging, patients with OI demonstrate osteopenia, fractures, and bone deformities. The bone deformities occur because of the plasticity of the bones. Other findings include hyperplastic callus formation, ossification of the interosseous membrane, and "popcorn" calcifications. "Popcorn" calcifications (arrow) usually occur in the metaphysis and epiphysis of the bone and are believed to result from microtrauma leading to disordered maturation of the growth plate.

References: Forlino A, Marini JC. Osteogenesis imperfect. *Lancet* 2016;387:1657–1671.
Renaud A, Aucourt J, Weill J. Radiographic features of osteogenesis imperfecta. *Insights Imaging* 2013;4:417–429.
Trejo P, Rauch F. Osteogenesis imperfecta in children and adolescents—new developments in diagnosis and treatment. *Osteoporosis Int* 2016;27:3427–3437.

44 Answer B. The table describes the four main types of osteogenesis imperfecta.

Type of osteogenesis imperfecta (OI)	Features
Type 1	**Mild** Fractures, minor deformities Normal stature Blue sclerae Dentinogenesis imperfecta may be present
Type 2	**Lethal** Fractures in utero Death due to respiratory insufficiency
Type 3	**Severe** Fractures, major deformities Very short stature Dentinogenesis imperfecta is frequent
Type 4	**Moderate** Fractures Short stature Variable sclerae Dentinogenesis imperfecta may be present

Reference: Renaud A, Aucourt J, Weill J. Radiographic features of osteogenesis imperfecta. *Insights Imaging* 2013;4:417–429.

45 Answer D. Bisphosphonate therapy is the most common medical treatment for children with osteogenesis imperfecta (OI). Bisphosphonate therapy consists of cyclic intravenous infusion. The result of this therapy on imaging is dense metaphyseal lines in the long bones which are parallel to the growth plate (arrow). Each line will correspond to the administration of the intravenous bisphosphonate. In the spine and long bones, bisphosphonate therapy results in a "bone within a bone" appearance.

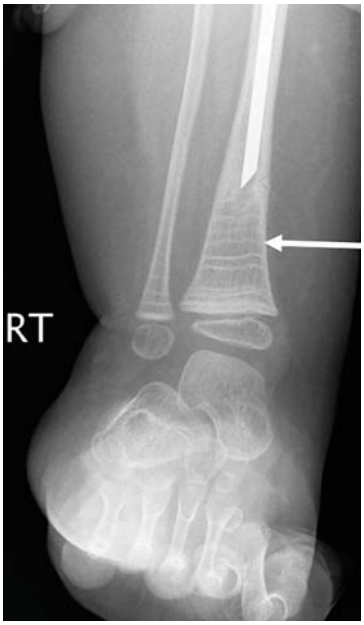

References: Renaud A, Aucourt J, Weill J. Radiographic features of osteogenesis imperfecta. *Insights Imaging* 2013;4:417–429.
Trejo P, Rauch F. Osteogenesis imperfecta in children and adolescents—new developments in diagnosis and treatment. *Osteoporosis Int* 2016;27:3427–3437.

46 Answer D. The image demonstrates a well-circumscribed epiphyseal tumor within the distal femur (arrows). Given the age of the patient and the epiphyseal location, the diagnosis is most likely a chondroblastoma. A chondroblastoma is an uncommon benign cartilaginous tumor most often occurring in the epiphysis or apophysis of long bones. It is most commonly seen in the femur. On plain film evaluation, the tumor is a well-defined oval or round lytic lesion located within the epiphysis or apophysis. On MRI, the tumor is lobulated and heterogenous with associated bone marrow edema. It may have a characteristic thin hypointense rim corresponding to siderosis within the tumor.

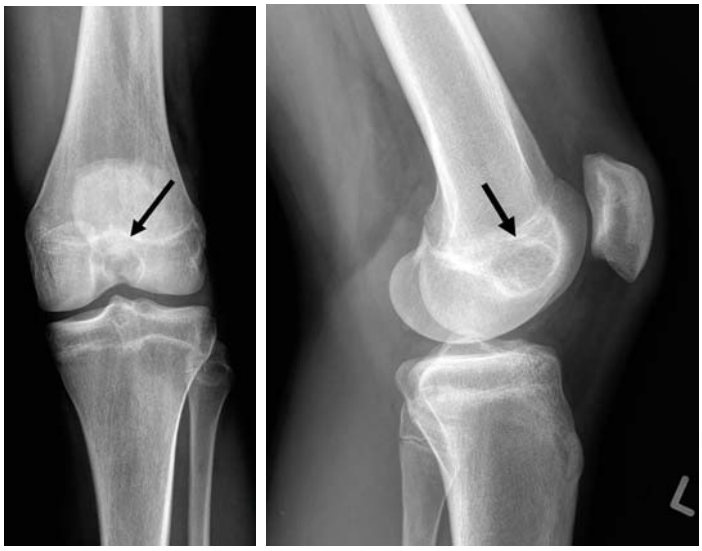

References: DeMattos CBR, Angsanunstsukh C, Akrader A, et al. Chondroblastoma and chondromyxoid fibroma. *J Am Acad Orthop Surg* 2013;21:225–233.
Wooten-Gorges SL. MR imaging of primary bone tumors and tumor-like conditions in children. *Magn Reson Clin N Am* 2009;17:469–487.

47 Answer C. Curettage and bone grafting is the recommended treatment for a chondroblastoma. Tumors sometimes may be widely excised when in bones such as the ribs or fibula. Recurrence rates of chondroblastoma are variable within the literature ranging from 5% to 40%.
Reference: DeMattos CBR, Angsanunstsukh C, Akrader A, et al. Chondroblastoma and chondromyxoid fibroma. *J Am Acad Orthop Surg* 2013;21:225–233.

48 Answer A. The image demonstrates an effusion of the right hip (arrow). In a patient of this age with hip pain and a hip effusion, the most likely diagnosis is transient synovitis. Transient synovitis of the hip is an acute but transient inflammation of the synovium of the hip. It typically occurs in patients 3 to 8 years old who present with hip pain, poor joint mobility, and a limp.

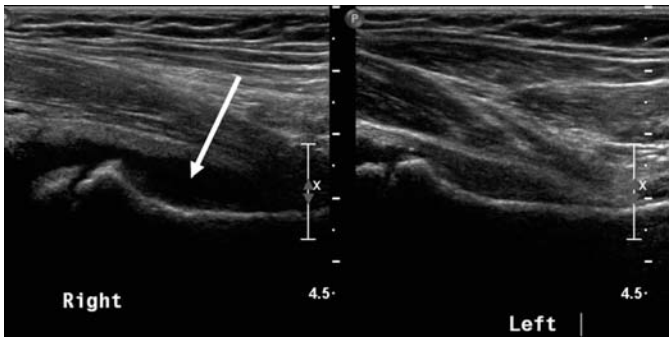

Reference: Paruso S, DiMartino A, Tarantino CC, et al. Transient synovitis of the hip: ultrasound appearance. *J Ultrasound* 2011;14:92–94.

49 **Answer A.** Sinding-Larsen-Johansson syndrome is an osteochondrosis of the inferior pole of the patella commonly seen between the ages of 10 and 14 years of age. It is similar to Osgood-Schlatter disease given that it is a result of repetitive microtrauma due to stress at the insertion of the patellar tendon on the lower pole of the patella. Imaging findings include fragmentation of the inferior pole of the patella (arrow) along with inflammation in Hoffa fat pad (arrowhead). It can be distinguished from patellar sleeve avulsion given the clinical history of chronic knee pain.

References: Dupuis CS, Westra SJ, Makris J, et al. Injuries and conditions of the extensor mechanism of the pediatric knee. *Radiographics* 2009;29:877–886.
Kuehnast M, Mahomed N, Mistry B. Sinding-Larsen-Johansson syndrome. *SAJCH* 2012;6:90–92.

50 **Answer D.** As noted in Answer 49, Sinding-Larsen-Johansson syndrome is an osteochondrosis of the inferior pole of the patella due to traction of the patellar ligament resulting in microtrauma. It is most commonly seen between the ages of 10 and 14 years. On MRI, there is edema of the inferior pole of the patella and proximal patellar tendon. Initial treatment is rest and anti-inflammatory medication such as NSAIDs.

References: Dupuis CS, Westra SJ, Makris J, et al. Injuries and conditions of the extensor mechanism of the pediatric knee. *Radiographics* 2009;29:877–886.
Kuehnast M, Mahomed N, Mistry B. Sinding-Larsen-Johansson syndrome. *SAJCH* 2012;6:90–92.

4 Pediatric Chest Radiology

Questions

1. Newborn presents with respiratory distress. What is the most reliable prenatal predictor of postnatal survival?

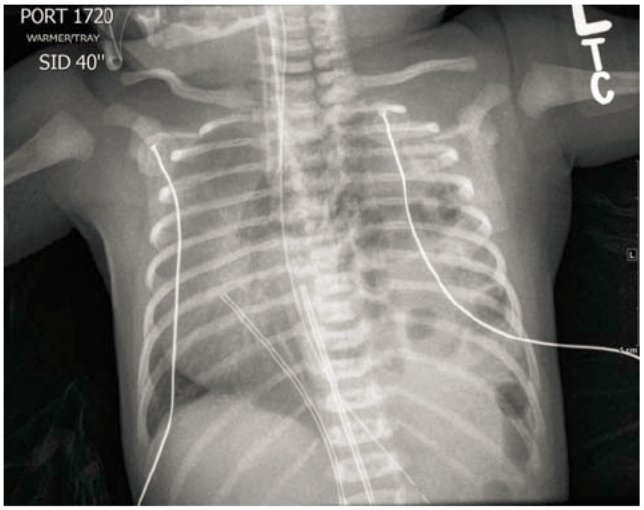

A. Liver herniation
B. Stomach herniation
C. Mediastinal shift
D. Pleural effusion

2. A 4-year-old male with trisomy 21, ventricular septal defect, and patent foramen ovale. CT exam is performed to evaluate for vascular anomalies and lung parenchymal disease.

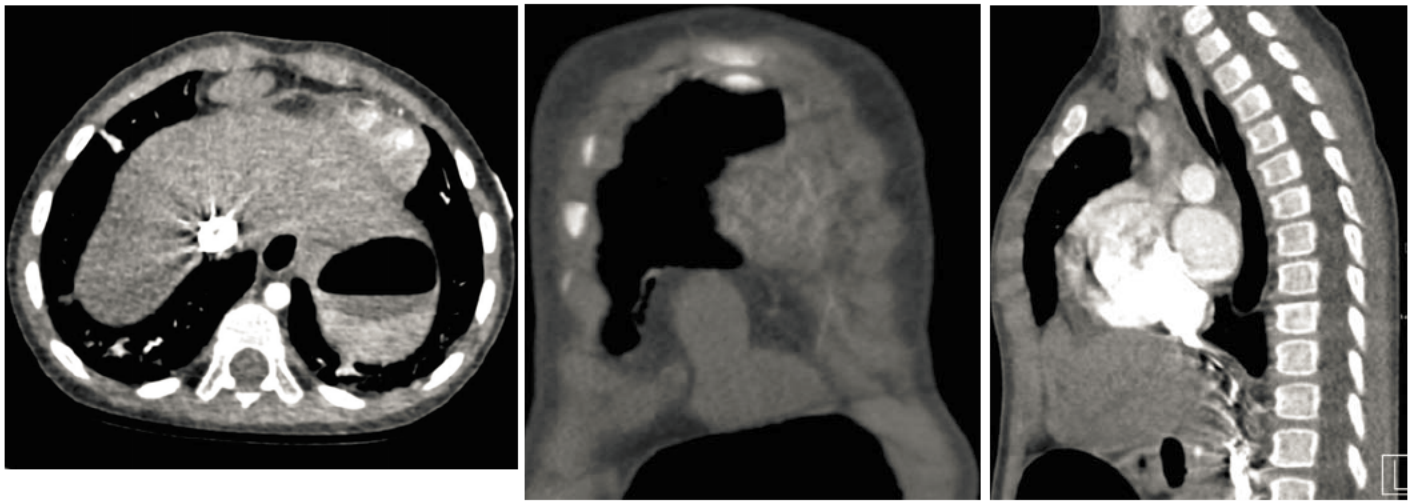

Which of the following diaphragmatic hernias is present?
A. Bochdalek
B. Morgagni
C. Central
D. Eventration

3. A 3-month-old female with prenatally diagnosed lung mass. What is the most likely diagnosis?

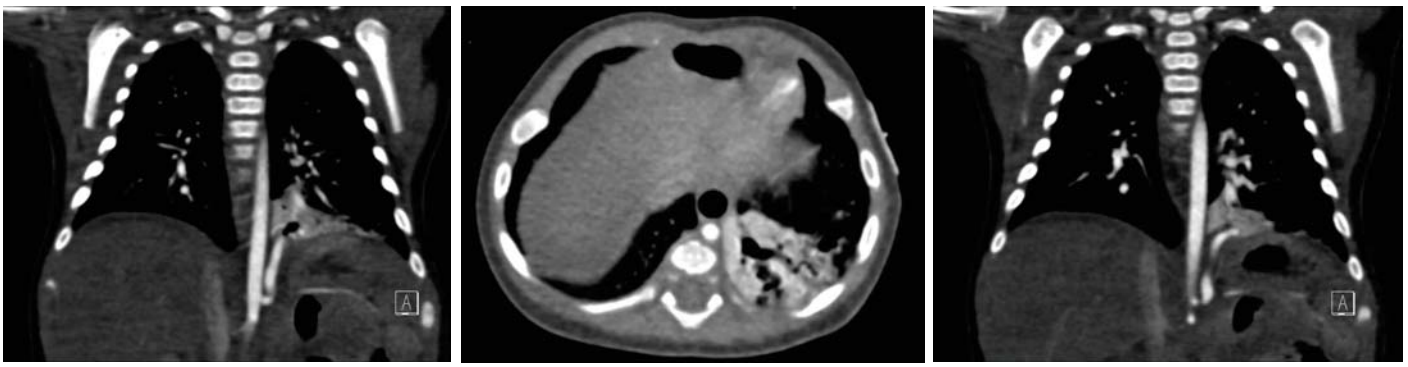

A. Bronchopulmonary sequestration
B. Congenital lobar overinflation
C. Swyer-James syndrome
D. Scimitar syndrome

4. History of abnormal prenatal US. Fetal MRI performed at 30 weeks gestational age and chest radiograph performed shortly after delivery.

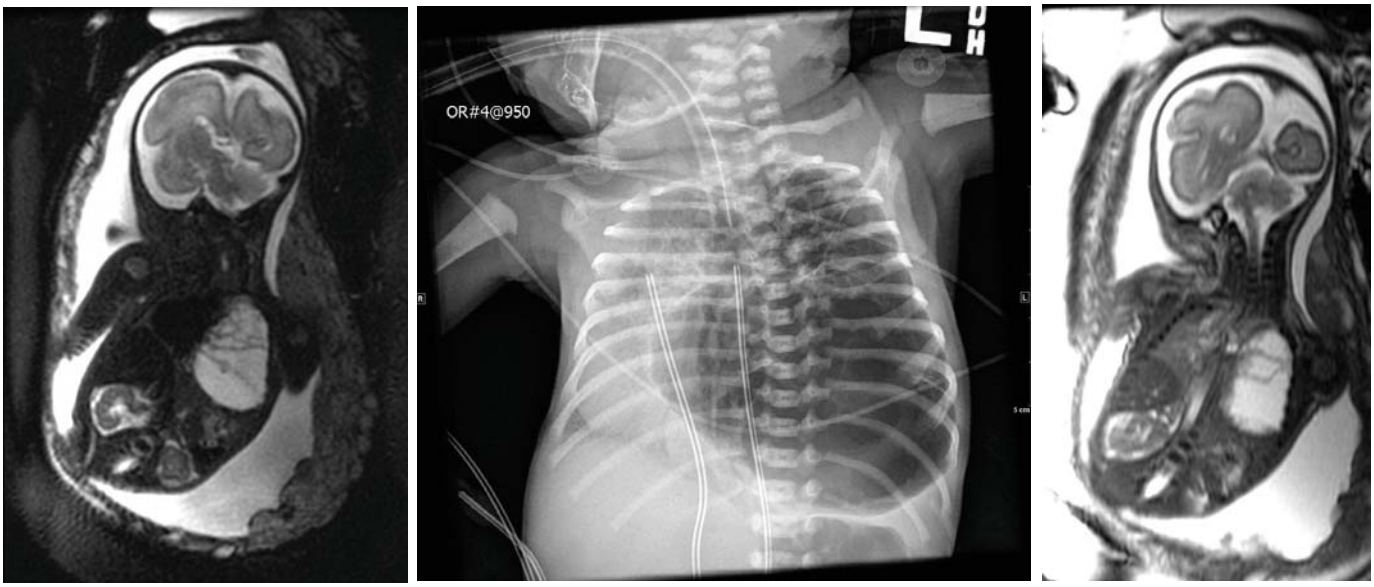

What is the most likely diagnosis?
A. Congenital lobar overinflation
B. Congenital diaphragmatic hernia
C. Congenital pulmonary airway malformation
D. Posttraumatic pneumatocele

5. Which subtype is associated with other congenital abnormalities and malignant potential?
A. Type 0
B. Type 1
C. Type 2
D. Type 3

6. A 2-month-old male infant with tachypnea and failure to thrive. What lobe is most commonly involved with this congenital lung abnormality?

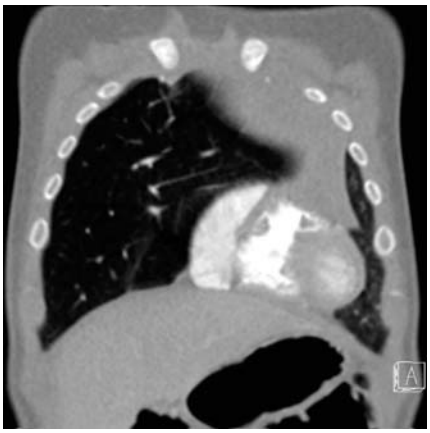
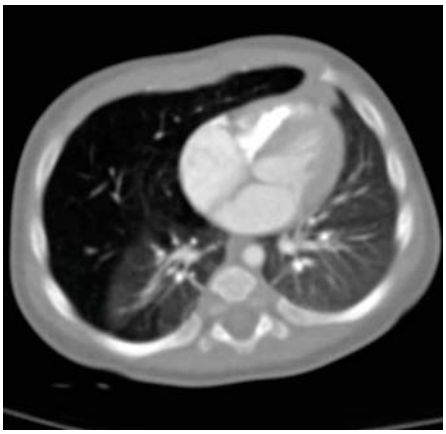
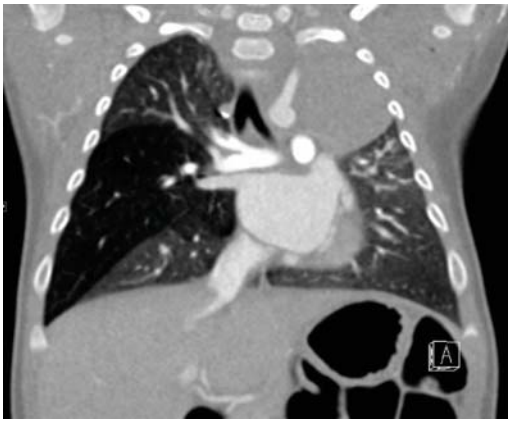
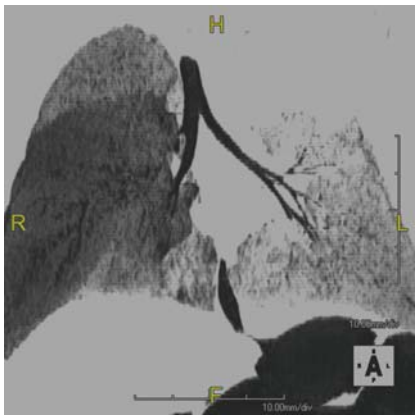

A. Right upper
B. Right lower
C. Left upper
D. Left lower

7. What is the most likely diagnosis?

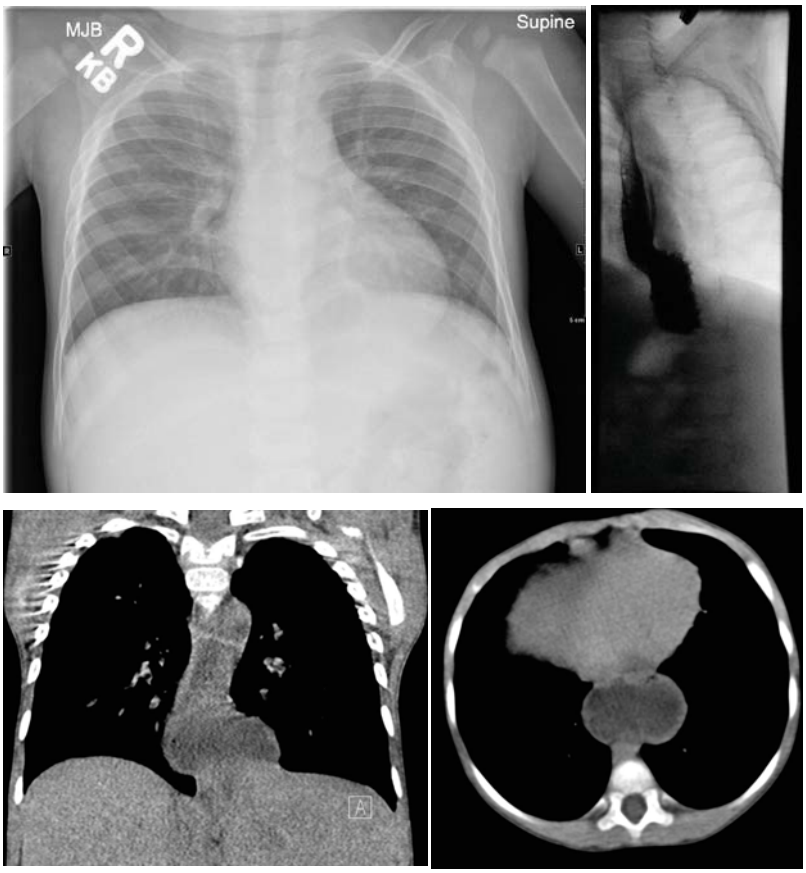

A. Achalasia
B. Foregut duplication cyst
C. Aspirated foreign body
D. Paraesophageal hernia

8. Which of the following thoracic lesions is classically located in the posterior mediastinum?

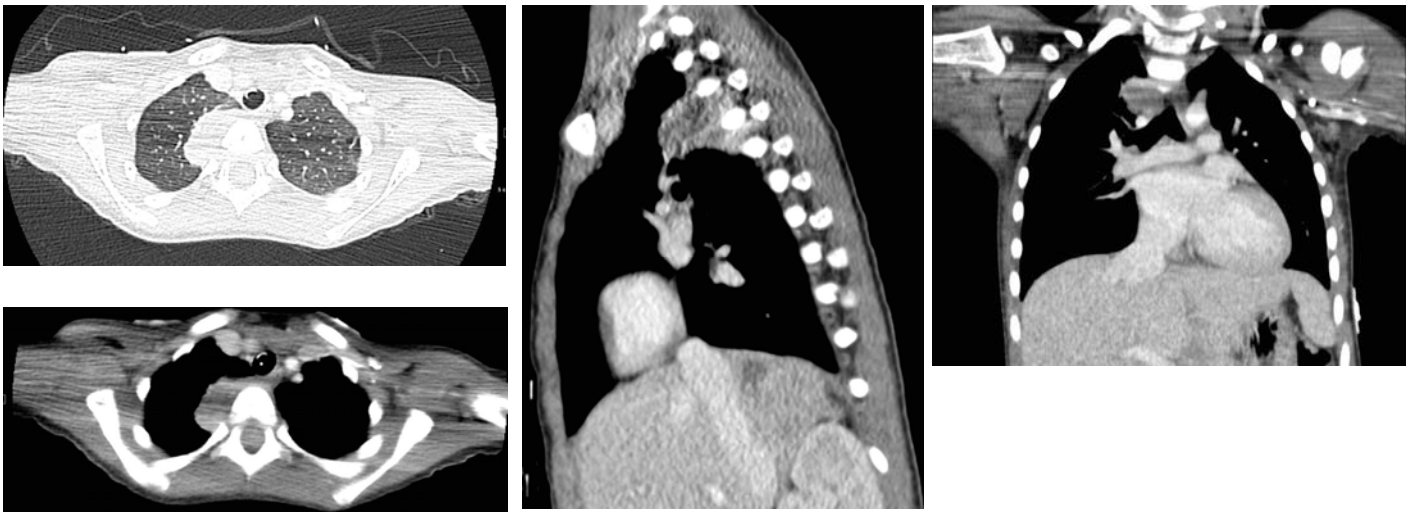

A. Mature teratoma
B. Neuroblastoma
C. Foregut duplication cyst
D. Lymphoma

9. What is the most common infective agent in the setting of round pneumonia?

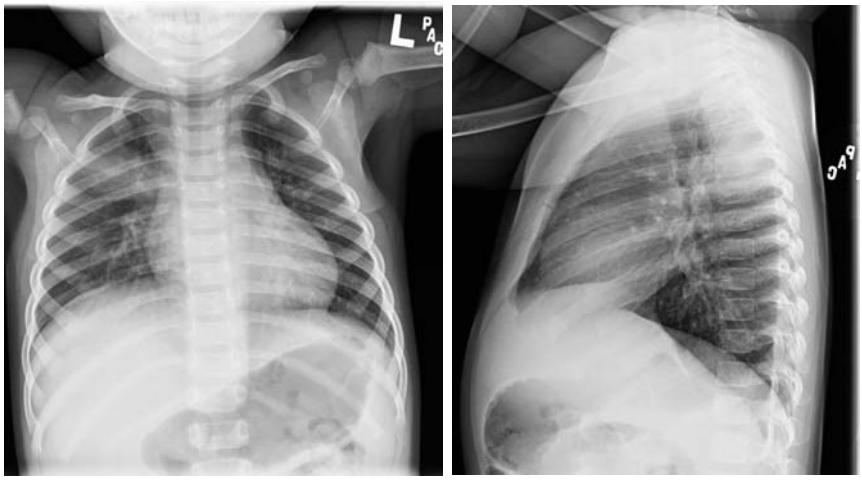

A. *Staphylococcus aureus*
B. *Streptococcus pneumoniae*
C. *Klebsiella pneumoniae*
D. *Mycoplasma pneumoniae*

10. A 6-month-old female with intermittent stridor and increased work of breathing. In the setting of suspected foreign body aspiration, what is the next best step?

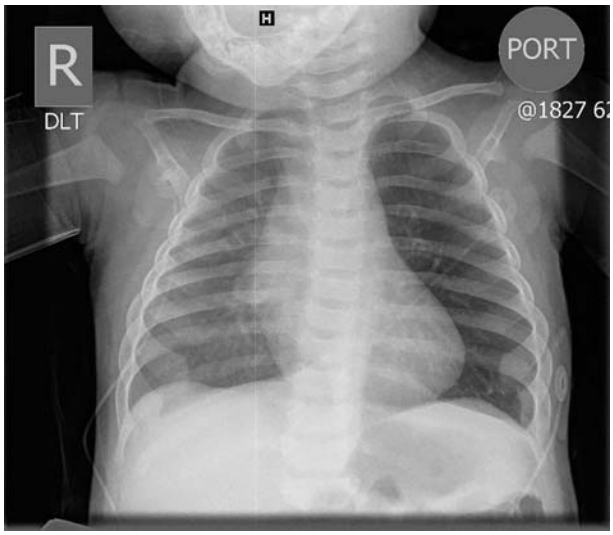

A. Administer broad-spectrum IV antibiotics
B. Perform bronchoscopy
C. Perform lateral decubitus chest radiographs
D. Perform chest CT

11. A 10-year-old female presents with recurrent lung infection. What is the most likely diagnosis?

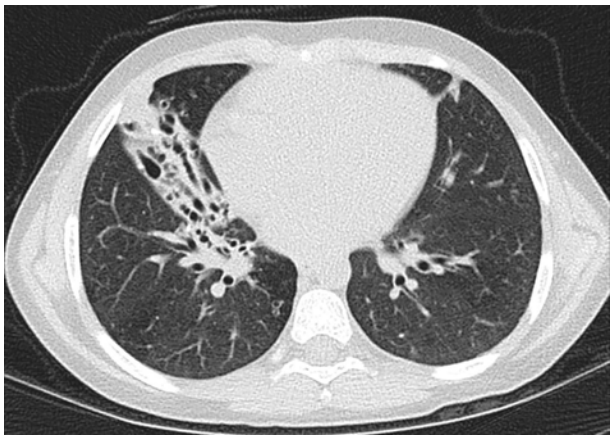

A. Pulmonary tuberculosis
B. Metastatic Wilms tumor
C. Cystic fibrosis
D. Cavitary pneumonia

12. A 19-month-old male with a history of cystic nephroma and DICER-1 mutation. What is the most likely primary lung malignancy demonstrated?

A. Non–small cell carcinoma
B. Mesothelioma
C. Pleuropulmonary blastoma
D. Ewing sarcoma

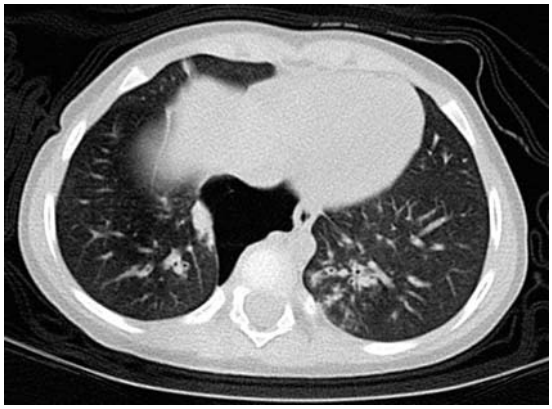

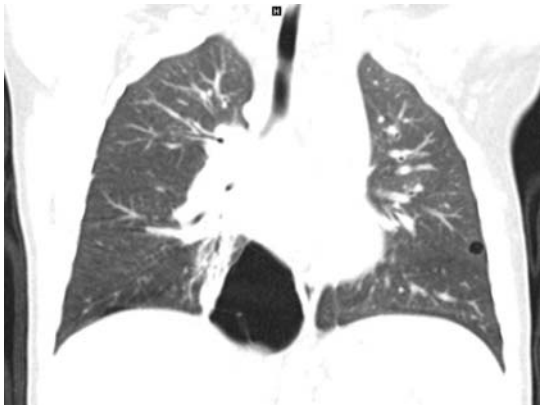

13. Neonate with situs inversus. What anatomic structure is depicted by the yellow arrow? The US correlation of the anatomic structure is provided.

A. Ascending aorta
B. Right pulmonary outflow tract
C. Thymus
D. Esophagus

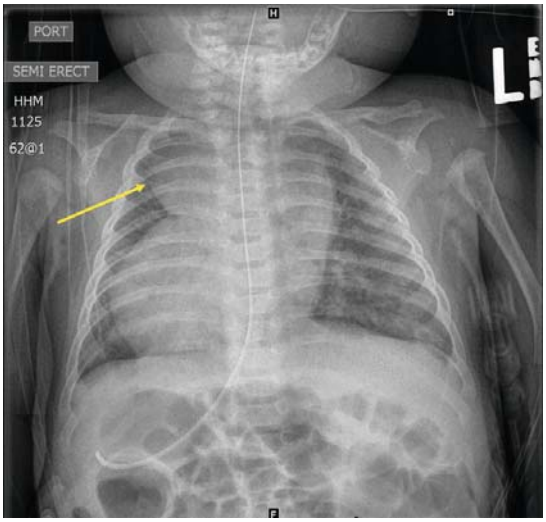

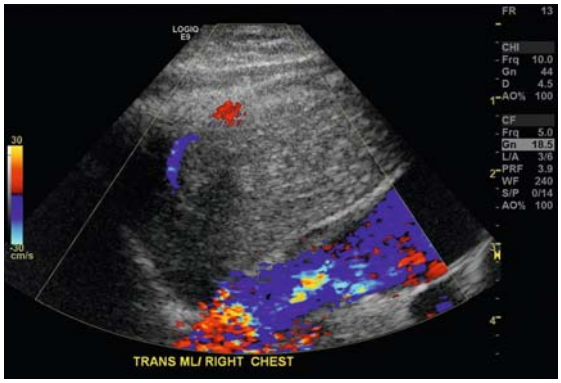

14. What are the top differential diagnoses for an anterior mediastinal mass?

A. Teratoma, foregut duplication cyst, lymphoma
B. Teratoma, thymoma, lymphoma
C. Aortic aneurysm, neuroblastoma, thyroid carcinoma
D. Bronchogenic cyst, paraganglioma, thymoma

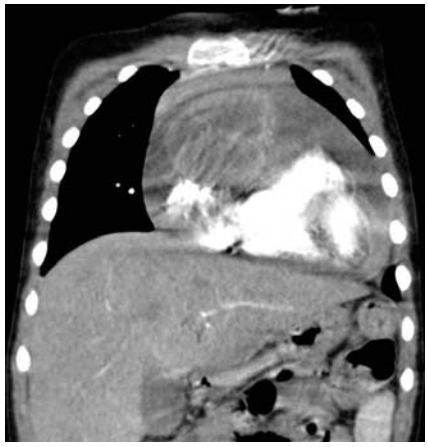

15. A 17-year-old female presents with an abnormal chest radiograph. What is the most likely diagnosis?

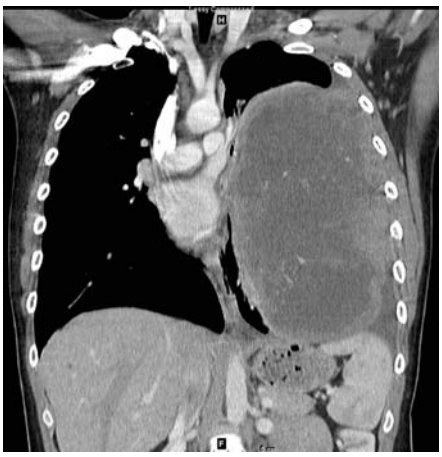

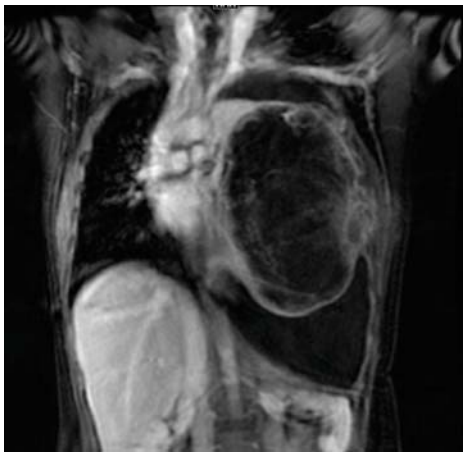

A. Small cell lung carcinoma
B. Mesothelioma
C. Ewing sarcoma
D. Neurofibroma

16. A 4-year-old female presents after liver transplant and airspace disease on chest imaging. What is the most likely infectious etiology based on the following imaging findings?

A. *Haemophilus influenza*
B. *Streptococcus pneumoniae*
C. *Mycobacterium tuberculosis*
D. *Neisseria gonorrhoeae*

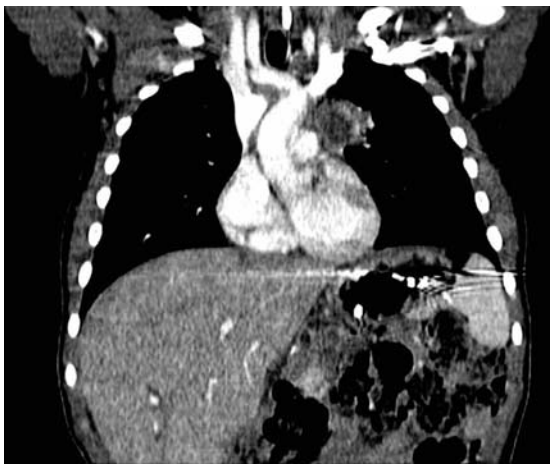


17. A 3-year-old female with abdominal mass felt by the patient's grandmother. What is the most likely malignancy present?

A. Lymphoma
B. Mature retroperitoneal teratoma
C. Colon carcinoma
D. Wilms

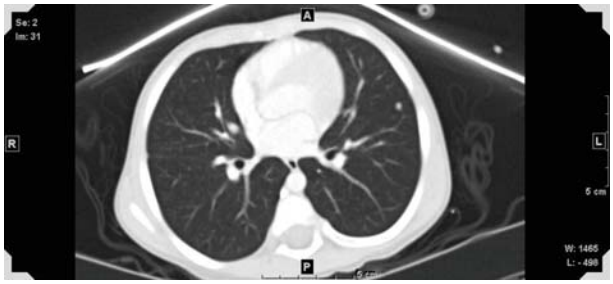

18. A 14-year-old male presents with a chest wall deformity. What measurement is commonly calculated to determine if the patient qualifies for surgical intervention?

A. Haller index
B. Quantitative lung index
C. Lung heart ratio
D. Congenital pulmonary airway malformation volume ratio

19. What surgical procedure was performed on this patient?

A. Video-assisted thoracoscopic surgery
B. Nuss procedure
C. Ravitch procedure
D. Pleurodesis

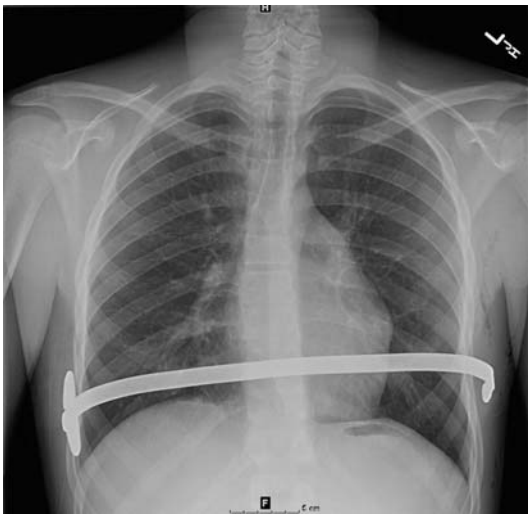

20. A 5-day-old presents with decreased respiratory effort and increased oxygen requirements. What is the most likely diagnosis?

A. Meconium aspiration
B. Transient tachypnea of the newborn
C. Pulmonary interstitial emphysema
D. Pneumatocele

21. A 14-year-old male is imaged after placement of a central venous catheter. What congenital vascular variant is present?

A. Vertical vein
B. Scimitar vein
C. Persistent left-sided superior vena cava
D. Pulmonary sling

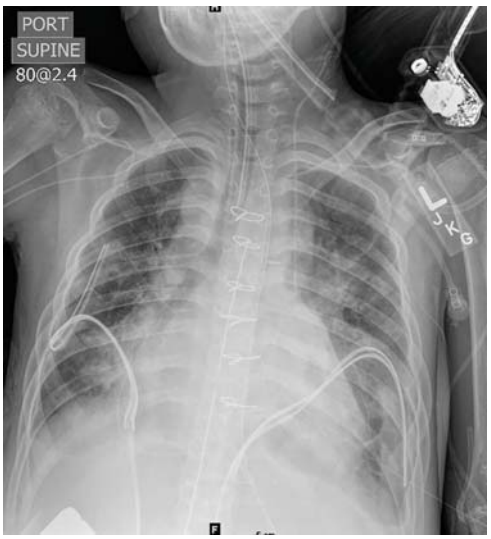

22. A newborn presents with increased work of breathing. Within what thoracic compartment is air abnormally located?

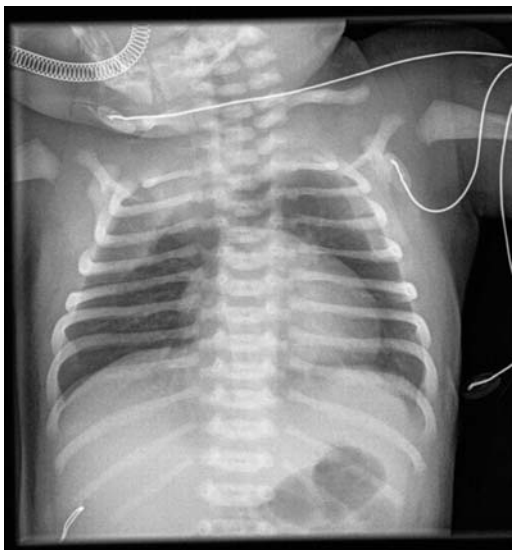
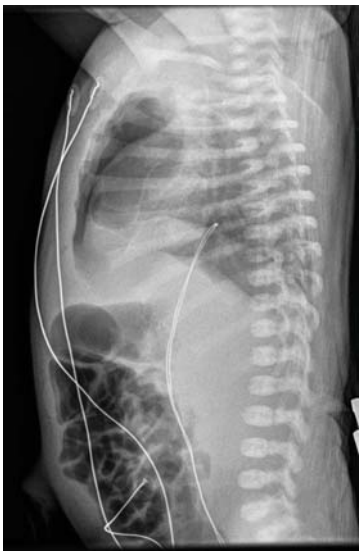
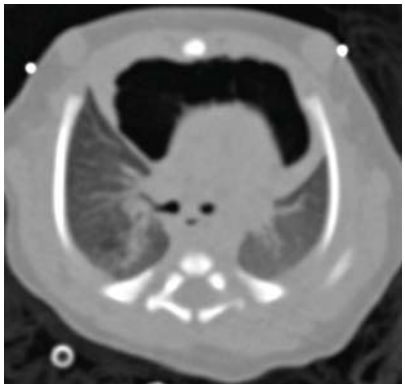
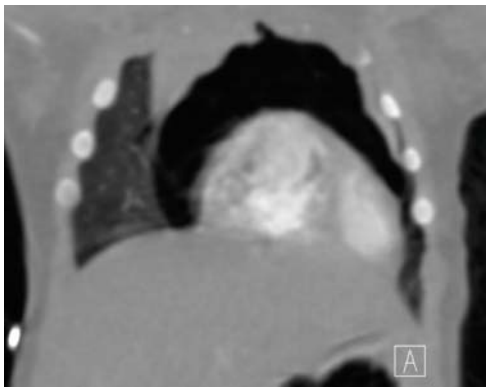

A. Mediastinum
B. Pericardium
C. Pleura
D. Peritoneum

23. A 17-year-old male presents with sepsis. What is the most likely diagnosis?

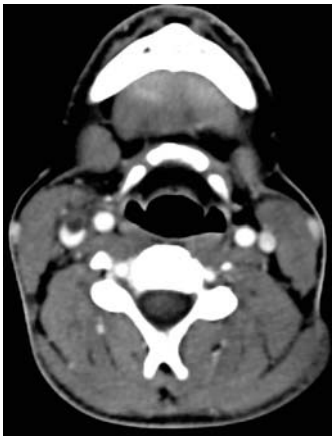
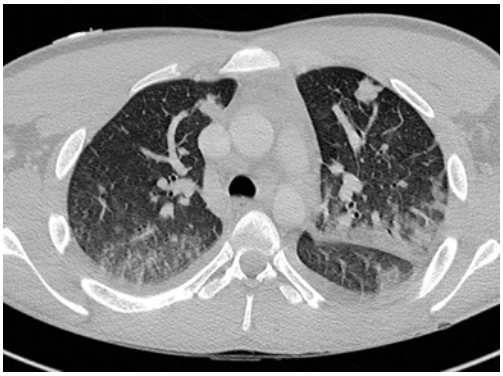


A. Pulmonary artery embolism
B. Lemierre syndrome
C. Aspergillosis
D. Legionnaires disease

24. A newborn male is diagnosed with multiple anomalies prenatally. After delivery, a nasogastric tube is inserted and a chest radiograph is obtained. What is the diagnosis?

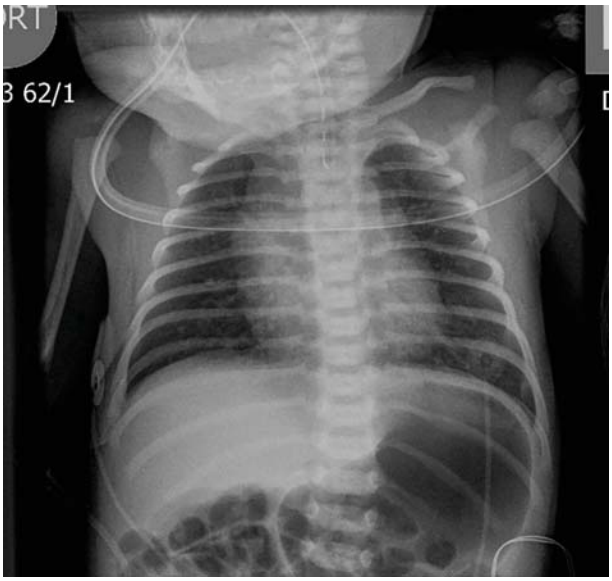

A. Malposition of the nasogastric tube into the tracheal airway
B. Esophageal atresia and tracheoesophageal fistula
C. Choanal atresia
D. Piriform aperture stenosis

25. What is the most common subtype of esophageal atresia and tracheoesophageal fistula?
A. Proximal fistula, distal atresia
B. Isolated fistula, H-type
C. Isolated esophageal atresia
D. Distal fistula, proximal atresia

26. A newborn presents with history of meconium-stained amniotic fluid. What complication in this setting leads to higher morbidity and mortality?

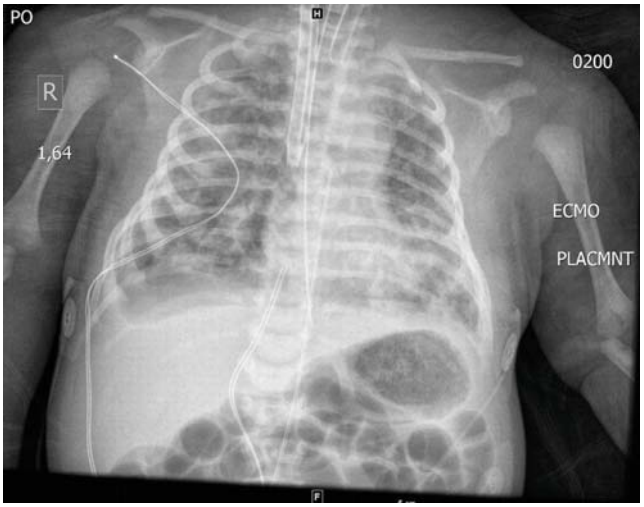

A. Reactive airway disease
B. Air leak
C. Pulmonary interstitial emphysema
D. Pulmonary hypertension

27. A 12-year-old male presents with recurrent lung disease. What is the most likely diagnosis?

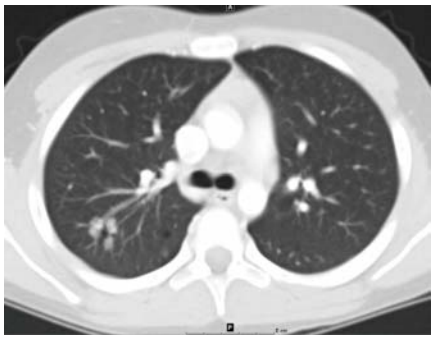

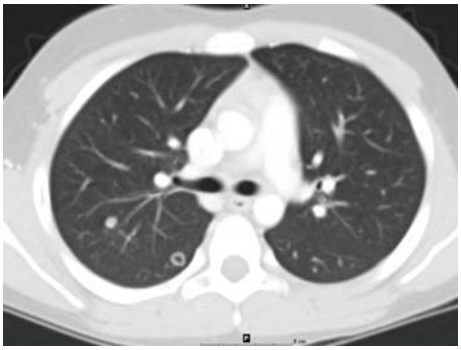

A. Posttransplant lymphoproliferative disorder
B. Tuberculosis
C. Aspergillosis
D. Papillomatosis

28. A 3-month-old male presents with a left humerus fracture. In addition to posterior rib fractures, what other fractured bone is considered highly specific for nonaccidental trauma or child abuse?

A. Long bone
B. Scapula
C. Pelvic
D. Clavicle

29. A 16-year-old male presents from outside hospital after motor vehicle collisions (car hit tree). What is the most appropriate next step?

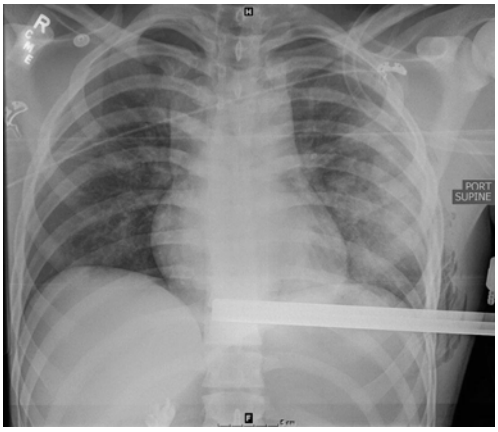

A. Chest ultrasound
B. Abdominal ultrasound
C. CT angiography of the chest
D. Surgical consultation

30. What is the diagnosis?

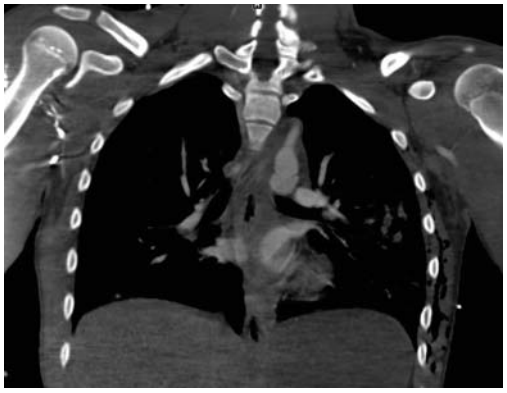

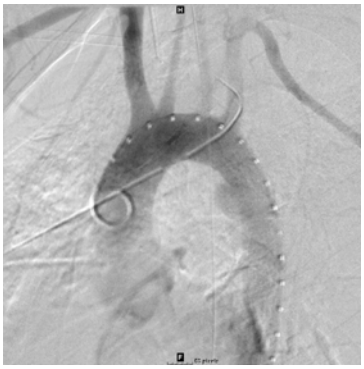

A. Aortic dissection
B. Aortic pseudoaneurysm
C. Tracheal rupture
D. Tension pneumothorax

31. A 30-day-old female with suspected vascular malformation. What is the most likely diagnosis?

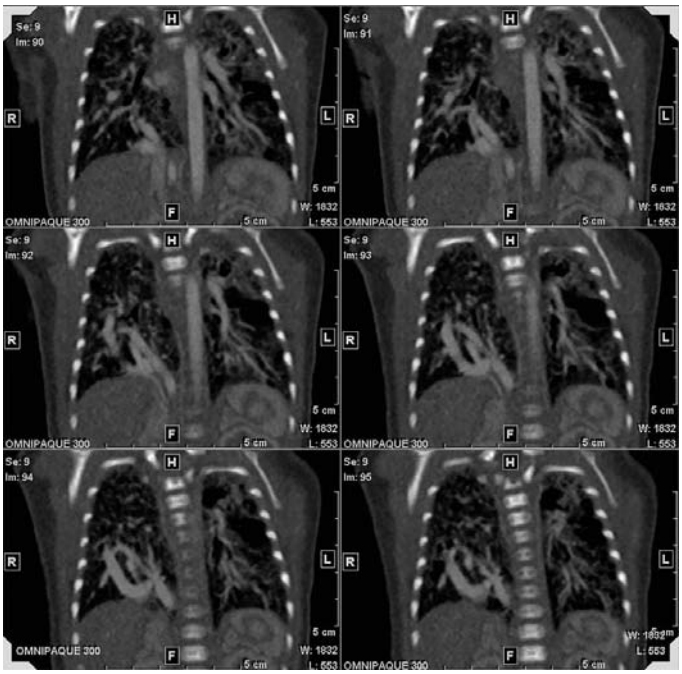

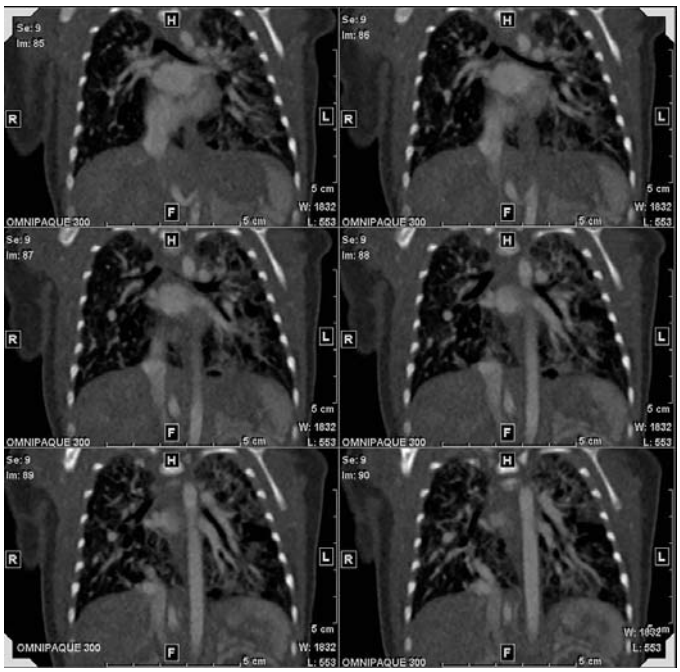

A. Scimitar syndrome
B. Pulmonary arteriovenous malformation
C. Total anomalous pulmonary venous return
D. Disrupted IVC with azygous continuation

32. An 8-month-old with bronchopulmonary dysplasia, hypoplastic left lung, and chronic pneumonia. Follow-up image performed at 3 years old is also presented. What is the likely diagnosis of the lucent left hemothorax on the most recent chest radiograph?

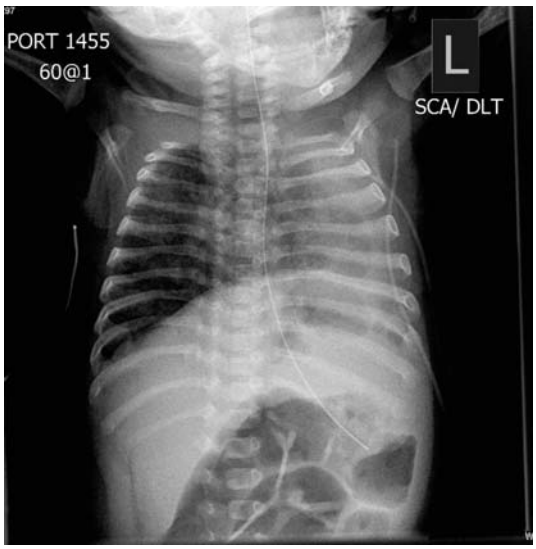

A. Poland syndrome
B. Swyer-James syndrome
C. Sickle cell disease
D. Foreign body aspiration

33. A 1-month-old with chest wall abnormality. Which of the following syndromes is included in the differential diagnoses of a hyperlucent hemithorax?

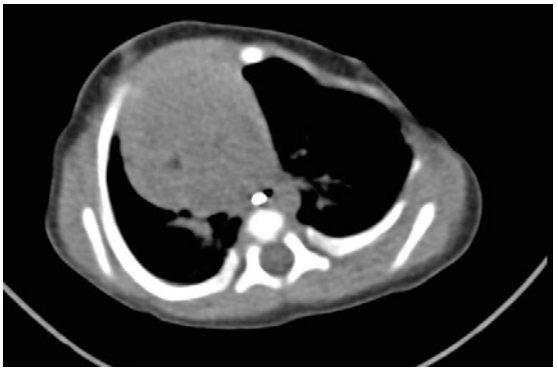

A. Poland syndrome
B. Thoracic outlet syndrome
C. Scimitar syndrome
D. Vanishing lung syndrome

Chest Radiology: Answers and Explanations

1 Answer A. Chest radiograph demonstrates a large left-sided diaphragmatic hernia with herniation of bowel contents into the left hemithorax. The stomach is inferior to the diaphragm. There is rightward mediastinal shift and small right hemithorax and lung. The left lung is not well visualized.
Congenital diaphragmatic hernia (CDH) is a developmental discontinuity of the diaphragm that allows abdominal contents to herniate into the chest. The diaphragmatic defect is usually posterolateral (Bochdalek hernia) but may be anterior retrosternal or peristernal (Morgagni hernia) or rarely central. A majority of diaphragmatic hernias occur on the left. Right-sided diaphragmatic hernias occur in only 10% to 15% of cases. Bilateral herniation is uncommon. With left-sided herniation, the stomach is often involved, whereas the liver is often involved when the hernia is on the right; however, the liver may herniate even with left-sided CDH. Both right- and left-sided hernias involve bowel. A sac may cover the herniated abdominal contents.
Pulmonary changes are most severe on the ipsilateral side but can also occur on the contralateral side. The contralateral side is almost always affected in CDH. Differing degrees of bilateral pulmonary hypoplasia may explain the variation in severity among neonates presenting with respiratory distress and CDH. Prognosis is worse in the setting of an abnormal chromosomal microarray, severe associated anomalies, right-sided defect, liver herniation, and lower fetal lung volume. The most reliable prenatal predictor of postnatal survival is absence of liver herniation.
References: Deprest J, et al. Prenatal management of the fetus with isolated congenital diaphragmatic hernia in the era of the TOTAL trial. *Semin Fetal Neonatal Med* 2014;19:338–348.
Mullassery D, Ba'ath ME, Jesudason EC, Losty PD. Value of liver herniation in prediction of outcome in fetal congenital diaphragmatic hernia: a systematic review and meta-analysis. *Ultrasound Obstet Gynecol* 2010;35:609–614.

2 Answer B. CT imaging of the chest demonstrates a small right anterior diaphragmatic hernia with herniated omentum and liver. Morgagni hernias are one of the congenital diaphragmatic hernias (CDH) and are characterized by herniation through the foramen of Morgagni. When compared to Bochdalek hernias, Morgagni hernias are:

- Anterior
- Right sided (90%)
- Small
- Rare (2% of CDH)
- Lower risk of prolapse

Reference: Aghajanzadeh M, et al. Clinical presentation and operative repair of Morgagni hernia. *Interact Cardiovasc Thorac Surg* 2012;15:608–611.

3 Answer A. There is a focal area of mixed consolidation and cystic change in the left lower lobe. There is an aortic branch that originates left lateral to the celiac artery with a separate ostium and courses cephalad to supply the left lower lobe lesion. The venous blood return of this lesion is to the left atrium through the inferior left pulmonary vein.
Bronchopulmonary sequestration (BPS) is a nonfunctioning mass of lung tissue, with airway and alveolar elements, that lacks normal communication with the tracheobronchial tree and that receives its arterial blood supply from the systemic circulation. The subtypes are classified anatomically, as follows:

- Intralobar sequestration (ILS)

Located within a normal lobe and lacks its own visceral pleura. ILS accounts for about 75% of BPS.

- Extralobar sequestration (ELS)

Located outside the normal lung and has its own visceral pleura. This lesion can also be located below the diaphragm. ELS accounts for about 25% of BPS and is more likely to be associated with other congenital anomalies.

- Hybrid BPS/CPAM lesions

In a hybrid lesion, BPS (either ILS or ELS) occurs in combination with a congenital pulmonary airway malformation (CPAM). These hybrid lesions have histologic features of CPAM and a blood supply from a systemic artery and have been reported in a substantial proportion of cases of BPS.

- Bronchopulmonary foregut malformation (BPFM)

This is a rare variant of sequestration in which the sequestered lung tissue is connected to the gastrointestinal tract. This may occur in either ILS or ELS. Occasionally, BPFM is used as a general term to include all foregut malformations.

BPS preferentially affects the lower lobes. Extralobar sequestrations almost always affect the left lower lobe; however, 10% of extralobar sequestrations can be subdiaphragmatic.

Traditionally, treatment has been a surgical resection. Extralobar sequestrations with their separate pleural investments can usually be removed sparing normal lung tissue, although, with an intralobar type, segmental resection or even lobectomy will be necessary.

References: Berrocal T, Madrid C, Novo S, et al. Congenital anomalies of the tracheobronchial tree, lung, and mediastinum: embryology, radiology, and pathology. *Radiographics* 2004;24(1):e17.

Franco J, Aliaga R, Domingo ML, et al. Diagnosis of pulmonary sequestration by spiral CT angiography. *Thorax* 1998;53(12):1089–1092.

4 Answer C.

5 Answer C. Fetal MRI demonstrates a large mass with multiple T2 hyperintense cysts within the left upper lobe of the lung. The left lower lung is collapsed. The right lung is small. There is left-to-right mediastinal shift. Neonatal chest radiography demonstrates a large lucent lesion within the left hemithorax with mass effect on the right lung and rightward mediastinal shift.

Congenital pulmonary airway malformation (CPAM), previously known as congenital cystic adenomatoid malformation (CCAM), is a developmental anomaly of the lower respiratory tract. Each type of CPAM has distinct pathologic characteristics:

Type 0 is the rarest form and originates from tracheal or bronchial tissue. The cysts are small, with a maximum diameter of 0.5 cm, and are lined with ciliated pseudostratified epithelium. This is a diffuse malformation that involves the entire lung. Gas exchange is severely impaired, and affected infants die at birth.

Type 1 is the most common form of CPAM. Type 1 lesions are comprised of distinct thin-walled cysts 2 to 10 cm in diameter. This type of CPAM has malignant potential. The clinical presentation of type 1 CPAMs depends primarily on the size of the cysts. Large cysts may be detected on prenatal ultrasound.

Type 2 lesions consist of multiple cysts 0.5 to 2 cm in diameter and solid areas that blend into adjacent normal tissue. Extralobar pulmonary sequestrations may have a similar appearance, but unlike type 2 CPAM, these have a systemic blood supply. Other congenital anomalies are observed in patients with type 2 CPAM. Type 2 CPAMs are not at risk for development of malignancy.

Type 3 CPAMs are often very large and can involve an entire lobe or several lobes. They can be a mixture of cystic and solid tissue or be entirely solid. Affected infants present in utero or at birth, usually with severe respiratory distress or death in the neonatal period. This type of CPAM has not been associated with malignancy.

Type 4 lesion cysts have a maximum diameter of 7 cm and consist of nonciliated, flattened, alveolar lining cells, with no mucus cells or skeletal muscle.

References: Biyyam DR, Chapman T, Ferguson MR, et al. Congenital lung abnormalities: embryologic features, prenatal diagnosis, and postnatal radiologic-pathologic correlation. *Radiographics* 2010;30(6):1721–1738.

Chen WS, Yeh GP, Tsai HD, et al. Prenatal diagnosis of congenital cystic adenomatoid malformations: evolution and outcome. *Taiwan J Obstet Gynecol* 2009;48(3):278–281.
Rosado-de-christenson ML, Stocker JT. Congenital cystic adenomatoid malformation. *Radiographics* 1991;11(5):865–886.

6 Answer C. There is an emphysematous and hyperexpanded right middle lobe, of both the medial and lateral segments. Congenital lobar overinflation (CLO) is a developmental anomaly of the lower respiratory tract that is characterized by hyperinflation of one or more of the pulmonary lobes. Other terms for CLO include congenital lobar emphysema and infantile lobar emphysema. Findings include hyperlucency on the affected lung with ipsilateral atelectasis, widened rib spaces, and diaphragmatic flattening. The mediastinum may be displaced away from the affected side and may herniate into the contralateral hemithorax. Patients typically present with respiratory distress, most commonly in the neonatal period, and usually within the first 6 months of life.
There is a predilection for certain lobes:
Left upper lobe, most common
Right middle lobe
Right upper lobe
Rare in the lower lobes
Even though the left upper lobe is the most commonly affected, the right lung is the most common side to be affected.
References: Berrocal T, Madrid C, Novo S, et al. Congenital anomalies of the tracheobronchial tree, lung, and mediastinum: embryology, radiology, and pathology. *Radiographics* 2004;24(1):e17.
Stigers KB, Woodring JH, Kanga JF. The clinical and imaging spectrum of findings in patients with congenital lobar emphysema. *Pediatr Pulmonol* 1992;14(3):160–170.

7 Answer B. Esophagram demonstrates extrinsic compression of the distal thoracic esophagus. CT demonstrates fluid-attenuation structure in the posterior mediastinum, which is intimately in contact with, and deforming, the esophagus.
Foregut duplication cysts or esophageal duplication cysts are congenital anomalies that arise during early embryonic development. They are most frequently found in the proximal small intestine, although they can also be found in the esophagus, stomach, and colon. Approximately 80% of cysts do not communicate with the esophageal lumen; the others generally run parallel to and communicate with the esophageal lumen. They are commonly lined by gastric epithelium. This ectopic gastric mucosa is prone to infection, perforation, and hemorrhage. Patients are generally asymptomatic but may complain of dysphagia because of esophageal compression.
References: Callahan MJ, Taylor GA. CT of the pediatric esophagus. *AJR Am J Roentgenol* 2003;181(5):1391–1396.
Wiechowska-Kozłowska A, Wunsch E, Majewski M, et al. Esophageal duplication cysts: endosonographic findings in asymptomatic patients. *World J Gastroenterol* 2012;18(11):1270–1272.

8 Answer B. CT demonstrates a heterogeneous right paraspinal mass. There is involvement of the right neural foramina at the levels of T3–T5. Neurogenic tumors represent more than 60% of posterior mediastinal masses. Neuroblastomas and ganglioneuroblastomas are malignant tumors that occur most commonly in children and originate from the sympathetic ganglia. Schwannomas and neurofibromas are benign lesions that arise from the intercostal nerve sheath.
Ganglioneuromas are benign lesions that arise from the sympathetic ganglia and are most common in young adults. Lesions that arise from paraganglionic cells include pheochromocytomas and paragangliomas. A spinal meningocele is a herniation of the meninges through a vertebral column defect or through a foramina. These are most commonly located posteriorly and in the lumbosacral region. Although rare, an anterior spinal meningocele will appear to be a posterior mediastinal mass

on imaging. Thoracic teratomas and lymphomas typically occur in the anterior mediastinum. Foregut duplication cysts are typically located in the middle mediastinum.

References: Durand C, Baudain P, Nugues F, Bessaguet S. Mediastinal and thoracic MRI in children. *Pediatr Pulmonol Suppl* 1999;18:60.
Nakazono T, White CS, Yamasaki F, Yamaguchi K, Egashira R, Irie H, et al. MRI findings of mediastinal neurogenic tumors. *AJR Am J Roentgenol* 2011;197(4):W643–W652.

9 Answer B. There is a rounded airspace opacity in the right upper lobe consistent with round pneumonia. The mean age of patients with round pneumonia is 5 years and 90% of patients who present with round pneumonia are younger than twelve. Rounded pneumonia is uncommon after the age of eight because collateral airways tend to be well developed by this age. The infective agent in round pneumonia is bacterial. There is no specific bacterium that causes round pneumonia, but because *Streptococcus pneumoniae* is the most common cause of chest infection, that it is the leading cause of round pneumonia. Follow-up radiographs are not necessary in asymptomatic children with uncomplicated community-acquired pneumonia (CAP). However, in children with complicated CAP or CAP that required intervention, follow-up radiographs help to ensure resolution.

References: Kim YW, Donnelly LF. Round pneumonia: imaging findings in a large series of children. *Pediatr Radiol* 2007;37(12):1235–1240.
Wagner AL, Szabunio M, Hazlett KS, et al. Radiologic manifestations of round pneumonia in adults. *AJR Am J Roentgenol* 1998;170(3):723–726.

10 Answer C. Chest radiography demonstrates asymmetric lucency of the left hemithorax as well as decreased pulmonary vascularity. Additionally, there is hyperinflation of the left lung. Differential considerations include left lung air trapping because of foreign body aspiration or sequela of infection (Swyer-James syndrome). Most foreign bodies are radiolucent. Less than 20% of aspirated foreign bodies are radiopaque. The sensitivity for detecting signs of foreign body aspiration improves over time. On chest radiographs, children have air trapping more often, whereas adults have atelectasis more often. The proportion of patients with foreign body aspiration who have normal findings on chest radiographs varies widely in the literature, and atelectasis or consolidation is often not appreciated for at least 24 hours. If foreign body aspiration is suspected, a normal finding on chest radiographs does not exclude the diagnosis. Expiratory chest radiographs are more sensitive for air trapping than inspiratory chest radiographs. Signs are enhanced lucency and relatively low diaphragm position. If the patient cannot cooperate, lateral decubitus views may demonstrate air trapping in the dependent lung. The gold standard diagnostic and therapeutic intervention is bronchoscopy.

References: Capitanio MA, Kirkpatrick JA. The lateral decubitus film. An aid in determining air-trapping in children. *Radiology* 1972;103(2):460–462.
Passàli D, Lauriello M, Bellussi L, et al. Foreign body inhalation in children: an update. *Acta Otorhinolaryngol Ital* 2010;30(1):27–32.

11 Answer C. CT imaging demonstrates cylindrical and varicose bronchiectasis within the medial right lower and middle lobes. The classic finding of chronic pulmonary involvement of cystic fibrosis is the presence of thick-walled bronchiectasis. These begin as cylindrical and progress through varicoid to cystic forms. The intervening lung is often densely fibrotic and retracted.

Although the entire lung is affected, there is a predilection for:

Central (perihilar) distribution

Upper lobes

Apical segment of lower lobes

Other features include hyperinflation, regions of consolidation, lymph node enlargement, and pneumothorax and pulmonary arterial hypertension.

HRCT has become an important exam in the monitoring of CF patients and is used to guide therapy and assess response to treatment. Scans are repeated every 6 to 18 months depending on the

institution and clinical course. Mucous plugging is of particular importance as it is thought to precede infective exacerbations, and thus, identification of such plugging may be used to trigger changes in therapy.

References: Helbich TH, Heinz-peer G, Fleischmann D, et al. Evolution of CT findings in patients with cystic fibrosis. *AJR Am J Roentgenol* 1999;173(1):81–88.
Maffessanti M, Polverosi R, Dalpiaz G, et al. *Diffuse lung diseases, clinical features, pathology, HRCT*. Milano, Italy: Springer Verlag, 2006.

12 **Answer C.** In the medial inferior right lower lobe abutting the cardiophrenic angle, there is a large cystic mass with multiple septations. In the inferior left upper lobe, there is a peripheral round cyst. Pleuropulmonary blastomas (PPB) are rare, variably aggressive, childhood primary intrathoracic malignancy. Risk factors suggesting a substantial risk of malignancy include:

- Type 4 CPAM—Type 4 CPAM should be considered malignant lesions because approximately 30% of PPB present in a purely cystic form that is indistinguishable from nonmalignant cysts. The presence of a systemic feeding vessel supports a diagnosis of CPAM rather than PBB.
- Cysts that are bilateral or multifocal—There is a substantial risk of malignancy for a child presenting with bilateral or multifocal lung cysts because type 4 CPAMs often have this appearance and carry a malignancy risk.
- Family history of PBB or related diseases—About 25% of PPBs are associated with a familial predisposition to dysplasia and metaplasia, presenting in other family members as PPB or a variety of other malignancies, most of which arise during childhood or early adulthood, as well as cystic lesions, including renal cystic disease, small bowel polyps, and childhood cancers or dysplasias.

Pneumothorax is a prominent feature of type 4 CPAM, occurring in about 40% of cases later diagnosed as PPB.

Reference: Priest JR, Williams GM, Hill DA, Dehner LP, Jaffe A. Pulmonary cysts in early childhood and the risk of malignancy. *Pediatr Pulmonol* 2009;44:14–30.

13 **Answer C.** On chest radiography, a soft tissue opacity is located at the right superior mediastinum. The US demonstrates a homogeneous soft tissue mass similar in echogenicity to the liver and spleen. The thymus is a lymphatic organ that plays a vital role in the development and maturation of the immune system during childhood, specifically T cells, which regulate cellular immunity, and B cells, which are instrumental in regulating humoral immunity. The thymus attains its maximum size during the first few months of life and does not grow any larger beyond puberty. As children grow older and their immune systems mature, the thymus undergoes physiologic involution. Ultimately, the thymus becomes replaced by fat, yet it maintains its original configuration.

On frontal chest radiographs in infants and young children, the thymus is strikingly large but difficult to distinguish from the cardiac silhouette. The thymus usually has smooth borders and remains visible on radiographs through the age of 3 years. The thymic wave sign, a scalloped or wavy contour of the organ, is created by the impression of the anterior reflection of the ribs. The thymic sail sign is a triangular, slightly convex right lobe of the thymus with a sharply demarcated base caused by the minor fissure.

On US images, the thymus in infants may have multiple linear or branching echogenic foci. The echogenicity of the thymus can be similar to slightly hypoechoic compared to the liver and spleen. The thymus is very pliable and does not cause compression or displacement of the adjacent structures. This finding can be a particularly important part of a real-time sonographic examination because cardiac pulsations and respiratory motions affect the shape of the thymus. In contrast, solid tumors or diffuse infiltrative processes are less malleable and more rigid.

References: Nasseri F, Eftekhari F. Clinical and radiologic review of the normal and abnormal thymus: pearls and pitfalls. *Radiographics* 2010;30:413–428.
Nishino M, Ashiku SK, Kocher ON, et al. The thymus: a comprehensive review. *Radiographics* 2006;26(2):335–348.

14 **Answer B.** There is a complex heterogeneous enhancing mass centered within the anterior mediastinum. The classic differential for anterior mediastinal masses includes the 4 Ts: "terrible" lymphoma, teratoma, thymoma, and thyroid carcinoma. Lymphoma is the most common anterior mediastinal mass in children. Although Hodgkin lymphoma typically occurs before age 10 years, non-Hodgkin lymphoma is common in both the first and second decades of life. Teratoma accounts for approximately 60% of all germ-cell tumors in the mediastinum. Most are asymptomatic; however, when large, affected patients may present with respiratory distress because of airway compromise. The presence of fat, fluid, and calcified components within an anterior mediastinal mass in a pediatric patient can help differentiate a teratoma from other types of mediastinal masses. Thymomas may be discovered incidentally, although about one-third of patients have symptoms related to local compression or invasion. About 40% of patients with thymomas present with a paraneoplastic syndrome, such as hypogammaglobulinemia, red cell aplasia, or, most commonly, myasthenia gravis. Middle mediastinal masses include vascular lesions, foregut duplication cysts (e.g., bronchogenic cyst), and lymphadenopathy. Posterior mediastinal masses include sympathetic ganglion tumors (e.g., neuroblastoma) and nerve sheath tumors (e.g., schwannoma).

Reference: Ranganath SH, Lee EY, Restrepo R, Eisenberg RL. Mediastinal masses in children. *AJR Am J Roentgenol* 2012;198:W197–W216. doi: 10.2214/AJR.11.7027. http://www.ajronline.org/doi/abs/10.2214/AJR.11.7027

15 **Answer C.** There is a large mass in the left hemithorax, which appears to arise from the left sixth rib. There is associated bony destruction. The mass is multiloculated and has an enhancing rim and septations. There is significant shift of the mediastinum, which is almost entirely within the right hemithorax. There is no invasion of the mass into the spinal canal or neural foramina. Ewing sarcomas of the chest wall are malignant tumors affecting children and young adults, originating from either the osseous structures or the soft tissues of the chest wall. On imaging, they are usually characterized as a large extrapulmonary invasive soft tissue masses that are heterogeneous due the presence of hemorrhage, necrosis, or cystic changes. Differential diagnoses of chest wall masses include rhabdomyosarcoma, osteosarcoma, chest wall and pleural metastatic disease, lymphoma, and solitary fibrous tumors of the pleura.

References: Saenz NC, Hass DJ, Meyers P, et al. Pediatric chest wall Ewing's sarcoma. *J Pediatr Surg* 2000;35(4):550–555.
Tateishi U, Gladish GW, Kusumoto M, et al. Chest wall tumors: radiologic findings and pathologic correlation: part 2. Malignant tumors. *Radiographics* 2003;23(6):1491–1508.

16 **Answer C.** There is a low-density mass located to the left of the aortic arch. The hypodense masses most likely hilar lymph nodes are visualized at the level of the left hilum. In primary pulmonary tuberculosis, the initial focus of infection can be located anywhere within the lung and may present with patchy areas of consolidation or lobar consolidation. Radiographic evidence of parenchymal infection is seen in 70% of children and 90% of adults. Cavitation is uncommon in primary TB. In most cases, the infection becomes localized and a caseating granuloma forms (tuberculoma), which usually eventually calcifies and is then known as a Ghon lesion. Infected children can present with ipsilateral hilar and contiguous mediastinal (paratracheal) lymphadenopathy, usually right sided. These nodes typically have low-density centers with rim enhancement on CT. Occasionally, these nodes may be large enough to compress adjacent airways resulting in distal atelectasis.

References: Jeong YJ, Lee KS. Pulmonary tuberculosis: up-to-date imaging and management. *AJR Am J Roentgenol* 2008;191(3):834–844.
Leung AN. Pulmonary tuberculosis: the essentials. *Radiology* 1999;210(2):307–322.

17 Answer D. The scout image from the CT examination demonstrates a soft tissue density in the left abdomen displacing bowel loops superiorly and to the right. There are pulmonary nodules in all lobes bilaterally. Wilms tumors are the most common pediatric renal mass, accounting for over 85% of cases and accounts for 6% of all childhood cancers. It typically occurs in early childhood with peak incidence between 3 and 4 years of age. Approximately 80% of these tumors are found before the age of 5 years. When part of a syndrome, they occur even earlier, typically before 24 months of age. Metastases are most commonly to the lung, the liver, and local lymph nodes. Similar to renal cell carcinoma, tumor thrombus into the renal vein, IVC, and right atrium is also characteristic of advanced disease.

References: Guermazi A. *Imaging of kidney cancer*. Berlin, Germany: Springer Verlag, 2006.
Lowe LH, Isuani BH, Heller RM, et al. Pediatric renal masses: Wilms tumor and beyond. *Radiographics* 2000;20(6):1585–1603.

18 Answer A.

19 Answer B. Pectus excavatum is a congenital chest wall deformity characterized by concave depression of the sternum, resulting in cosmetic and radiographic alterations. The Haller index (maximal transverse diameter/narrowest AP length of chest) is used to assess severity of incursion of the sternum into the mediastinum. A normal Haller index is 2.5. Significant pectus excavatum has an index >3.25, representing the standard for determining candidacy for repair.

Surgical options include metal bar insertion, rib osteotomies, disconnection of the sternum from costal cartilages, and even reversal of the sternum. The Nuss procedure is a minimally invasive procedure where a concave bar is inserted substernally. It has largely replaced the Ravitch procedure, which was significantly more invasive.

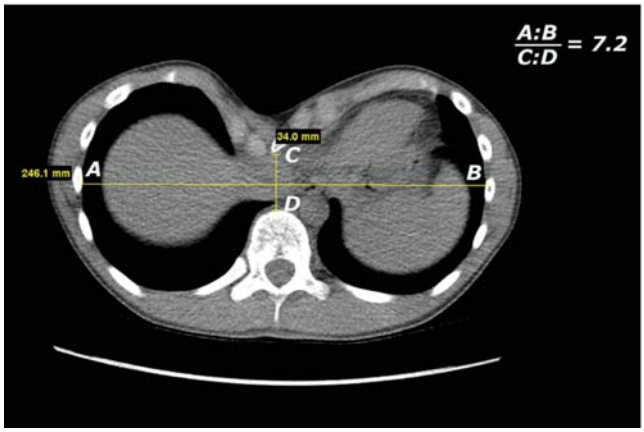

References: Haller AJ, Kramer SS, Lietman SA. Use of CT scans in selection of patients for pectus excavatum surgery: a preliminary report. *J Pediatr Surg* 1987;22(10):904–906. http://dx.doi.org/10.1016/S0022-3468(87)80585-7
Jaroszewski DE, Fonkalsrud EW. Repair of pectus chest deformities in 320 adult patients: 21 year experience. *Ann Thorac Surg* 2007;84(2):429–433.

20 Answer C. Chest radiograph demonstrates left lung hyperinflation and multiple rounded lucencies in the left lung. Pulmonary interstitial emphysema (PIE) refers to the abnormal location of air within the pulmonary interstitium and lymphatics. It typically results from rupture of overdistended alveoli following barotrauma in infants who have hyaline membrane disease. Meconium aspiration is encountered in term infants and presents with high lung volumes, asymmetric patchy lung opacities, and occasionally pneumothorax because of small airway obstruction. Transient tachypnea of the newborn (TTN), also known as retained fetal fluid or wet lung disease, presents in the neonate as tachypnea for the first few hours of life, lasting up to 1 day. The images in TTN typically demonstrate pulmonary edema and small pleural effusions. Pneumatoceles are intrapulmonary air-filled cystic spaces that can have a variety of sizes and appearances. They may contain air–fluid levels and are usually the result of ventilator-inducted lung injury in neonates or postpneumonic.

References: Cleveland RH. A radiologic update on medical diseases of the newborn chest. *Pediatr Radiol* 1996;25(8):631–637.
Greenough A, Dixon AK, Roberton NR. Pulmonary interstitial emphysema. *Arch Dis Childhood* 1984;59:1046–1051.

21 **Answer C.** Right upper extremity PICC line is coiled back upon itself with tip at level of right brachial artery. Left internal jugular vein catheter tip terminates in the lower portion of a persistent left-sided SVC (PLSVC). A PLSVC is the most common congenital venous anomaly in the chest and can result in a right-to-left shunt. The majority of cases are asymptomatic and the presence of the vessel is only identified incidentally during CT scanning of the chest or as a result of line placement as in this example. There are different possible drainage sites:
1. Coronary sinus: functionally insignificant because venous return from the head, neck, and upper limbs is delivered to the right atrium
2. Left atrium: results in a right-to-left shunt, which is usually not large enough to cause cyanosis or symptoms

References: Kellman GM, Alpern MB, Sandler MA, et al. Computed tomography of vena caval anomalies with embryologic correlation. *Radiographics* 1988;8(3):533–556.
Pretorius PM, Gleeson FV. Case 74: right-sided superior vena cava draining into left atrium in a patient with persistent left-sided superior vena cava. *Radiology* 2004;232(3):730–734.

22 **Answer A.** There is air in the mediastinum with mass effect and deviation of the thymus to the right. Pneumomediastinum is the presence of extraluminal gas within the mediastinum. Gas may originate from the lungs, trachea, central bronchi, esophagus, and peritoneal cavity and track from the mediastinum to the neck or abdomen. Etiologies include blunt or penetrating chest trauma, surgery, esophageal perforation, tracheobronchial perforation, barotrauma, infection, and idiopathic.
A pneumopericardium can usually be distinguished from pneumomediastinum, because air in the pericardial sac should not rise above the anatomic limits of the pericardial reflection on the proximal great vascular pedicle. Also, on radiographs obtained with the patient in the decubitus position, air in the pericardial sac will shift immediately, whereas air in the mediastinum will not shift in a short interval between films.
Occasionally, it may not be possible to distinguish pneumopericardium from pneumomediastinum on plain film.

References: Bejvan SM, Godwin JD. Pneumomediastinum: old signs and new signs. *AJR Am J Roentgenol* 1996;166(5):1041–1048. doi: 10.2214/ajr.166.5.8615238.
Karoui M, Bucur PO. Images in clinical medicine. Pneumopericardium. *N Engl J Med* 2008;359(14):e16. doi: 10.1056/NEJMicm074422.

23 **Answer B.** There is a thrombus within the right internal jugular vein. Peripheral, nodular-shaped opacities are visualized in the upper lobes. Patchy consolidations are seen in the lungs. Lemierre syndrome refers to thrombophlebitis of the jugular vein with distant metastatic sepsis in the setting of initial oropharyngeal infection such as pharyngitis/tonsillitis with or without peritonsillar or retropharyngeal abscess. Bacteremia and distal infective thromboembolism is common (lungs most commonly affected); however, almost any organ may be involved. An anaerobic gram-negative bacillus, Fusobacterium necrophorum, is responsible for a majority of cases and gives rise to the term necrobacillosis.

Reference: O'brien WT, Lattin GE, Thompson AK. Lemierre syndrome: an all-but-forgotten disease. *AJR Am J Roentgenol* 2006;187(3):W324.

24 **Answer B.**

25 Answer D. There is a feeding tube with its tip at the level of the T3 vertebral body. There is gas in the stomach and bowel loops. Esophageal atresia refers to an absence in contiguity of the esophagus because of an inappropriate division of the primitive foregut into the trachea and esophagus. This is the most common congenital anomaly of the esophagus. It is frequently associated with a tracheoesophageal fistula. The types of esophageal atresia/tracheoesophageal fistula can be divided into:

- Proximal atresia with distal fistula: 85%
- Isolated esophageal atresia: 8% to 9%
- Isolated fistula (H-type): 4% to 6%
- Double fistula with intervening atresia: 1% to 2%
- Proximal fistula with distal atresia: 1%

The presence of air in the stomach and bowel in the setting of esophageal atresia implies that there is a distal fistula if feeding tube insertion has been attempted. This may show the tube blind looping and turning back at the upper thoracic part of the esophagus or heading into the trachea and/or bronchial tree.

Esophageal atresias are frequently associated with various other anomalies (50% to 75% of cases). They include:

- Other intestinal atresias
  - Duodenal atresia
  - Jejunoileal atresia
  - Anal atresia
- Annular pancreas
- Pyloric stenosis
- VACTERL association inclusive of congenital cardiac anomalies
- CHARGE syndrome
- Increased incidence of chromosomal anomalies such as
  - Trisomy 21
  - Trisomy 18

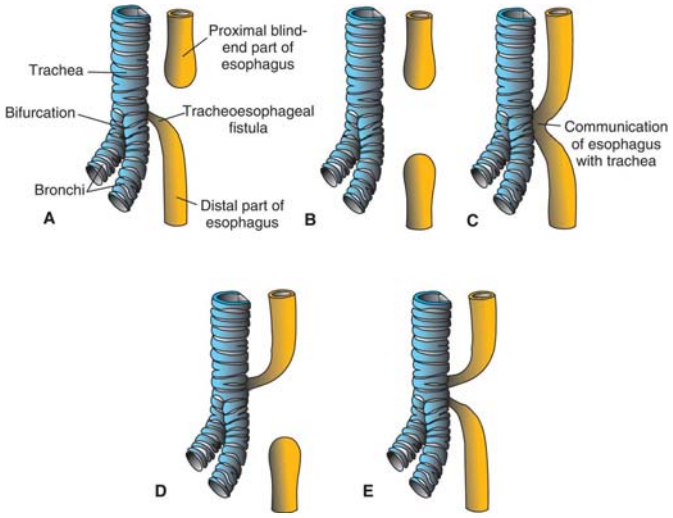

Reference: Berrocal T, Madrid C, Novo S, et al. Congenital anomalies of the tracheobronchial tree, lung, and mediastinum: embryology, radiology, and pathology. *Radiographics* 2004;24(1):e17.

26 Answer D. Bilateral interstitial and airspace opacities are most compatible with meconium aspiration. ECMO catheters are in place. Meconium aspiration syndrome (MAS) occurs secondary to intrapartum or intrauterine aspiration of meconium, usually in the setting of fetal distress and usually in term or postterm infants. The mortality rate for MAS resulting from severe parenchymal pulmonary disease and pulmonary hypertension is as high as 20%. Other complications include air leak syndromes (e.g., pneumothorax, pneumomediastinum, pneumopericardium), which occur in 10% to 30% of infants with MAS. The neurologic disabilities of survivors are not due primarily to the aspiration of meconium but rather by in utero pathophysiology, including chronic hypoxia and acidosis.

Reference: Ghidini A, Spong CY. Severe meconium aspiration syndrome is not caused by aspiration of meconium. *Am J Obstet Gynecol* 2001;185(4):931–938. ISSN: 0002-9378.

27 **Answer D.** There are well-defined, rounded, pulmonary nodules, many with cavitation, located in both lungs. Tracheobronchial or recurrent respiratory papillomatosis is a disease caused by the human papillomavirus (HPV). Imaging typically demonstrates airway wall (e.g., laryngeal, tracheal) thickening or nodularity and multiple pulmonary nodules and masses. The larger nodules are more likely to cavitate. The posterior, dependent lungs are more likely to be seeded. Most nodules grow slowly; however, rapid growth may represent conversion to squamous cell carcinoma.

References: Jhun BW, et al. The clinical, radiological, and bronchoscopic findings and outcomes in patients with benign tracheobronchial tumors. *Yonsei Med J* 2014;55(1):84–91.
Marchiori E, et al. Tracheobronchial papillomatosis with diffuse cavitary lung lesions. *Pediatr Radiol* 2010;40(7):1301–1302; author reply 1303.

28 **Answer B.** In addition to the left humerus fracture, there are nondisplaced fractures of the left fifth, sixth, and seventh lateral ribs without associated callus formation. The high-specificity skeletal fractures for nonaccidental trauma (NAT) include:

- Bucket-handle or corner fractures
- Ribs (especially posterior)
- Scapula (e.g., acromion)
- Spine (especially spinous processes)
- Sternum

The classical metaphyseal corner or bucket-handle fracture is virtually pathognomonic for NAT. Rib fractures are very common and highly specific for NAT in children <2 years old. Fractures of the acromion, sternum, and spinous processes are so rare in other conditions and therefore are considered a high specificity for NAT.

Rib fractures are easily overlooked on radiographs. These fractures are usually not evident on radiographs in the acute stage, as little displacement occurs. They are typically identified in the healing stage as a result of callus formation. It is imperative to routinely include oblique views of the chest while performing the skeletal survey to adequately diagnose rib fractures in the setting of NAT.

References: Kleinman PL, Kleinman PK, Savageau JA. Suspected infant abuse: radiographic skeletal survey practices in pediatric health care facilities. *Radiology* 2004;233(2):477–485.
Lonergan GJ, Baker AM, Morey MK, et al. From the archives of the AFIP. Child abuse: radiologic-pathologic correlation. *Radiographics* 2003;23(4):811–845.

29 **Answer C.** CT angiography of the chest. Approximately 25% of deaths from blunt trauma arise from chest injuries, although up to 50% of deaths are at least partially related to thoracic injuries. It is essential to diagnose and treat emergent thoracic injuries quickly, and imaging plays an essential role in diagnosing these injuries. The imaging manifestations of thoracic trauma are diverse and include musculoskeletal, pleural, pulmonary, and mediastinal findings. The most devastating injury to the thorax from blunt trauma is acute aortic injury or transection, and the most common thoracic injury is a rib fracture. ACR Appropriateness Criteria® topic on "Blunt Chest Trauma—Suspected Aortic Injury", supports the use of chest CT angiography (CTA) in combination with chest radiography without reservation. The authors reported evidence that CTA is highly sensitive (with a high negative predictive value) in evaluating suspected traumatic aortic injury when there are no signs of direct aortic injury. CTA is also highly specific for aortic injury, such that most centers have now abandoned invasive aortography in the initial assessment of patients with suspected aortic injury from trauma.

References: Calhoon JH, Trinkle JK. Pathophysiology of chest trauma. *Chest Surg Clin N Am* 1997;7(2):199–211.
Ungar TC, Wolf SJ, Haukoos JS, et al. Derivation of a clinical decision rule to exclude thoracic aortic imaging in patients with blunt chest trauma after motor vehicle collisions. *J Trauma* 2006;61(5):1150–1155.

30 **Answer B.** Chest radiography demonstrates an abnormally widened mediastinum. CT angiography of the chest and aortic angiography demonstrates pseudoaneurysm formation at the isthmus of the descending thoracic aorta.

Trauma to the aorta may result in:

- Aortic laceration: a tear in the intima, which may extend through the vessel wall; the tear is typically transverse
- Aortic transection: laceration of all three layers of the vessel wall, also known as aortic rupture
- Aortic pseudoaneurysm: aortic rupture contained by adventitia or periaortic tissue
- Aortic intramural hematoma: hematoma within the wall of the aorta

An aortic dissection is a longitudinal tear in the aortic wall and is rarely a sequelae of trauma. Aortic pseudoaneurysms are contained ruptures of the aorta in which the majority of the aortic wall has been breached, and luminal blood is held in only by a thin rim of the remaining wall or adventitia. They typically occur from focal aortic. The pseudoaneurysms typically occur along the undersurface of the aortic isthmus at or near the site of the ductus arteriosus. The isthmus is a portion of the proximal descending thoracic aorta between the left subclavian artery origin and the ligamentum arteriosum. Tethering of the aorta by the ligamentum arteriosum is believed to account for the high frequency of aortic injury in this region. Aortic injury is a surgical emergency. Treatment is with an aortic stent graft or open repair. An aortic stent graft is demonstrated in the following image.

References: Creasy JD, Chiles C, Routh WD, et al. Overview of traumatic injury of the thoracic aorta. *Radiographics* 1997;17(1):27–45. Kuhlman JE, Pozniak MA, Collins J, et al. Radiographic and CT findings of blunt chest trauma: aortic injuries and looking beyond them. *Radiographics* 1998;18(5):1085–1106.

31 **Answer B.** There is a pulmonary AVM in the right lower lobe with arterial supply from the right inferior phrenic artery and drainage into the suprahepatic IVC, with additional large branches emanating from the nidus to supply the right middle lobe and superior segment right lower lobe. Pulmonary arteriovenous malformations (PAVMs) are rare vascular anomalies of the lung in which abnormally dilated vessels provide a right-to-left shunt between the pulmonary artery and vein. They are generally considered direct high-flow, low-resistance fistulous connections between the pulmonary arteries and veins.

They can be classified as simple, complex, or diffuse:

- Simple type: most common; has a single segmental artery feeding the malformation. The feeding segmental artery may have multiple subsegmental branches that feed the malformation but must have only one single segmental level.
- complex type: have multiple segmental feeding arteries.
- diffuse type: rare. The diffuse form of the disease is characterized by hundreds of malformations. Some patients can have a combination of simple and complex AVMs within a diffuse lesion.

These are often unilateral. Although can potentially affect any part of the lung, there is a predilection toward the lower lobes.
PAVMs have been described in association with a number of conditions including hereditary hemorrhagic telangiectasia (HHT).
References: Lee EY, Boiselle PM, Cleveland RH. Multidetector CT evaluation of congenital lung anomalies. *Radiology* 2008;247(3):632–648.
Suchin CR, Whitman GJ, Chew FS. Pulmonary arteriovenous malformation. *AJR Am J Roentgenol* 1996;167(3):648.

32 **Answer B.** The initial image demonstrates left lung with upper lobe opacification and cystic changes/air trapping at the left base. The subsequent image demonstrates a hyperlucent and small left lung with decreased vascularity. Swyer-James syndrome (SJS) is a rare lung condition that manifests as unilateral hemithorax lucency as a result of postinfectious obliterative bronchiolitis. The condition typically follows a viral respiratory infection such as adenoviruses or *Mycoplasma pneumoniae* infection in infancy or childhood. It is generally characterized on radiographs by a unilateral small lung with hyperlucency and air trapping. CT shows the affected lung as being hyperlucent with diminished vascularity. The size of the majority of the affected lobes is smaller, although occasionally, they can be normal.
Reference: Shi HS, Yang F, Han P, et al. Findings of chest radiograph and spiral computed tomography in Swyer-James syndrome. *Chin Med Sci J* 2006;21(1):53–56.

33 **Answer A.** There is deformity of the left chest wall with dysplastic left-sided ribs, which are somewhat irregular and truncated, with straightening of expected curvature. The left fifth rib is shortened relative to the other ribs. There is also hypoplasia of the overlying musculature, particularly along the inferior aspect of the anterior chest wall. Poland syndrome refers to a congenital unilateral absence of the pectoralis major and minor muscles and is a recognized cause of unilateral hyperlucent hemithorax. The abnormality is usually evident at birth because of an asymmetry of the chest and frequent and ipsilateral abnormalities, most frequently syndactyly.
Reference: Jeung MY, Gangi A, Gasser B, et al. Imaging of chest wall disorders. *Radiographics* 1999;19(3):617–637.

5 Pediatric Neuroradiology

Questions

Brain

1. A 1-day-old infant male born at 39 weeks of gestational age with a history of abnormal prenatal ultrasound and MRI. What is the correct diagnosis?

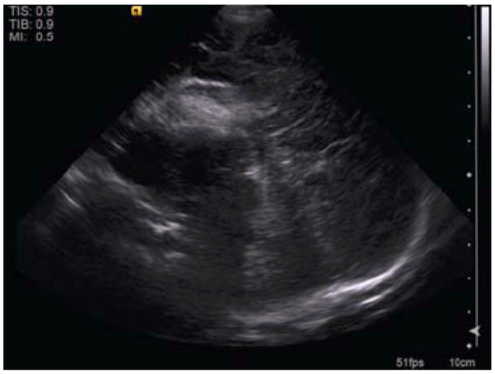

A. Holoprosencephaly
B. Dandy-Walker sequence
C. Agenesis of the corpus callosum
D. Septo-optic dysplasia

2. A 15-year-old female presents with seizure disorder and evaluation for VP shunt malfunction.

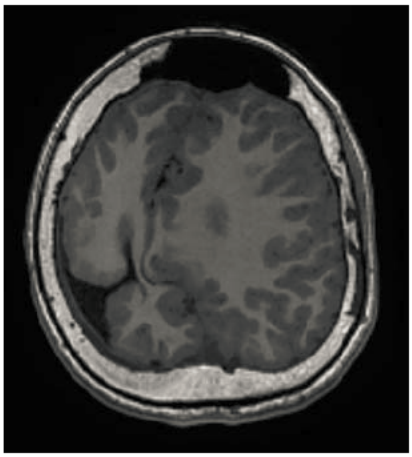

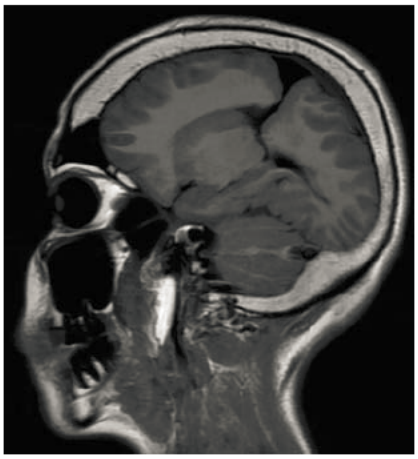

Schizencephaly is commonly associated with which of the following cerebral anomalies?
A. Holoprosencephaly
B. Agenesis of the corpus callosum
C. Lissencephaly
D. Gray matter heterotopia

3. A 2-year-old female presents to the emergency department with increased head circumference and possible VP shunt malfunction.

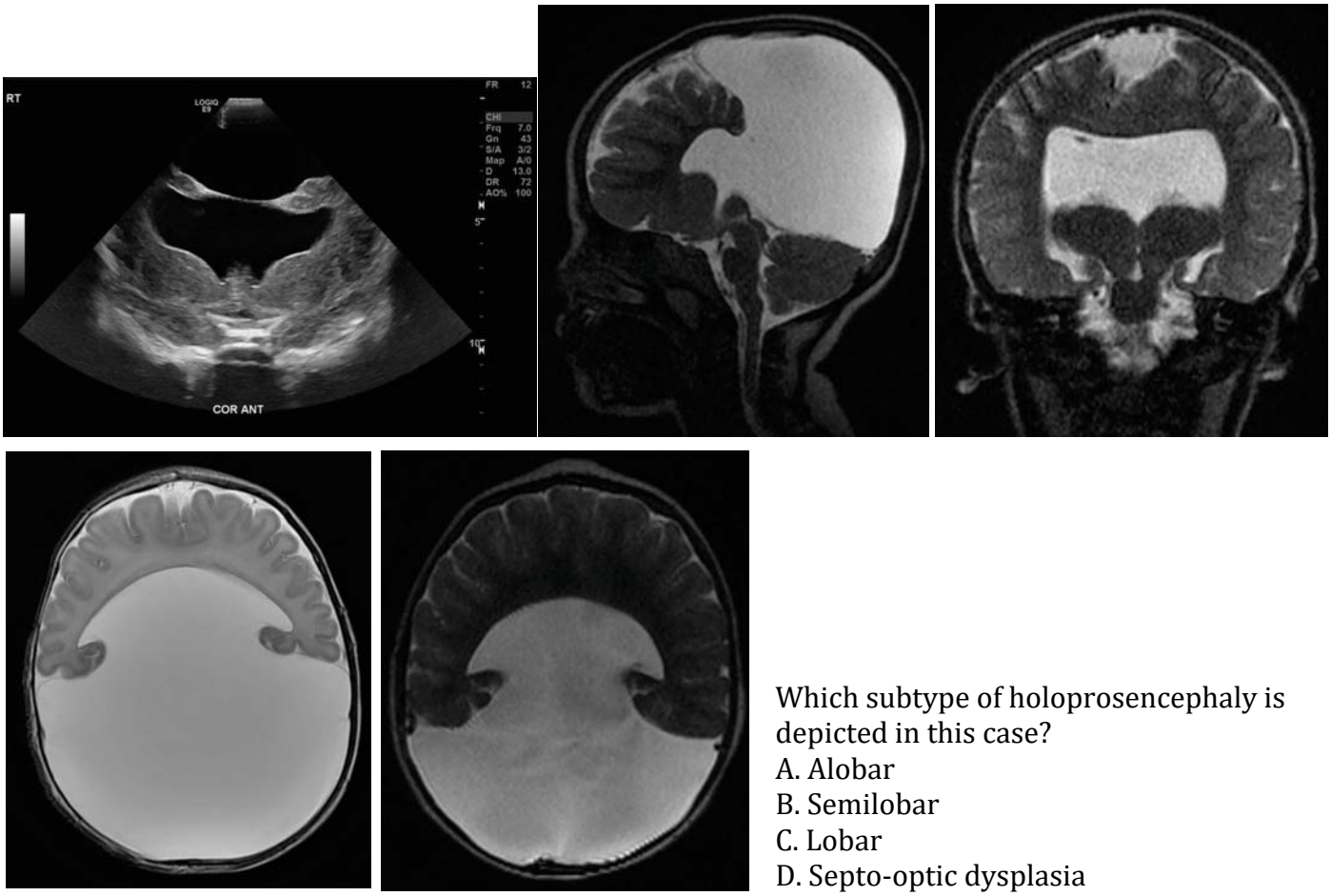

Which subtype of holoprosencephaly is depicted in this case?
A. Alobar
B. Semilobar
C. Lobar
D. Septo-optic dysplasia

4. A 4-year-old female presents with headache.

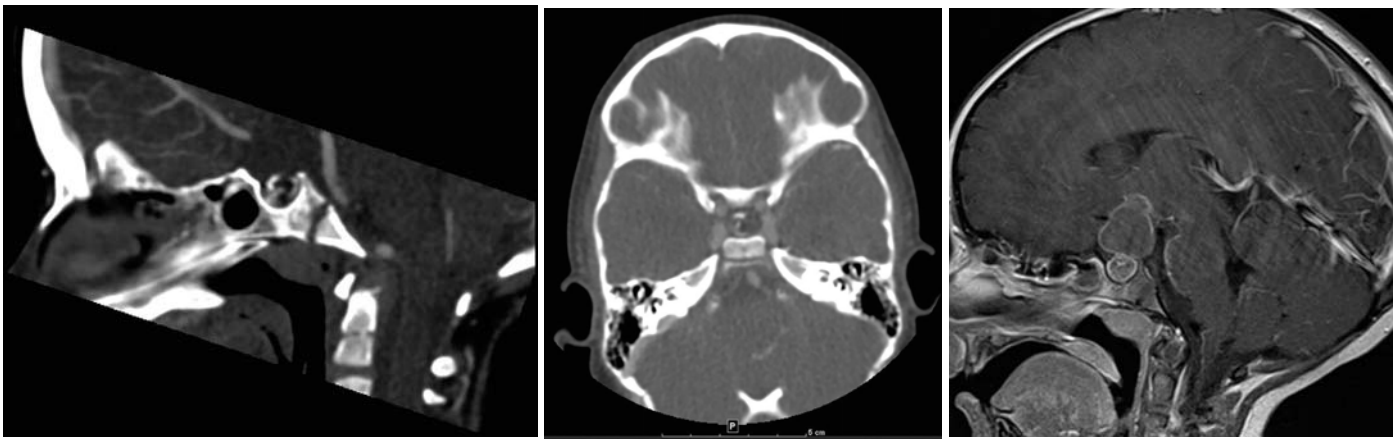

What is the most likely diagnosis?
A. Chordoma
B. Langerhans cell histiocytosis
C. Anterior communicating artery aneurysm
D. Craniopharyngioma

5. A 4-year-old male presents with precocious puberty, early penile growth, and testicular enlargement.

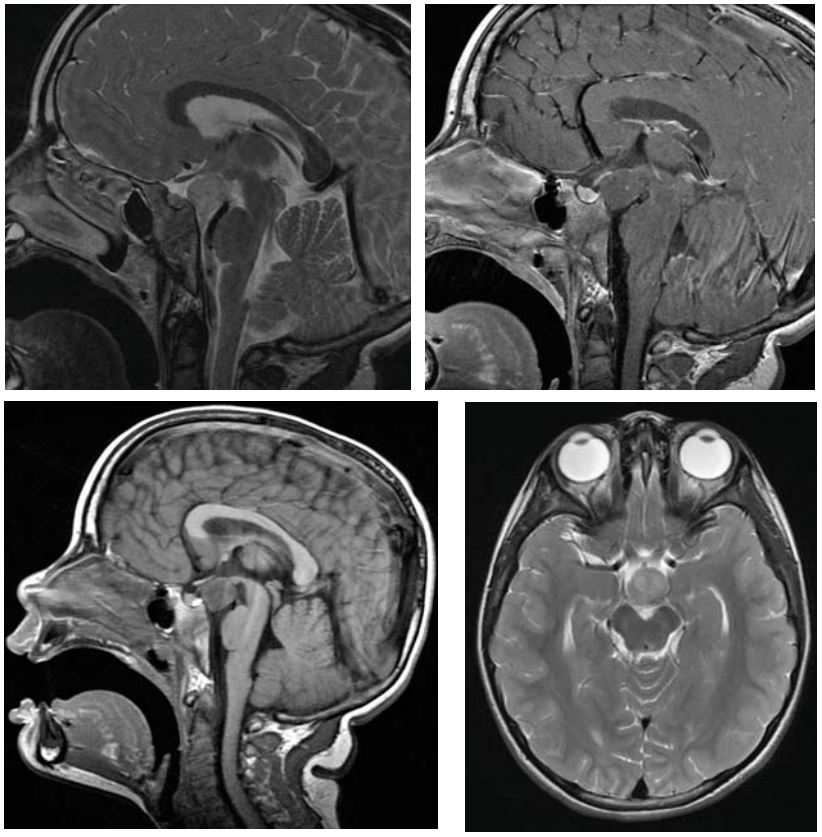

What is the most likely diagnosis?
A. Lipoma
B. Hypothalamic hamartoma
C. Langerhans cell histiocytosis
D. Germinoma

6. A 15-year-old female presents with daily headaches for 1 week and vomiting.

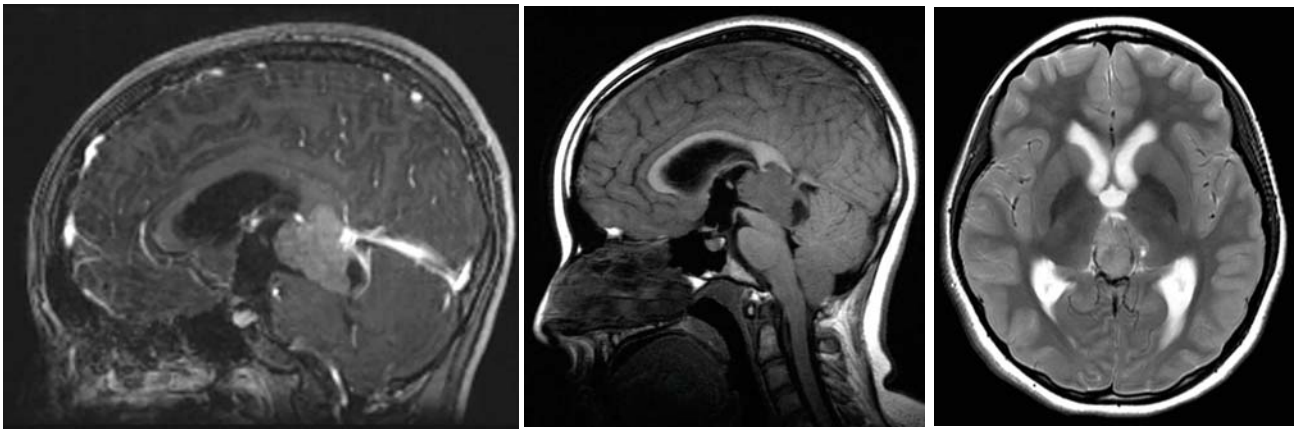

What is the most likely diagnosis?
A. Pineoblastoma
B. Craniopharyngioma
C. Meningioma
D. Ependymoma

7. Pineal region tumors may cause which of the following?
A. Diabetes insipidus
B. Parinaud syndrome
C. Gynecomastia
D. Seborrheic dermatitis

8. An 11-year-old male presents with vomiting, dizziness, headache, and personality changes.

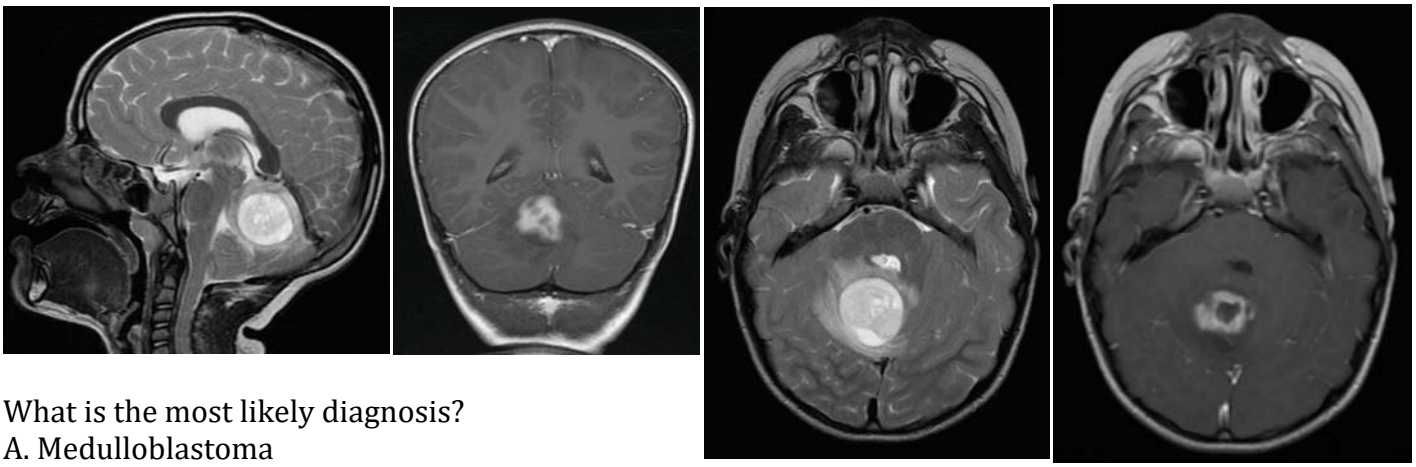

What is the most likely diagnosis?
A. Medulloblastoma
B. Pilocytic astrocytoma
C. Meningioma
D. Dermoid cyst

9. A 12-year-old male presents with progressive ataxia of the past few weeks.

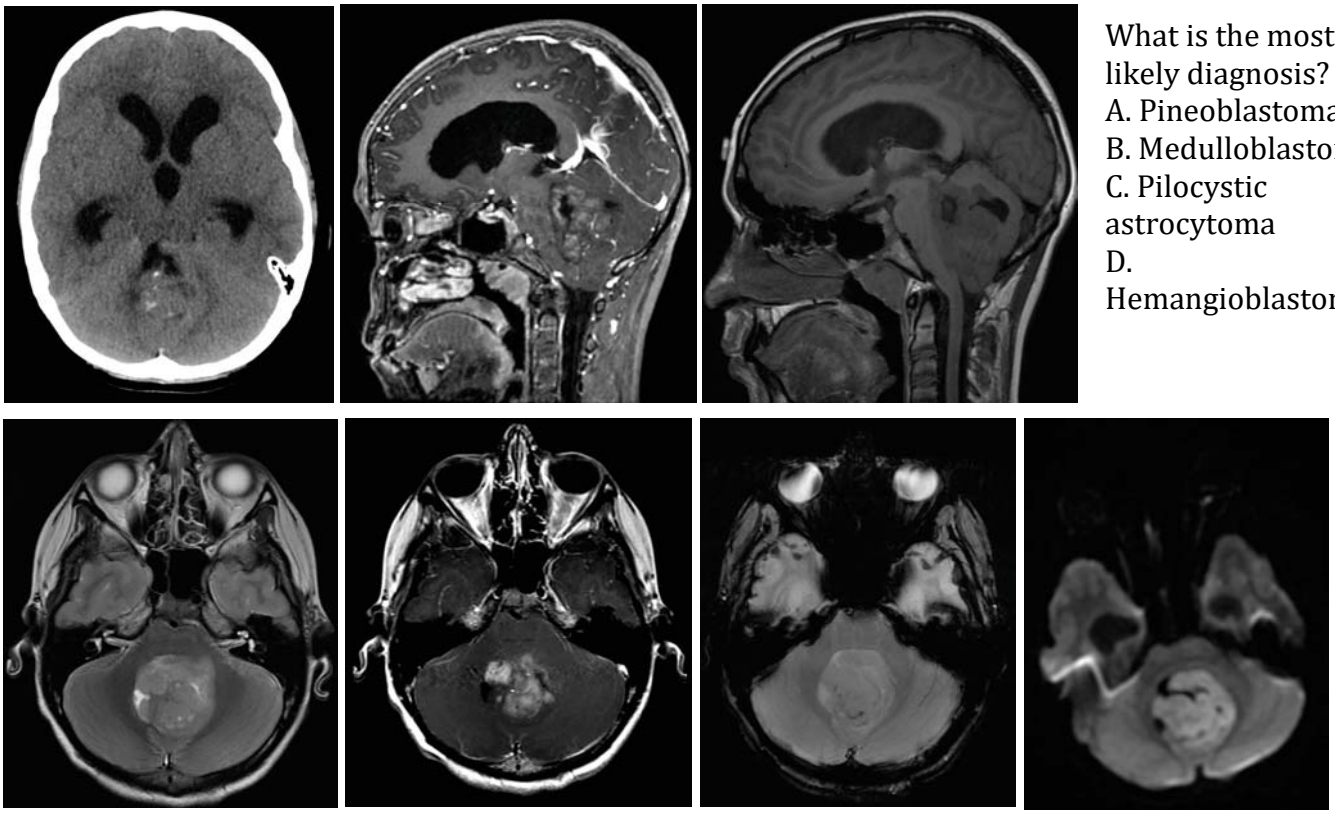

What is the most likely diagnosis?
A. Pineoblastoma
B. Medulloblastoma
C. Pilocystic astrocytoma
D. Hemangioblastoma

10. What is the next best step?
A. Spine imaging to exclude drop metastases
B. Cerebral angiography to delineate feeding vessels
C. Chemotherapy
D. Surgical resection

11. A 2-day-old female presents with abnormal antenatal imaging. Images from fetal MRI performed at 22 weeks of gestational age and sagittal MRI of the brain performed at 2 days of age.

What is the most likely diagnosis?
A. Neurofibromatosis type 1
B. Chiari II malformation
C. Dandy-Walker malformation
D. Subarachnoid cyst

12. A 4-year-old male patient presents with a history of developmental delay. What is the diagnosis?

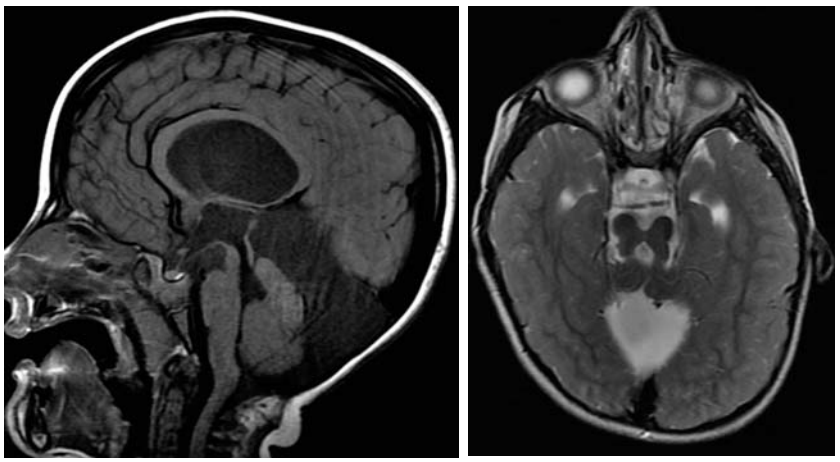

A. Dandy-Walker malformation
B. Posterior fossa arachnoid cyst
C. Mega cisterna magna
D. Joubert syndrome

13. A 5-month-old female presents for the evaluation of congenital fibrosis of extraocular muscles.

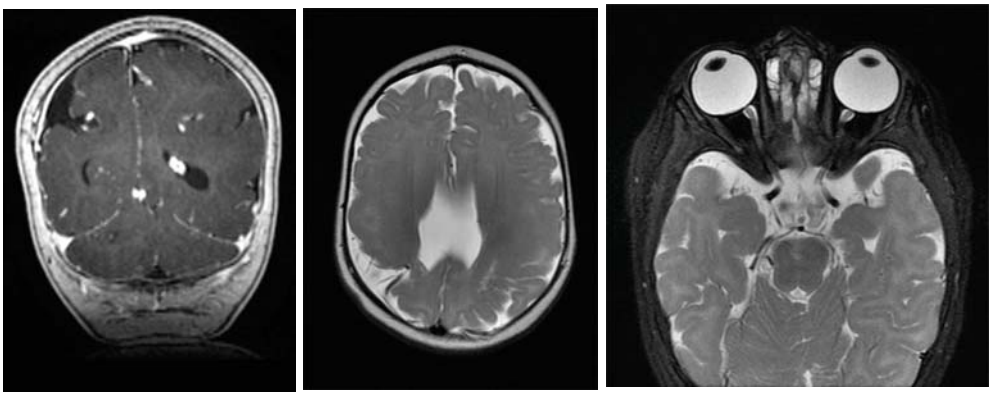

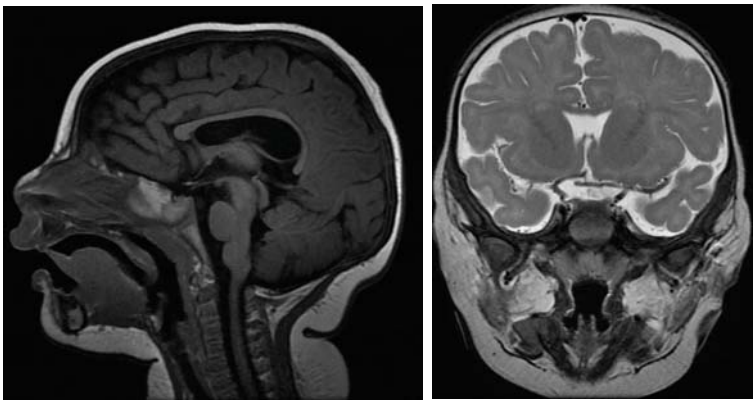

What is the most likely diagnosis?
A. Absence of the corpus callosum
B. Neurofibromatosis type 1
C. Lobar holoprosencephaly
D. Septo-optic dysplasia

14. An 18-year-old male presents with imaging for follow-up of congenital brain abnormality. What syndrome is demonstrated?

A. Sturge-Weber
B. Tuberous sclerosis
C. Neurofibromatosis type 2
D. Neurofibromatosis type 1

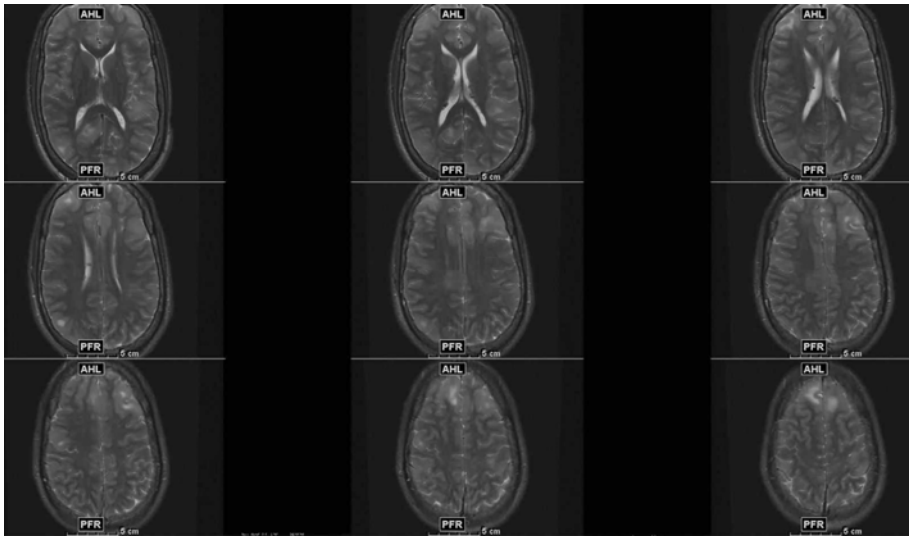

15. In this syndrome, what is the next most common body system affected?
A. Genitourinary
B. Gastrointestinal
C. Cardiovascular
D. Pulmonary

16. Term infant born with hydrocephalus, which was originally diagnosed at 20 weeks of gestation on fetal ultrasound.

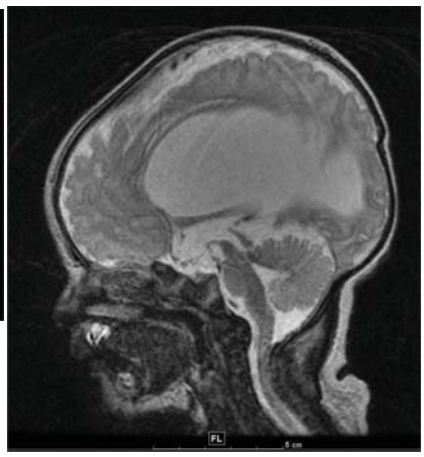

What is the most likely etiology of this congenital hydrocephalus?
Chiari I malformation
B. Chiari II malformation
C. Aqueductal stenosis
C. Down syndrome

17. A 6-year-old female presents from outside hospital with a history of newly diagnosed brain mass.

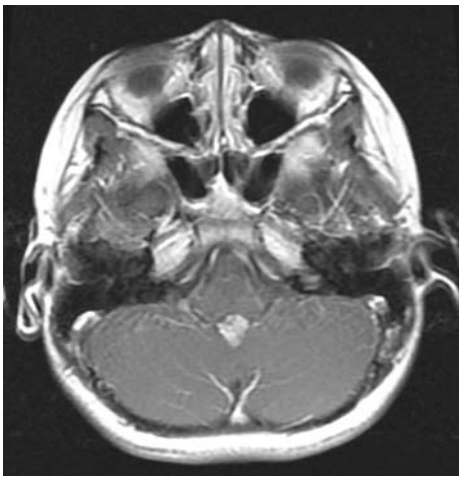

What is the most likely diagnosis?
A. Choroid plexus papilloma
B. Hemangioblastoma
C. Juvenile pilocytic astrocytoma
D. Metastatic neuroblastoma

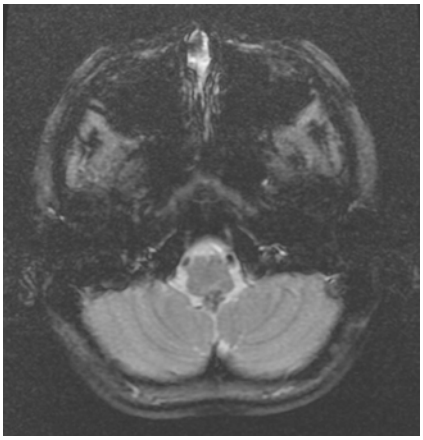

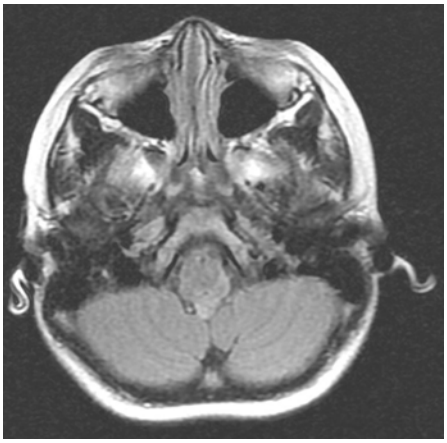

18. A 24-day-old female presents with macrocephaly.

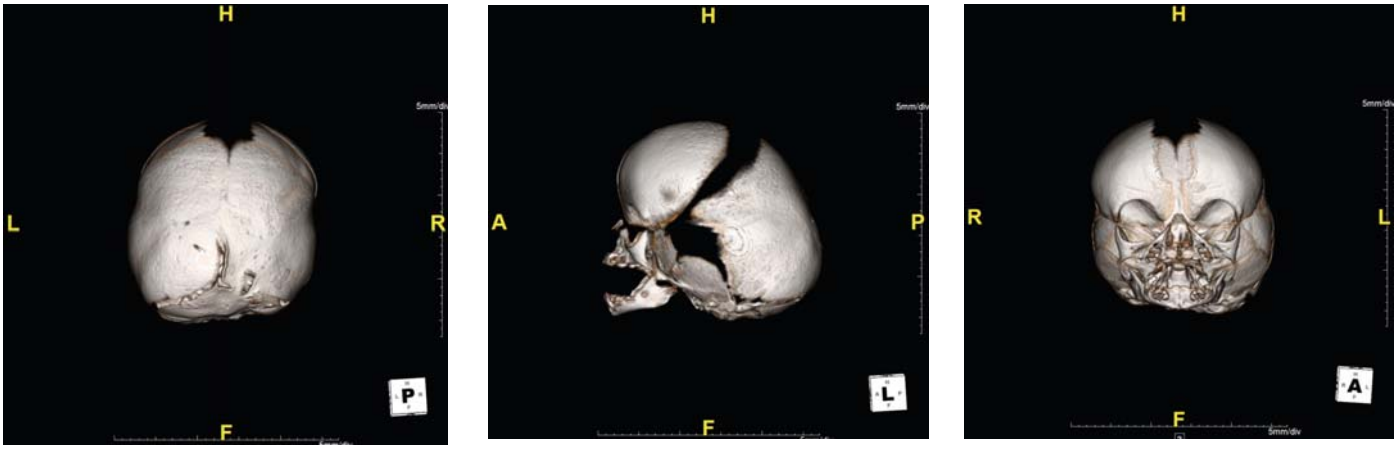

What is the diagnosis?
A. Langerhans cell histiocytosis
B. Multiple myeloma
C. Myelodysplasia
D. Craniosynostosis

19. A 2-week-old male presents with a history of nasal congestion.

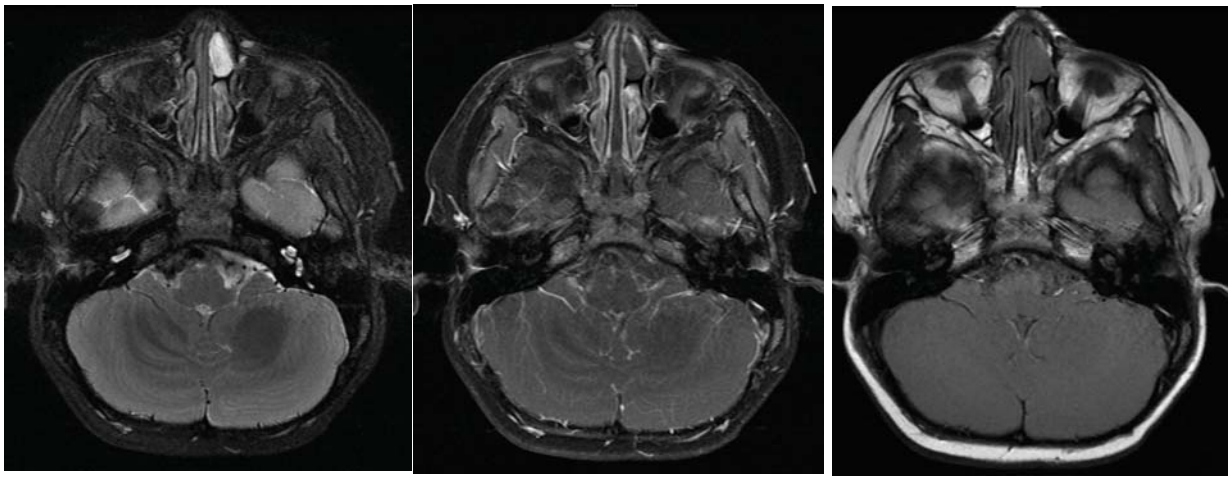

What is the diagnosis?
A. Glioma
B. Encephalocele
C. Fungal infection
D. Angiofibroma

20. A 17-year-old male status post fall from second story window. What is the diagnosis?

A. Meningocele
B. Epidural hematoma
C. Langerhans cell histiocytosis
D. ADEM

21. A 1-year-old female presents with high-output congestive heart failure and increased head size.

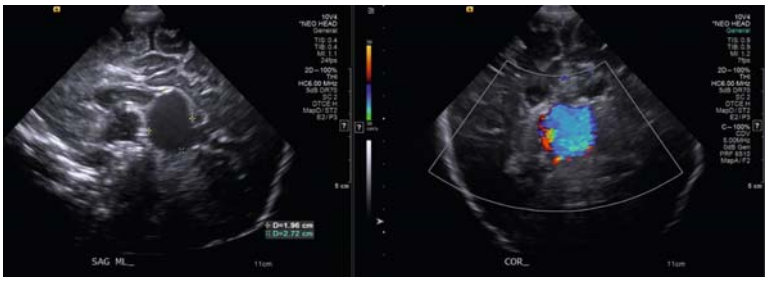

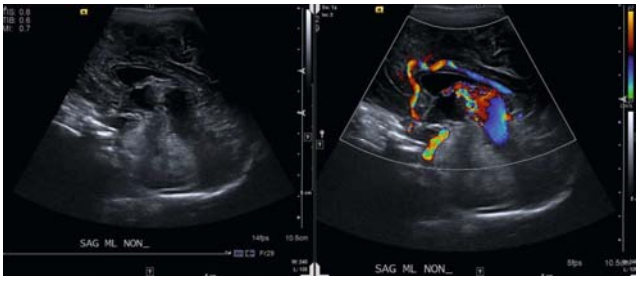

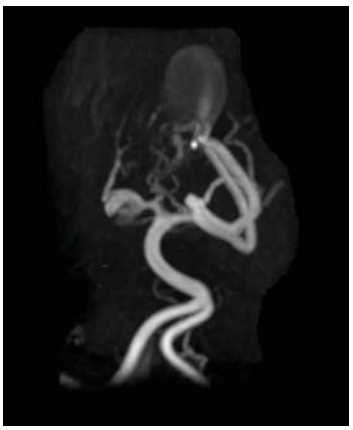

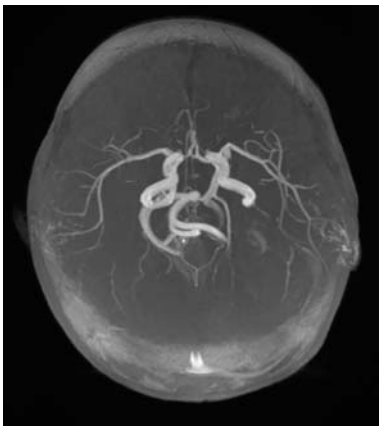

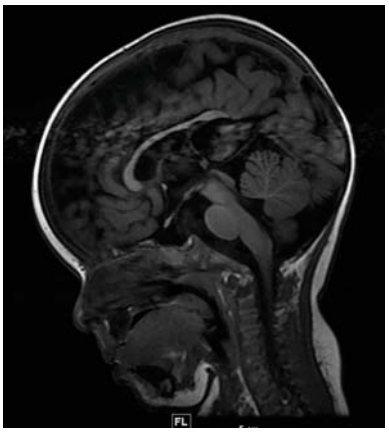

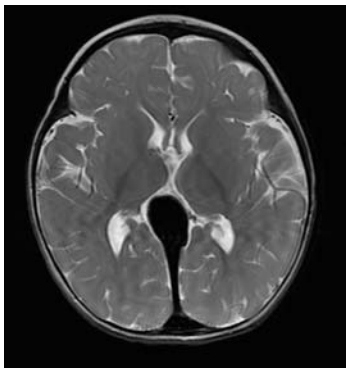

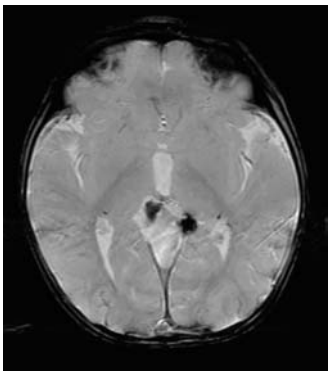

What is the diagnosis?
A. Dural venous thrombosis
B. Pineoblastoma
C. Trilateral retinoblastoma
D. Vein of Galen aneurysmal malformation

22. What is the most appropriate next step for management?
A. Embolization
B. Surgical resection
C. Radiotherapy
D. Thermal ablation

23. A 1-day-old female presents with abnormal antenatal ultrasound and microcephaly.

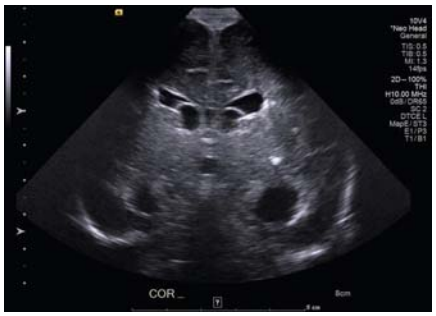

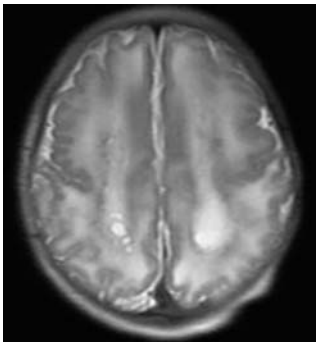

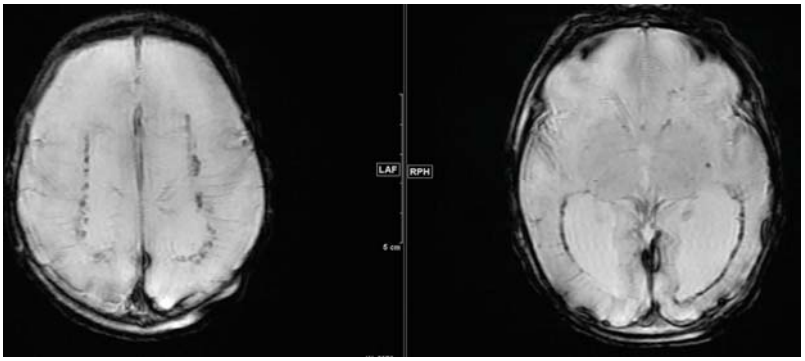

What is the most likely etiology of the intracranial abnormality?
A. Cytomegalovirus (CMV) infection
B. Middle cerebral artery (MCA) infarction
C. Congenital aqueductal stenosis
D. Sturge-Weber syndrome

24. A 3-month-old with failure to thrive.

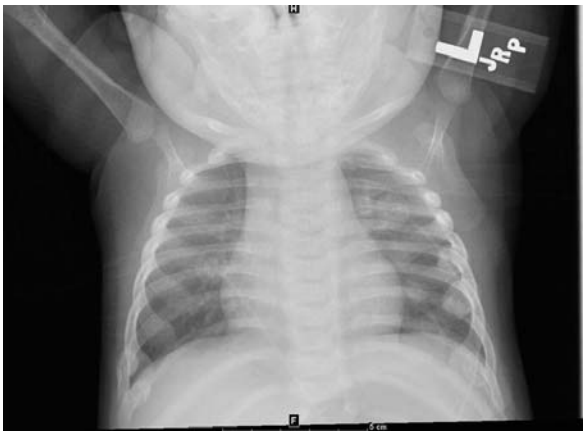


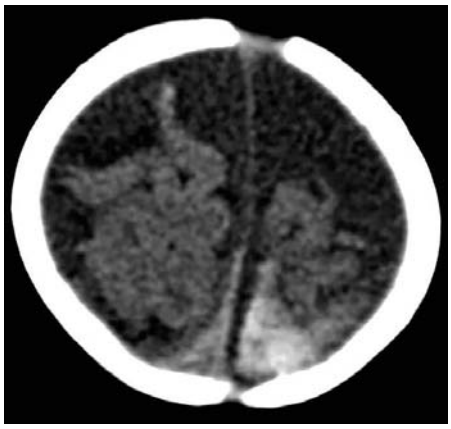

What is the most likely diagnosis?
A. Nonaccidental trauma (child abuse)
B. Osteogenesis imperfecta
C. Congenital syphilis
D. Hemophilia

25. A 7-month-old male presents with palpable nodules on the parietal scalp, as well as on the left maxillary alveola.

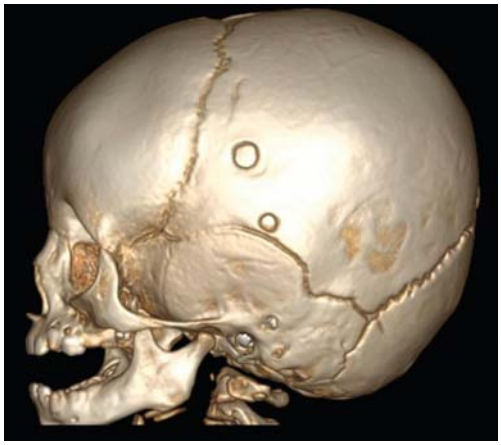

What is the most likely diagnosis?
A. Multiple myeloma
B. Langerhans cell histiocytosis
C. Neuroblastoma metastatic disease
D. Cephalohematoma

26. A 6-year-old male presents with left foot tremor.

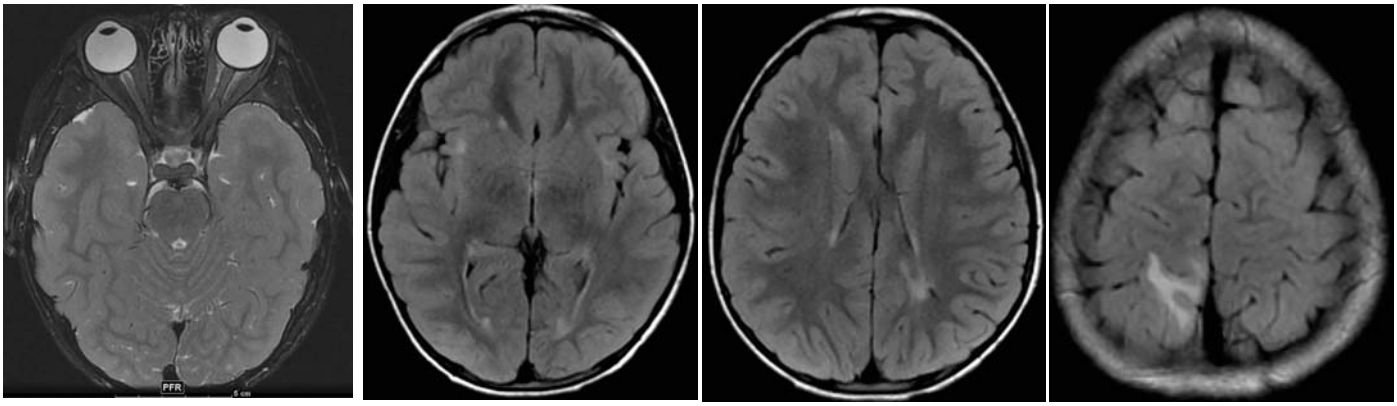

What is the most likely
diagnosis?
A. Multiple sclerosis
B. Leukodystrophy
C. Acute disseminated encephalomyelitis
D. TORCH infection

27. An 11-year-old male presents with headache and visual disturbance.

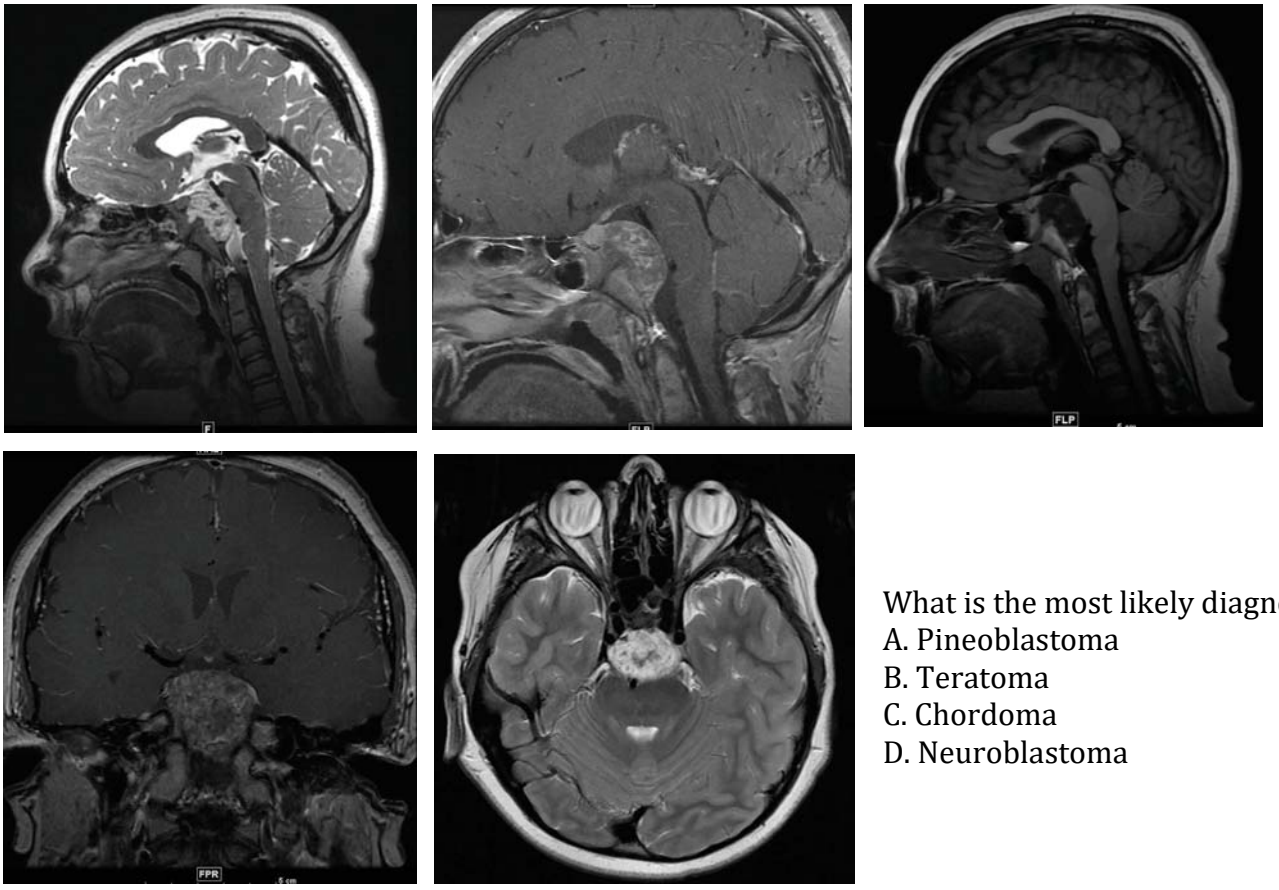

What is the most likely diagnosis?
A. Pineoblastoma
B. Teratoma
C. Chordoma
D. Neuroblastoma

Head and Neck

28. A 4-year-old male transferred from outside hospital with sore throat, stiff neck. After review of the neck radiograph, what is the recommended next step?

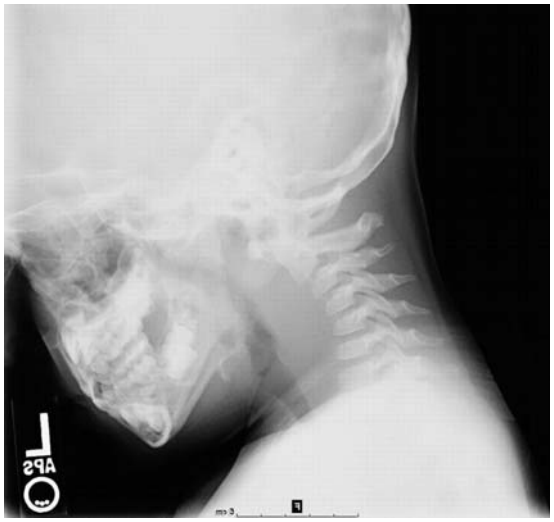

A. Surgery consultation
B. CT neck with contrast
C. IV antibiotics
D. IV steroids

29. What is the diagnosis?

A. Croup
B. Retropharyngeal abscess
C. Retained foreign body
D. Epiglottitis

30. A 4-week-old male presents with a history of trisomy 21 and respiratory distress. What is the most likely diagnosis?

A. Choanal atresia
B. Nasal dermoid
C. Nasolacrimal duct mucocele
D. Nasal encephalocele

31. An otherwise healthy 15-year-old boy presents with symptoms of left nasal congestion. What is the most likely diagnosis?

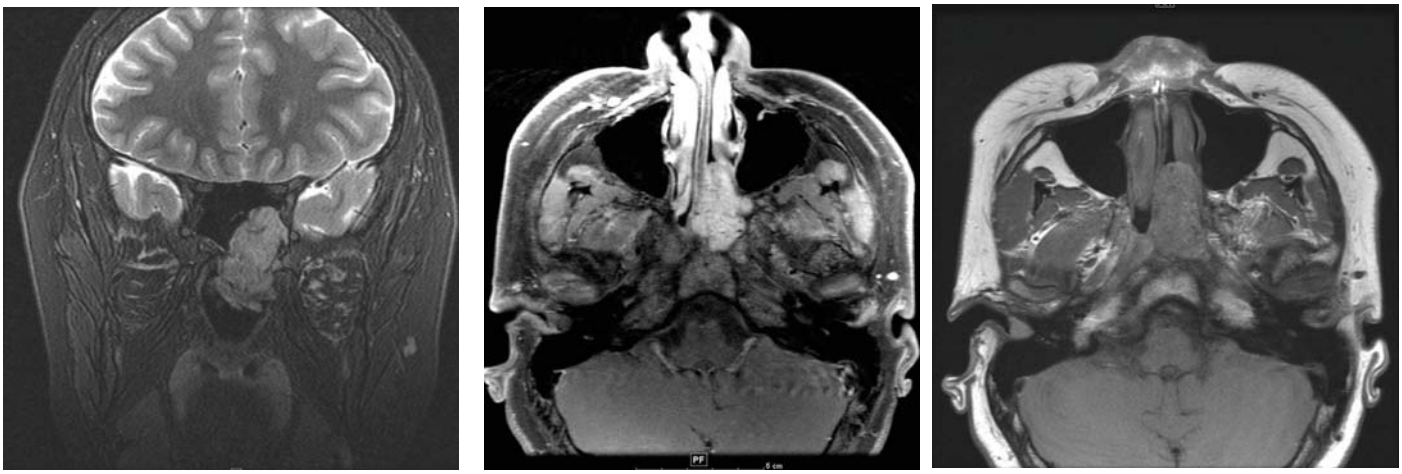

A. Rhabdomyosarcoma
B. Langerhans cell histiocytosis
C. Sinonasal aspergillosis
D. Juvenile nasopharyngeal angiofibroma

32. What is the most common feeding vessel of this mass?

A. Internal maxillary artery
B. Ophthalmic artery
C. Facial artery
D. Vertebral artery

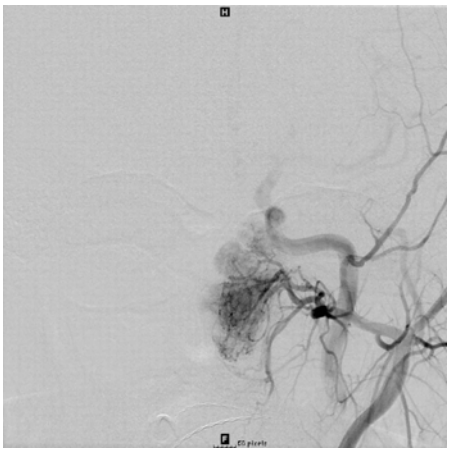

33. A 4-month-old male presents with abnormal ophthalmic examination. What is the most likely diagnosis?

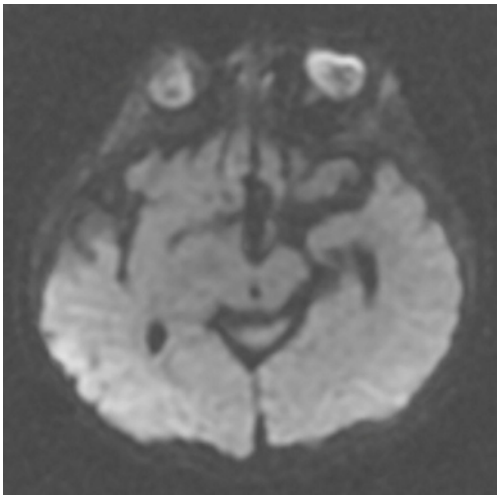

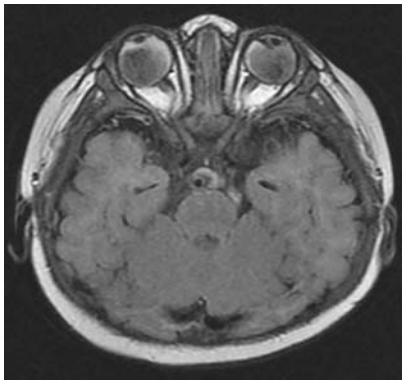

A. Persistent primary hyperplastic vitreous
B. Retinoblastoma
C. Retinopathy of prematurity
D. Orbital toxocariasis

34. A 3-year-old male presents with left neck mass. What is the most likely diagnosis?

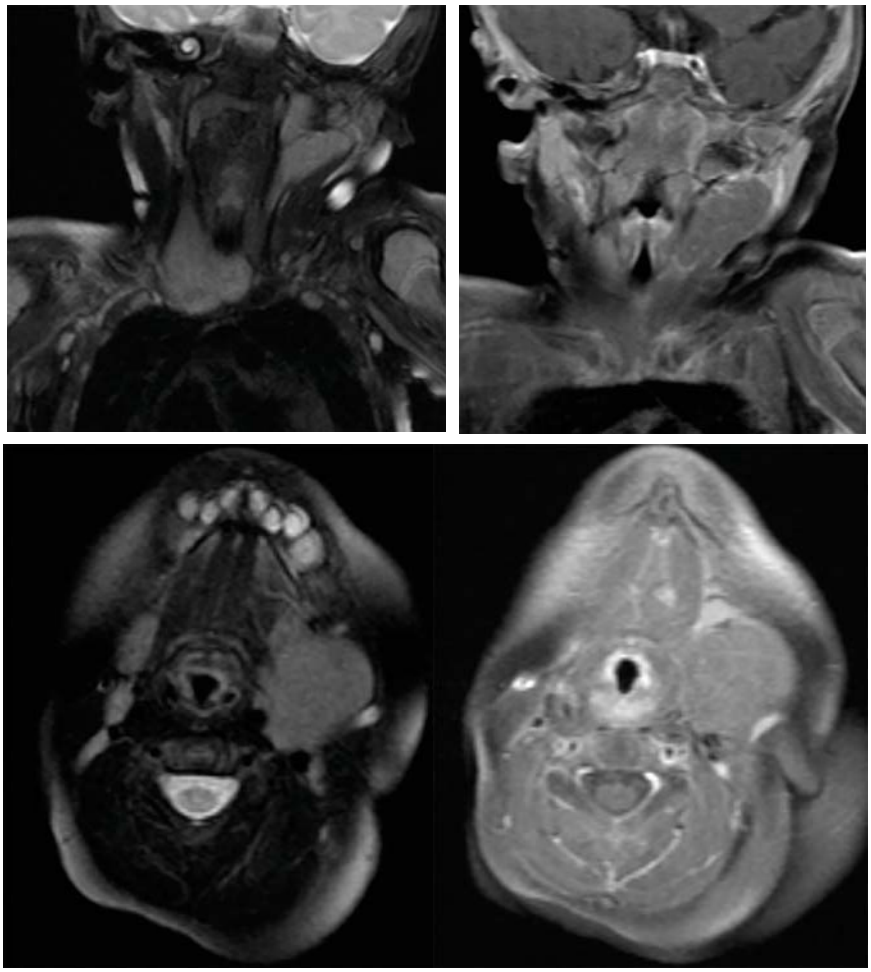

A. Rhabdomyosarcoma
B. Ectopic thymus
C. Papillary thyroid carcinoma
D. Thyroglossal duct cyst

35. A 4-year-old male presents with right facial swelling. Which salivary gland is most likely involved?

A. Parotid
B. Submandibular
C. Sublingual
D. Minor

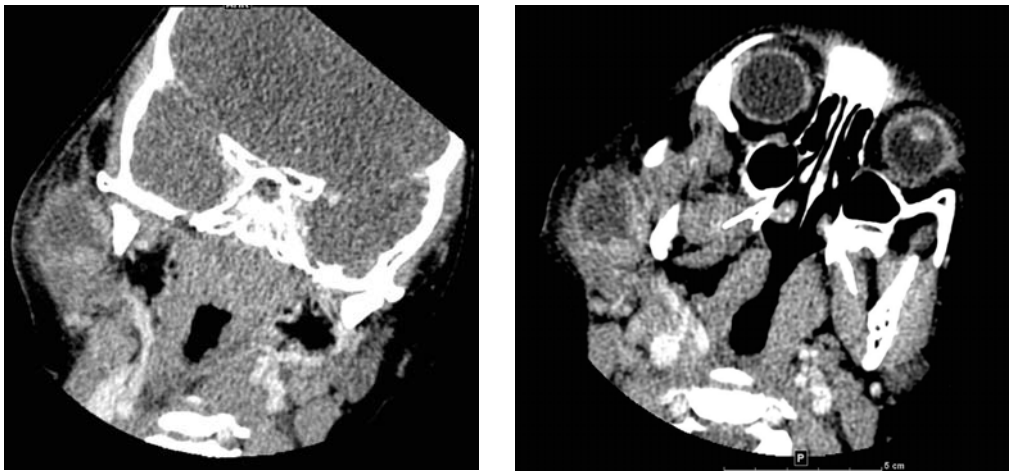

36. A 4-year-old female presents with neck mass in the suprasternal notch. What is the most likely diagnosis?

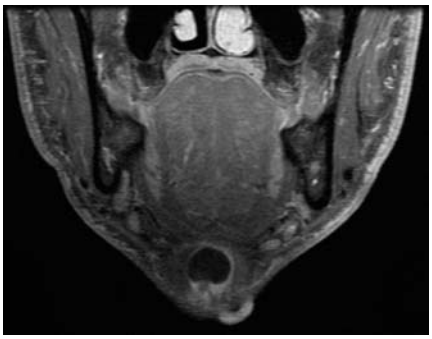

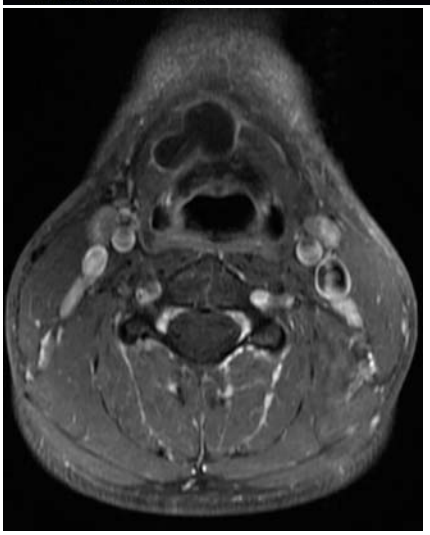

A. Thyroglossal duct cyst
B. Thyroiditis
C. Ectopic thymus
D. Branchial apparatus cyst

37. A 2-month-old with antenatally diagnosed neck mass. What is the most likely diagnosis?

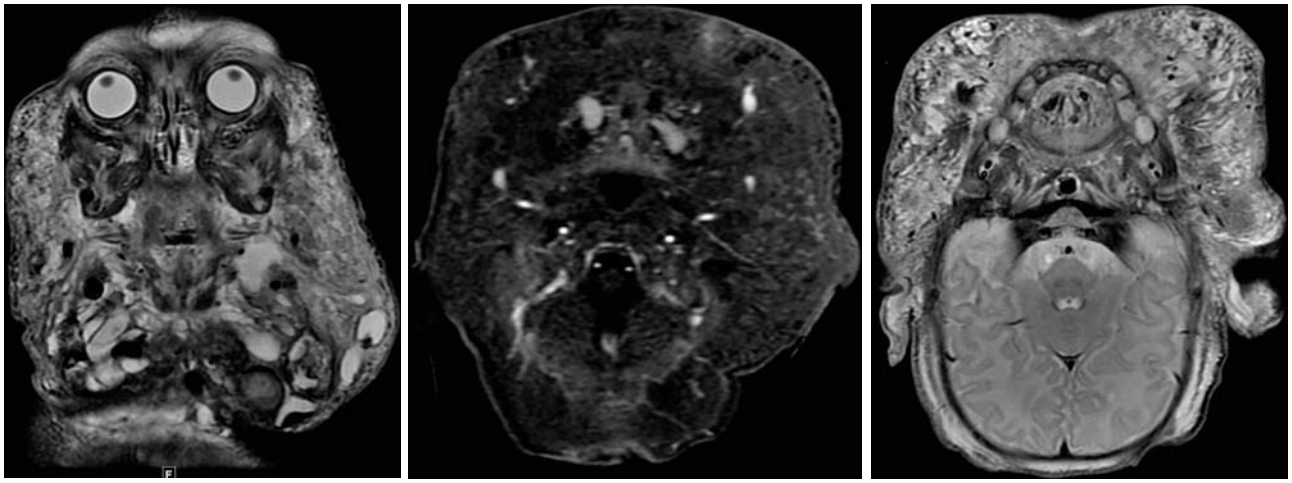

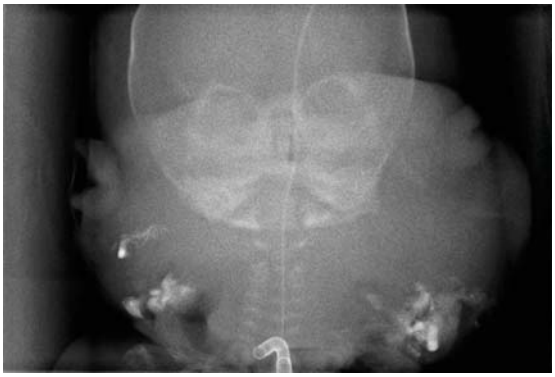

A. Cervical teratoma
B. Venolymphatic malformation
C. Thyroglossal duct cyst
D. Second branchial cleft cyst

38. A 29-day-old female presents with right neck swelling. What is the most likely diagnosis?

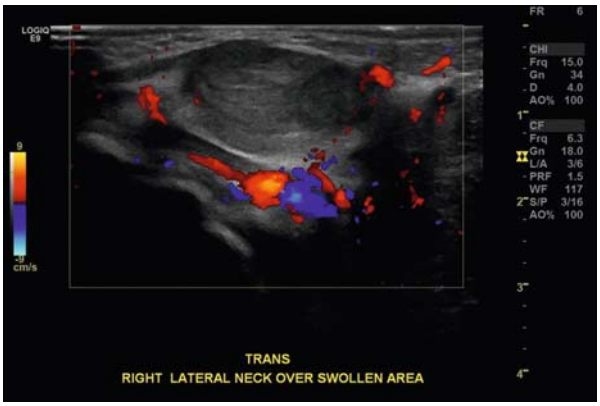

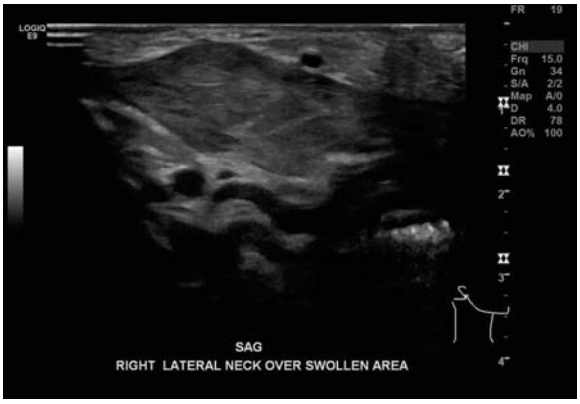

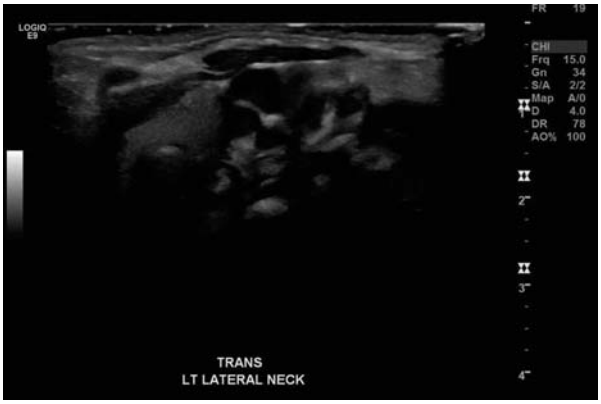

A. Lymphoma
B. Hemangioma
C. Fibromatosis colli
D. Lymphadenitis

Spine

39. A 20-year-old pregnant female carrying a fetus of 20 weeks of gestational age.

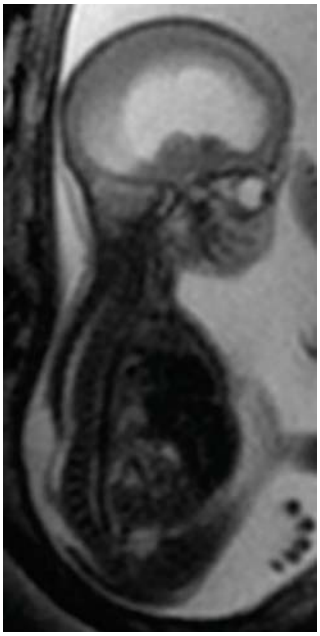

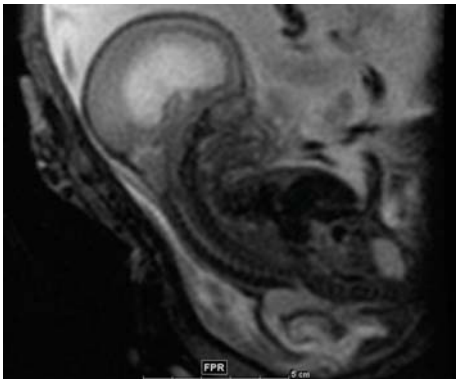

What is the most likely diagnosis?
A. Dandy-Walker malformation
B. Megalencephaly
C. Chiari I malformation
D. Chiari II malformation

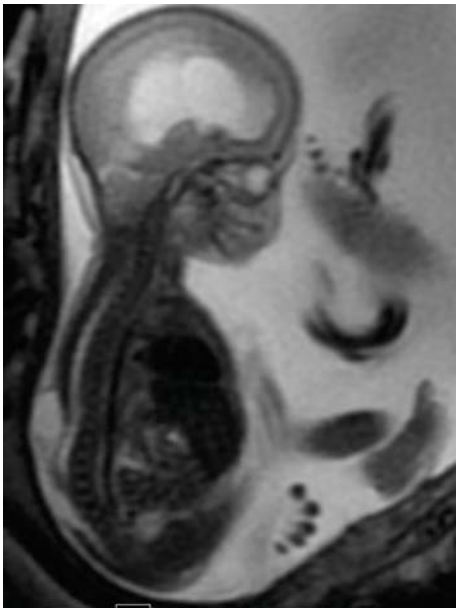

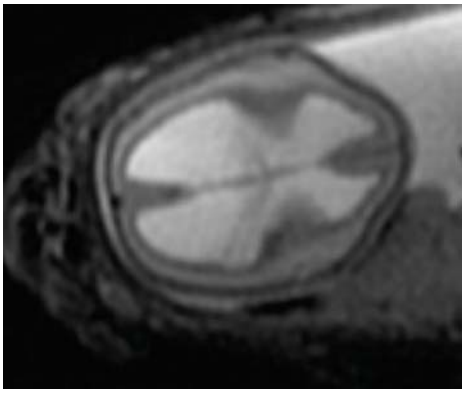

40. A 3-year-old female presents with short stature.

What is the most likely diagnosis?
A. Jeune syndrome
B. Achondroplasia
C. Thanatophoric dwarfism
D. Ollier disease

41. An 18-year-old male presents with a history of chronic osteomyelitis and back pain.

What is the most likely diagnosis?
A. Discitis osteomyelitis
B. Vertebral compression fracture
C. Vertebral hemangioma
D. Scheuermann disease

42. A 9-year-old male presents with multiple anomalies.

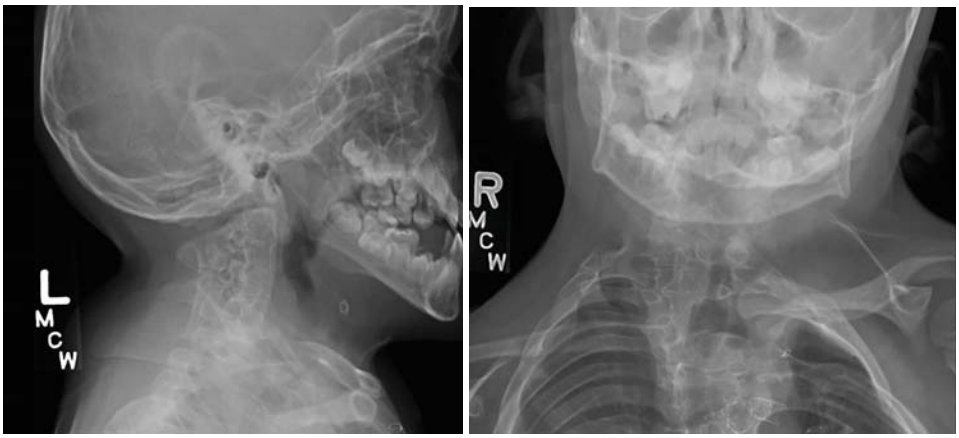

What is the most likely diagnosis?
A. Klippel-Feil syndrome
B. Morquio syndrome
C. Gorham disease
D. Osteogenesis imperfecta

43. A 15-year-old male presents with back pain and progressive lower extremity weakness.



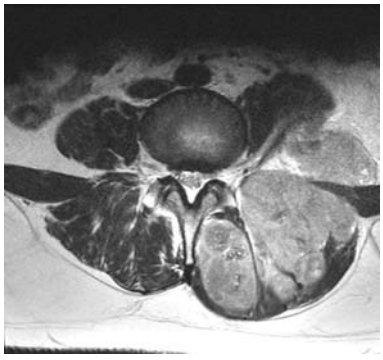

What is the most likely diagnosis?
A. Myelomeningocele
B. Langerhans cell histiocytosis
C. Ewing sarcoma
D. Ependymoma

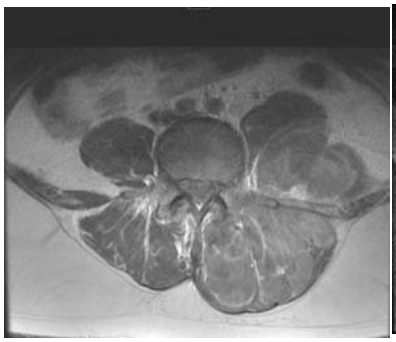
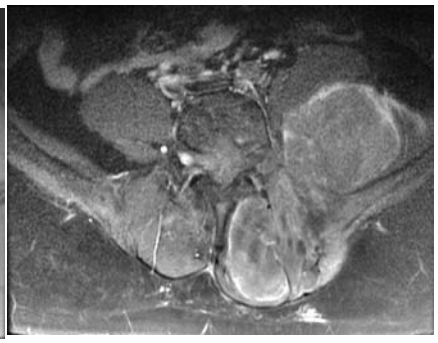


44. A 14-year-old female presents with back pain.

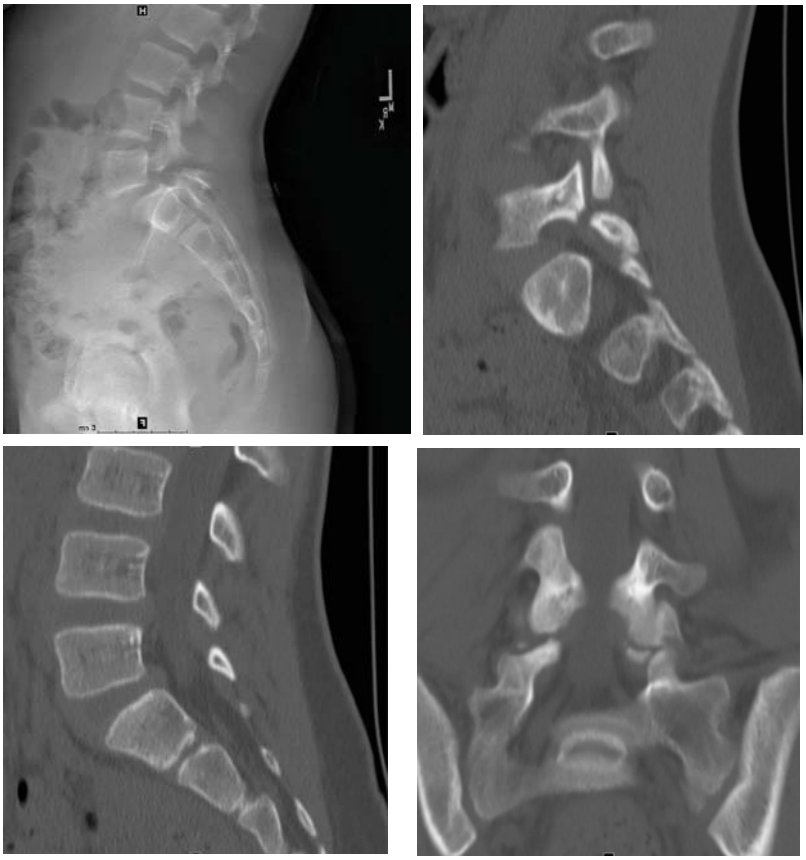

What is the most likely diagnosis?
A. Vertebral hemangioma
B. Spondylolysis
C. Sickle cell disease
D. Gaucher disease

45. A former premature infant with a history of anal atresia.

Which of the following CNS abnormalities is most commonly associated with maternal diabetes?
A. Chiari II malformation
B. Diastematomyelia
C. Caudal regression syndrome
D. Chordoma

46. A 17-year-old female presents with a long history of UTI.

What is the most likely diagnosis?
A. Rhabdomyosarcoma
B. Ovarian torsion
C. Ewing sarcoma
D. Sacrococcygeal teratoma

47. A 14-year-old male presents with neck pain.

What is the most likely diagnosis?
A. Ewing sarcoma
B. Osteogenic sarcoma
C. Osteoblastoma
D. Metastatic neuroblastoma

Neuroradiology: Answers and Explanations

Brain

1 **Answer C.** The neonatal head ultrasound images demonstrate an echogenic midline mass superior to the third ventricle. There is dilation of the lateral ventricles, colpocephaly, and absence of the corpus callosum. Agenesis of the corpus callosum (ACC) is the most common developmental abnormality, resulting from failure of commissuration and can occur for a number of reasons including genetic, metabolic, or vascular abnormalities, but in most cases, the cause is not found. The term "ACC" implies that the entire structure has failed to form, but in other fetuses, the corpus callosum may fail to form in part leading to the term "hypoplasia of the corpus callosum." In the context of the detection of antenatal malformations, ACC is much more common than hypoplasia of the corpus callosum.
Imaging findings often include ventriculomegaly, colpocephaly (dilation of the trigones and occipital horns), and absent cavum septum pellucidum. In the sagittal plane, there is a radial, spoke-wheel, or sunray appearance of the gyri from the expected location of the corpus callosum. The echogenic midline mass in this case is consistent with an interhemispheric lipoma. Half of all midline intracranial lipomas are associated with ACC.

References: Barkovich AJ, et al. Congenital malformations of the brain and skull. In: Barkovich AJ, Raybaud C (eds). *Pediatric neuroimaging*, 5th ed. Philadelphia, PA: Lippincott Williams & Wilkins, 2012:367–568.
Craven I, Bradburn MJ, Griffiths PD. Antenatal diagnosis of agenesis of the corpus callosum. *Clin Radiol* 2015;70(3):248–253.

2 **Answer D.** Brain MRI images demonstrate right open lip schizencephaly with a cleft of CSF extending from the pial margin of the right frontoparietal lobe to the ependymal margin of the right lateral ventricle. This schizencephaly cleft is lined by polymicrogyria. Schizencephaly is a rare cortical malformation that manifests as a gray matter–lined cleft extending from the ependyma to the pia mater. This malformation is thought to be a result of an acquired in utero insult affecting the germinal zone prior to neuronal migration.
There are two types of schizencephaly: type 1 or open lip and type 2 or closed lip. Closed-lip MRI findings include irregular tract of gray matter extending from cortical surface to ventricle. The gray matter lining can appear dysplastic (lumpy/bumpy on margin of cleft or at gray–white interface). Open lip can appear wide and wedge shaped or with nearly parallel walls. The gray matter lining cleft may be harder to discern than in closed lip. The most common signs/symptoms include seizures (more common with unilateral clefts), mild motor deficit ("congenital" hemiparesis), developmental delay, paresis, microcephaly, and spasticity.
Schizencephaly is frequently associated with other cerebral anomalies including:

- Septo-optic dysplasia
- Gray matter heterotopia
- Absent septum pellucidum

References: Barkovich AJ, Kjos BO. Schizencephaly: correlation of clinical findings with MR characteristics. *Am J Neuroradiol* 1992;13(1):85–94.
Nabavizadeh SA, Zarnow D, Bilaniuk LT, Schwartz ES, Zimmerman RA, Vossough A. Correlation of prenatal and postnatal MRI findings in schizencephaly. *Am J Neuroradiol* 2014;35(7):1418–1424. doi:10.3174/ajnr.A3872.

3 Answer A. Head ultrasound and brain MRI demonstrate a monoventricle, large dorsal cyst, fused thalami, and fused anterior cerebral mantle. Alobar holoprosencephaly is the most severe form of holoprosencephaly and consists of complete lack of separation of the cerebral hemispheres with a large posterior monoventricle. Single midline structures such as the falx, interhemispheric fissure, septum pellucidum, and corpus callosum are absent, whereas paired midline structures are fused, including the thalami and basal ganglia. Affected patients suffer from dysmorphic facies, microcephaly, seizures, and developmental delay.

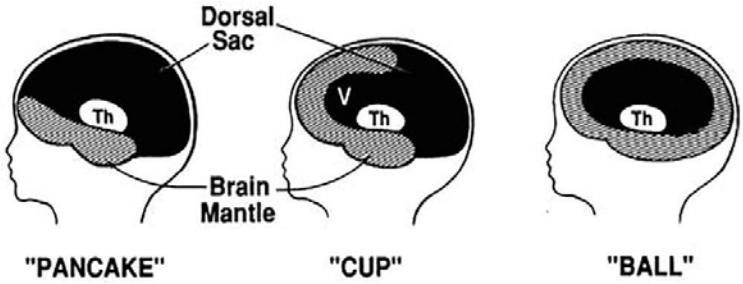

Diagram of three morphologic types of alobar holoprosencephaly (and semilobar holoprosencephaly) in sagittal view. Pancake type: The flattened residual brain mantle at the base of the brain with a correspondingly large dorsal sac. Cup type: This type has more brain mantle but it does not cover the monoventricle. The dorsal sac communicates widely with the monoventricle. Ball type: Brain mantle completely covers the monoventricle, and a dorsal sac may or may not be present. Th, thalami; V, ventricle.
(Modified from McGahn JP, Ellis W, Lindfors KK, et al. Congenital cerebrospinal fluid-containing intracranial abnormalities: sonographic classification. *J Clin Ultrasound.* 1988;16:531–544.)

Holoprosencephaly is a spectrum of congenital abnormalities characterized by incomplete separation of the cerebral hemispheres. Abnormalities range from incomplete formation of the falx cerebri and interhemispheric fissure to a complete lack of separation of the cerebral hemispheres with a large monoventricle. There are three types which include alobar, semilobar, and lobar (septo-optic dysplasia).

Midline facial abnormalities in the setting of alobar holoprosencephaly include:

- Cyclopia
- Ethmocephaly (small narrow-set eyes with absence of nose)
- Cebocephaly (small narrow-set eyes with a flattened nose and one nostril)
- Cleft palate and lip
- Solitary maxillary central incisor

Facial malformations of any kind should trigger very careful evaluation of brain. “The face predicts the brain.”

References: Barkovich AJ. Congenital malformations of the brain and skull. In: Barkovich AJ (ed). *Pediatric neuroimaging*, 4th ed. Philadelphia, PA: Lippincott Williams & Wilkins, 2005:291–439.
Winter TC. *Diagnostic imaging: obstetrics*, 2nd ed. Philadelphia, PA: Lippincott Williams & Wilkins, 2011:1–2.

4 Answer D. On CT, there is a mildly hypodense nonenhancing sellar and suprasellar lesion. The sellar component of this mass has associated calcification. MRI demonstrates a T1/T2 hyperintense cystic-appearing sellar and suprasellar mass with peripheral enhancement. There is GRE hypointensity within the sellar component. The lesion causes deformity and displacement upon the optic apparatus. Craniopharyngioma is the most common suprasellar mass in children. Craniopharyngiomas arise from the metaplastic squamous epithelial rests along the hypophysis. They are more common in males. The vast majority arise within the suprasellar cistern; however, they may arise within the sella turcica and occasionally the third ventricle. There is a bimodal age distribution with children between the ages of 5 and 10 exhibiting the adamantinomatous type and second peak in the fifth and sixth decade. Clinical presentation includes visual disturbances related to compression of the optic chiasm, pituitary

hypofunction related to compression of the gland or hypothalamus, and/or symptoms of increased intracranial pressure.
Imaging findings typically include a cystic or solid and cyst mass. Approximately 80% to 90% of all craniopharyngiomas have a cystic component. Smaller lesions may be purely solid. The vast majority have calcification and enhance after administration of IV contrast. Rim enhancement may be seen around the cystic portions of these tumors, and the solid portions typically demonstrate more avid, solid enhancement. The cystic component is frequently hyperintense on T2 and may be hypointense, isointense, or hyperintense on T1.
Reference: Sartoretti-Schefer S, et al. MR differentiation of adamantinous and squamous-papillary craniopharyngioma. *Am J Neuroradiol* 1997;18:77–87.

5 Answer B. There is a nonenhancing mass associated with the tuber cinereum. The pituitary stalk and posterior pituitary bright spot are present. This case illustrates the characteristic appearance of a hamartoma of the tuber cinereum. The mass is isointense to gray matter on T1 imaging and sits just anterior to the mammary bodies at the level of the floor of the third ventricle.
Hamartomas are benign nonneoplastic lesions that are likely congenital in origin. Many are symptomatic, but symptoms may be more common in children and typically include gelastic seizures, "fits of laughter," and precocious puberty. Knowledge of this lesion and its radiologic and clinical presentations usually allows the diagnosis to be established in most cases. Atypical imaging findings including marked hyperintensity on T2 or lesion larger than 1.5 cm raise the possibility of hypothalamic glioma.
Reference: Boyko OB, et al. Hamartomas of the tuber cinereum: CT, MR and pathologic findings. *AJNR Am J Neuroradiol* 1991;12:309–314.

6 Answer A. MR imaging demonstrates a lobulated mixed cystic and solid enhancing pineal region mass, isointense to gray matter on T2 and T1 images, and containing several small internal foci of GRE hypointensity. There is extension to the left splenium of the corpus callosum and possible involvement of the midbrain. There is associated expansion of the third and lateral ventricles as well as periventricular T2 hyperintensity, consistent with moderate hydrocephalus. There is mild downward displacement of the cerebellar tonsils.
Tumors of pineal cell origin (pineoblastoma and pineocytoma) comprise only 15% of pineal region masses. Unlike germ cell tumors, which show a marked predilection in males, tumors of pineal cell origin occur equally among men and woman. Tumors of pineal origin frequently calcify. Calcification of the pineal gland in a child under 7 years of age should raise suspicion of tumor. After 7 years of age, the pineal gland begins to show calcification, which increases with age. Parinaud syndrome is a cluster of abnormalities of eye movement and pupil dysfunction with paralysis of upward gaze (downward gaze is usually preserved). This syndrome is associated with young patients with brain tumors in the pineal gland or midbrain.
MRI is most useful in characterizing masses in the pineal region. Tumors arising in the parapineal region in a child are usually gliomas arising from the tectal plate, whereas tumor arising in the parapineal region in adults may represent gliomas or meningiomas arising from the tentorium. Tumors of germ cell origin occur in children as do pineoblastomas, whereas pineocytomas are generally seen in adults.
Reference: Smirniotopoulos JG, et al. Pineal region masses: differential diagnosis. *Radiographics* 1992;12:577–596.

7 **Answer B.** Parinaud syndrome is a cluster of abnormalities of eye movement and pupil dysfunction with paralysis of upward gaze (downward gaze is usually preserved). This syndrome is associated with young patients with brain tumors in the pineal gland or midbrain.

8 **Answer B.** On MRI, there is a large, round right cerebellar mass with T2 hyperintensity, internal mural nodules, and peripheral contrast enhancement. There is mass effect on the fourth ventricle and left midline shift. Astrocytomas are the most common brain tumors of childhood with 60% occurring in the posterior fossa (40% in the cerebellum, 20% in the brain stem). Most of them are juvenile pilocytic astrocytomas (JPA), which are WHO grade 1 benign tumors. Differential diagnosis of cystic cerebellar masses includes hemangioblastomas, which have similar appearance to JPA. These are more common in young adults and children and are usually part of von Hippel-Lindau disease. Medulloblastoma and ependymomas usually have a shorter clinical history. They are typically centered on the fourth ventricle, isodense or hyperdense on nonenhanced CT, and characteristically not cystic. However, purely solid JPAs do occur.
As a rule, JPAs arise from the midline and can extend into the cerebellar hemispheres. Most are large at presentation (>5 cm). The tumor usually consists of a cyst with a solid nodule within the cyst wall. The cyst is most typically adjacent to the tumor (no peripheral enhancement), but in 40%, it may develop within it as a cyst-like necrotic center (peripheral enhancement). The frequency of JPA is equal in boys and girls usually occurring between birth and 9 years of age. The symptoms (headaches, early morning vomiting, ataxia) develop gradually over several months to become persistent and acute.
References: Campbell JW, Pollack IF. Cerebellar astrocytomas in children. *J Neurooncol* 1996;28:223–231.
Rashidi M, DaSilva VR, Minagar A, Rutka JT. Nonmalignant pediatric brain tumors. *Curr Neurol Neurosci Rep* 2003;3:200–205.

9 **Answer B.** On CT, there is a heterogeneous soft tissue mass centered at the fourth ventricle with foci of internal calcification. There is lateral and third ventriculomegaly. On MRI, there is an enhancing mass within the posterior fossa in the midline. The mass has restricted diffusion indicating that the mass is densely cellular. There is also GRE susceptibility, which indicates a component of hemorrhage or mineralization. There is extension of the mass out the left foramen of Luschka. There is mass effect on the fourth ventricle causing enlargement of the lateral ventricles. There is also periventricular edema. The major differential diagnostic consideration of a midline posterior fossa mass in children is a fourth ventricular ependymoma. These typically expand rather than compress the fourth ventricle. Less commonly, cerebellar astrocytomas may occur in the midline; however, they are typically hemispheric lesions.
Medulloblastoma comprise up to one-third of all pediatric posterior fossa tumors. They occur more commonly in boys and arise from the medullary velum of the fourth ventricle from primitive neuroectoderm. In children, they are typically midline masses associated with the inferior vermis. Subarachnoid seeding of the leptomeninges is very common at presentation; therefore, screening of the spine is recommended to exclude spread. On unenhanced CT, medulloblastomas are typically hyperdense relative to brain parenchyma because of their dense cellularity. Calcification, cystic change and/or hemorrhage may be present in up to 10% to 20% of lesions. On MRI, most medulloblastomas are mildly hypointense to brain parenchyma on T1 and vary in signal intensity on T2 images. These masses avidly enhance after contrast administration. As CSF seeding is common at presentation, imaging with contrast of the whole neuraxis is recommended to identify drop metastases and leptomeningeal spread. Although rare, extraneural spread is reported. Treatment typically consists of surgical resection, radiation therapy, and chemotherapy, with the prognosis strongly influenced by surgical resection, presence of CSF metastases at the time of diagnosis, and expression of the c-erbB-2 (HER2/neu) oncogene.
Reference: Nueller DP, Moore SA, Sato Y, Yuh WTC. MR spectrum of medulloblastoma. *Clin Imaging* 1992;16:250–255.

10 **Answer A.** Spine imaging to exclude drop metastases. CSF seeding is common in the setting of medulloblastoma therefore imaging with contrast of the whole neuraxis is recommended to identify drop metastases and leptomeningeal spread.

11 **Answer C.** Fetal MRI demonstrates bilateral ventriculomegaly. The septum pellucidum is absent. There is a small and upward tilted vermis and large posterior fossa CSF intensity space, which is continuous with the fourth ventricle. Postnatal MRI demonstrates marked lateral ventriculomegaly with moderate third ventricular enlargement and a large posterior fossa cyst. There is partial agenesis of the cerebellar vermis with upward tilted vermian remnant. There are bilateral small cerebellar hemispheres.
The Dandy-Walker complex (which includes Dandy-Walker malformation [DWM] and its variants) is a congenital anomaly believed to be related to an in utero insult to the fourth ventricle leading to complete or partial outflow obstruction of CSF. As a result, there is cyst-like dilation of the fourth ventricle, which protrudes up between the cerebellar hemispheres to prevent their fusion, and there is incomplete formation of all or part of the inferior vermis. DWMs are associated with hydrocephalus in 75% of cases. In addition, a significant number of patients are associated with supratentorial anomalies including dysgenesis of the corpus callosum, migrational anomalies, and encephaloceles. The radiologic hallmark of DWM is communication of a retrocerebellar cyst with the fourth ventricle.
Reference: Barkovich AJ, Kjos BO, Norman D, Edwards MS. Revised classification of posterior fossa cysts and cyst-like malformations based on the results of multiplanar MR imaging. *AJR Am J Roentgenol* 1989;153:1289–1300.

12 **Answer D.** MRI demonstrates a hypoplastic superior cerebellar vermis and dysplastic inferior cerebellar vermis. There is a dysmorphic fourth ventricle, which has “batwing” appearance. There is a hypoplastic cerebellar vermis with hypoplasia of the superior cerebellar peduncle resembling the “molar tooth sign” in the midbrain. There is an elongated and thinned superior cerebellar peduncle and interpeduncular fossa. The size of the brainstem is smaller than the normal appearance. There is a retrocerebellar mega cisterna magna with supracerebellar extension. There is partial agenesis of the septum pellucidum.
Joubert syndrome (JS) is a very rare, autosomal recessive condition. It is characterized by agenesis of cerebellar vermis, abnormal eye movements with nystagmus, episodes of hyperpnea and apnea, delayed generalized motor development, retinal coloboma and dystrophy, and, sometimes, multicystic kidney disease. A spectrum of cerebellar developmental anomalies are categorized into compete or incomplete cerebellar agenesis, medial aplasia/hypoplasia, and lateral aplasia/hypoplasia. These anomalies in cerebellar development may result in prominent CSF spaces or CSF collections/cystic dilation of the fourth ventricle (giant cisterna magna, Dandy-Walker malformations) in the posterior fossa. The predominant abnormality in Joubert syndrome is aplasia or hypoplasia of the vermis, particularly the superior portion. These patients have dysplastic cerebellar tissue including heterotopic and dysplastic cerebellar nuclei; abnormal development of the inferior olivary nuclei; and incomplete formation of the pyramidal decussation. It is an autosomal recessive disorder.

The characteristic appearance of Joubert syndrome includes:

- Diminutive vermis
- Enlarged fourth ventricle that is “batwing” shaped
- Superior cerebellar peduncles are vertically oriented and elongated in the AP direction
- Separation or disconnection of the cerebellar hemispheres, which are apposed by not fused in the midline

Reference: Friede RL, Boltshauser E. Uncommon syndromes of cerebellar vermis aplasia. I: Joubert Syndrome. *Dev Med Child Neurol* 1978;20:758–763.

13 **Answer D.** There is an absent septum pellucidum and dysmorphic appearance of the lateral ventricles. The corpus callosum is present but is dysmorphic. Right cerebral gray matter–lined cleft extending to the right lateral ventricle, compatible with closed-lip schizencephaly. There is extensive polymicrogyria in the left parietal occipital lobe and right occipital, parietal, and temporal lobes. The cerebellar vermis appears small and dysplastic. The optic nerves and chiasm appear small.
Septo-optic dysplasia (SOD), also known as de Morsier syndrome, is a condition characterized by optic nerve hypoplasia and absence of septum pellucidum and, in two-thirds of patients, hypothalamic–pituitary dysfunction. It is best thought of as being part of the holoprosencephaly spectrum. Clinical presentation of septo-optic dysplasia is varied and mostly dependent of whether or not it is associated with schizencephaly (~50% of cases). This association is used to define two forms of the condition:

- Not associated with schizencephaly
  - Visual apparatus more severely affected
  - Hypothalamic–pituitary dysfunction present in 60% to 80% of patients
  - May present as hypoglycemia in the neonatal period
  - Small pituitary gland with hypoplastic or absent infundibulum and ectopic posterior pituitary seen as focus of T1 high signal intensity in median eminence of hypothalamus
  - Olfactory bulbs may be absent (Kallmann syndrome)
- Associated with schizencephaly
  - Optic apparatus less severely affected
  - Cortical anomalies: polymicrogyria and cortical dysplasia
  - May be etiologically different
  - Sometimes referred to as septo-optic dysplasia plus
- In addition, a number of other associations are recognized including:
  - Rhombencephalosynapsis
  - Chiari II malformation
  - Aqueductal stenosis

MRI is the modality of choice for assessing septo-optic dysplasia. Imaging may demonstrate a "point down" appearance of the lateral ventricular frontal horns on coronal images, absent septum pellucidum, hypoplastic pituitary stalk, hypoplastic optic chiasm/optic nerves, and globes.
References: Barkovich AJ, Fram EK, Norman D. Septo-optic dysplasia: MR imaging. *Radiology* 1989;171(1):189–192.
Sener RN. Septo-optic dysplasia associated with cerebral cortical dysplasia (cortico-septo-optic dysplasia). *J Neuroradiol* 1996;23(4):245–247.

14 **Answer B.** There are multiple calcified subependymal nodules and cortical thickening in all lobes of the brain. There are enhancing tubers in the left frontal lobe. There are enhancing subependymal nodules at the right foramen of Monro. Tuberous sclerosis was classically described as presenting in childhood with a triad (Vogt triad) of:

- Seizures: absent in one-quarter of individuals
- Mental retardation: up to half have normal intelligence
- Adenoma sebaceum: only present in about three-quarters of patients

Tuberous sclerosis has a significant number of manifestations, involving many organ systems.

The most common manifestations are:

- Cortical or subependymal tubers and white matter abnormalities
- Renal angiomyolipomas (AML)
- Cardiac rhabdomyoma
- Cutaneous findings: adenoma sebaceum

After the neurological manifestations of TS, renal manifestations are the second most common clinical feature; four types of lesions can occur: autosomal dominant polycystic kidney disease lesions, isolated renal cyst(s), angiomyolipomas (AMLs), and renal cell carcinomas.
Cortical/subcortical tubers are commonly located in the frontal lobe and demonstrate high T2 and low T1 with only 10% of tubers showing enhancement. The tubers frequently calcify after 2 years of age. The subependymal hamartomas are often associated with calcification. Lesion enhancement is variable and is not a useful feature in distinguishing them from subependymal giant cell astrocytomas (SEGA). Subependymal giant cell astrocytomas' peak occurrence is 8 to 18 years of age and tends to be large and demonstrates growth. These lesions tend to have intense enhancement. The white matter abnormalities demonstrate variable appearance, with nodular, ill-defined, cystic and band-like lesions seen. One way to differentiate tuberous sclerosis from multiple sclerosis is that radial bands are thought to be relatively specific for tuberous sclerosis.
References: Goh S, Butler W, Thiele EA. Subependymal giant cell tumors in tuberous sclerosis complex. *Neurology* 2004;63(8):1457–1461.
Takanashi J, Sugita K, Fujii K, et al. MR evaluation of tuberous sclerosis: increased sensitivity with fluid-attenuated inversion recovery and relation to severity of seizures and mental retardation. *AJNR Am J Neuroradiol* 1995;16(9):1923–1928.

15 **Answer A.** Genitourinary. After the neurological manifestations of TS, renal manifestations are the second most common clinical feature; four types of lesions can occur: autosomal dominant polycystic kidney disease lesions, isolated renal cyst(s), angiomyolipomas (AMLs), and renal cell carcinomas.

16 **Answer C.** Aqueductal stenosis. Head ultrasound demonstrates that the lateral ventricles are moderately enlarged and very little extra-axial fluid is seen. The fourth ventricle is decompressed. Brain MRI demonstrates moderate to marked ventriculomegaly with enlargement of the lateral and third ventricles. The fourth ventricle is normal in size. The cerebral aqueduct is incompletely visualized and appears narrow. Aqueductal stenosis (AS) is the most common cause of congenital obstructive hydrocephalus but can also be seen in adults as an acquired abnormality. Antenatal ultrasound can show features of fetal hydrocephalus with a near-normal posterior fossa. There can be secondary thinning of the cortical mantle as well as secondary macrocephaly. MRI demonstrates enlargement of the lateral and third ventricles. The aqueduct may show narrowing and funnelling superiorly. The fourth ventricle is classically not dilated. One must exclude causes of secondary obstruction such as aqueductal or tectal plate tumor. An MRI CSF flow study is helpful, and the absence of a flow void signal intensity on sagittal T2 images at the aqueductal level has been suggested as a sign of aqueductal stenosis.
References: Mcmillan JJ, Williams B. Aqueduct stenosis. Case review and discussion. *J Neurol Neurosurg Psychiatr* 1977;40(6):521–532. doi:10.1136/jnnp.40.6.521.
Stoquart-El Sankari S, Lehmann P, Gondry-Jouet C, et al. Phase-contrast MR imaging support for the diagnosis of aqueductal stenosis. *AJNR Am J Neuroradiol* 2009;30(1):209–214.

17 Answer A. MRI images demonstrate a mass in the caudal aspect of the fourth ventricle. This rounded mass has high T1 signal, isointense T2 signal, areas of low signal on GRE, and homogeneous enhancement. Differential consideration for a mass centered in the fourth ventricle include:

Medulloblastoma	Arises from vermis or roof of fourth ventricle (superior medullary velum) Small round blue cells: hyperdense on CT 50% have CSF dissemination at diagnosis Solid, enhancing mass within fourth ventricle Hydrocephalus in > 90%
Ependymoma	Arises from floor of fourth ventricle "Plastic" tumor squeezes out lateral recesses and foramen of Magendie Intratumoral cysts and hemorrhage common 2/3 are infratentorial within fourth ventricle. Heterogeneous and enhancing mass
Pilocytic astrocytoma	Cyst with enhancing mural nodule Typically cerebellar hemisphere rather than intraventricular 60% are cerebellar; 30% optic nerve/chiasm
Brainstem glioma	Intrinsic to brainstem, not fourth ventricle May be dorsally exophytic, project posteriorly into fourth ventricle
Subependymoma	Inferior fourth ventricle, obex (60%) Middle-aged and older adults T2 hyperintense lobular mass No or mild enhancement is typical.
Choroid plexus papilloma	40% involve fourth ventricle (posterior medullary velum), CPA, and foramina of Luschka Fourth ventricle common location in adults Lateral ventricle more common in child Lobular and vibrantly enhancing mass

There are three types of choroid plexus tumor (CPT):

- Choroid plexus papilloma (CPP) (WHO grade I)
- Atypical choroid plexus papilloma (aCPP) (grade II)
- Choroid plexus carcinoma (CPCa) (grade III)

Classic imaging appearance of CPP is a child with enhancing lobulated (cauliflower-like) mass in atrium of lateral ventricle. CPPs occur in proportion to amount of choroid plexus. CPP is typically located in the following locations:

- 50% in lateral ventricle (usually atrium)
- 40% in fourth ventricle and/or foramina of Luschka
- 5% in third ventricle (roof)

References: Jaiswal AK, Jaiswal S, Sahu RN, et al. Choroid plexus papilloma in children: diagnostic and surgical considerations. *J Pediatr Neurosci* 2009;4(1):10–16.
Smith A, Smirniotopoulos J, Horkanyne-Szakaly I. From the radiologic pathology archives: intraventricular neoplasms: radiologic-pathologic correlation. *Radiographics* 2013;33(1):21–43.

18 Answer D. There is mid to posterior sagittal synostosis as well as synostosis of the right lambdoid suture resulting in some scaphocephaly and asymmetric posterior brachycephaly. There is also likely synostosis of the transverse occipital suture/synchondrosis between the occipital portion of the basiocciput and the squamosal occipital bone. Craniostenosis or craniosynostosis refers to premature closure of one or more of the cranial sutures. Isolated premature closure of the sagittal suture is most common. Unilateral or bilateral premature closure of the coronal suture is the next most common followed by premature of the metopic suture. Depending on which suture prematurely fuses, there are characteristic deformities of the skull and orbits. For example, premature closure of the sagittal suture results in limited transverse growth of the skull, namely, dolichocephaly or scaphocephaly, which is an increased anterior–posterior dimension. Plagiocephaly refers to premature closure of a single coronal or lambdoid suture. In the majority of cases, plagiocephaly is seen with closure of a single coronal suture, resulting in elevation of the lesser wing of the sphenoid bone leading to the "harlequin" appearance of the orbit.

Craniosynostosis is usually an isolated abnormality although it can be associated with a variety of syndromes. Such conditions include Apert syndrome, hypophosphatasia, Crouzon disease (craniofacial dysostosis), and Treacher Collins syndrome (mandibulofacial dysostosis).
Reference: Mafee MF, Valvassori GE. Radiology of the craniofacial anomalies. *Otolaryngol Clin North Am* 1981;14:939–988.

19 Answer B. There is a mass within and expanding the left midanterior nasal cavity. The mass is noted to extend superiorly to the level of the cribriform plate. This mass is hypointense on T1 and hyperintense on T2. There is no internal enhancement within the mass. Nasal encephaloceles are in most cases a form of neural tube defect particularly common in Southeast Asia. They are herniation of cranial content through a bony defect in the anterior skull base into the nasal area. Nasal encephaloceles usually present at birth with symptoms of obstruction or other complications. It presents as an external swelling on the nose. The swelling is usually soft, with normal overlying skin, and increases in size on coughing/straining. Symptomatic patients usually present with obstruction or rhinorrhea. Nasal encephaloceles are typically identified in association with a discernible cranial bone defect. Best imaging practices include multiplanar MRI to delineate soft tissues and intracranial relationships and bone CT to define osseous anatomy (except nasofrontal region in infants).
Reference: Tirumandas M, et al. Nasal encephaloceles: a review of etiology, pathophysiology, clinical presentations, diagnosis, treatment, and complications. *Childs Nerv Syst* 2013;29(5):739–744.

20 Answer B. There is an 11-mm-wide crescent-shaped hyperdense extra-axial hematoma overlying the left posterior convexity parietal region. Extradural hematoma (EDH), also known as an epidural hematoma, is a collection of blood that forms between the inner surface of the skull and outer layer of the dura, which is called the periosteal layer. They are commonly associated with a history of trauma and associated skull fracture. The source of bleeding is usually a torn meningeal artery (most commonly, the middle meningeal artery). EDHs are typically biconvex in shape and can cause a mass effect with herniation. They are usually limited by cranial sutures, but not by venous sinuses. Both CT and MRI are suitable to evaluate EDHs. When the blood clot is evacuated promptly (or treated conservatively when small), the prognosis of EDHs is generally good.
Reference: Irie F, Le Brocque R, Kenardy J, et al. Epidemiology of traumatic epidural hematoma in young age. *J Trauma* 2011;71(4):847–853.

21 Answer D. US demonstrates an anechoic, vascular structure at the level of the tentorium with mild mass effect on the right lateral ventricle. MRI and MRA demonstrate prominent galenic/transfalcine perimesencephalic vein with associated hypogenesis of the corpus callosum posteriorly. Vein of Galen aneurysmal malformations (VGAM), probably better termed as median prosencephalic arteriovenous fistula, are uncommon intracranial anomalies that tend to present dramatically during early childhood with features of a left-to-right shunt and high-output cardiac failure. These malformations account for <1% to 2% of all intracranial vascular malformations but are the cause of 30% of cerebral vascular malformations presenting in the pediatric age group. It is also the most common antenatally diagnosed intracranial vascular malformation. There may be an increased male predilection.

References: Bhattacharya JJ, Thammaroj J. Vein of galen malformations. *J Neurol Neurosurg Psychiatr* 2003;74(Suppl 1):i42–i44. Nicholson AA, Hourihan MD, Hayward C. Arteriovenous malformations involving the vein of Galen. *Arch Dis Child* 1989;64(12):1653–1655.

22 **Answer A.** Angiography remains the gold standard in full characterization of the lesion. It enables to individually catheterize feeding vessels. Venous drainage is via the median prosencephalic vein (MPV), the straight sinus (if present) and then out via the transverse/sigmoid sinuses. By definition, there should be no drainage to other components of the deep venous system. Prior to endovascular intervention, prognosis was dismal, with 100% mortality without treatment and 90% mortality following surgical attempts. Ideally, embolization is deferred until 6 months of age for choroidal VGM and later for mural types, to allow the cavernous sinus to mature. If cardiac failure is refractory to medical management, embolization may be performed sooner. Both venous and arterial embolization is possible, depending on the number of feeders, and controversy persists in regard to the optimum approach.

23 **Answer A.** US demonstrates bilateral ventriculomegaly, bilateral periventricular hyperechogenicity with shadowing consistent with calcification, and bilateral complex but predominantly cystic changes in both germinal matrices consistent with subacute hemorrhage. The lenticulostriate arteries are hyperechogenic consistent with vasculopathy. MRI demonstrates moderate dysmorphic ventriculomegaly, periventricular calcifications, and subependymal cysts, including prominent bilateral subependymal cysts near the foramen of Monro. Abnormal gyration pattern with bilateral polymicrogyria as well as frontal predominant undersulcation.
Congenital cytomegalovirus infection results from intrauterine fetal infection by cytomegalovirus (CMV). CMV is the most common cause of intrauterine infection and most common cause of congenital infective and brain damage. Antibodies to CMV are seen in 30% to 60% of pregnant women, but only 2.5% have a primary infection during pregnancy, and this can result in fetal infection in approximately 30% of cases. The vast majority (90%) of infected babies are asymptomatic at birth, but some may go on to develop symptoms after 6 to 9 months.
US imaging findings include fetal intracranial calcification: mainly periventricular calcification (hyperechogenic foci), considered one of the most common features; fetal hydrocephalus; heterogeneous appearing brain parenchyma; microcephaly; and intraventricular adhesions.

MR brain imaging findings include:

- Microcephaly
- Migrational abnormalities: lissencephaly, pachygyria, and schizencephaly
- White matter lesions: predominantly parietal or posterior white matter involvement with spared rim in immediately periventricular and subcortical white matter
- Ventriculomegaly and subarachnoid space enlargement
- Delayed myelination
- Periventricular and temporal pole cysts

References: Ceola AF, Angtuaco TL. US case of the day. Congenital cytomegalovirus infection. *Radiographics* 1999;19(5):1385–1387. Malinger G, Lev D, Zahalka N, et al. Fetal cytomegalovirus infection of the brain: the spectrum of sonographic findings. *AJNR Am J Neuroradiol* 2003;24(1):28–32.

24 **Answer A.** Chest radiography demonstrates bilateral healing rib fractures. Noncontrast head CT demonstrated intermediate density extra-axial (subdural) fluid at the frontal convexities and hyperdense extra-axial (subdural) hemorrhage along the posterior interhemispheric fissure and at the apex. The presence of skull fractures and/or intracranial hemorrhage particularly in infants in the absence of known trauma to explain such injuries should raise the suspicion of child abuse. Head injury is the leading cause of morbidity and mortality in these abused children. Brain injury may be the result of direct trauma, aggressive shaking, or strangulation/suffocation. There is little or no evidence of external trauma.

The most common type of intracranial hemorrhage in the setting of child abuse is subdural hematoma although subarachnoid, epidural, intraventricular, and cortical hemorrhages are also manifestations of NAT. Bilateral retinal hemorrhages are highly suggestive of child abuse. Complex skull fractures and cerebral infarction are also diagnostic harbingers of child abuse.
Reference: Sato Y, Yuh WTC, Smith WL. Head injury in child abuse: evaluation with MR imaging. *Radiology* 1989;173:653–657.

25 Answer B. Images demonstrate two lytic lesions in the left parietal region and one at the apical parietal region. The skeleton is the most commonly involved organ system in Langerhans cell histiocytosis (LCH) and is by far the most common location for single-lesion LCH, often referred to as eosinophilic granuloma (EG). Patients may have one or, less commonly, many lesions.

The most common locations are the skull and long bones:
- Skull: approximately 50%
- Pelvis: 23%
- Femur: 17%
- Ribs: 8% (most common in adults)
- Humerus: 7%
- Mandible: 7%
- Spine

Skull radiographic imaging findings include:
- Solitary or multiple punched out lytic lesions without sclerotic rim
- Double-contour or beveled-edge appearance may be seen due to greater involvement of the inner versus the outer table (hole within a hole) sign
- Button sequestrum representing residual bone
- Geographic skull

Prognosis is excellent when disease is confined to the skeleton, especially if it is a solitary lesion, with the majority of such lesions spontaneously resolving by fibrosis within 1 to 2 years.
Reference: David R, Oria RA, Kumar R, et al. Radiologic features of eosinophilic granuloma of bone. *AJR Am J Roentgenol* 1989;153(5):1021–1026.

26 **Answer C.** MRI demonstrates multifocal areas of FLAIR hyperintensity throughout the cerebral white matter, as well as left optic nerve thickening/hyperintensity, and extraocular muscle thickening. Acute disseminated encephalomyelitis is an immune-mediated demyelinating disease related to an antecedent viral infection or vaccination. The cause is believed to be an allergic or autoimmune (cell-mediated) response against the myelin basic protean because of cross-reaction with viral proteins. ADEM has most commonly been associated with measles; however, it has also been associated with chickenpox, rubella, mumps, and other viral agents.

Both clinically and on MRI, ADEM may appear identical to the initial presentation of multiple sclerosis. Patients may present with symptoms and focal neurologic deficits typically within 2 to 3 weeks following a viral illness. In addition to focal neurologic deficits, unlike multiple sclerosis, ADEM is not infrequently associated with seizures. ADEM more common involved white matter especially in the subcortical region; however, gray matter may also be involved. MRI typically demonstrates multiple hyperintense foci on T2. These lesions may or may not enhance. ADEM is a monophasic process; therefore, no new lesions should develop after 6 months following initial presentation. The diagnosis of ADEM can usually be made by clinical history and CSF analysis.

Reference: Mader I, Stock KW, Ettlin T, Probst A. Acute disseminated encephalomyelitis: MR and CT features. *AJNR Am J Neuroradiol* 1996;17:104–109.

27 **Answer C.** There is a well-circumscribed and heterogeneously enhancing extradural mass extending dorsally from the posterior sphenoid body and clivus. The mass is T2 bright and has some internal areas of mixed signal and areas of mineralization. Chordomas arise in locations where notochordal remnants are found. They occur most commonly at the sacrum although not infrequently found at the clivus or upper cervical spine. They are considered benign neoplasms; however, they grow quite invasively especially at the skull base where they can invade the neural foramen and cavernous sinus or extend into the middle cranial fossa.

On CT, a calcified matrix may be present and regions of bony erosion or destruction are best visualized. On MRI, the signal characteristics of chordoma are variable. These tumors are typically hypointense on T1 and hyperintense on T2. Most chordomas enhance. The differential considerations include chondrosarcoma, metastatic disease, multiple myeloma, and lymphoma.

Reference: Myers SP, Hirsch WJ Jr, Curtin HD, Barnes I, Skhear LN, Sen C. Chordomas of the skull base: MR features. *AJNR Am J Neuroradiol* 1992;13:1627–1636.

Head and Neck

28 Answer B. The lateral neck radiograph demonstrates abnormal thickening of the prevertebral soft tissues. Please note that the lateral neck position in this case is suboptimal due to the neck in flexion. The pediatric neck should be positioned in extension for the lateral radiograph since neutral or flexion position can lead to false positive preverterbral soft tissue thickening due to redundancy of the soft tissues. It may be difficult to obtain correct radiographic positioning due to neck stiffness at the time of presentation.

CT is excellent at evaluating the neck soft tissues in an emergency setting when there is potential narrowing of the patient's airway and inability to obtain optimal radiographic positioning. CT imaging of the neck should be performed with intravenous contrast to differentiate fluid masses (abscess) from phlegmonous thickening (retropharyngeal cellulitis). It is important to note that CT imaging can lead to false-positive and false-negative results with respect to detecting pus. Therefore, surgical exploration may need to be carried out on the basis of clinical presentation.

29 Answer B. Neck radiograph demonstrates abnormal thickening of the prevertebral soft tissues. CT demonstrates a low-density collection with incomplete peripheral enhancement in the left parapharyngeal space consistent with a retropharyngeal abscess. Retropharyngeal abscesses are most frequently encountered in children, with 75% of cases occurring before the age of 5 years and often in the first year of life. This is likely due to the combination of prominent retropharyngeal nodal tissue and frequency of middle ear and nasopharyngeal infections. There may be a slight male predilection. Presentation is variable. In some instances, children present with nonspecific symptoms including generalized irritability, fever, and decreased appetite.

Radiographs demonstrate soft tissue swelling posterior to the pharynx, with a widening of the prevertebral soft tissues. This appearance cannot be distinguished from a prevertebral abscess, and careful evaluation of the vertebral bodies and disc spaces is important. CT is excellent at evaluating the neck, and timeliness is essential given potential narrowing of the airway. CT imaging should be obtained with IV contrast to allow differentiation of fluid collections from phlegmonous thickening (retropharyngeal cellulitis). It is important to note however that CT has a insignificant rate of both false-positive (10%) and false-negative (13%) rates with respect to detecting pus, and as such, surgical exploration may need to be carried out on the basis of clinical presentation. Treatment is similar in principle to that of other infected collections usually requiring both surgical drainage (usually performed via a transoral route) and intravenous antibiotics. In some instances, antibiotics alone may suffice, when collections are small.

With a prompt diagnosis, appropriate antibiotics and drainage when necessary, almost all patients recover uneventfully. Serious complications in developed nations with prompt access to imaging and antibiotic are uncommon; however, complacency needs to be avoided as retropharyngeal can lead to potentially life-threatening complications.

References: Coulthard M, Isaacs D. Retropharyngeal abscess. *Arch Dis Child* 1991;66(10):1227–1230.

Craig FW, Schunk JE. Retropharyngeal abscess in children: clinical presentation, utility of imaging, and current management. *Pediatrics* 2003;111(6 Pt 1):1394–1398.

30 **Answer A.** There is unilateral right-sided choanal atresia with a fluid level along the right nasal cavity. The left side is normal. Choanal atresia refers to a lack of formation of the choanal openings. It can be unilateral or bilateral. Approximately two-third of cases are unilateral. It frequently presents in neonates where it is one of the most common causes of nasal obstruction. There is a recognized female predilection. Unilateral choanal atresias present late and can be asymptomatic or present with rhinorrhoea, whereas bilateral atresias can present with neonatal respiratory distress (infants are obligate nose breathers). Another finding is failure to pass a nasogastric tube.

Structurally, there are two main types:

- Osseous: 90%
- Membranous: 10%

Syndromic associations include:

- CHARGE syndrome
- Crouzon syndrome
- DiGeorge syndrome
- Amniotic band syndrome
- Fetal alcohol syndrome
- Treacher Collins syndrome

Other associations include:

- Intestinal malrotation
- Craniosynostosis
- Congenital heart disease

Axial CT scans are the best modality and can demonstrate:

- Unilateral or bilateral posterior nasal narrowing with an obstruction
- Airway <3 mm (measurement done at the reference level of the pterygoid plates in the axial plane)
- Air–fluid level above the obstruction point
- Thickening of the vomer
- Medial bowing of posterior maxillary sinus

Treatment options include endoscopic perforation (for membranous types) and full choanal reconstruction.

References: Hengerer AS, Brickman TM, Jeyakumar A. Choanal atresia: embryologic analysis and evolution of treatment, a 30-year experience. *Laryngoscope* 2008;118(5):862–866.
Tadmor R, Ravid M, Millet D, et al. Computed tomographic demonstration of choanal atresia. *AJNR Am J Neuroradiol* 1984;5(6):743–745.

31 **Answer D.** MRI demonstrates a heterogeneously enhancing mass originating in the posterior nasal cavity in the region of the sphenopalatine foramen extending into the medial aspect of the pterygopalatine fossa. This mass extends superiorly through the floor of the sphenoid into the left sphenoid sinus. There is involvement of the anterior left vidian canal within the sphenoid. The mass extends anteriorly into the nasal cavity and posteriorly into the nasopharynx.

32 **Answer A.** External carotid angiography and polyvinyl alcohol particle embolization of left nasopharyngeal tumor via distal internal maxillary artery.
Juvenile nasopharyngeal angiofibromas (JNA) are a rare benign but locally aggressive vascular tumor. Juvenile nasopharyngeal angiofibromas occur almost exclusively in males and usually in adolescence. They account for only 0.5% of all head and neck tumors but are the most common of benign nasopharyngeal neoplasms. The presentation is typically with obstructive symptoms, epistaxis, and chronic otomastoiditis because of obstruction of the Eustachian tube.
CT is particularly useful at delineating bony changes. Typically, a lobulated nonencapsulated soft tissue mass is demonstrated centered on the sphenopalatine foramen (which is often widened) and usually bowing the posterior wall of the maxillary antrum anteriorly. There is marked contrast enhancement following administration of contrast, reflecting the prominent vascularity. Angiography is often useful both in defining the feeding and in preoperative embolization.

Supply of these tumors is usually via:

- External carotid artery: majority
- Internal maxillary artery
- Ascending pharyngeal artery
- Palatine arteries
- Internal carotid artery: less common, usually in larger tumors
- Sphenoidal branches
- Ophthalmic artery

References: Duvall AJ, Moreano AE. Juvenile nasopharyngeal angiofibroma: diagnosis and treatment. *Otolaryngol Head Neck Surg* 1988;97(6):534–540.
Kania RE, Sauvaget E, Guichard JP, et al. Early postoperative CT scanning for juvenile nasopharyngeal angiofibroma: detection of residual disease. *AJNR Am J Neuroradiol* 2005;26(1):82–88.

33 **Answer B.** There are mildly enhancing mineralized T2 hypointense masses present within the bilateral globes, which are fairly symmetric in appearance. There is no extension into the surrounding intraorbital structures. Retinoblastomas are the most common intraocular neoplasm found in childhood. Presentation is most frequently with leukocoria or loss of red-eye reflex. Overall, approximately 30% to 40% are bilateral and often synchronous. The bilateral occurrence is even higher in inherited forms and tends to occur at a younger age. They are generally characterized by a heterogeneous retinal mass with calcifications, necrotic components, and increased vascularization on Doppler ultrasound/enhancement on CT/MRI. MRI is the modality of choice for pretreatment staging on retinoblastoma. Prognosis depends on the stage. Overall, the cure rate has risen to over 90% in first world nations.
References: de Graaf P, Barkhof F, Moll AC, et al. Retinoblastoma: MR imaging parameters in detection of tumor extent. *Radiology* 2005;235(1):197–207.
Kaufman LM, Mafee MF, Song CD. Retinoblastoma and simulating lesions. Role of CT, MR imaging and use of Gd-DTPA contrast enhancement. *Radiol Clin North Am* 1998;36(6):1101–1117.

34 **Answer B.** In the left neck, there is a slightly lobulated, oblong slightly T2 hyperintense, minimally enhancing lesion in the left paracervical, submandibular, and carotid spaces.
Also notable, there is a slightly asymmetric morphology of the thymic gland with prominence on the right. Signal characteristics of this gland are similar to the lesion in the left neck.
Ectopic thymus can occur anywhere along the caudal descent of the thymopharyngeal duct (migration of the thymus from the third and fourth branchial pouches to the anterior mediastinum) and also found rarely in the posterior mediastinum and dermis. Ectopic thymic tissue may manifest as a neck mass, which can be mistaken for a pathologic process.
Also, as the thymopharyngeal duct undergoes atrophy, thymic remnants may develop into cysts. Because the parathyroid glands similarly arise from the third and fourth pharyngeal pouches, ectopic parathyroid glands, and hence parathyroid adenomas, may appear anywhere near or within the thyroid or thymus.
Reference: Nasseri F, Eftekhari F. Clinical and radiologic review of the normal and abnormal thymus: pearls and pitfalls. *Radiographics* 2010;30(2):413–428. doi:10.1148/rg.302095131.

35 **Answer A.** In the region of the right parotid gland, there is a rounded fluid density. There is surrounding thick enhancement with overlying soft tissue swelling. Given the patient's age, differential considerations include an infected or inflamed branchial cleft cyst.

Acute inflammation of parotid gland in a child can be cause by:
- Bacterial: Localized bacterial infection ± abscess
  - Usually because of ascending infection.
  - May result from adjacent cellulitis.
  - *Staphylococcus aureus* (50% to 90%) > *Streptococcus*, *Haemophilus*, *E. coli*, and *anaerobes*.
  - Neonatal suppurative parotitis may be bilateral because of bacteremia.
    - More common in premature infants, males
- Viral: Usually from systemic viral infection
  - Mumps paramyxovirus most common cause (so-called epidemic parotitis)
  - Also influenza, parainfluenza, coxsackie A and B, ECHO, and lymphocytic choriomeningitis viruses
  - CMV and adenovirus reported with HIV infection
- Calculus induced: Ductal obstruction by sialolith
- Autoimmune: Acute episode of chronic disease
  - Sjögren syndrome
  - Mikulicz syndrome
  - Sicca syndrome, acute phase
- Juvenile recurrent parotitis (JRP): Intermittent idiopathic episodes of parotid inflammation
  - Recurrent episodes mimic mumps.
  - Patient often has unilateral symptoms but bilateral imaging abnormalities.
  - Sialographically mimics Sjögren syndrome.

Top differential considerations:
- Infected first branchial cleft anomaly
- Parotid infantile hemangioma
- Salivary gland neoplasms
- Parotid sialosis
- Benign lymphoepithelial lesions of HIV
- Parotid sarcoidosis

References: Francis CL, et al. Pediatric sialadenitis. *Otolaryngol Clin North Am* 2014;47(5):763–778.

Spiegel R, et al. Acute neonatal suppurative parotitis: case reports and review. *Pediatr Infect Dis J* 2004;23(1):76–78.

36 Answer A. On US, in the midline at the suprasternal region, just below level of thyroid, is a hypoechoic rounded mass with posterior acoustic enhancement and internal echogenic debris. On MRI, there is a T2 hyperintense cystic neck lesion with rim enhancement extending between the hyoid bone and laryngeal prominence.

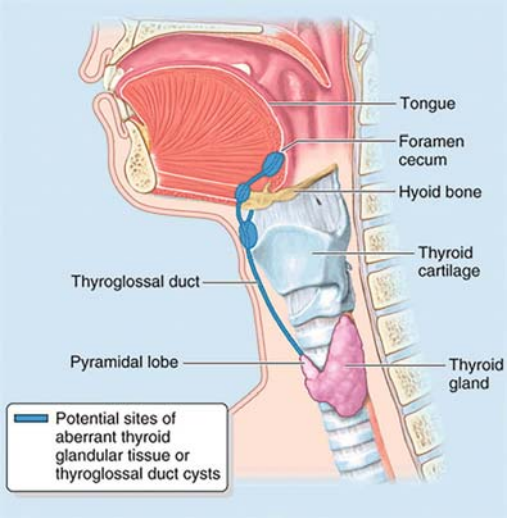

Thyroglossal duct vestiges. (From Moore KL, Dalley AF, Agur AM. *Clinically Oriented Anatomy*, 7th Ed. Philadelphia, PA: Wolters Kluwer Health 2014:1041.)

Thyroglossal duct cysts (TGDC) are the most common congenital neck cyst. They are typically located in the midline and are the most common midline neck mass in young patients. Thyroglossal duct cysts typically present during childhood (90% before the age of 10) or remain asymptomatic until they become infected, in which case they can present at any time. Thyroglossal duct cysts account for 70% of all congenital neck anomalies and are the second most common benign neck mass, after lymphadenopathy. Presentation is typically either as a painless rounded midline anterior neck swelling or, if infected, as a red warm painful lump. It may move with swallowing and classically elevates on tongue protrusion.

The cysts can occur anywhere along the course of the thyroglossal duct, although infrahyoid location is most common:

- Suprahyoid: 20% to 25% (less common in adults ~5%)
- At the level of hyoid bone: approximately 30% (range 15% to 50%)
- Infrahyoid: approximately 45% (range 25% to 65%)

Typically, they are located in the midline with those off-midline characteristically located next to the thyroid cartilage. Nearly all thyroglossal duct cysts are located within 2 cm of the midline, with more inferior lesions tending to be off-midline. Ectopic thyroid tissue may be present.

Unless infected, they are painless, fluctuant masses, which spread the strap muscles. The fluid is usually anechoic and the walls are thin, without internal vascularity. However, in some cases, the internal fluid may contain debris. This is particularly the case in an adult patient where cysts may be complex heterogeneous masses. If there is associated infection, there may be surrounding inflammatory change.

References: Ahuja AT, King AD, King W, et al. Thyroglossal duct cysts: sonographic appearances in adults. *AJNR Am J Neuroradiol* 1999;20(4):579–582.

Meuwly JY, Lepori D, Theumann N, et al. Multimodality imaging evaluation of the pediatric neck: techniques and spectrum of findings. *Radiographics* 2005;25(4):931–948. doi:10.1148/rg.254045142

37 Answer B. Extensive multiloculated bilateral transspatial mixed venolymphatic malformation demonstrating innumerable small fluid-filled cysts involving the face and neck with extension inferiorly to the anterior chest wall and superior mediastinum. Percutaneous sclerotherapy for treatment of bilateral neck lymphatic malformation was performed. The neck radiograph demonstrates retained contrast from the procedure.

Lymphatic malformations are benign vascular lesions that arise from embryological disturbances in the development of the lymphatic system. They encompass a wide spectrum of related abnormalities, including cystic lymphatic lesions, angiokeratoma, destructive lymphatic malformations that occur in bones (Gorham-Stout syndrome), lymphatic and chylous leak conditions, and lymphedema. Symptoms

of lymphatic malformations are related to the anatomical location of these lesions, as well as to the extent of involvement of the local anatomical structures.
Lymphatic malformations can be seen in any anatomic region but are more commonly seen in lymphatic-rich areas, such as the head and neck (45% to 52%), axilla, mediastinum, groin, and retroperitoneum. These malformations are thought to be the result of abnormal development of the embryonic lymphatics or lymphatic jugular sacs, with failure of these structures to connect or drain into the venous system. In some patients, ectatic adjacent veins can be seen in association with a cystic lymphatic lesion. There are three morphologic types of cystic lymphatic lesions: macrocystic, microcystic, and combined. Histologically, cystic lymphatic malformations are composed of vascular spaces filled with eosinophilic and protein-rich fluid. Hemorrhage within the cystic spaces is common, indicating recent trauma or spontaneous intralesional bleeding.
Large cystic lymphatic lesions can be diagnosed in utero using ultrasound as early as the beginning of the second trimester, but lesions are more commonly noted at birth; the vast majority are evident by 2 years of age. Unlike hemangiomas, lymphatic malformations persist throughout life, grow proportionately with the size of the patient, and do not undergo involution as does hemangioma. The prenatal diagnosis of cervical lymphatic malformations has significant clinical implications. They may be associated with airway obstruction, and prenatal diagnosis can influence the mode, timing, and place of delivery. The term “cystic hygroma” should not be applied to typical lymphatic malformation masses for two reasons. Firstly, the -oma suffix suggests a neoplasm, which it is not. Secondly, this term is prevalent in the obstetric vernacular to denote posterior cervical cystic lesions that are associated with severe, often lethal, chromosomal anomalies. However, it is crucial to distinguish “hygroma” from typical lymphatic malformations seen postnatally, because the latter is not associated with chromosomal abnormalities or syndromes.
CT or MRI can clearly demonstrate the anatomic extent of cystic lesions and their relationship to soft tissues, muscle, and vascular structures.
Reference: Elluru RG, Balakrishnan K, Padua HM. Lymphatic malformations: diagnosis and management. *Semin Pediatr Surg* 2014;23(4):178–185. doi:10.1053/j.sempedsurg.2014.07.002

38 Answer C. There is a round hypoechoic heterogeneous fusiform lesion within the right sternocleidomastoid muscle. The lesion has internal vascularity similar to the adjacent musculature. Fibromatosis colli is a rare form of infantile fibromatosis that occurs within the sternocleidomastoid muscle (SCM). Presentation is usually with torticollis and is most frequently related to birth trauma (e.g., forceps delivery) or malposition in the womb. Ultrasound is the imaging modality of choice. The SCM is diffusely enlarged in a fusiform manner, with resultant shortening when the head is turned away from the affected side (mastoid process drawn inferiorly toward the ipsilateral head of clavicle). Echogenicity of the SCM may vary. Color Doppler may reveal a high-resistance waveform. The enlarged area often moves synchronously with the rest of the SCM muscle on real-time sonography. It is a self-limiting condition and usually resolves within 4 to 8 months and is treated conservatively with physiotherapy.
References: Crawford SC, Harnsberger HR, Johnson L, et al. Fibromatosis colli of infancy: CT and sonographic findings. *AJR Am J Roentgenol* 1988;151(6):1183–1184.
Patrick LE, O'shea P, Simoneaux SF, et al. Fibromatoses of childhood: the spectrum of radiographic findings. *AJR Am J Roentgenol* 1996;166(1):163–169.

Spine

39 Answer D. Fetal MRI demonstrates ventriculomegaly with the lateral ventricles measuring up to 14 mm in maximum dimension bilaterally at the level of the atria (10 mm and above is considered enlarged). There is a small posterior fossa with low-lying hindbrain elements. There is a large dorsal neural arch dysraphic defect starting near the T8–T9 level and extending from the lower thoracic to midlumbar spine associated with a fluid-filled sac. Spinal cord and neural elements course along the dorsal aspect of the thoracolumbar dysraphic defect.

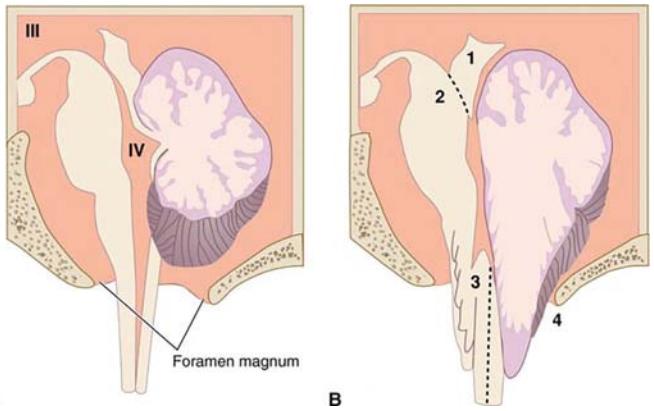

Chiari malformation. Midsagittal section. A: Normal cerebellum, fourth ventricle, and brainstem. B:Abnormal cerebellum, fourth ventricle, and brainstem showing the common congenital anomalies: (1) beaking of the tectal plate, (2) aqueductal stenosis, (3) kinking and transforaminal herniation of the medulla into the vertebral canal, and (4) herniation and unrolling of the cerebellar vermis into the vertebral canal. An accompanying meningomyelocele is common. (Reprinted from Fix JD. *BRS neuroanatomy*. Baltimore, MD: Williams & Wilkins; 1996:72, with permission.)

Chiari II malformation, also known as Arnold-Chiari malformation, is a relatively common congenital malformation of the spine and posterior fossa characterized by myelomeningocele (lumbosacral spina bifida aperta) and a small posterior fossa with descent of the brainstem and cerebellar tonsils. The presentation can be divided according to the age of the individual (although most will have lifelong sequelae) as follows:

- Neonatal
  - Myelomeningocele
  - Brainstem dysfunction resulting in cranial nerve palsies
  - Neurogenic bladder
- Child
  - Musculoskeletal
  - Hydrocephalus
- Young adult
  - Syrinx and scoliosis

Classical signs described on ultrasound include the lemon sign and the banana cerebellum sign. There may also be evidence of fetal ventriculomegaly because of obstructive effects as a result of downward cerebellar herniation. Additionally, many of the associated malformations (e.g., corpus callosal dysgenesis) may be identified. MRI is the modality of choice for detecting and characterizing the full constellation of findings associated with Chiari II malformations:

Posterior fossa

- Small posterior fossa with a low attachment of the tentorium and low torcula.
- Brainstem appears “pulled” down with an elongated and low-lying fourth ventricle.
- Tectal plate appears beaked: inferior colliculus is elongated and points posteriorly, with resulting angulation of the aqueduct, which results in aqueductal stenosis and hydrocephalus.
- Cerebellar tonsils and vermis are displaced inferiorly through foramen magnum, which appears crowded.

Spine

- Spina bifida aperta/myelomeningocele
- Tethered cord

References: Curnes JT, Oakes WJ, Boyko OB. MR imaging of hindbrain deformity in Chiari II patients with and without symptoms of brainstem compression. *AJNR Am J Neuroradiol* 1989;10(2):293–302.
El gammal T, Mark EK, Brooks BS. MR imaging of Chiari II malformation. *AJR Am J Roentgenol* 1988;150(1):163–170.

40 Answer B. Radiographs demonstrate relative shortening of the long bones, including the femurs, shortening of the ribs, flaring of the physis of the long bones, brachydactyly, narrowing of the lumbar interpeduncular distance, bullet-shaped vertebral bodies, widening of the intervertebral disc spaces, and disproportionate length of the fibula relative to the tibia. There is rounding of the bilateral iliac wings. There is a trident appearance of the iliac spines. Lack of ossification in the bilateral femoral heads is consistent with hypertrophy of the cartilages. MR evaluation of the brain demonstrates a somewhat horizontal orientation of the clivus suggesting skull base dysplasia, which can be seen in achondroplasia. There is narrowing of the foramen magnum at the cervicomedullary junction. Achondroplasia is a congenital genetic disorder resulting in rhizomelic dwarfism and is the most common skeletal dysplasia. There are numerous classical radiographic signs.

The skull and spine findings include:
Skull

- Relatively large cranial vault with small skull base
- Prominent forehead with depressed nasal bridge
- Narrowed foramen magnum
- Cervicomedullary kink
- Relative elevation of the brainstem resulting in a large suprasellar cistern and vertically oriented straight sinus
- Communicating hydrocephalus (because of venous obstruction at sigmoid sinus)

Spine

- Posterior vertebral scalloping
- Progressive decrease in interpedicular distance in lumbar spine
- Gibbus: thoracolumbar kyphosis with bullet-shaped/hypoplastic vertebra (not to be confused with Hurler syndrome)
- Short pedicle canal stenosis
- Laminar thickening
- Widening of intervertebral discs
- Increased angle between sacrum and lumbar spine

There is often a danger of cervical cord compression because of narrowing of the foramen magnum. Treatment varies and is usually orthopedic, particularly to correct kyphoscoliosis as well as neurosurgical to decompress the foramen magnum or shunt hydrocephalus. Overall prognosis is good, with near-normal life expectancy in heterozygous individuals. When homozygous, the condition is usually fatal because of respiratory compromise.

References: Kao SC, Waziri MH, Smith WL, et al. MR imaging of the craniovertebral junction, cranium, and brain in children with achondroplasia. *AJR Am J Roentgenol* 1989;153(3):565–569.
Wang H, Rosenbaum AE, Reid CS, et al. Pediatric patients with achondroplasia: CT evaluation of the craniocervical junction. *Radiology* 1987;164(2):515–519.

41 **Answer D.** There is moderate thoracic kyphosis measuring approximately 60 degrees. There is exaggeration of the normal lumbar lordosis. There is mild anterior wedging and loss of height of multiple contiguous thoracic vertebral bodies. Scheuermann disease, also known as juvenile kyphosis, juvenile discogenic disease, or vertebral epiphysitis, is a common condition, which results in kyphosis of the thoracic or thoracolumbar spine. There is a strong hereditary predisposition (perhaps autosomal dominant) with a high degree of penetrance and variable expressivity and occurs in the thoracic spine in up to 75% of cases, followed by the thoracolumbar spine combined and occasionally lumbar and rarely cervical spine.
To apply the label of classical Scheuermann disease, one needs to meet a number of criteria (Sorensen classification):

- Thoracic spine kyphosis >40 degrees (normal 25 to 40 degrees)
- Thoracolumbar spine kyphosis >30 degrees (normal 0 degrees)

and

- At least three adjacent vertebrae demonstrating wedging of >5 degrees

The condition is associated with Schmorl nodes, limbus vertebrae, scoliosis (~25%), and spondylolisthesis.

Other signs include:

- Vertebral end-plate irregularity because of extensive disc invagination
- Intervertebral disc space narrowing, more anteriorly

References: Blumenthal SL, Roach J, Herring JA. Lumbar Scheuermann's. A clinical series and classification. *Spine* 1987;12(9):929–932. Summers BN, Singh JP, Manns RA. The radiological reporting of lumbar Scheuermann's disease: an unnecessary source of confusion amongst clinicians and patients. *Br J Radiol* 2008;81(965):383–385.

42 **Answer A.** There are multiple cervical spine anomalies with fusion at multiple levels as well as markedly abnormal morphology throughout the spine. There is elevation of the left scapula. Klippel-Feil syndrome (KFS) is a complex heterogeneous entity that results in cervical vertebral fusion. Two or more nonsegmented cervical vertebrae are usually sufficient for diagnosis. There is a recognized female predilection. The classic clinical triad of a short neck, low hairline, and restricted neck motion is considered to be present in <50% of patients with this syndrome.
Associations and imaging findings

- Sprengel deformity of the shoulder
- Anomalies of the aortic arch and branching vessels, for example, carotid and subclavian arteries
- Spinal scoliosis
- Intervertebral disc herniation
- Cervical spondylosis
- Renal abnormalities, for example, unilateral renal agenesis
- Vertebral fusion
- Anteroposterior narrowing of the vertebral bodies (wasp-waist sign)
- Hemivertebrae
- Spina bifida

Reference: Ulmer JL, Elster AD, Ginsberg LE, et al. Klippel-Feil syndrome: CT and MR of acquired and congenital abnormalities of cervical spine and cord. *J Comput Assist Tomogr* 1993;17(2):215–224.

43 **Answer C.** There is a large cellular appearing left paraspinal soft tissue mass, which extends into the posterior paraspinal musculature and into the left lower pelvis displacing the and extending into the iliac vessels and psoas muscles. The lesion extends through the neural foramina on the left from L5 through S2–S3 and into the left lateral and ventral epidural space filling the spinal canal and effacing the CSF with displacement of the nerve roots posteriorly into the right from the level of L4–L5 through S3. There is also involvement of the right neural foramen at L5–S1.
Ewing sarcoma is a small, round cell tumor, which accounts for one-quarter of all primary bone tumors during childhood. It has a peak incidence during the second decade and is very rare after 30 years of age. Typical complaints of patients with Ewing sarcoma are pain and swelling of the affected bone. The most commonly affected bones are the femur, pelvis, and other long bones of the extremities. Vertebrae are affected in <5% of the cases and may present with nerve root or spinal cord compression. The prognosis is usually poor.
Ewing sarcoma is the second most common highly malignant primary bone tumors of childhood after osteosarcoma, typically arising from medullary cavity with invasion of the Haversian system and typically occurs in children and adolescents between 10 and 20 years of age. It is rare in African Americans. Ewing sarcoma is a small round blue cell tumor with regular-sized primitive-appearing cells. It is closely related to the soft tissue tumors pPNET, Askin tumor, and neuroepithelioma, which collectively are referred to as Ewing sarcoma family of tumors (ESFT). Ewing sarcoma of the spine is a rare condition that appears with a clinical triad of local pain, neurological deficit, and palpable mass.

As far as location within long bones, the tumor is almost always metadiaphyseal or diaphyseal:
Middiaphysis: 33%
Metadiaphysis: 44%
Metaphysis: 15%
Epiphysis: 1% to 2%

References: Dini LI, Mendonca R, Gallo P. Primary Ewing's sarcoma of the spine. *Arq Neuropsiquiatr* 2006;64(3-A):654–659.
Goktepe AS, Alaca R, Mohur H, Coskun U. Paraplegia: an unusual presentation of Ewing's sarcoma. *Spinal Cord* 2002;40(7):367–369. doi:10.1038/sj.sc.3101326.

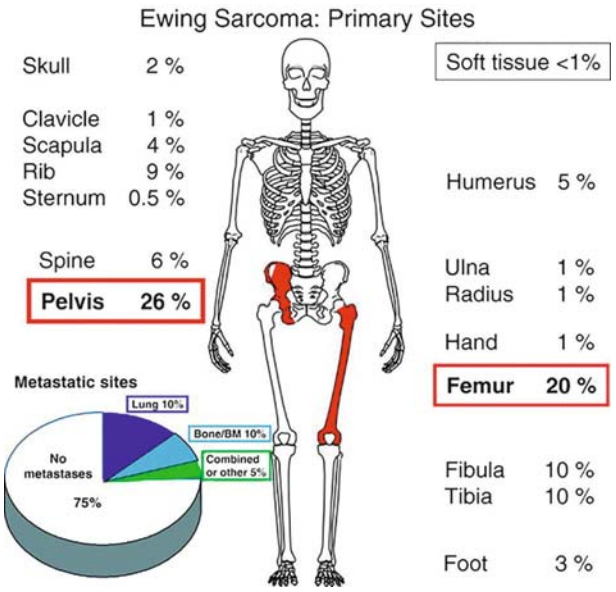

44 **Answer B.** There is spondylolysis at L5 with associated 8 mm grade 2 anterolisthesis of L5 on S1. Spondylolysis is a defect in the pars interarticularis of the neural arch, the portion of the neural arch that connects the superior and inferior articular facets. It is commonly known as pars interarticularis defect or more simply as pars defect. Spondylolysis is present in approximately 5% of the population and higher in the adolescent athletic population. Spondylolysis is commonly asymptomatic. Symptomatic patients often have pain with extension and/or rotation of the lumbar spine. Approximately 25% of individuals with spondylolysis have symptoms at some time. It is a common cause of low back pain in adolescents and in particular athletes.

The "Scotty dog." On the oblique radiograph of the lumbar spine, the appearance of the posterior elements is commonly referred to as resembling the side view of a "Scotty dog." In this oblique radiograph, the "Scotty dog" is outlined by (*dots*). The superior articular process (*white arrow*) represents the dog's ear; the pedicle (*black arrow*), the dog's muzzle; the inferior articular process (*small arrows*), the dog's front leg; and the pars interarticularis (p), the dog's neck. Spondylolysis is believed to be caused by repeated microtrauma, resulting in stress fracture of the pars interarticularis. A dysplastic pars is usually present. Genetics are also believed to be a factor. It is more common in men than in women. Traumatic pars defects result from high-energy trauma where there is hyperextension of the lumbar spine and are rare in a congenitally normal vertebra.

Location

- 90% of cases of spondylolysis occur at the L5 level and 10% occur at L4 level
- Unilateral or bilateral

Associations

- 65% of patients with spondylolysis will progress to spondylolisthesis
- Spina bifida occulta

Imaging features

- Scotty dog sign: on oblique radiographs, a break in the pars interarticularis can have the appearance of a collar around the dog's neck
- Inverted Napoleon hat sign

Surgery is only considered in rare circumstances as most cases respond to conservative management.

References: Jinkins JR, Matthes JC, Sener RN, et al. Spondylolysis, spondylolisthesis, and associated nerve root entrapment in the lumbosacral spine: MR evaluation. *AJR Am J Roentgenol* 1992;159(4):799–803.
Syrmou E, Tsitsopoulos PP, Marinopoulos D, et al. Spondylolysis: a review and reappraisal. *Hippokratia* 2010;14(1):17–21.

45 **Answer C.** Spine radiograph and MRI demonstrates midthoracic and lower lumbar segmentation/formation anomalies. There is a hydrosyringomyelia of the low-lying conus medullaris. Caudal regression syndrome (CRS) represents a spectrum of structural defects of the caudal region. Malformations vary from isolated partial agenesis of the coccyx to lumbosacral agenesis. In an antenatal setting, there are associations with maternal diabetes (type I or type II) and polyhydramnios.

Imaging appearances can significantly vary depending on the severity of regression. In general, the following may be seen:

- Lumbosacral vertebral body dysgenesis/hypogenesis
- Level of atresia/dysgenesis is usually below L1 and often limited to sacrum
- Truncated, blunt spinal cord terminating above the expected level
- Severe canal narrowing rostral to last intact vertebra

References: Singh SK, Singh RD, Sharma A. Caudal regression syndrome—case report and review of literature. *Pediatr Surg Int* 2005;21(7):578–581.
Stroustrup Smith A, Grable I, Levine D. Case 66: caudal regression syndrome in the fetus of a diabetic mother. *Radiology* 2004;230(1):229–233.

46 **Answer D.** There is a mixed cystic solid heterogeneous mass in the presacral space closely associated with the sacrum, distal sigmoid colon, and rectum. There are heterogeneous cystic components of the mass, with several T1 hypointense and T2 hyperintense cysts and several T1 and T2 intermediate intensity cysts, possibly representing cysts containing hemorrhage or proteinaceous material.
Sacrococcygeal teratoma (SCT) refers to a teratoma arising in the sacrococcygeal region. The coccyx is almost always involved. It is the most common congenital tumor in the fetus and neonate. The tumor is composed of the all three germ cells (i.e., ectoderm, mesoderm, and endoderm).

Pathology-based classification:
Benign (mature): most common
Malignant (immature)

Location-based classification system according to the American Academy of Pediatric Surgery Section Survey:
Type I: developing only outside the fetus (can have small presacral component); accounts for the majority of cases
Type II: extrafetal with intrapelvic presacral extension
Type III: extrafetal with abdominopelvic extension
Type IV: tumor developing entirely in the fetal pelvis

An SCT can be benign or malignant depending on whether mature or immature. The majority, however, tend to be benign. Those presenting in older infants tend to have a higher malignant potential, which those presenting in utero have a poor prognosis because of complications.
Complications include:

- High-output cardiac failure from AV shunting: which in turn can cause hydrops fetalis
- Ureteric obstruction
- Gastrointestinal tract obstruction
- Compression of underlying nerves: giving urinary/fecal incontinence
- Anemia
- Dystocia

- Tumor rupture

References: Avni FE, Guibaud L, Robert Y, et al. MR imaging of fetal sacrococcygeal teratoma: diagnosis and assessment. *AJR Am J Roentgenol* 2002;178(1):179–183.
Danzer E, Hubbard AM, Hedrick HL, et al. Diagnosis and characterization of fetal sacrococcygeal teratoma with prenatal MRI. *AJR Am J Roentgenol* 2006;187(4):W350–W356. doi:10.2214/AJR.05.0152

47 Answer C. There is an expansile, mixed lytic/sclerotic lesion involving the right C3 lamina. Osteoblastomas are rare and benign primary bone tumors. They may be locally aggressive and tend to affect the axial skeleton more often than their histologic relative, osteoid osteoma. Patients typically present around the second to third decades of life. With spinal lesions, a painful scoliosis is a common presenting symptom. Otherwise, it presents with an insidious onset of dull pain, worse at night, with minimal response to salicylates in only 7% of patients (unlike osteoid osteoma). The area will characteristically be swollen and tender with a decreased range of motion.
Osteoblastoma is histologically similar to an osteoid osteoma except that it is much larger. The tumor is bone and osteoid forming and is comprised of osteoblasts. There is high associated vascularity.

Location
- Spinal column: often involves the posterior column
- Cervical spine
- Sacrum
- Metaphysis and distal diaphysis of the long bones

Osteoblastomas can have a wide range of radiographic patterns. Lesions are typically larger than 2 cm. On radiography, lesions tend to be expansile and predominantly lytic with a rim of reactive sclerosis. There may be surrounding sclerosis or periostitis in up to 50% of cases.

References: Atesok KI, Alman BA, Schemitsch EH, et al. Osteoid osteoma and osteoblastoma. *J Am Acad Orthop Surg* 2012;19(11):678–689.
Kroon HM, Schurmans J. Osteoblastoma: clinical and radiologic findings in 98 new cases. *Radiology* 1990;175(3):783–790.
Shaikh MI, Saifuddin A, Pringle J, et al. Spinal osteoblastoma: CT and MR imaging with pathological correlation. *Skeletal Radiol* 1999;28(1):33–40.

6 Pediatric Vascular Radiology

Questions

1. A 9-day-old presents with history of congenital stridor. An upper GI was performed (Fig. A). The most likely diagnosis is:

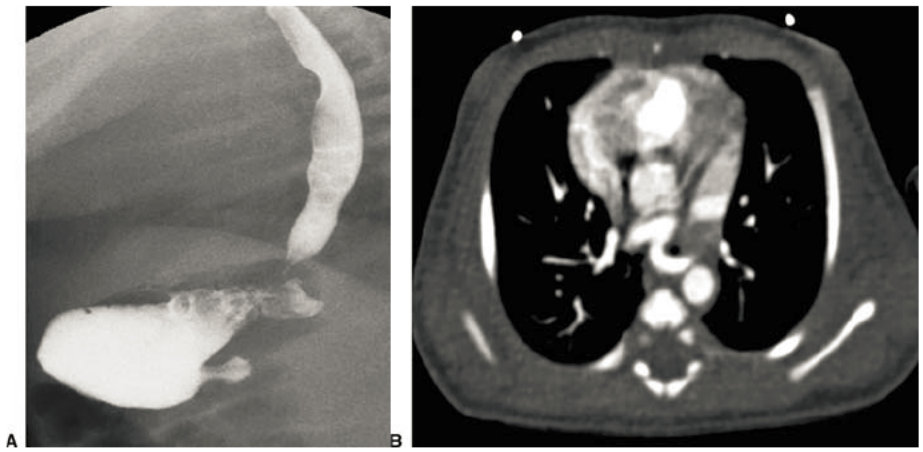

A. Pulmonary artery sling
B. Right arch with aberrant left subclavian
C. Tracheomalacia
D. Esophageal stenosis

2. Which of the following would reduce the dose to the child when performing the upper GI examination:
A. Use of an antiscatter grid
b. Reducing the magnification
C. Increasing the source to skin distance
D. Increasing the pulse rate

3. Concerning the diagnosis in Question 1, a type II is classified as having the following characteristic:
A. Carina in a normal location at the level of T4 to T5
B. Low carina at the level of T6
C. High carina at the level of T3
D. Tracheal bronchus

4. A right and left renal angiogram was performed on a 15-year-old female. What is the most likely diagnosis?

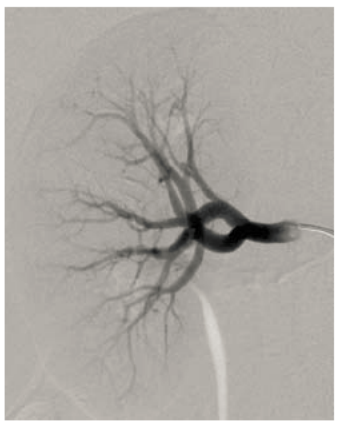

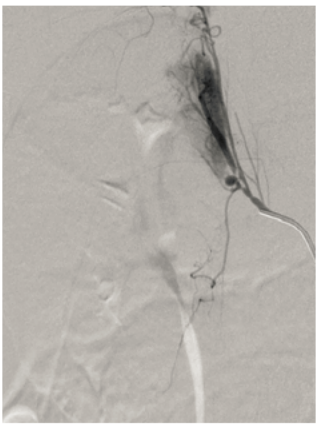

A. Autosomal dominant polycystic kidney disease
B. Atherosclerosis
C. Fibromuscular dysplasia
D. Segmental arterial mediolysis

5. Of the following choices, what is the most common presenting sign of the disease in Question 4?
A. Chest pain
B. Headache
C. No presenting signs or symptoms
D. Hypertension

6. The most common subtype of this disease in Question 4 is the following:
A. Medial
B. Perimedial
C. Intimal
D. Serosal

7. The indications for percutaneous intervention in a patient with the disease in Question 4 include which of the following?
A. Resistant hypertension
B. Intolerance to hypertensive medications
C. Renal impairment
D. Noncompliance with hypertensive medications
E. A and C only
F. All of the above

8. A 2-day-old presents with history of a two-vessel cord and Williams syndrome. Which of the following are TRUE?

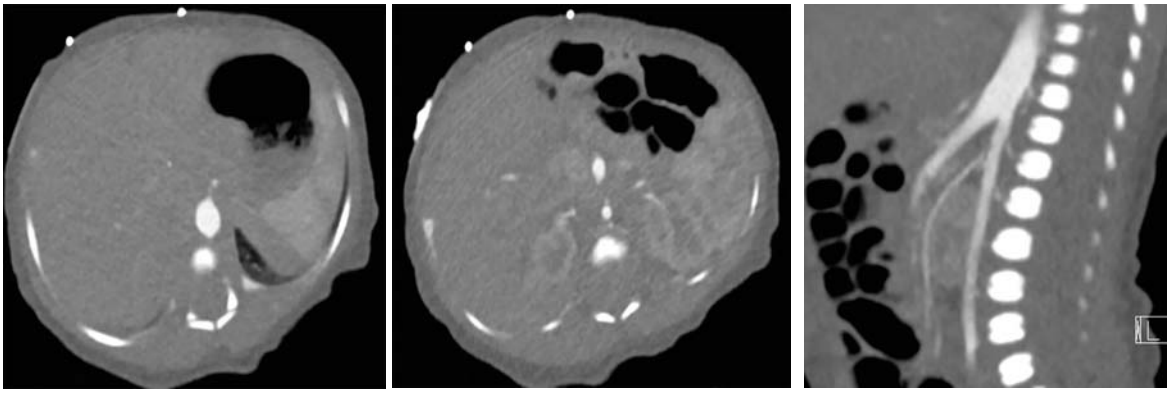

A. The infrarenal aorta is decreased in caliber.
B. The infrarenal aorta is enlarged in caliber.
C. The superior mesenteric artery is normal in caliber.
D. The superior mesenteric artery is decreased in caliber.

9. In the pediatric population, which is the first-line imaging modality to evaluate the disorder shown in Question 8?
A. Ultrasound with Doppler
B. Contrast-enhanced MRI
C. Contrast-enhanced CT
D. Subtraction angiography

10. A commonly occurring collateral pathway to supply the lower extremities in the disorder shown in Question 8 is:
A. Intercostal arteries to inferior mesenteric artery to hemorrhoidal arteries to external iliac arteries
B. Intercostal arteries to inferior mesenteric artery to infrarenal abdominal aorta
C. Superior mesenteric artery to inferior mesenteric artery to hemorrhoidal arteries to external iliac arteries
D. Superior mesenteric artery to inferior mesenteric artery to infrarenal abdominal aorta

11. An 18-month-old with elevated liver function tests presents for MRI following abnormality noted on recent abdominal sonogram. The following axial and volume-rendered images were obtained.

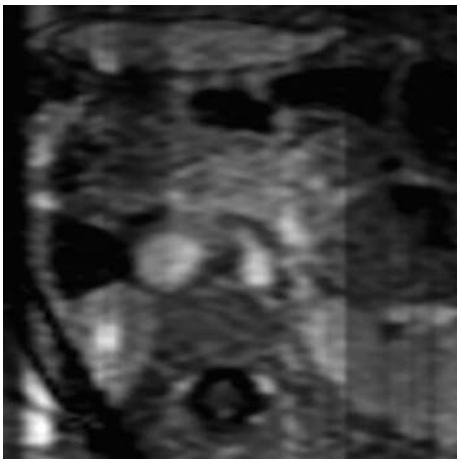
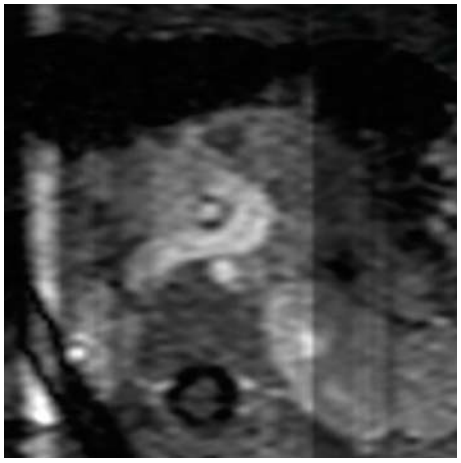
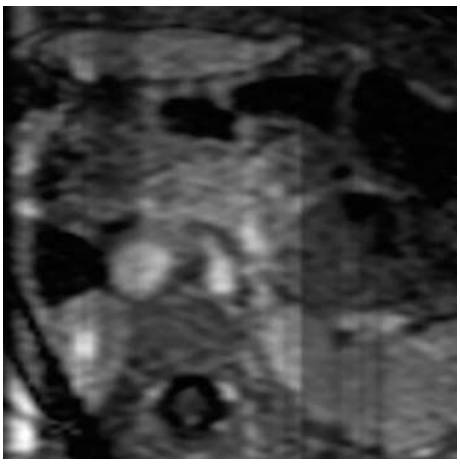
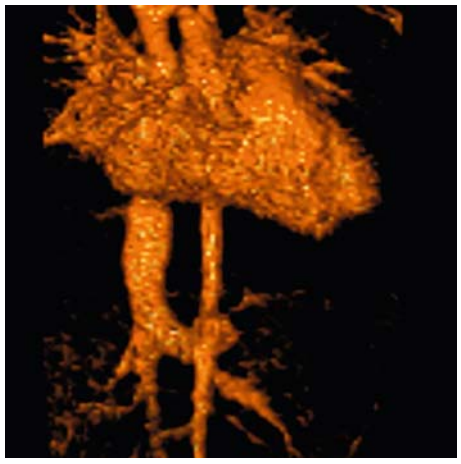

The most likely explanation for the prominent vessel extending below the SMA axis is:
A. Arteriovenous fistula
B. Aneurysmal dilatation of the left renal vein
C. Congenital portosystemic shunt
D. Interrupted IVC

12. What is the most likely classification of the abnormality shown in Question 11?
A. Type 1
B. Type 2
C. Type 3
D. Type 4

13. Type 1 congenital extrahepatic portosystemic shunts are associated with which of the following?
A. Conserved portal vein supply
B. Hepatoblastoma
C. Congenital heart disease
D. Male predilection

14. A 17-year-old underwent a contrast-enhanced CT angiogram of the chest.

What is the most common symptom in older children presenting with this diagnosis?
A. Shortness of breath
B. Chest pain
C. Hemoptysis
D. Syncope
E. Tachypnea

15. What is the most common risk factor for the diagnosis in Question 14 in a child?
A. Septicemia
B. Dehydration
C. Malignancy
D. Congenital thrombophilia
E. Central venous catheter

16. Which of the following is a chronic complication of children following the diagnosis in Question 14?
A. Left ventricular dysfunction
B. Vascular dissection
C. Pneumonia
D. Pulmonary hypertension

17. An 8-year-old underwent a contrast-enhanced MRI of the chest.

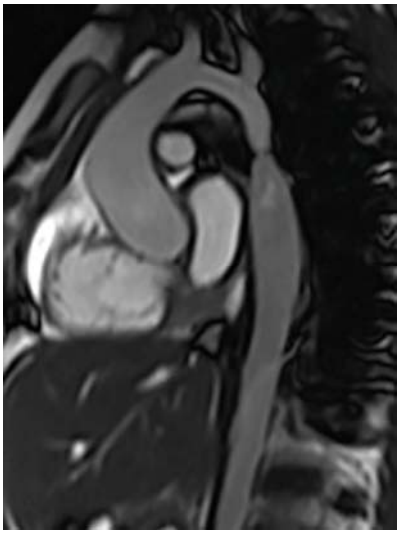

Which of the following is TRUE concerning this diagnosis?
A. Female predominance
B. Clinical presents with lower body hypertension
C. Bicuspid aortic valve that is seen <10% of affected patients
D. Can be associated with cerebral artery aneurysms

18. Which of the following is the advantage of imaging the disorder in Question 17 with MRI in comparison to CT?
A. Increased spatial resolution
B. Multiplanar imaging capability
C. Ability to quantify collateral flow
D. Improved diagnostic accuracy

19. What is the preferred technique in neonates and infants for repair of the condition in Question 17?
A. End-to-end anastomosis
B. Left subclavian flap anastomosis
C. Extra-anatomic bypass
D. Angioplasty

20. A 10-year-old with history of tracheomalacia underwent a contrast-enhanced CT evaluation of the chest.

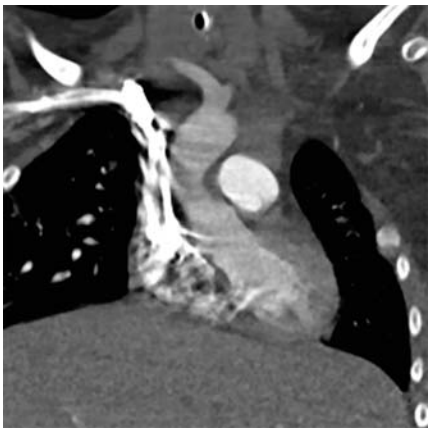
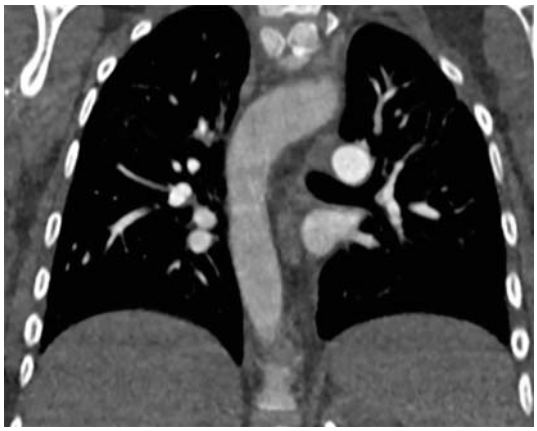
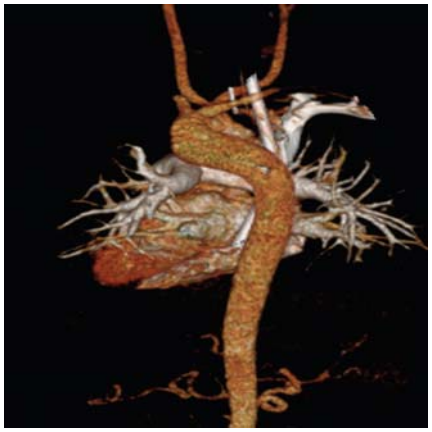

What is the diagnosis?
A. Double aortic arch
B. Left aortic arch with aberrant left subclavian artery
C. Normal left aortic arch
D. Circumflex aortic arch

21. Is the abnormality in Question 20 a vascular ring?
A. Yes, the vascular ring is completed by the ligamentum.
B. Yes, the vascular ring is completed by a vessel passing adjacent to the trachea and esophagus.
C. No, the ligamentum is on the contralateral side and does complete the vascular ring.
D. No, there is no vessel passing adjacent to the trachea and esophagus to complete the vascular ring.

22. Which of the following is TRUE concerning aortic arch anomalies?
A. Circumflex aortic arch is usually an isolated anomaly.
B. Right aortic arch with aberrant left subclavian artery is commonly associated with congenital heart disease.
C. Right dominant double aortic arch is usually an isolated anomaly.
D. Left dominant double aortic arch is commonly associated with congenital heart disease.

23. A 5-month-old with history of high fever underwent a contrast-enhanced MRA.

What is the most likely diagnosis?
A. Anomalous left coronary artery
B. Henoch-Schonlein Purpura
C. Kawasaki disease
D. Polyarteritis nodosa
E. Takayasu arteritis

24. Additional findings of the disorder in Question 23 are which of the following?
A. Diffuse lymphadenopathy
B. Hydrops of the gallbladder
C. Atrial myxoma
D. Extrapleural sequestration

25. Initial imaging evaluation of the coronary arteries in the disorder is performed using which modality?
A. MRI/MRA
B. CT angiography
C. Echocardiography
D. Conventional angiography

Vascular Radiology: Answers and Explanations

1 Answer A. A pulmonary artery sling causes an anterior impression on the esophagus (arrow) and a posterior impression on the trachea because of the left pulmonary artery passing between the trachea and esophagus (arrow in B). The left pulmonary artery arises from the posterior aspect of the right pulmonary artery. This condition occurs because of the obliteration of the primitive left sixth aortic arch.

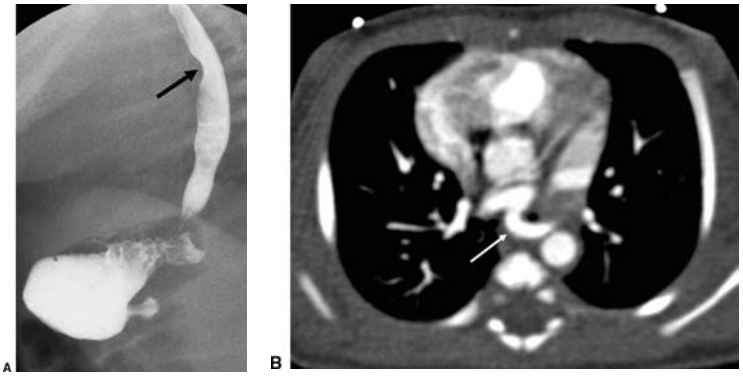

A right arch with an aberrant left subclavian artery would produce a posterior impression on the esophagus, not an anterior impression.

Tracheomalacia is a condition where there is flaccidity of the airway wall and supporting cartilage. On imaging, there is collapse of the tracheal lumen most pronounced during expiration or coughing. This condition is associated with vascular rings such as pulmonary artery sling but is not demonstrated on this image.

Single-contrast barium upper gastrointestinal study demonstrates an anterior impression on the esophagus (arrow in A). There is no evidence of significant esophageal narrowing.

References: Lee EY, Dorkin H, Vargas SO. Congenital pulmonary malformations in pediatric patients: review and update on etiology, classification, and imaging findings. *Radiol Clin N Am* 2011;49(5):921–948.

Yedururi S, Guillerman P, Chung T, et al. Multimodality imaging of tracheobronchial disorders in children. *Radiographics* 2008;28(3):e29. doi:http://dx.doi.org/10.1148/rg.e29.

2 Answer B. When the magnification increases, the field of view becomes smaller. Unfortunately, when the field of view becomes smaller and the magnification increases, the dose also increases. Reducing the magnification or enlarging the field of view will therefore decrease the radiation dose.

The antiscatter grid attenuates scattered radiation. Given that detection of this scattered radiation decreases image quality, it is often necessary to use the grid in larger patients. With removal of the scattered radiation, the primary dose of radiation must be increased to replace the scattered dose at the image receptor. In pediatric patients, the smaller body produces less scatter, and therefore, use of a grid only minimally improves image quality. Children under the age of 3 to 5 years generally can be imaged without the grid with similar image quality.

Decreasing the source to skin distance (SSD) will decrease the dose to the child. The inverse square law states that the intensity of radiation of the beam is inversely proportional to the square of the SSD. Because of this, decreasing the SSD will decrease the dose to the child, and increasing the SSD will increase the dose to the child.

The pulse rate is the number of fluoroscopic images the fluoroscopy machine creates per second. Increasing the pulse rate would increase the number of images per second and therefore increase the dose. Decreasing the pulse rate would decrease the number of images per second and decrease the dose.

Reference: Hernanz-Schulman M, Strauss K, Bercha IH. Fluoroscopy and radiation safety content for radiologists. http://www.imagegently.org/Portals/6/Radiologists/Background4radiologists.pdf

3 Answer B. A type II pulmonary artery sling is characterized by a low position of the carina at the level of T6. A type II pulmonary artery sling is associated with long-segment tracheal stenosis, a T-shaped carina, and a bridging bronchus.

Types of Pulmonary Artery Slings

Type 1	Position of carina: NORMAL (T4–T5)
Type 2	Position of the carina: LOW (T6) Associated with long-segment tracheal stenosis, T-shaped carina, bridging bronchus

Reference: Lee EY, Dorkin H, Vargas SO. Congenital pulmonary malformations in pediatric patients: review and update on etiology, classification, and imaging findings. *Radiol Clin N Am* 2011;49(5):921–948.

4 Answer C. Right and left renal angiograms demonstrate a normal right main renal artery but an early upper pole branch with irregular narrowing and a small aneurysm (arrow in A). The left main renal artery also has irregular stenosis and two small aneurysms (arrows in B). These findings are most compatible with fibromuscular dysplasia, particularly in this age group. Fibromuscular dysplasia is a nonatherosclerotic disease involving medium-sized vessels, most commonly the renal and extracranial carotid and vertebral arteries. Percutaneous transluminal renal angioplasty is the treatment of choice for renal fibromuscular dysplasis.

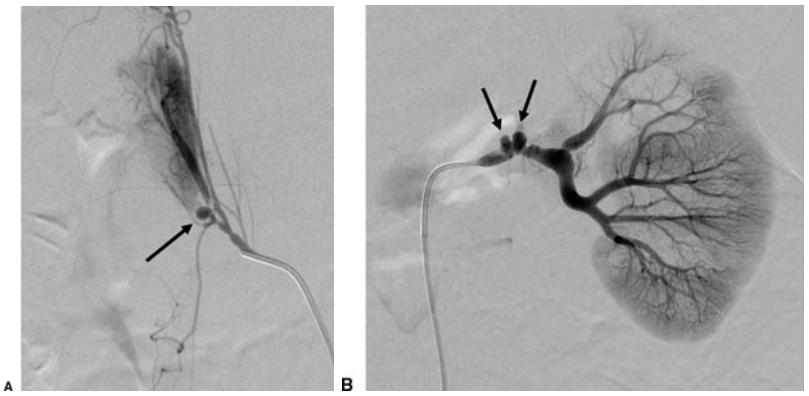

References: Meuse MA, Turba UC, Sabri SS, et al.
Treatment of renal artery fibromuscular dysplasia. *Tech Vasc Interv Radiol* 2010;13:126–133.
O'Connor SC, Gornik HL. Recent developments in the understanding and management of fibromuscular dysplasia. *J Am Heart Assoc* 2014;3(6):e001259. doi:10.1161/JAHA.114.001259.

5 Answer D. The most common presenting sign of fibromuscular dysplasia is hypertension followed by headache.

Most Common Presenting Signs and Symptoms of Fibromuscular Dysplasia

Presenting symptom	%
Hypertension	64
Headache	52
Pulsatile tinnitus	28
Dizziness	26
Cervical bruit	22
Neck pain	22

Reference: O'Connor SC, Gornik HL. Recent developments in the understanding and management of fibromuscular dysplasia. *J Am Heart Assoc* 2014;3(6):e001259. doi:10.1161/JAHA.114.001259.

6 Answer A. The most common histopathologic subtypes of fibromuscular dysplasia are medial (70%), perimedial (15% to 25%), and intimal fibrodysplasia (1% to 2%). Both medial and perimedial fibrodysplasia tend to develop stenosis and aneurysms, whereas intimal fibrodysplasia develops smooth focal or tubular narrowing.

Reference: Meuse MA, Turba UC, Sabri SS, et al. Treatment of renal artery fibromuscular dysplasia. *Tech Vasc Interv Radiol* 2010;13:126–133.

7 Answer F. Per the American College of Cardiology, the indications for percutaneous intervention in fibromuscular dysplasia include resistant hypertension, intolerance to antihypertensive medications, noncompliance with antihypertensive medications, and renal impairment. Other reasons for intervention are renal artery dissection and renal artery aneurysm.

References: Meuse MA, Turba UC, Sabri SS, et al. Treatment of renal artery fibromuscular dysplasia. *Tech Vasc Interv Radiol* 2010;13:126–133.
O'Connor SC, Gornik HL. Recent developments in the understanding and management of fibromuscular dysplasia. *J Am Heart Assoc* 2014;3(6):e001259. doi:10.1161/JAHA.114.001259.

8 Answer A. This patient has narrowing of the infrarenal aorta (arrows) consistent with middle aortic syndrome. The etiologies of this disorder include genetic causes such as Williams syndrome, Alagille syndrome, and neurofibromatosis. Additionally, vasculitis such as Takayasu arteritis and intrauterine infection such as rubella have been associated with this disorder.

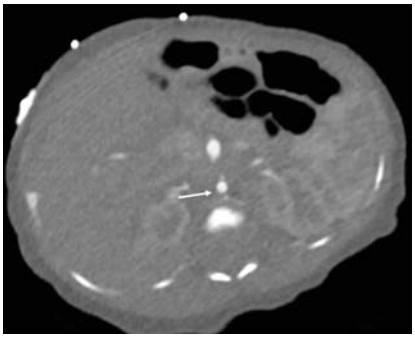

References: Kim SM, Jung IM, Min SI, et al. Surgical treatment of middle aortic syndrome with takayasu arteritis or midaortic dysplastic syndrome. *Eur J Endovasc Surg* 2015;50:206–212.
Rumman RK, Nickel C, Matsuda-Abedini M, et al. Disease beyond the arch: a systemic review of middle aortic syndrome in childhood. *Am J Hypertens* 2015;28:833–846.

9 Answer A. Given the lack of ionizing radiation and the ability to perform without sedation, ultrasound with Doppler is the imaging modality of choice to initially evaluate a child with suspected middle aortic syndrome.

10 Answer C. The most commonly occurring collateral pathways in abdominal aortoiliac stenosis are
1. Superior mesenteric artery to inferior mesenteric artery to hemorrhoidal arteries to external iliac arteries
2. Intercostal, subcostal, and lumbar arteries to superior gluteal and iliolumbar arteries to internal iliac arteries to external iliac arteries
3. Intercostal, subcostal, and lumbar arteries to circumflex arteries to external iliac arteries

Reference: Sebastia C, Quiroga S, Boye R, et al. Aortic stenosis: spectrum of diseases depicted at multisection CT. *Radiographics* 2003;23:S79–S91.

11 Answer C. There is connection of the splenic and superior mesenteric vein (arrow) to the inferior vena cava consistent with a congenital extrahepatic portosystemic shunt. This is a condition in which the portomesenteric blood drains into a systemic vein therefore bypassing the liver.

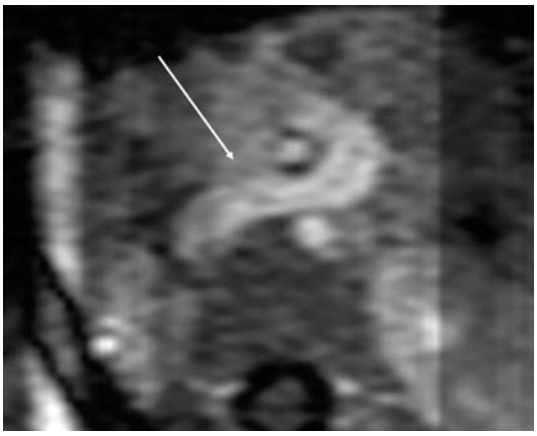

References: Alonso-Gamarra E, Parrion M, Perez A, et al. Clinical and radiologic manifestations of congenital extrahepatic portosystemic shunts: a comprehensive review. *Radiographics* 2011;32:707–722.
Kobayashi N, Niwa T, Kirikoshi H, et al. Clinical classification of congenital extrahepatic portosystemic shunts. *Hepatol Res* 2010;40:585–593.

12 Answer B. Congenital portosystemic shunts are initially classified as intrahepatic or extrahepatic. In this case, the abnormal connection is extrahepatic. Extrahepatic shunts are classified into type 1 where there is absence of the intrahepatic portal venous supply or type 2 in which the intrahepatic portal venous supply is present. In this case, no portal vein is present, so it is a type 2 extrahepatic portosystemic shunt.

References: Alonso-Gamarra E, Parrion M, Perez A, et al. Clinical and radiologic manifestations of congenital extrahepatic portosystemic shunts: a comprehensive review. *Radiographics* 2011;32:707–722.
Kobayashi N, Niwa T, Kirikoshi H, et al. Clinical classification of congenital extrahepatic portosystemic shunts. *Hepatol Res* 2010;40:585–593.

13 Answer C. Type 1 congenital extrahepatic portosystemic shunts are characterized by congenital absence of the portal vein and multiple associated anomalies such as polysplenia, congenital heart defects, and malrotation. Additionally, there is a female predilection. Type 2 congenital extrahepatic portosystemic shunts have a portal vein supply, no gender predilection, and fewer associated anomalies.

Reference: Alonso-Gamarra E, Parrion M, Perez A, et al. Clinical and radiologic manifestations of congenital extrahepatic portosystemic shunts: a comprehensive review. *Radiographics* 2011;32:707–722.

14 Answer B. The axial image demonstrates a pulmonary embolism within the left pulmonary artery extending into the segmental vessels (arrow). Although children may present with all of the listed symptoms, in older children, 84% of cases present with pleuritic chest pain.

Reference: Thacker PG, Lee EY. Pulmonary embolism in children. *AJR Am J Roentgenol* 2015;204:1278–1288.

15 Answer E. The most common risk factor for pulmonary embolism in both neonates and older children is a central venous catheter. Additional risk factors in neonates are dehydration, septicemia, and peripartum asphyxia. In older children, other risk factors are malignancy, renal disease, surgery or trauma, renal disease, and congenital thrombophilia. Ninety-six to ninety-eight percent of children have an identifiable risk factor with 88% having two more risk factors present.
Reference: Thacker PG, Lee EY. Pulmonary embolism in children. *AJR Am J Roentgenol* 2015;204:1278–1288.

16 Answer D. Chronic complications of a pulmonary embolus in children are recurrence, pulmonary hypertension possibly leading to right heart failure, and complications related to anticoagulation therapy.
Reference: Thacker PG, Lee EY. Pulmonary embolism in children. *AJR Am J Roentgenol* 2015;204:1278–1288.

17 Answer D. The images demonstrate focal narrowing of the postductal thoracic aorta (arrows) consistent with coarctation. Coarctation of the aorta is a congenital narrowing of the aorta. There is a male predominance with a male-to-female ratio of 1.5:1. The clinical presentation is upper body hypertension with lower body hypoperfusion. This condition is associated with multiple other anomalies including bicuspid aortic valve, cerebral aneurysms, Turner syndrome, and Noonan syndrome. A bicuspid aortic valve is seen in 20% to 85% of patients with coarctation.

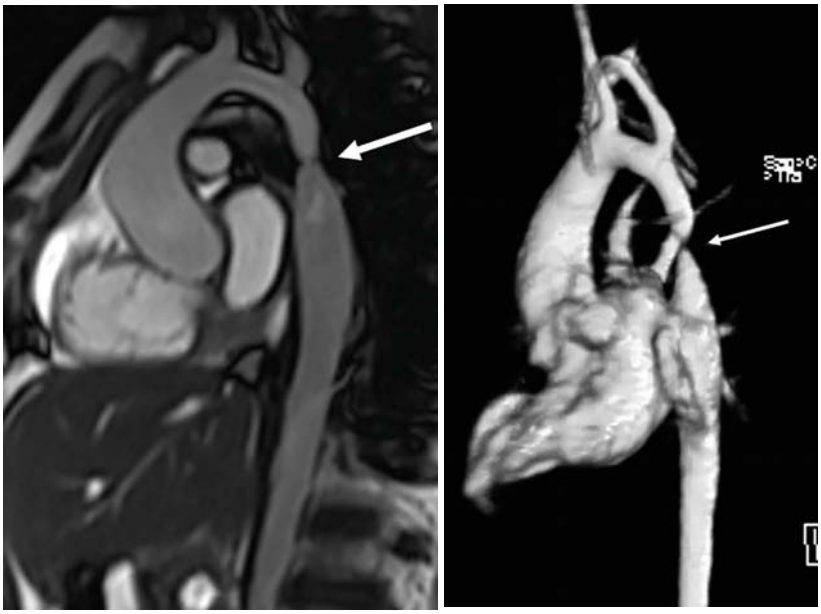

References: Nance JW, Ringel RE, Fishman EK. Coarctation of the aorta in adolescents and adults: a review of clinical features and CT imaging. *J Cardiovasc Comput Tomogr* 2016;10:1–12.
Sebastia C, Quiroga S, Boye R, et al. Aortic stenosis: spectrum of diseases depicted at multisection CT. *Radiographics* 2003;23:S79–S91.

18 Answer C. MRI has several advantages over CT in imaging coarctation including the lack of ionizing radiation and the ability to use phase contrast imaging to quantify collateral flow and flow and velocity across the area of narrowing. CT has higher spatial resolution and can be acquired more rapidly than MRI. Both modalities have multiplanar imaging capability, and there has been no proven difference in diagnostic accuracy when comparing these modalities.
Reference: Nance JW, Ringel RE, Fishman EK. Coarctation of the aorta in adolescents and adults: a review of clinical features and CT imaging. *J Cardiovasc Comput Tomogr* 2016;10:1–12.

19 Answer A. The preferred method of repair in a neonate or infant is end-to-end anastomosis. This repair has decreased risk of recoarctation and reintervention with improved outcomes.
Reference: Nance JW, Ringel RE, Fishman EK. Coarctation of the aorta in adolescents and adults: a review of clinical features and CT imaging. *J Cardiovasc Comput Tomogr* 2016;10:1–12.

20 Answer D. A circumflex aortic arch is when the aorta passes to the left the trachea but courses posteriorly to the trachea and esophagus when becoming the descending aorta. This is most often associated with an anomalous right subclavian artery, but a normal branching pattern can be seen.

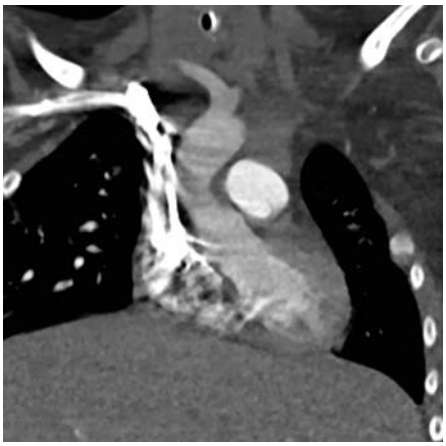
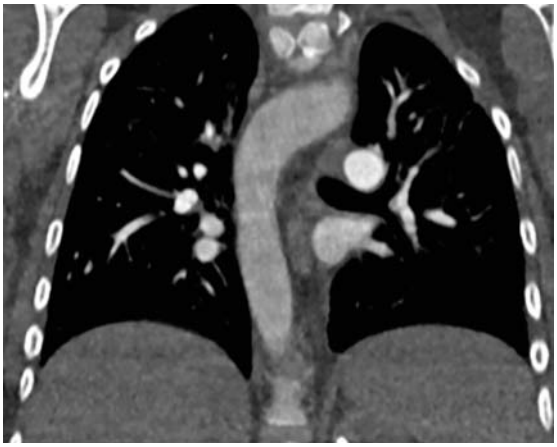


References: Smith BM, Lu JC, Dorfman AL, et al. Rings and slings revisited. *Magn Reson Imaging Clin N Am* 2015;23:127–135. Weinberg PM. Aortic arch anomalies. *J Cardiovasc Magn Reson* 2006;8:633–643.

21 Answer A. A circumflex aortic arch always forms a vascular ring. The ring is completed by the right ductus or ligamentum connecting the descending aorta to the pulmonary artery. The ligamentum cannot be visualized on imaging.

References: Smith BM, Lu JC, Dorfman AL, et al. Rings and slings revisited. *Magn Reson Imaging Clin N Am* 2015;23:127–135. Weinberg PM. Aortic arch anomalies. *J Cardiovasc Magn Reson* 2006;8:633–643.

22 Answer C. A double aortic arch, whether right dominant, codominant, or left dominant, is usually an isolated anomaly.

Arch anomaly	Association with CHD
Right aortic arch with aberrant left subclavian artery	Usually isolated
Double aortic arch	Usually isolated
Right aortic arch with mirror image branching pattern	Associated with CHD such as TOF, truncus arteriosus, and VSD
Circumflex aortic arch	Associated with CHD such as VSD, DORV, and coarctation

Reference: Smith BM, Lu JC, Dorfman AL, et al. Rings and slings revisited. *Magn Reson Imaging Clin N Am* 2015;23:127–135.

23 **Answer C.** The image demonstrates aneurysms of the left anterior descending coronary artery (arrow). Given the aneurysms, the most likely diagnosis is Kawasaki disease. Kawasaki disease is a self-limiting vasculitis that occurs in infants and young children. It is characterized by an initial acute phase of up to 14 days and a convalescent phase that lasts months to years. Patients experience a high fever minimally responsive to antipyretics. Conjunctivitis occurs in 85% of children. Additional symptoms include diarrhea, abdominal pain, vomiting, scrotal swelling, and arthritis. Coronary artery aneurysms occur in 20% of untreated children, most of which occur during the convalescent phase.

References: Pipitone N, Versari A, Hunder GG, et al. Role of imaging in the diagnosis of large and medium-sized vessel vasculitis. *Rheum Dis Clin N Am* 2013;39:593–608.
Weiss PF. Pediatric vasculitis. *Pediatr Clin N Am* 2012;59:407–423.

24 **Answer B.** Although patients with Kawasaki disease have unilateral cervical lymphadenopathy in 25% of cases, diffuse lymphadenopathy is unusual. Hydrops of the gallbladder along with diarrhea, vomiting, and abdominal pain can be seen. During the acute phase, patients may present with valvulitis, pericarditis, or myocarditis. Aneurysms are seen in the coronary arteries but additionally can be seen in visceral vessels such as the mesenteric and renal arteries.

References: Khanna G, Sargar K, Baszis KW. Pediatric vasculitis: recognizing multisystemic manifestations at body imaging. *Radiographics* 2015;35:849–865.
Weiss PF. Pediatric vasculitis. *Pediatr Clin N Am* 2012;59:407–423.

25 **Answer C.** Per the American Heart Association, patients with Kawasaki disease should be initially evaluated with echocardiography. This should be followed by reevaluation by echocardiography at 2 weeks and 6 to 8 weeks. Echocardiography has shown to have high sensitivity and specificity for evaluating coronary artery alterations.

Reference: Pipitone N, Versari A, Hunder GG, Salvarani C. Role of imaging in the diagnosis of large and medium-sized vessel vasculitis. *Rheum Dis Clin N Am* 2013;39:593–608.

7 Pediatric Cardiac Radiology

Questions

1. A 3-year-old patient with a history of congenital heart disease status post repair who presents for a cardiac MRI.

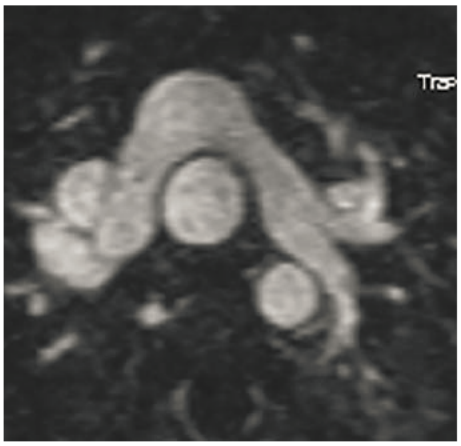

What is this patient's underlying diagnosis?
A. Tetralogy of Fallot (TOF)
B. Hypoplastic left heart (HLHS)
C. Total anomalous pulmonary venous return (TAPVR)
D. D-transposition of the great arteries (D-TGA)

2. Regarding the diagnosis in Question 1, which is TRUE?
A. There is ventriculoarterial discordance and atrioventricular discordance.
B. There is ventriculoarterial discordance and atrioventricular concordance.
C. There is ventriculoarterial concordance and atrioventricular discordance.
D. There is ventriculoarterial concordance and atrioventricular concordance.

3. The most common postoperative complication following surgical correction of the diagnosis in Question 1 is:
A. Coronary artery occlusion
B. Pulmonary vein stenosis
C. Mitral insufficiency
D. Aortic stenosis

4. Newborn presents with the following frontal radiograph of the chest.

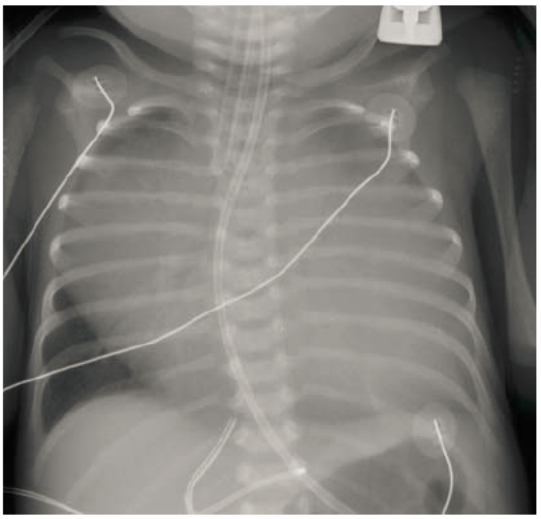

What is the most likely diagnosis?
A. Atrial–septal defect (ASD)
B. Ebstein anomaly
C. Tetralogy of Fallot (TOF)
D. Total anomalous pulmonary venous return (TAPVR)

5. In regard to the diagnosis in Question 4, the pulmonary vascularity is:
A. Increased
B. Normal
C. Decreased

6. The following is a surgical treatment for correction of the disorder in Question 4:
A. Tricuspid valvuloplasty
B. Jatene arterial switch
C. Left subclavian flap repair
D. Unroofing of the coronary artery

7. A 4-year-old patient presents with the following radiograph of the chest.

What is the diagnosis?
A. Partial anomalous pulmonary venous return (PAPVR)
B. TOF with aortopulmonary collateral
C. Ventricular septal defect (VSD)
D. Atrial septal defect (ASD)

8. Which of the following is an anomaly commonly associated with the disorder in Question 7?
A. Pleuropulmonary blastoma
B. Horseshoe lung
C. Congenital absence of the pericardium
D. Cor triatriatum

9. In a pediatric patient, what is the next step in imaging the disorder in Question 7?
A. CT angiogram
B. MR angiogram
C. Echocardiogram
D. Cardiac catheterization

10. An MRI of a 7-year-old patient with a history of a cardiac mass. Balanced gradient echo (A), first-pass perfusion (B), and delayed enhancement (C) imaging were performed.

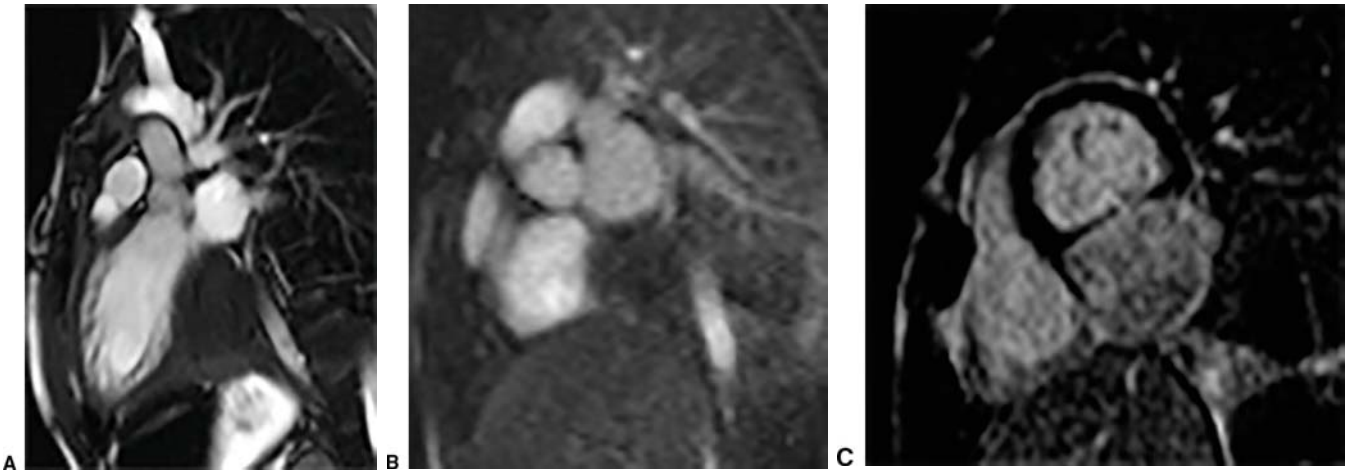

The most likely diagnosis is the following:
A. Rhabdomyoma
B. Myxoma
C. Fibroma
D. Lipoma
E. Teratoma

11. A typical imaging characteristic of the tumor in Question 10 is the following:
A. Strong first-pass perfusion
B. Typical location within the pericardium
C. Hyperenhancement on myocardial delayed enhancement
D. Hypoechoic appearance on echocardiography

12. Which of the following concerning a cardiac fibroma is TRUE?
A. It may remain stable for years or regress.
B. Asymptomatic patients are most often treated with chemotherapy.
C. Recurrence following surgery is common.
D. Arrhythmias are uncommon.

13. An MR angiogram of a 10-year-old male with chest pain was performed.

What is the diagnosis?
A. Anomalous left coronary artery from the right coronary cusp
B. Anomalous right coronary artery from the left coronary cusp
C. Anomalous left coronary artery from the pulmonary artery
D. Anomalous right coronary artery from the pulmonary artery
E. Normal coronary anatomy

14. Which imaging modality is commonly used for confirmation of the abnormality in Question 13?:
A. Echocardiography
B. Ventilation Perfusion Scan
C. ECG-gated CT Angiography
D. T1 mapping with myocardial delayed enhancement

15. What defines a high origin of a coronary artery?
A. 1 cm above the aortic annulus
B. 2 cm above the aortic annulus
C. 1 cm above the sinus of Valsalva
D. 2 cm above the sinus of Valsalva
E. 1 cm above the sinotubular junction
F. 2 cm above the sinotubular junction

16. Which of the following is a potentially hemodynamically significant coronary artery anomaly?
A. Duplication of the left or right coronary artery
B. High origin of the coronary artery
C. Interarterial course of a coronary artery
D. Prepulmonic course of a coronary artery
E. Transseptal course of a coronary artery
F. Retroaortic course of a coronary artery

17. A cardiac MRI was performed on a 3-year-old patient with congenital heart disease.

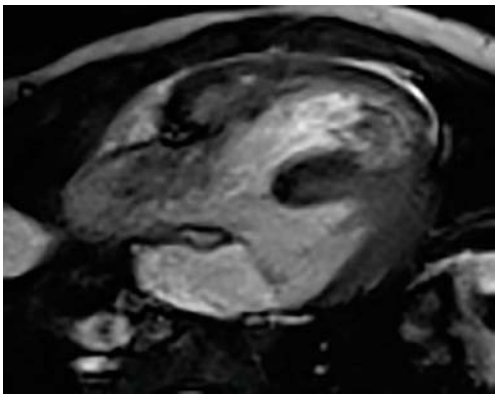

What is the diagnosis?
A. Transposition of the great arteries (TGA)
B. Total anomalous pulmonary venous return (TAPVR)
C. Cor triatriatum
D. Tetralogy of Fallot (TOF)
E. Hypoplastic left heart syndrome (HLHS)

18. Which of the following is NOT a characteristic of the disorder in Question 17?
A. Overriding aorta
B. Ventriculoseptal defect (VSD)
C. Right ventricular hypertrophy
D. Anomalous pulmonary venous return
E. Main and/or branch pulmonary artery obstruction
F. Pulmonary valve atresia

19. The most common coronary anomaly associated with the diagnosis in Question 17 is the following:
A. Right coronary artery from the left anterior descending artery (LAD)
B. Right coronary artery from the left circumflex artery
C. Right coronary artery from the left main
D. Left coronary artery from the right coronary artery

20. Which of the following is NOT a postoperative complication of the disorder in Question 17?
A. Left ventricular dysfunction
B. Right ventricular dysfunction
C. Residual ventricular septal defect (VSD)
D. Aortic insufficiency
E. Pulmonic insufficiency

21. A 2-day-old patient who presents with respiratory distress. Initial chest radiograph was performed.

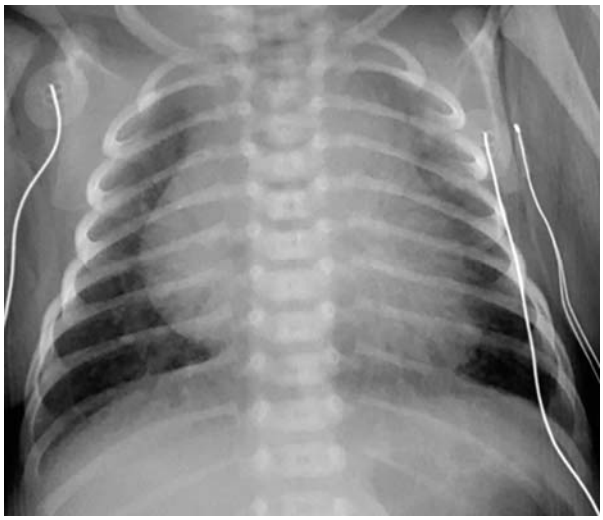

Which of the following is NOT a potential diagnosis for this patient?
A. Truncus arteriosus
B. Tetralogy of Fallot (TOF)
C. Transposition of the great arteries (TGA)
D. Hypoplastic left heart syndrome (HLHS)

22. A cardiac MRI was performed. Below is a four chamber balanced gradient echo image (A) and a sagittal image from an MRA (B).

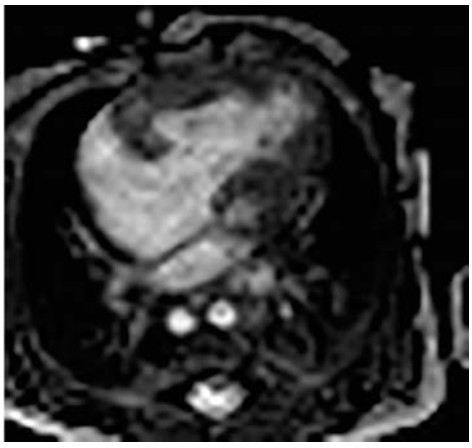
A


B

What is the diagnosis?
A. Truncus arteriosus
B. Tetralogy of Fallot (TOF)
C. Transposition of the great arteries (TGA)
D. Hypoplastic left heart syndrome (HLHS)

23. In a neonate with the disorder in Question 22, how are the coronary arteries perfused prior to surgical intervention?
A. Left to right flow through the ductus arteriosus during ventricular systole
B. Left to right flow through the ductus arteriosus during ventricular diastole
C. Right to left flow through the ductus arteriosus during ventricular systole
D. Right to left flow through the ductus arteriosus during ventricular diastole

24. Which of the following is TRUE in regards to the Norwood procedure for surgical correction of hyoplastic left heart syndrome?
A. Stage 1 of the Norwood procedure is typically the creation of a bidirectional Glenn shunt.
B. Stage 1 of the Norwood procedure is typically performed at 1 month of life.
C. Stage 2 of the Norwood procedure is typically the creation of a Blalock-Taussig shunt.
D. Stage 2 of the Norwood procedure is typically performed at 2 months of life.
E. Stage 3 of the Norwood procedure is typically the creation of a modified Fontan.
F. Stage 3 of the Norwood procedure is typically performed at 6 months of life.

25. A cardiac examination was performed on a child but was complicated by motion artifact. Which of the following is a technique that can be used to reduce motion artifact when imaging this child?
A. Radial k-space filling
B. Changing the field of view (FOV)
C. Decreasing the pixel size
D. Gradient moment nulling

Cardiac Radiology: Answers and Explanations

1 Answer D. The patient is status post arterial switch operation and a LeCompte maneuver for transposition of the great arteries. In this surgery, the coronaries are excised from the aorta and the ascending aorta, and main pulmonary artery is switched. The LeCompte maneuver involves placing the ascending aorta (asterisk) posterior to the bifurcation of the main pulmonary artery. This maneuver reduces the risk of compression or kinking of the coronary arteries.

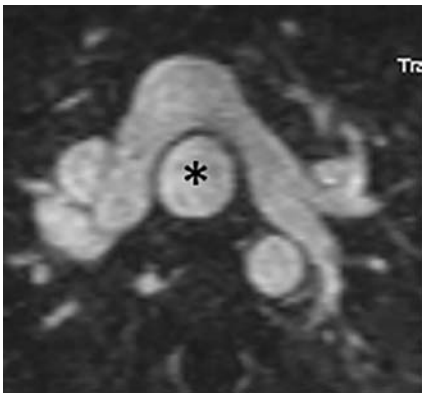

Reference: Gaca AM, Jaggers JJ, Dudley LT, et al. Repair of congenital heart disease: a primer—part 1. *Radiology* 2008;247:617–631.

2 Answer B. In dextrotransposition of the great arteries (D-TGA), there is ventriculoarterial discordance but atrioventricular concordance. The aorta arises from the morphological right ventricle, and the main pulmonary artery arises from the morphological left ventricle. The left atrium enters the left ventricle, and the right atrium enters the right ventricle consistent with atrioventricular concordance. In congenitally corrected or L-transposition of the great arteries (L-TGA), there is atrioventricular and ventriculoarterial discordance.

References: Gaca AM, Jaggers JJ, Dudley LT, et al. Repair of congenital heart disease: a primer—part 1. *Radiology* 2008;247:617–631. Warnes CA. Transposition of the great arteries. *Circulation* 2006;114:2699–2709.

3 Answer A. An obstructed coronary artery leading to myocardial ischemia is the most common cause of morbidity and mortality following an arterial switch operation (ASO) for D-TGA. This risk is most common in the initial 3 months following ASO. Additionally, neoaortic root dilation occurs in nearly all patients post ASO, and neoaortic valve regurgitation occurs in most patients post ASO. Less common long-term sequelae are supravalvular pulmonary stenosis and aortic stenosis.

Reference: Villafane J, Lantin-Hermoso MR, Bhatt AB, et al. D-transposition of the great arteries. *J Am Coll Cardiol* 2014;64:498–511.

4 Answer B. The characteristic appearance of Ebstein anomaly on a chest radiograph is marked cardiomegaly with decreased pulmonary vascularity. Although tetralogy of Fallot also may present with decreased vascularity on radiograph, it does not typically present with marked cardiomegaly. In Ebstein anomaly, there is displacement of the septal and posterior leaflets (arrows) of the tricuspid valve into the right ventricle forming an atrialized portion of the right ventricle.

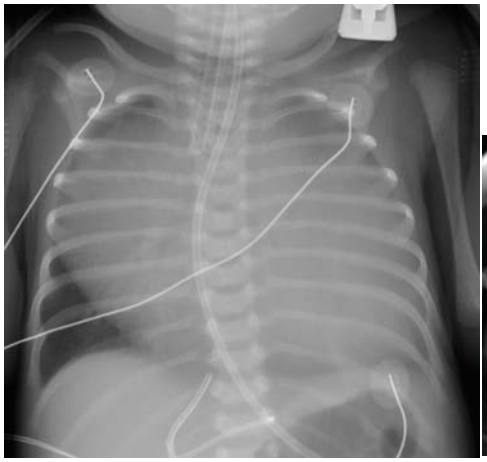

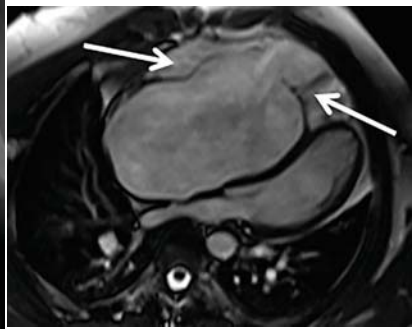

Reference: Epstein ML. Tricuspid atresia, stenosis, and regurgitation. In: Moss AJ, Allen HD, eds. *Moss and adams' heart disease in infants, children, and adolescents: including the fetus and young adult*, 7th ed. Philadelphia, PA: Wolters Kluwer Health/Lippincott Williams & Wilkins, 2008:817–834.

5 Answer C. Although the degree of abnormality varies in patients with Ebstein anomaly, the pulmonary vascularity would be typically decreased. During ventricular systole, much of the cardiac output is sent retrograde into the true right atrium rather than antegrade into the true right ventricle and main pulmonary artery.

Reference: Epstein ML. Tricuspid atresia, stenosis, and regurgitation. In: Moss AJ, Allen HD, eds. *Moss and adams' heart disease in infants, children, and adolescents: including the fetus and young adult*, 7th ed. Philadelphia, PA: Wolters Kluwer Health/Lippincott Williams & Wilkins, 2008:817–834.

6 Answer A. Management of Ebstein anomaly can be variable depending on the severity of the disease. Biventricular repair involving tricuspid valvuloplasty such as cone reconstruction may be performed. Tricuspid valve replacement is another surgical procedure used in Ebstein anomaly repair. Single ventricle repair involving a bidirectional cavopulmonary anastomosis (Glenn) and/or a total cavopulmonary anastomosis (Fontan) may be needed for a poorly functioning right ventricle.

References: Gaca AM, Jaggers JJ, Dudley T, et al. Repair of congenital heart disease: a primer-part 1. *Radiology* 2008;247:617–631. Jinghao Z, Kai L, Yanhui H, et al. Individualized surgical treatments for children with Ebstein anomaly. *Thorac Cardiovasc Surg* 2016 [Epub ahead of print].

7 Answer A. On the chest radiograph, there is a prominent vessel within the right hemithorax (arrow in Fig. **A**) consistent with an anomalous pulmonary vein draining to the inferior vena cava. This finding is consistent with a right lower lobe anomalous pulmonary venous connection. The pulmonary veins normally drain into the left atrium. In partial anomalous pulmonary venous, some of the veins drain anomalously into the systemic venous system rather than to the left atrium (arrow in Fig. **B**).
In this case, the right lung is also decreased in size in comparison to the left with elevation of the right hemidiaphragm. This finding in addition to the partial anomalous pulmonary venous return is consistent with hypogenetic lung syndrome or scimitar syndrome. In this syndrome, the right lung partially drains to the inferior vena cava with a variable degree of lung hypoplasia. The right pulmonary artery may be hypoplastic or aplastic.

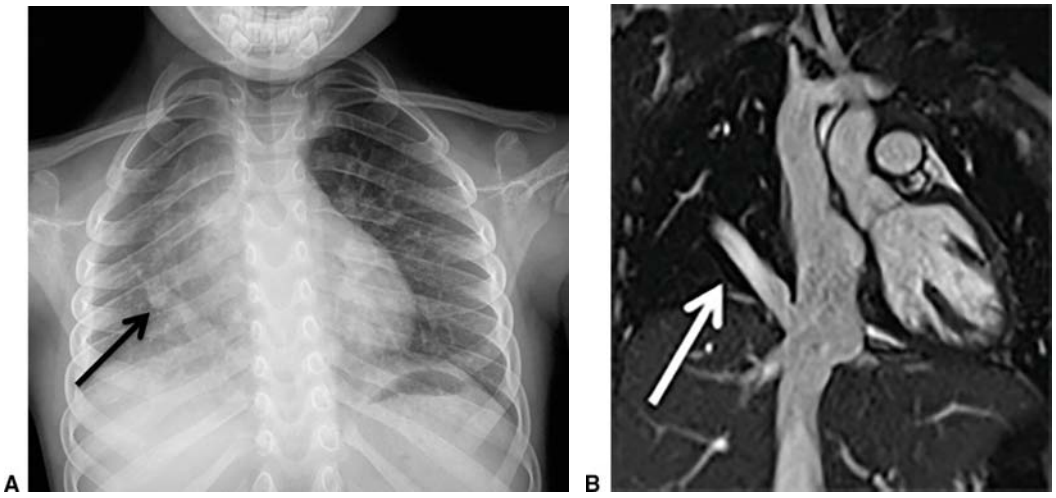

Reference: Konen E, Raviv-Zilka L, Cohen RA, et al. Congenital pulmonary venolobar syndrome: spectrum of helical CT findings with emphasis on computerized reformatting. *Radiographics* 2003;23:1175–1184.

8 Answer B. As noted above, this patient presents with not only partial anomalous pulmonary venous return (PAPVR) but also hypogenetic lung syndrome or scimitar syndrome. Patients with scimitar have associated anomalies including congenital heart disease, particularly sinus venosus atrial septal defects (ASD), bronchogenic cysts, accessory diaphragms, and hernias. Scimitar syndrome is also associated with horseshoe lung where an isthmus of the right lung base extends posteriorly joining the posterobasal segments of the right and left lung.

Reference: Konen E, Raviv-Zilka L, Cohen RA, et al. Congenital pulmonary venolobar syndrome: spectrum of helical CT findings with emphasis on computerized reformatting. *Radiographics* 2003;23:1175–1184.

9 Answer C. A chest radiograph is the initial screening modality used to evaluate patients with suspected partial anomalous pulmonary venous return (PAPVR). Given that it is noninvasive, echocardiogram is the next imaging modality in evaluating pediatric patients with this disorder. If additional imaging is desired, cross-sectional imaging such MRI/MR angiography and CT/CT angiography can be performed. MRI is usually preferred given the lack of ionizing radiation and the ability to characterize pulmonary and systemic flow. CT would be preferred if evaluation of the lung parenchyma is desired. Cardiac catheterization is performed for endovascular procedures or if additional hemodynamic data is needed.

Reference: Sung LY, Ting C, Varghese C, Hellinger JC. Scimitar syndrome. In: Reid JR, Paladin A, Davros WJ, et al. (eds). *Pediatric radiology*. New York, NY: Oxford University Press, 2013:105–109.

10 Answer C. The most likely diagnosis is a cardiac fibroma. Fibromas are low in signal on balanced gradient echo imaging (arrow), do not demonstrate first-pass perfusion (+), and do demonstrate myocardial delayed enhancement (asterisk). Rhabdomyoma could be considered, but rhabdomyomas do not demonstrate myocardial delayed enhancement.

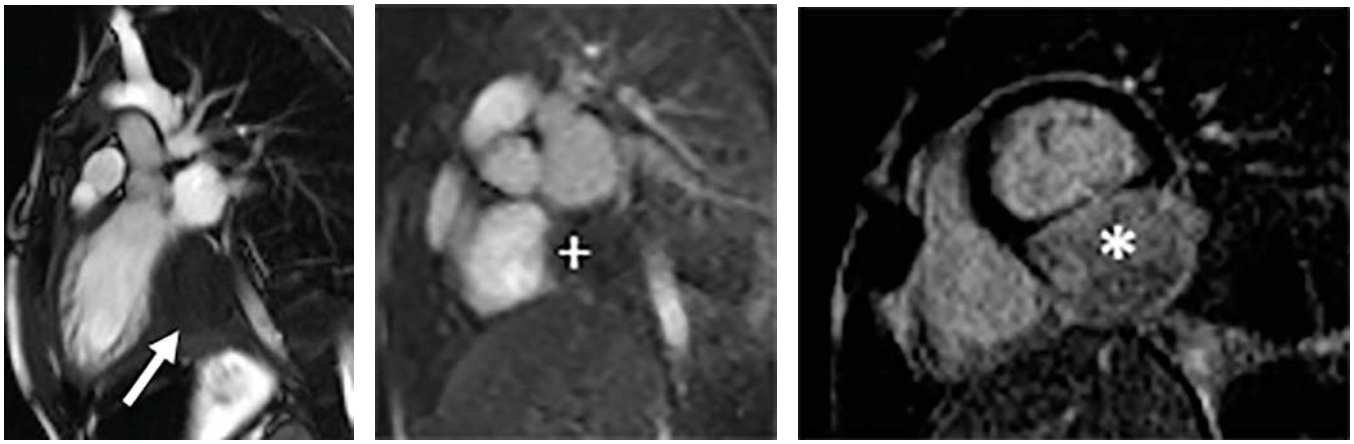

The table below describes characteristics of select pediatric cardiac masses (from Beroukhim et al. 2011).

Tumor	Location	T1	T2	First-pass perfusion (FPP)	Myocardial delayed enhancement (MDE)
Fibroma	Intramyocardial, ventricular septum, or free wall	Variable	Variable	No	Positive
Rhabdomyoma	Intramyocardial or intracavitary	Variable	Bright	No	Negative
Myxoma	Left atrium typically	Variable	Bright	No	Variable
Hemangioma	Variable	Dark	Bright	Strong	Variable but if positive homogenous
Malignant	Variable but infiltrative	Variable	Variable	Variable	Variable but if positive heterogeneous

Reference: Beroukhim RS, Prakash A, Buechel ERV, et al. Characterization of cardiac tumors in children by cardiovascular magnetic resonance imaging. *J Am Coll Cardiol* 2011;58:1044–1054.

11 **Answer C.** Cardiac fibromas demonstrate strong delayed hyperenhancement on myocardial delayed imaging. They are most often heterogeneous on T1- and T2-weighted imaging. They do not demonstrate first pass perfusion. The lesions are most often echogenic on echocardiography. There location is usually intramyocardial involving either the ventricular septum or ventricular free wall.

References: Beroukhim RS, Prakash A, Buechel ERV, et al. Characterization of cardiac tumors in children by cardiovascular magnetic resonance imaging. *J Am Coll Cardiol* 2011;58:1044–1054.
Grebenc ML, Rosado de Christenson M, Burke AP, et al. Primary cardiac and pericardial neoplasms: radiologic-pathologic correlation. *Radiographics* 2000;20:1073–1103.

12 **Answer A.** Cardiac fibromas may be stable for years or even regress. Although one-third of patients may be asymptomatic, presenting symptoms may include arrhythmias, heart failure, or sudden death. If patients are symptomatic, these tumors are resected. Patients may even benefit from partial resection of more extensive tumors. Postsurgical recurrence is rare.

Reference: Grebenc ML, Rosado de Christenson M, Burke AP, et al. Primary cardiac and pericardial neoplasms: radiologic-pathologic correlation. *Radiographics* 2000;20:1073–1103.

13 **Answer B.** The images demonstrate the right coronary artery (arrow) originating for the left coronary cusp consistent with an anomalous right coronary artery. The right coronary artery takes a tangential course to the aortic root and an interarterial course between the right ventricular outflow tract on the aorta.

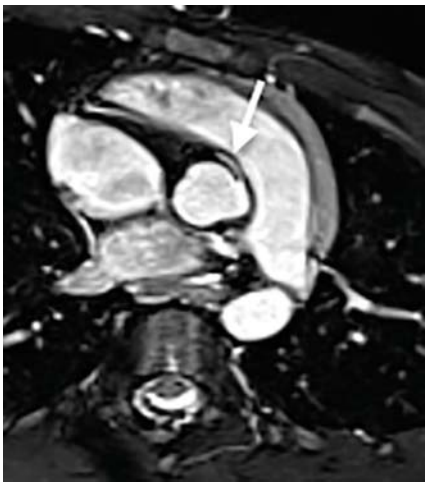

Reference: Shriki JE, Shinbane JS, Rashid MA, et al. Identifying, characterizing, and classifying congenital anomalies of the coronary arteries. *Radiographics* 2012;32:453–468.

14 **Answer C.** Although history and physical examination is initially used to screen patients for coronary artery anomalies, imaging modalities are needed for detection. Cross-sectional imagings, such as MRA and CTA, are modalities often used to directly visualize the origin of the coronary arteries. Echocardiography can also be used, but this modality is less precise than cross-sectional imaging.

Reference: Angelini P. Novel imaging of coronary artery anomalies to assess their prevalence, the causes of clinical symptoms, and the risk of sudden cardiac death. *Circ Cardiovasc Imaging* 2014;7:747–754.

15 **Answer E.** A high origin of a coronary artery is defined as >1 cm above the sinotubular junction of the ascending aorta. This anomaly is not hemodynamically significant but can have significance in patients undergoing aortic valve surgery. Additionally, there is a reported increased incidence of high origin of the right coronary artery in patients with bicuspid aortic valves.

Reference: Shriki JE, Shinbane JS, Rashid MA, et al. Identifying, characterizing, and classifying congenital anomalies of the coronary arteries. *Radiographics* 2012;32:453–468.

16 **Answer C.** Potentially hemodynamically significant coronary anomalies include the interarterial course of the coronary artery, origin of the coronary artery from the pulmonary artery, and coronary artery fistulas. In an interarterial course, the anomalous coronary artery, either the left coronary from the right cusp or the right coronary from the left cusp, takes a course between the pulmonary artery and the aorta. The interarterial course is more associated with sudden cardiac death. Other features that may increase the risk of sudden cardiac death are a slit-like orifice, acute angle between the anomalous coronary artery and the aorta, and an intramural aortic segment.

References: Biko DM, Chung C, Hitt SM, et al. High-resolution coronary MR angiography for evaluation of patients with anomalous coronary arteries: visualization of the intramural segment. *Pediatr Radiol* 2015;45:1146–1152.
Shriki JE, Shinbane JS, Rashid MA, et al. Identifying, characterizing, and classifying congenital anomalies of the coronary arteries. *Radiographics* 2012;32:453–468.

17 **Answer D.** The findings are consistent with tetralogy of Fallot (TOF). In the provided image, there is right ventricular hypertrophy (arrow), an overriding aorta (+) and a ventricular septal defect (asterisk). TOF is the most common cyanotic congenital heart disease. Classically, the TOF consists of (1) obstruction of the right ventricular outflow tract, (2) ventricular septal defect, (3) overriding aorta, and (4) right ventricular hypertrophy.

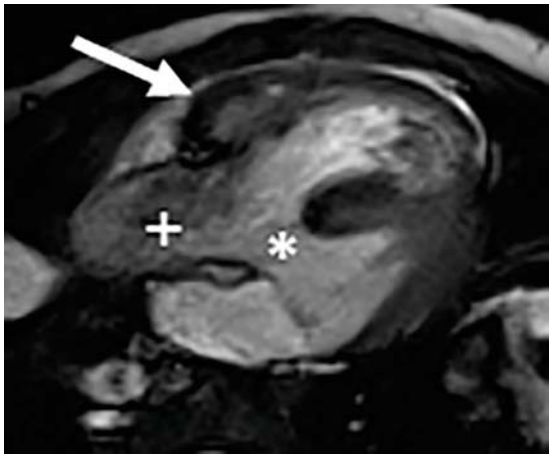

References: Lapierre C, Dubois J, Rypens F, et al. Tetralogy of Fallot: preoperative assessment with MR and CT imaging. *Diagn Interv Imaging* 2016;97:531–541.
Norton KI, Tong C, Glass RB, Nielsen JC. Cardiac MR imaging assessment following tetralogy of Fallot repair. *Radiographics* 2006;26:197–211.

18 **Answer D.** As noted in the explanation for Question 17, TOF consists of (1) obstruction of the right ventricular outflow tract, (2) ventricular septal defect, (3) overriding aorta, and (4) right ventricular hypertrophy. The degree of obstruction in TOF is variable ranging from mild obstruction of the right ventricular outflow tract to main or branch pulmonary artery obstruction, to pulmonary atresia. TOF with pulmonary atresia is the most severe form of this disease.

References: Lapierre C, Dubois J, Rypens F, et al. Tetralogy of Fallot: preoperative assessment with MR and CT imaging. *Diagn Interv Imaging* 2016;97:531–541.
Norton KI, Tong C, Glass RB, Nielsen JC. Cardiac MR imaging assessment following tetralogy of Fallot repair. *Radiographics* 2006;26:197–211.

19 **Answer A.** Coronary artery anomalies are present in tetralogy of Fallot (TOF) in approximately 5% of cases with the most common anomaly being the right coronary artery arising from the left anterior descending artery (LAD). This finding is important to report as it may change the surgical approach to this disorder. Additionally, a right aortic arch is seen in 25% of patients, an atrial septal defect is seen in 5% of patients, and a left superior vena cava is seen in 11% of patients.

Reference: Lapierre C, Dubois J, Rypens F, et al. Tetralogy of Fallot: preoperative assessment with MR and CT imaging. *Diagn Interv Imaging* 2016;97:531–541.

20 Answer D. Surgical repair in tetralogy of Fallot (TOF) involves removing the right ventricular obstruction. This most often involves placement of a transannular patch or conduit in addition to closure of the ventricular septal defect (VSD) and infundibular muscle resection. Postoperative complications of surgical intervention in these patients include residual VSD, pulmonic insufficiency and subsequent right ventricular enlargement and dysfunction, residual pulmonic stenosis, tricuspid insufficiency, right ventricular outflow tract aneurysm, conduit obstruction, and left ventricular dysfunction.

Reference: Norton KI, Tong C, Glass RB, Nielsen JC. Cardiac MR imaging assessment following tetralogy of Fallot repair. *Radiographics* 2006;26:197–211.

21 Answer B. The pulmonary vascularity is increased on the presented radiograph. Truncus arteriosus, transposition of the great arteries, and hypoplastic left heart syndrome all may present with increased pulmonary vascularity. Given the right ventricular outflow tract obstruction, tetralogy of Fallot and Ebstein anomaly usually present with decreased or normal vascularity on chest radiograph.

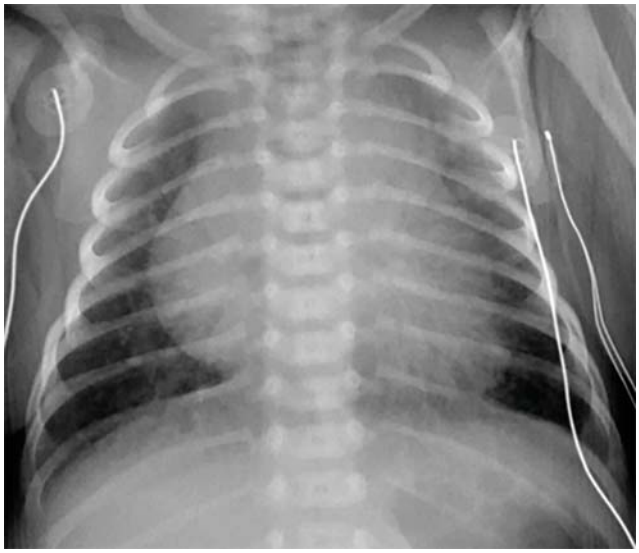

Reference: Ferguson EC, Krishnamurthy R, Oldham SA. Classic imaging signs of congenital cardiovascular abnormalities. *Radiographics* 2007;27:1323–1334.

22 Answer D. Hypoplastic left heart syndrome (HLHS) is a spectrum which involves hypoplasia or absence of the left ventricle with hypoplasia of the ascending aorta. In this case, the left ventricle is severely hypoplastic (arrow) with flow to the aorta supported via the right ventricle consistent with this syndrome. There may be mitral and/or aortic valve stenosis or atresia. The neonate born with this disorder is dependent on the ductus arteriosus for maintenance of systemic perfusion.

References: Bardo DM, Frankel DG, Applegate KE, et al. Hypoplastic left heart syndrome. *Radiographics* 2001;21:705–717.
Greenleaf CE, Urencio JM, Salazar JD, et al. Hypoplastic left heart syndrome: current perspectives. *Transl Pediatr* 2016;5:142–147.

23 Answer D. In hypoplastic left heart syndrome (HLHS), the ductus arteriosus must be maintained for systemic perfusion. At birth, the blood flow is right to left across the ductus arteriosus during ventricular systole which perfuses the systemic circulation. In ventricular diastole, the flow across the ductus arteriosus is left to right. Blood flow is also retrograde into the ascending aorta during ventricular diastole which perfuses the coronary arteries.
Reference: Bardo DM, Frankel DG, Applegate KE, et al. Hypoplastic left heart syndrome. *Radiographics* 2001;21:705–717.

24 Answer E. The Norwood procedure is a 3-stage surgical procedure performed in patients with single ventricle physiology such as hypoplastic left heart syndrome (HLHS). In this staged procedure, the right ventricle becomes the systemic pump. It is designed to protect the pulmonary vascular bed and transition an infant to definitive repair. See the table below.

	Intervention	Typical age of surgery
Stage 1	Divide pulmonary artery and create neoaorta Create Blalock-Taussig shunt (shunt between subclavian artery and ipsilateral pulmonary artery)	First few days of life
Stage 2	Remove Blalock-Taussig shunt Create bidirectional Glenn shunt (superior vena cava to pulmonary artery anastomosis)	3 months–6 months
Stage 3	Fontan (inferior vena cava to pulmonary artery anastomosis) Bidirectional Glenn shunt remains	18 months–4 years

References: Bardo DM, Frankel DG, Applegate KE, et al. Hypoplastic left heart syndrome. *Radiographics* 2001;21:705–717.
Gaca AM, Jaggers JJ, Dudley LT, Bissett GS. Repair of congenital heart disease: a primer-part 1. *Radiology* 2008;247:617–631.

25 Answer A. There are several techniques to correct of ghosting or smearing of an MR image from either voluntary or involuntary patient motion. The use of radial k-space filling as opposed to rectilinear k-space filling is one of these techniques. Using this technique, data are acquired in radial sections which vary the phase-encoding direction. This disperses the patient motion over radial sections rather than rectilinear sections, which improve image quality. The table below summarizes a few techniques to correct several common MR artifacts caused by motion.

Type of artifact	MR techniques for correction	Explanation
Ghosting and Smearing	Radial k-space filling	Data is acquired in radial sections varying the phase-encoding direction and dispersing the patient motion over radial sections
	Cardiac gating	k-space lines acquired during a certain phase of each heart beat
	Respiratory gating	k-space lines acquired during a certain phase of respiration
Pulsatile Flow Artifact	Gradient moment nulling	Application of gradient pulses to eliminate phase shifts produced by the moving protons
	Saturation pulse	RF pulse applied perpendicular or parallel to the imaging plane to eliminate ghosting from moving structures

Reference: Morelli JN, Runge VM, Ai F, et al. An image-based approach to understanding the physics of MR artifacts. *Radiographics* 2011;31:849–866.

8 Pediatric Multisystem Radiology

Questions

1. An 11-year-old female presents with chronic visual disturbance. What neurocutaneous syndrome is manifested with these findings?

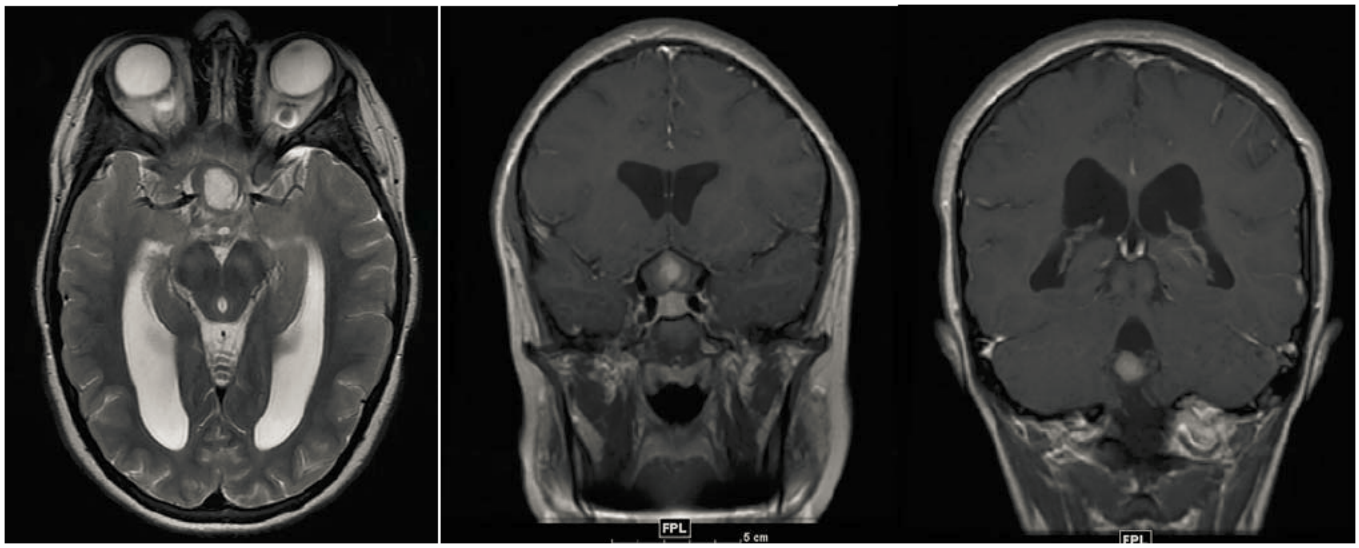

A. Neurofibromatosis type 1
B. Neurofibromatosis type 2
C. Sturge-Weber
D. Metachromatic leukodystrophy

2. What cutaneous finding is associated with this syndrome?
A. Port-wine stain
B. Café au lait spot
C. Facial angiofibroma
D. Vitiligo

3. A 13-year-old female presents with history of left functional hemispherectomy to alleviate refractory epilepsy. Which syndrome is the likely cause of her seizure disorder?

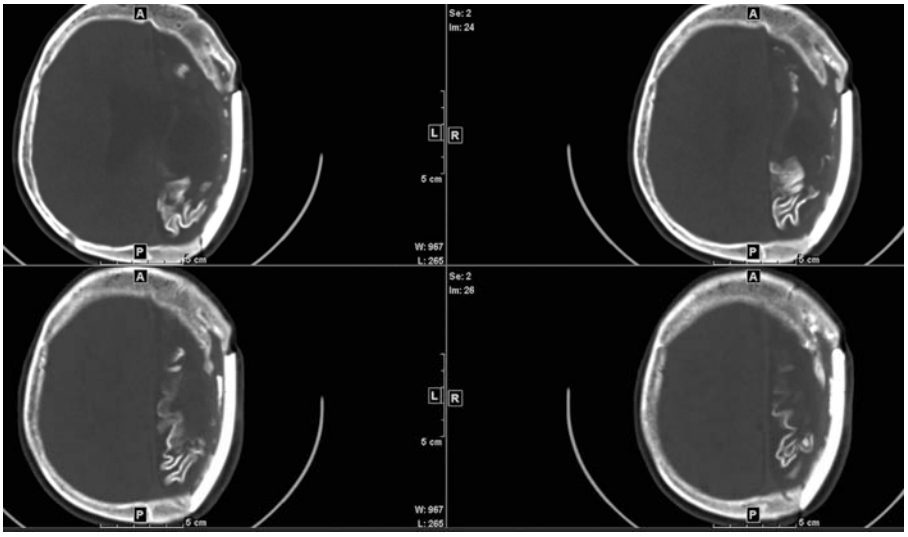

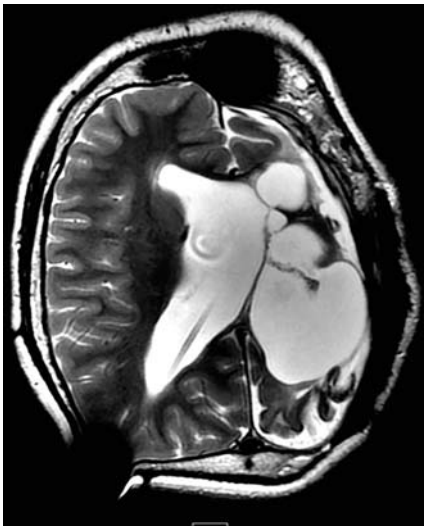

A. Neurofibromatosis type 1
B. Neurofibromatosis type 2
C. Sturge-Weber
D. Tuberous sclerosis

4. What cutaneous finding is associated with this syndrome?
A. Port-wine stain
B. Café au lait spot
C. Facial angiofibroma
D. Vitiligo

5. A newborn presents with abnormal prenatal ultrasound. Which of the following antenatal findings is most associated with this postnatal radiographic finding?

A. Rocker bottom foot
B. Microcephaly
C. Polydactyly
D. Cerebral ventriculomegaly

6. What is the most likely diagnosis?
A. Trisomy 13
B. Trisomy 18
C. Trisomy 21
D. Trisomy 23

7. A 21-day-old female presents with abnormal ophthalmic examination. What syndrome is associated with the imaging findings?

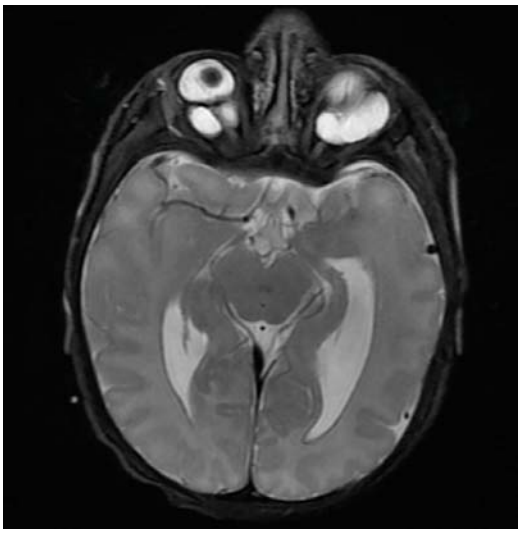

A. Chiari II malformation
B. CHARGE
C. Tuberous sclerosis
D. Sturge-Weber

8. A 10-year-old male presents with tall stature and history of spontaneous pneumothorax. What syndrome does this patient likely have?

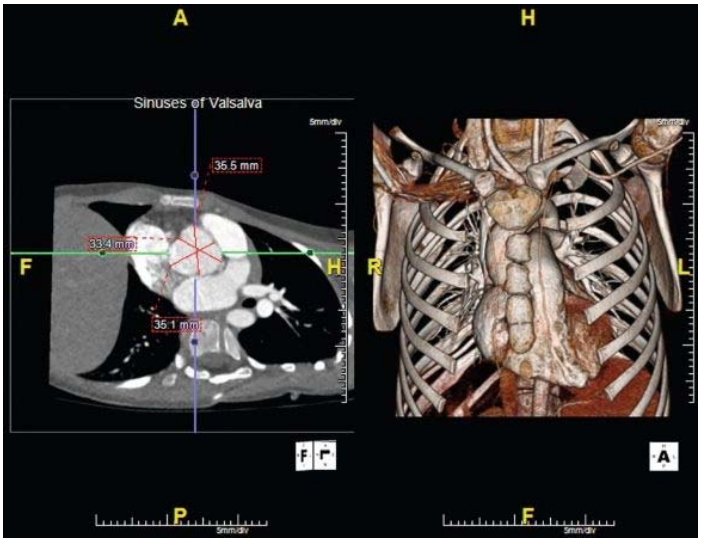

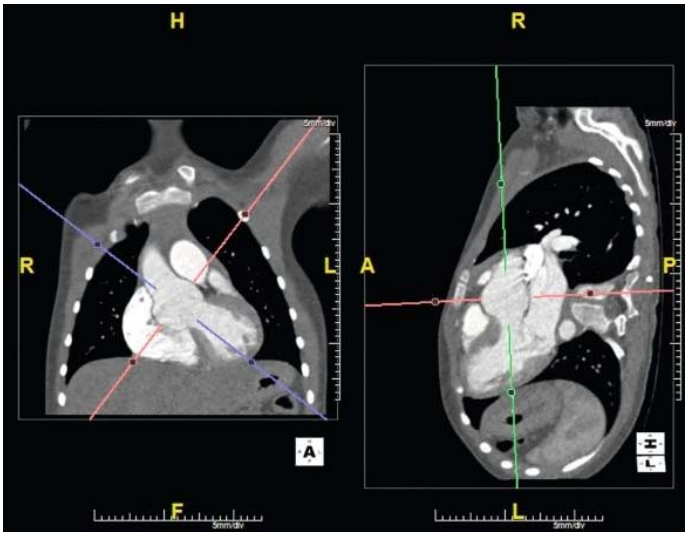

A. Down
B. Marfan
C. McCune-Albright
D. Birt-Hogg-Dube

9. What measurement threshold (in millimeters) is used to determine if intervention is required to correct a dilated or aneurysmal aortic root in this syndrome?
A. 25
B. 35
C. 45
D. 55

10. A 4-month-old female presents for imaging surveillance. Which of the following syndromes corresponds to this patient's imaging findings?

A. von Hippel-Lindau
B. Neurofibromatosis type 1
C. Neurofibromatosis type 2
D. Beckwith-Wiedemann

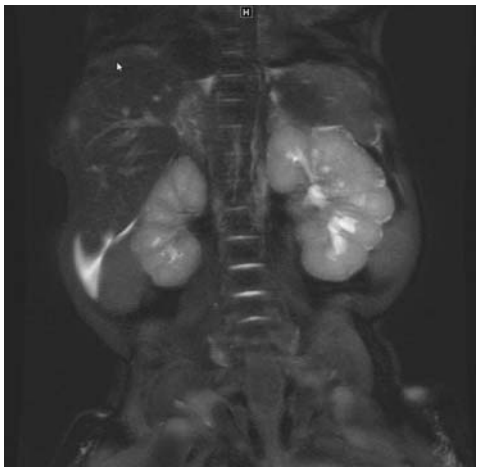

11. Which of the following syndromes are included in the WT1-related Wilms tumor syndromes?
A. Neurofibromatosis type 2
B. von Hippel-Lindau
C. Denys-Drash syndrome
D. Down syndrome

12. A 26-year-old female presents with 33-week-old fetus with neck mass identified on US and MR. Which syndrome is most commonly associated with this fetal neck mass?

A. Klinefelter
B. Turner
C. Patau
D. Edward

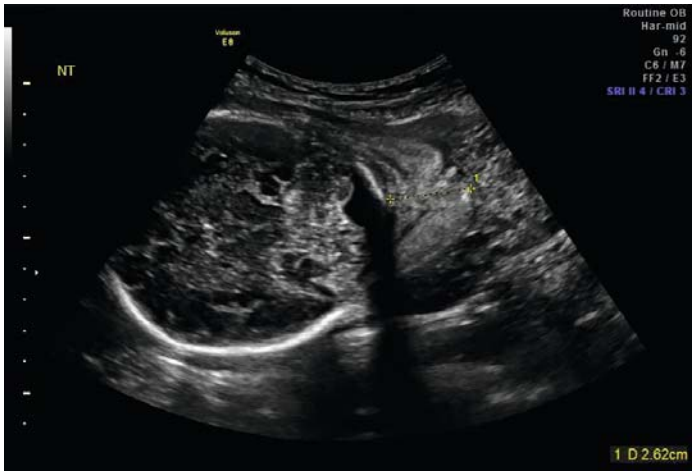

13. What is the most appropriate time frame (gestational age in weeks) during pregnancy should the nuchal translucency scan be performed when screening for aneuploidy?
A. 8 to 10
B. 11 to 13
C. 14 to 16
D. 17 to 19

14. A 17-year-old female presents with recurrent joint dislocation. Which of the following syndromes or diseases is most commonly associated with joint laxity and recurrent joint dislocation?

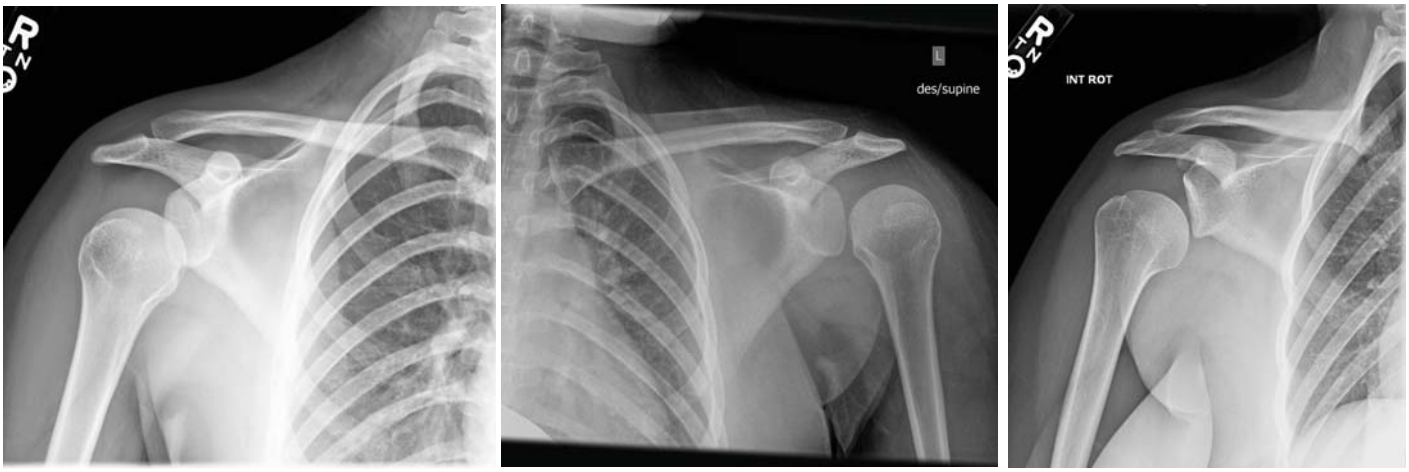

A. Trisomy 21
B. Osteogenesis imperfecta
C. Ehlers-Danlos syndrome
D. Gaucher disease

15. What is the most common inheritance pattern of this syndrome or disease?
A. Autosomal recessive
B. Autosomal dominant
C. X-linked recessive
D. X-linked dominant

16. A 10-month-old with DiGeorge syndrome is status post thoracic surgery. Which of the following cardiothoracic abnormalities is most associated with DiGeorge syndrome?

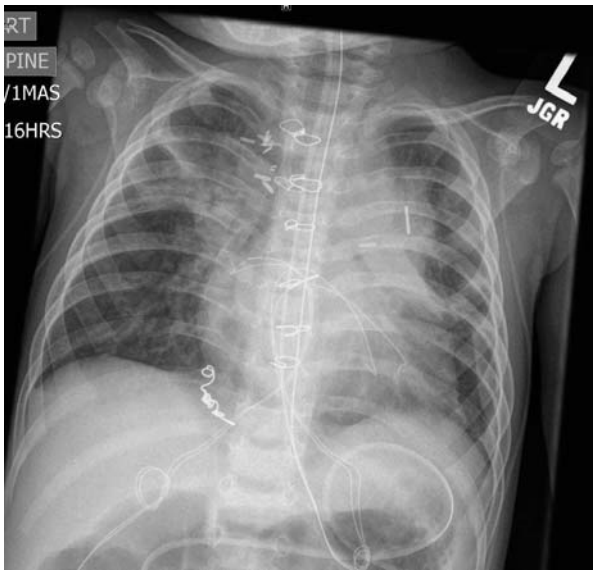

A. Aortic coarctation
B. Tetralogy of Fallot
C. Tricuspid atresia
D. Mitral valve regurgitation

17. Which of the following chromosomal deletions is responsible for DiGeorge syndrome?
A. 13
B. 18
C. 21
D. 22

18. A 17-year-old female presents with a vascular anomaly. Which of the following is the most likely syndrome depicted?

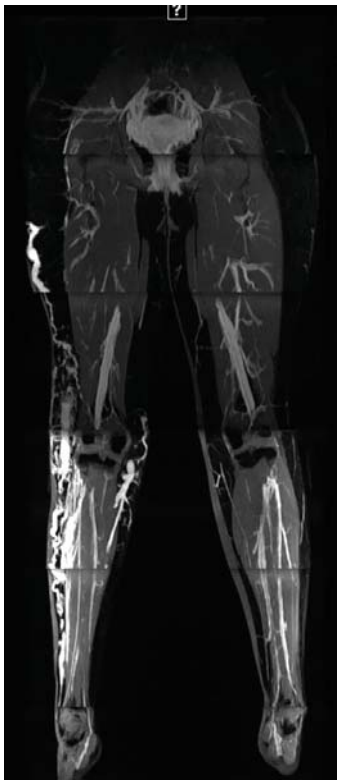

A. Klippel-Trenaunay-Weber
B. Hemihypertrophy
C. Beckwith-Wiedemann
D. Maffucci

19. An 8-year-old female presents with history of small bowel transplant. What organism is most commonly associated with this disease process?

A. Cytomegalovirus
B. *Mycobacterium tuberculosis*
C. *Escherichia coli*
D. Epstein-Barr virus

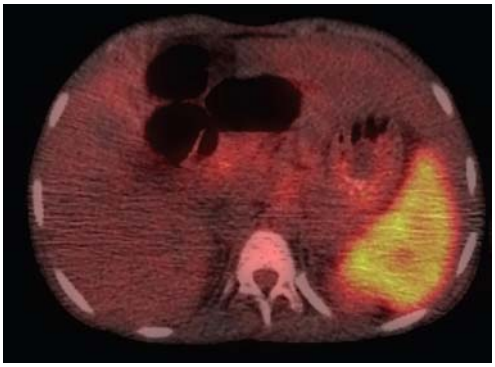

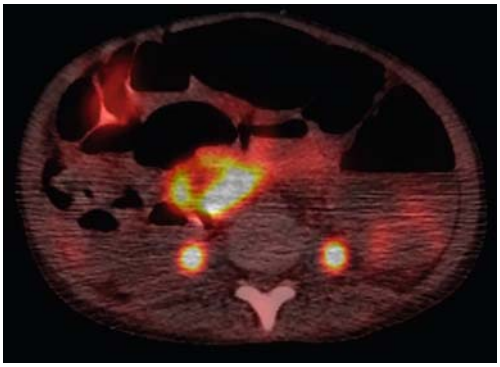

20. An 8-week-old female presents with multiple congenital anomalies including anal atresia. Given the following imaging abnormalities, what is the most likely diagnosis?

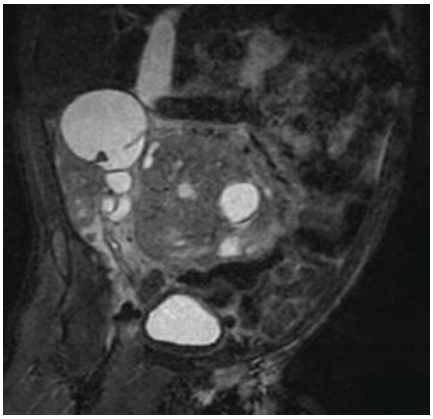

A. VACTERL association
B. Beckwith-Wiedemann syndrome
C. Scheuermann disease
D. Denys-Drash syndrome

21. A 3-year-old patient presents to the emergency room with complaints of a headache. A CT scan of the brain was obtained, and a coronal image is shown below (Image A). This is compared to a coronal image from a limited MR of the brain performed a year before the current study (Image B). What is the next best step in management?

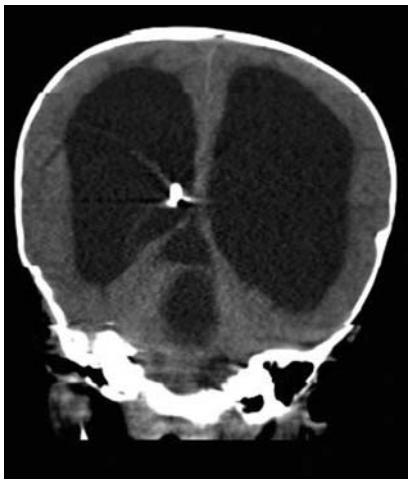

Image A

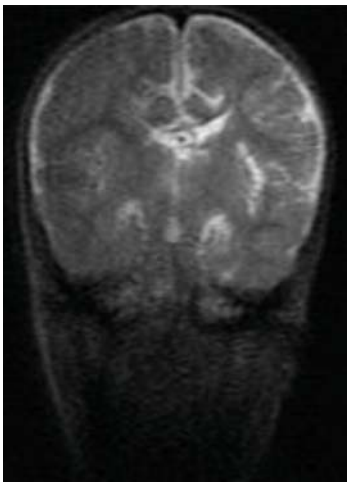

Image B

A. Whole-body MR
B. No further management is needed
C. Plain film skeletal survey to evaluate for nonaccidental trauma (NAT)
D. Plain film shunt series

22. A shunt series was subsequently ordered to evaluate the integrity of the patient's ventriculoperitoneal (VP) shunt catheter described in Question 21. The catheter was noted to be intact, but the distal tip was noted to be kinked (Image A). Because of this finding, an ultrasound exam of the area surrounding the tip was performed and a representative image is shown below (Image B). Concerning the most likely diagnosis, which of the following is true?

Image A

Image B

A. This entity usually develops within the first week after shunting.
B. If infection is present, the wall of the lesion should be excised but the CSF shunt can be left in place.
C. Fine needle aspiration is sometimes used to differentiate this lesion from ascites.
D. The formation of this lesion is a contraindication for future use of the peritoneal cavity in CSF shunting.

23. Regarding transependymal flow of CSF, which of the following is true?
A. It is a form of increased interstitial edema that occurs due to a decrease in intraventricular pressures.
B. CT is more sensitive for the detection of transependymal flow of CSF than MR.
C. Without intervention, this entity ultimately progress to cerebral atrophy and gliosis.
D. This finding is pathognomonic for CSF shunt malfunction.

24. What is the most common imaging sign of increased intracranial pressure?
A. Flattening of the posterior globes
B. Low cerebellar tonsils
C. Empty sella
D. Large ventricles

25. What is the most sensitive MRI sign of hydrocephalus?
A. Papilledema
B. Sutural splaying
C. Enlargement of the temporal horns of the lateral ventricles
D. Venous expansion

26. Chest radiographs obtained on a 16-year-old female are shown below.
Which of the following condition does this patient most likely have?
A. Neurofibromatosis I
B. Tuberous sclerosis
C. Sickle cell anemia
D. von Hippel-Lindau syndrome

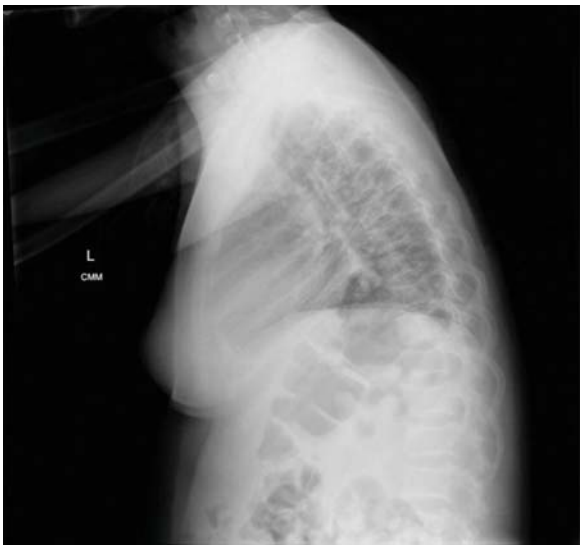

27. A few months later, the same patient described in Question 26 presents with fever, chest pain, and cough. A radiograph obtained on the patient is shown below.

Given the patient's clinical history, which of the following would be the most likely treatment for the patient's symptoms?
A. Oral outpatient antibiotic therapy
B. No treatment is necessary
C. Antiviral therapy
D. Hydration, transfusion, supplemental oxygen, and analgesia on an inpatient basis

28. Which of the following additional tests would be of most benefit to the patient described in Questions 27 and 28?
A. Transcranial Doppler
B. I-123 MIBG scan
C. Barium enema
D. Voiding cystourethrogram (VCUG)

29. Regarding the imaging evaluation of juvenile idiopathic arthritis (JIA) in children, which of the following is true?
A. There are well-established imaging protocols to evaluate JIA.
B. Radiographs are a good modality for evaluating synovitis.
C. MR imaging has been shown to detect approximately twice as many erosions as radiographs or ultrasound.
D. Temporomandibular joints are only affected in one of the subtypes of JIA.

30. Regarding Langerhans cell histiocytosis (LCH), which of the following is true?
A. Vertebra plana is pathognomonic of this condition.
B. The liver is involved in a majority of cases.
C. The most common manifestation of LCH in the central nervous system is diabetes insipidus.
D. The multifocal multisystem form is the most common subtype.

Multisystem Radiology: Answers and Explanations

1 Answer A. There is an enhancing mass at the optic pathway and hypothalamic region consistent with glioma. There is also an enhancing exophytic mass arising from the right dorsolateral aspect of the medulla also consistent with glioma. Neurofibromatosis (NF) type 1 (NF1) is a disease characterized by the growth of noncancerous tumors called neurofibromas. These are located on or just underneath the skin, as well as in the brain and peripheral nervous system. They may also form in other body parts, including the eye and orbit.

Ophthalmologic manifestations of NF-1 include the following:

- Lisch nodules
- Plexiform neurofibromas
- Choroid hamartomas
- Retinal tumors
- Optic nerve gliomas
- Prominent corneal nerves

An estimated 15% to 40% of children with NF1 have optic nerve glioma or visual pathway gliomas involving the optic nerve, chiasm, or optic tract. Some of these lesions are asymptomatic. Bilateral optic nerve gliomas are almost pathognomonic for NF1. Optic nerve gliomas are locally invasive and slow growing with low malignant potential. However, chiasmatic gliomas may invade the hypothalamus and third ventricle, causing obstructive hydrocephalus.

Reference: Listernick R, Charrow J, Greenwald MJ, Esterly NB. Optic gliomas in children with neurofibromatosis type 1. *J Pediatr* 1989;114(5):788–792.

2 Answer B. Café au lait spot. Flat pigmented lesions of the skin called café au lait spots are hyperpigmented lesions that may vary in color from light brown to dark brown; this is reflected by the name of the condition, which means “coffee with milk.” The borders may be smooth or irregular. These spots can grow from birth and can continue to grow throughout the person's lifetime. Having six or more café au lait spots > 5 mm in diameter before puberty, or > 15 mm in diameter after puberty, is a diagnostic feature of neurofibromatosis type I, but other features are required to diagnose NF-1.

A port-wine stain (nevus flammeus), also commonly called a firemark, is almost always a birthmark; in rare cases, it can develop in early childhood. It is caused by a vascular anomaly (a capillary malformation in the skin). Port-wine stains are named for their coloration, which is similar in color to port-wine, a fortified red wine from Portugal. Port-wine stains may be part of a syndrome such as Sturge-Weber syndrome or Klippel-Trénaunay-Weber syndrome.

Facial angiofibromas (adenoma sebaceum) is a rash of reddish spots or bumps, which appears on the nose and cheeks in a butterfly distribution. They consist of blood vessels and fibrous tissue. Facial angiofibromas are one of the classic dermatological findings of tuberous sclerosis.

Ataxia telangiectasia can cause features of early aging such as premature graying of the hair. It can also cause vitiligo (an autoimmune disease causing loss of skin pigment resulting in a blotchy “bleach-splashed” look) and warts, which can be extensive and recalcitrant to treatment.

References: Crino PB, Nathanson KL, Henske EP. The tuberous sclerosis complex. *N Engl J Med* 2006;355(13):1345–1356.
Nowak CB. The phakomatoses: dermatologic clues to neurologic anomalies. *Semin Pediatr Neurol* 2007;14(3):140–149.

3 **Answer C.** CT demonstrates pial and leptomeningeal vascular calcifications with a small left cerebral hemisphere and distortion of the left lateral ventricle. MRI redemonstrates postsurgical changes of left-sided craniotomy and hemispherectomy. There is left cerebral atrophy and gyriform susceptibility along the residual left cerebral hemisphere. Sturge-Weber syndrome, or encephalotrigeminal angiomatosis, is a phakomatosis characterized by facial port-wine stains and pial angiomas. The diagnosis is usually suspected with the presence of congenital facial cutaneous hemangioma (also known as port-wine stain or facial nevus flammeus). This feature is almost always present and usually involves the ophthalmic division (V1) of the trigeminal nerve. If the V1 territory of the trigeminal nerve is not involved, Sturge-Weber syndrome is unlikely.

The differential is a combination of that for multiple intracranial calcifications, cerebral hemiatrophy, and leptomeningeal enhancement, and therefore includes the following:

- Cerebral arteriovenous malformation (AVM)
- Infection (including TORCH infection)
- Neurocysticercosis
- PHACE syndrome
- Healed cortical infarct
- Radiotherapy
- Gobbi syndrome

References: Comi AM. Update on Sturge-Weber syndrome: diagnosis, treatment, quantitative measures, and controversies. *Lymphat Res Biol* 2007;5(4):257–264.
Griffiths PD. Sturge-Weber syndrome revisited: the role of neuroradiology. *Neuropediatrics* 1996;27(06):284–294.

4 **Answer A.** Port-wine stain. A port-wine stain (nevus flammeus), also commonly called a firemark, is almost always a birthmark; in rare cases, it can develop in early childhood. It is caused by a vascular anomaly (a capillary malformation in the skin). Port-wine stains are named for their coloration, which is similar in color to port-wine, a fortified red wine from Portugal. Port-wine stains may be part of a syndrome such as Sturge-Weber syndrome or Klippel-Trénaunay-Weber syndrome.
Flat pigmented lesions of the skin called café au lait spots are hyperpigmented lesions that may vary in color from light brown to dark brown; this is reflected by the name of the condition, which means "coffee with milk." The borders may be smooth or irregular. These spots can grow from birth and can continue to grow throughout the person's lifetime. Having six or more café au lait spots > 5 mm in diameter before puberty, or > 15 mm in diameter after puberty, is a diagnostic feature of neurofibromatosis type I, but other features are required to diagnose NF-1.
Facial angiofibromas (adenoma sebaceum) is a rash of reddish spots or bumps, which appears on the nose and cheeks in a butterfly distribution. They consist of blood vessels and fibrous tissue. Facial angiofibromas are one of the classic dermatological findings of tuberous sclerosis.
Ataxia telangiectasia can cause features of early aging such as premature graying of the hair. It can also cause vitiligo (an autoimmune disease causing loss of skin pigment resulting in a blotchy “bleach-splashed” look) and warts, which can be extensive and recalcitrant to treatment.
References: Crino PB, Nathanson KL, Henske EP. The tuberous sclerosis complex. *N Engl J Med* 2006;355(13):1345–1356.
Nowak CB. The phakomatoses: dermatologic clues to neurologic anomalies. *Semin Pediatr Neurol* 2007;14(3):140–149.

5 Answer D. The abdominal radiograph demonstrates two lucent regions in the upper abdomen (double bubble) consistent with duodenal atresia in the setting of trisomy 21. The two bubbles represent the stomach lumen and the duodenal bulb, respectively. Down syndrome (or trisomy 21) is the most common trisomy and also the commonest chromosomal disorder. It is a major cause of intellectual disability and also has numerous multisystem manifestations.

Antenatal "soft markers" for aneuploidy include

- Nuchal fold thickness >6 mm
- Hypoplastic nasal bone
- Echogenic intracardiac focus
- Echogenic bowel
- Shortened humerus
- Shortened femur
- Single umbilical artery
- Renal pyelectasis

Structural abnormalities include

- Cardiac
  - Atrioventricular septal defect (AVSD)
- Abdominal
  - Duodenal atresia
  - Esophageal atresia
- Central nervous system
  - Ventriculomegaly
- Craniofacial/calvarial
  - Short maxilla
  - Mild brachycephaly

Reference: Smith-Bindman R, Hosmer W, Feldstein VA, et al. Second-trimester ultrasound to detect fetuses with Down syndrome: a meta-analysis. *JAMA* 2001;285(8):1044–1055.

6 Answer C. Trisomy 21. Aneuploidy refers to an abnormal number of chromosomes and is a type of chromosomal abnormality. There are large number potential aneuploidic anomalies. The most common three aneuploidies encountered in the obstetric and pediatric population include trisomy 21 (most common), trisomy 18, and trisomy 13. The double bubble demonstrated on the abdominal radiograph is most consistent with duodenal atresia in the setting of trisomy 21. Trisomy 13 also called Patau syndrome presents with heart defect, brain or spinal cord abnormalities, microphthalmia, polydactyly, cleft lip/palate, and hypotonia. Trisomy 18 also called Edwards syndrome present with intrauterine growth restriction, low birth weight, heart defects, abnormal head shape, micrognathia, and clenched fists with overlapping fingers. Trisomy 23 is also known as XXY male syndrome, and Klinefelter syndrome is associated with male infertility, gynecomastia, small testes, and reduced facial and body hair.

Reference: Estroff JA. Imaging clues in the prenatal diagnosis of syndromes and aneuploidy. *Pediatr Radiol* 2012;42(Suppl 1):5–23. https://doi.org/10.1007/s00247-011-2264-3

7 Answer B. There is bilateral microphthalmia and retro-ocular cyst-like structures consistent with coloboma. The bilateral olfactory apparatus are absent. CHARGE syndrome is an acronym that classically describes a combination of head and neck, cardiac, CNS, and genitourinary disorders:
C: Coloboma
H: Heart defects (congenital heart disease)
A: Atresia (choanal)
R: Retardation (mental)
G: Genital hypoplasia
E: Ear abnormalities/deafness
Coloboma is collective term encompassing any focal discontinuity in the structure of the eye. Colobomas are due to failure of closure of the choroidal fissure posteriorly. Typically, colobomas are bilateral, small and are not accompanied by other deeper abnormalities. It occurs along the inferomedial aspect of the globe and optic nerve. On CT or MRI, the affected globe is usually small with

a focal posterior defect in the globe with vitreous herniation. A retrobulbar fluid-density cyst may be present.

References: Simmons JD, LaMasters D, Char D. Computed tomography of ocular colobomas. *AJR Am J Roentgenol* 1983;141(6):1223–1226.
Tellier AL, Cormier-daire V, Abadie V, et al. CHARGE syndrome: report of 47 cases and review. *Am J Med Genet* 1998;76(5):402–409.

8 Answer B. CTA of the chest demonstrates a dilated aortic root/ascending aorta measuring up to 3.6 cm at the sinuses of Valsalva. Marfan syndrome is a multisystem connective tissue disease with autosomal dominant inheritance of defect in fibrillin 1 gene. The affected patients are tall with long disproportionate extremities, have pectus excavatum and arachnodactyly, and may also experience upward and lateral optic lens dislocation. Cardiovascular disease is common, particularly aortic root dilatation and dissection, which is the most common cause of sudden death in these patients. Cardiovascular complications are predominantly due to cystic medial necrosis of the vessels and are the most frequent cause of death. Aortic root dilatation and myxomatous degeneration of the mitral valve resulting in mitral valve regurgitation are the most two common cardiac manifestations. Among the total number of patients with root aneurysms, those with a diagnosis of Marfan syndrome dominate the younger age range but they are nevertheless a minority of all patients with ascending aortic aneurysm. They are prone to acute dissection, and prior to the introduction of prophylactic root replacement, this was the cause of death in two-thirds of all patients and often at a young age.

References: Ha HI, Seo JB, Lee SH, et al. Imaging of Marfan syndrome: multisystemic manifestations. *Radiographics* 2007;27(4):989–1004.
Treasure T, Takkenberg JJM, Pepper J. Surgical management of aortic root disease in Marfan syndrome and other congenital disorders associated with aortic root aneurysms. *Heart* 2014;100(20):1571–1576. doi:10.1136/heartjnl-2013-305132.

9 Answer C. 45 mm. Current guidelines for the management of valvular heart disease state that irrespective of the presence and severity of aortic valve regurgitation, surgery should be considered in patients with Marfan syndrome with risk factors (family history of dissection, size increase 2 mm/year in repeated examinations) who have aortic root disease with a maximum ascending aortic diameter of ≥45 mm.

Reference: Treasure T, Takkenberg JJ, Pepper J. Surgical management of aortic root disease in Marfan syndrome and other congenital disorders associated with aortic root aneurysms. *Heart* 2014;100(20)1571–1576. doi:10.1136/heartjnl-2013-305132.

10 Answer D. US demonstrates a mixed solid–cystic mass in the upper left kidney. MRI demonstrates an enlarged left kidney containing a collection of multiple cysts within the medulla of the upper pole, as well as multiple peripheral subcortical cysts. Left nephrectomy was performed, and pathology demonstrated a focus of Wilms tumor present in a background of nephroblastomatosis. Beckwith-Wiedemann syndrome (BWS) is a congenital overgrowth disorder. The syndrome is characterized by omphalocele, macroglossia, gigantism, neonatal hypoglycemia, hemihypertrophy, hepatosplenomegaly, nephromegaly, cardiac anomalies, adrenal cytomegaly, pancreatic islet cell hyperplasia, facial nevus flammeus, and ear lobe creases. There is a high risk (about 10%) of development of embryonal neoplasms, particularly Wilms tumor in the child with BWS, especially those with hemihypertrophy.

References: Andrews MW, Amparo EG. Wilms' tumor in a patient with Beckwith-Wiedemann syndrome: onset detected with 3-month serial sonography. *AJR Am J Roentgenol* 1993;160(1):139–140.
Choyke PL, Siegel MJ, Oz O, et al. Nonmalignant renal disease in pediatric patients with Beckwith-Wiedemann syndrome. *AJR Am J Roentgenol* 1998;171(3):733–737.

11 Answer C. Denys-Drash syndrome. The WT1-related Wilms tumor (WT) syndromes are a group of hereditary disorders caused by alterations in a gene known as WT1. This group of disorders includes:

- WAGR (Wilms tumor–aniridia–genitourinary malformation–retardation) syndrome
- Denys-Drash syndrome (DDS)
- Frasier syndrome (FS)
- Genitourinary anomalies (abnormalities of the reproductive and urinary systems) syndrome

Patients with Denys-Drash syndrome may develop the following clinical features:

- Higher risk of developing Wilms tumor (the risk is estimated to be more than 90%)
- Abnormal or undermasculinized reproductive organs in boys
- Normal or abnormal female reproductive organs
- Higher risk of developing gonadoblastoma (a tumor of the developing reproductive organs, including the ovaries and testes)
- End-stage renal (kidney) disease: patients may develop renal failure, often in association with a condition known as diffuse mesangial sclerosis

In addition to the WT1-related Wilms tumor syndromes, there are a number of other genetic conditions associated with the development of WT. Some of these conditions include the following:

- Beckwith-Wiedemann syndrome
- Li-Fraumeni syndrome
- Neurofibromatosis type 1
- Sotos syndrome
- Fanconi anemia syndrome
- Bloom syndrome
- Simpson-Golabi-Behmel syndrome
- Perlman syndrome
- Trisomy 18

Patients with these conditions have a greater risk of developing a malignant tumor of the kidney known as Wilms tumor (WT) or nephroblastoma. Wilms tumor is the most common type of kidney cancer affecting children. Very rarely, WT can occur in adults.

Reference: Lowe LH, Isuani BH, Heller RM, et al. Pediatric renal masses: Wilms tumor and beyond. *Radiographics* 2000;20(6):1585–1603.

12 **Answer B.** US demonstrates an echogenic soft tissue mass at the posterior neck. MR was performed to assess for pulmonary lymphangiectasia in the setting of genetically proven Turner syndrome. The cystic hygroma is demonstrated (white arrows).

Cystic hygromas can occur as an isolated finding or in association with other birth defect as part of a syndrome. They result from environmental factors, genetic factors, or unknown factors.

Environmental causes for cystic hygroma include:

- Maternal viral infections, such as parvovirus of fifth disease
- Maternal substance abuse, such as abuse of alcohol

Genetic syndromes with cystic hygroma as a clinical feature:

- The majority of prenatally diagnosed cystic hygromas are associated with Turner syndrome, also referred to as 45X, which is the most common of sex chromosome abnormalities in females.
- Chromosome abnormalities such as trisomies 13, 18, and 21
- Noonan syndrome

The pattern of inheritance for these syndromes varies depending upon the specific syndrome. Isolated cystic hygroma can be inherited as an autosomal recessive disorder for which parents are "silent" carriers. Finally, a cystic hygroma can occur from an unknown cause.

Other imaging findings in Turner syndrome include:

- Increased nuchal thickness
- Increased nuchal translucency
- Coarctation of the aorta
- Bicuspid aortic valve
- Horseshoe kidney/pelvic kidney
- IUGR
- Hydrops fetalis
- Short fetal limbs

Reference: Chen C-P, Chien S-C. Prenatal sonographic features of Turner syndrome. *J Med Ultrasound* 2007;15:251–257.

13 **Answer B.** 11 to 13 weeks. A nuchal translucency scan (also called first trimester of pregnancy screening) is carried out during weeks 11 to 13 of a pregnancy. The scan uses ultrasound to screen for Down syndrome or other chromosomal or inherited conditions in the fetus. Other nonchromosomal conditions, such as neural tube defects, abdominal wall defects, limb abnormalities, and some congenital heart disease, can also be detected at this stage of the pregnancy.
Screening can determine the likelihood of risk of an abnormality but does not diagnose the condition. If screening does identify a possible risk, it does not necessarily mean there is an abnormality present but does mean that further testing is necessary. A nuchal translucency scan is combined with the mother's age and results of a blood test showing the mother's pregnancy hormone levels to provide a "combined risk."

Without the blood test, screening is 75% accurate for predicting Down syndrome. With the blood test, the accuracy increases to 85%. Women who return a high-risk result from the screening will be offered formal genetic testing using other procedures, such as amniocentesis or chorion villus sampling (CVS).
Reference: ACOG Committee on Practice Bulletins. ACOG Practice Bulletin No. 77: screening for fetal chromosomal abnormalities. *Obstetr Gynecol* 2007;109(1):217–227.

14 **Answer C.** The right and left glenohumeral joints appear subluxed or dislocated. This patient with known Ehlers-Danlos syndrome (EDS) belongs to a group of collagen disorders or hereditary connective tissue disease. There are at least 10 subtypes with variable inheritance patterns. The majority are autosomal dominant. EDS clinically manifests by skin hyperelasticity and fragility, joint hypermobility, and blood vessel fragility with bleeding diathesis. Skeletal findings include hemarthrosis (especially knees), recurrent joint dislocation including spontaneous dislocation of the temporomandibular joint, precocious osteoarthritis, kyphoscoliosis, and spondylolisthesis.
Reference: Ayres JG, Pope FM, Reidy JF, et al. Abnormalities of the lungs and thoracic cage in the Ehlers-Danlos syndrome. *Thorax* 1985;40(4):300–305.

15 **Answer B.** Autosomal dominant.

16 **Answer B.** This patient was treated for tetralogy of Fallot, major aortopulmonary collateral arteries, and hypoplastic pulmonary arteries. A right ventricular outflow track transjugular patch was placed in addition to patch closure of an ASD and VSD. The 22q11.2 deletion syndrome, also known as the DiGeorge syndrome (DGS) or velocardiofacial syndrome, is a syndrome where a small portion of the chromosome 22 is lost and results in a variable but a recognizable pattern of physical and behavioral features. The classic triad of features of DGS on presentation is conotruncal cardiac anomalies, hypoplastic thymus, and hypocalcemia.

The most common cardiac defects account for two-thirds of the cardiac anomalies seen in patients with DGS and include the following:

- Interrupted aortic arch
- Truncus arteriosus
- Tetralogy of Fallot
- Atrial or ventricular septal defects (ASDs, VSDs)
- Vascular rings

References: Alikaşifoğlu M, Malkoç N, Ceviz N, et al. Microdeletion of 22q11 (CATCH 22) in children with conotruncal heart defect and extracardiac malformations. *Turk J Pediatr* 2000;42(3):215–218.
McDonald-McGinn DM, Sullivan KE. Chromosome 22q11.2 deletion syndrome (DiGeorge syndrome/velocardiofacial syndrome). *Medicine (Baltimore)* 2011;90:1–18.

17 **Answer D.** Chromosome 22 deletion.

18 Answer A. MRI demonstrates an extensive venous vascular malformation of the right lower extremity, which extends from the level of the groin to the distal tibiotalar joint and involves both the subcutaneous and intramuscular compartments. Klippel-Trenaunay syndrome (KTS) is a complex congenital disorder characterized by the classic triad of capillary malformation, venous malformation, and limb overgrowth, with or without lymphatic malformation. In KTS, the persistence of embryonic avalvular venous structures, most notably the lateral vein of the thigh (lateral marginal vein of Servelle) and sciatic vein, can result in dilated tortuous varicosities, with superficial ones being more often located over the anterolateral thigh and leg.
MRI with and without gadolinium contrast is the imaging study of choice to define the nature and extent of vascular anomalies in patients with KTS. MRI provides the highest diagnostic accuracy in the evaluation of the underlying venous and lymphatic abnormalities, as well as soft tissue and bony overgrowth. Venous malformations show uniform enhancement, whereas lymphatic malformations demonstrate rim or septal enhancement of cyst walls. Fluid–fluid levels and high T2 signal intensity are characteristic of lymphatic malformations. The presence of phleboliths as signal voids is characteristic of venous malformations.

Hemihypertrophy or hemihyperplasia describes an asymmetry in size between the right and left side of the body. This can arise sporadically as isolated hemihypertrophy or it can arise as part of a syndrome:

- Beckwith-Wiedemann syndrome
- Proteus syndrome
- Klippel-Trénaunay syndrome
- Neurofibromatosis type 1
- Hemihyperplasia-multiple lipomatosis (HHML)
- McCune-Albright syndrome
- Langer-Giedion syndrome

Beckwith-Wiedemann syndrome (BWS) is a congenital overgrowth disorder characterized by:

- Macroglossia (most common clinical finding)
- Otic dysplasia
- Omphalocele
- Localized gigantism/macrosomia
- Hemihypertrophy
- Cardiac anomalies
- Pancreatic islet cell hyperplasia
- Organomegaly
  - Nephromegaly
  - Hepatosplenomegaly

Maffucci syndrome is a congenital nonhereditary mesodermal dysplasia characterized by multiple enchondromas with soft tissue venous malformations (hemangiomas). On imaging, it is usually portrayed by a short limb with metaphyseal distortions because of multiple enchondromas, which may appear grotesque, and soft tissue masses with phleboliths depicting hemangiomas.

References: Flors L, et al. MR imaging of soft-tissue vascular malformations: diagnosis, classification, and therapy follow-up. *Radiographics* 2011;31:1321–1340; discussion: 1340–1341.
Roebuck DJ, Howlett DC, Frazer CK, et al. Pictorial review: the imaging features of lower limb Klippel-Trenaunay syndrome. *Clin Radiol* 1994;49(5):346–350.

19 **Answer D.** PET imaging demonstrates diffusely increased FDG uptake identified within the spleen, which is enlarged in size concerning for lymphomatous involvement. Multiple enlarged mesenteric and retroperitoneal lymph nodes are also present and demonstrate increased FDG uptake.
Posttransplant lymphoproliferative disorders (PTLD) are lymphoid and/or plasmacytic proliferations that occur in the setting of solid organ or allogeneic hematopoietic cell transplantation as a result of immunosuppression. They are among the most serious and potentially fatal complications of transplantation. While the majority appear to be related to the presence of Epstein-Barr virus (EBV), EBV-negative disease does occur.
The range of appearances is large due to the number of possible sites. In general, extranodal involvement is three to four times more common than is nodal involvement and resembles primary lymphoma of those organs:

- Solid organs (liver, spleen, kidney)
  - Nodules or diffuse infiltration
- Bowel
  - Circumferential wall thickening
  - Aneurysmal dilatation
  - Ulceration/perforation
- Lung
  - Nodules or diffuse infiltration
- Brain
- Nodes
  - Nonspecific nodal enlargement, similar to other lymphomas
  - Most commonly affecting mediastinum (either lymphadenopathy or anterior mediastinal mass) or retroperitoneum (either as lymphadenopathy or mass)

References: Pickhardt PJ, Siegel MJ, Hayashi RJ, et al. Posttransplantation lymphoproliferative disorder in children: clinical, histopathologic, and imaging features. *Radiology* 2000;217(1):16–25.
Meador TL, Krebs TL, Cheong JJ, et al. Imaging features of posttransplantation lymphoproliferative disorder in pancreas transplant recipients. *AJR Am J Roentgenol* 2000;174(1):121–124.

20 **Answer A.** Left hand radiograph demonstrates polydactyly of the first digit. MRI of the abdomen demonstrates bilateral dysplastic kidneys with multiple cysts, hydronephrosis, and an ectopically located left kidney. Spine radiograph and MRI demonstrate segmentation and fusion anomalies in the upper lumbar spine with associated kyphosis.
VACTERL is an acronym that describes a nonrandom constellation of congenital anomalies. It is not a true syndrome as such and is equivalent to the VATER anomaly.
The acronym VACTERL derives from the following:

V: Vertebral anomalies

- Hemivertebrae
- Congenital scoliosis
- Caudal regression
- Spina bifida

A: Anorectal anomalies

- Anal atresia

C: Cardiac anomalies; cleft lip

TE: Tracheoesophageal fistula +/− esophageal atresia

R: Renal anomalies; radial ray anomalies

L: Limb anomalies

- Polydactyly
- Oligodactyly

At least three of the above features (in each category) are considered necessary for the diagnosis of this condition.

Reference: Solomon BD, et al. An approach to the identification of anomalies and etiologies in neonates with identified or suspected VACTERL (vertebral defects, anal atresia, tracheo-esophageal fistula with esophageal atresia, cardiac anomalies, renal anomalies, and limb anomalies) association. *J Pediatr* 2014;164:451–457.e1.

21 Answer D. The coronal image (A) from the patient's CT scan demonstrates interval development of marked ventriculomegaly when compared to the patient's prior MR (B) when the ventricles were not dilated. In addition, there is a small amount of low attenuation in the periventricular white matter surrounding the superior aspect of the right lateral ventricle compatible with transependymal flow of CSF. A high-attenuation structure is seen coursing through the right ventricle, which represents a portion of a shunt catheter. Therefore, these findings raise the concern for shunt malfunction.
Conventional radiography is primarily performed to evaluate for breaks in the shunt, shunt disconnections, or distal catheter migration of the shunt. A typical shunt series includes frontal and lateral radiographs of the head and neck and frontal radiographs of the chest and abdomen and is indicated given the patient's history. The purpose of the shunt series is to image the entire course of the shunt.
Nonaccidental trauma (NAT) can manifest with subdural hematomas. However, there is no evidence of subdural hematomas on the images nor is there anything in the history to suggest the possibility of nonaccidental trauma. Therefore, a skeletal survey consisting of plain radiographs of the axial and appendicular skeleton is not indicated.
The most important clinical application of whole-body MR imaging in children, as in adults, is the staging of malignant disease and screening for metastatic spread. However, the use of whole-body MR imaging to evaluate other multisystem disease processes such as chronic recurrent multifocal osteomyelitis is increasing. Nevertheless, a whole-body MR exam is not indicated in this setting.

References: Chavhan GB, Babyn PS. Whole-body MR imaging in children: principles, technique, current applications, and future directions. *Radiographics* 2011;31(6):1757–1772.
Donnelly LF. *Pediatric imaging the fundamentals*. Philadelphia, PA: Elsevier/Saunders, 2009.
Ho ML, Rojas R, Eisenberg RL. Cerebral edema. *Am J Roentgenol* 2012;199(3):W258–W273.
Lonergan GJ, Baker AM, Morey MK, et al. From the archives of the AFIP. Child abuse: radiologic-pathologic correlation. *Radiographics* 2003;23(4):811–845.
Wallace AN, McConathy J, Menias CO, et al. Imaging evaluation of CSF shunts. *Am J Roentgenol* 2014;202(1):38–53.

22 Answer C. The image provided from an ultrasound exam surrounding the tip of the VP shunt demonstrates a well-circumscribed anechoic cystic lesion with internal septations (Image B). In a patient with suspected shunt malfunction, the findings are most consistent with a CSF pseudocyst. In addition, the septated nature of the pseudocyst indicates the lesion may be infected.
Pseudocyst formation is a common cause of distal VP shunt catheter obstruction. Pseudocysts are loculated collections of CSF that form around the terminal end of the catheter. In patients with ventriculoperitoneal shunts, pseudocysts are caused by peritoneal adhesions or migration of the greater omentum over the shunt tip. Pseudocysts can also develop around ventriculopleural shunts because of adhesions caused by chronic pleural irritation. Conventional radiography may show coiling of the distal catheter within an intra-abdominal soft tissue mass or loculated pleural effusion.

Definitive diagnosis can be made by CT or ultrasound showing a loculated fluid collection surrounding the catheter tip. The time from the last shunting procedure to the development of an abdominal pseudocyst ranges from 3 weeks to 5 years and is usually not within the first week.
CSF pseudocysts can sometimes be differentiated from ascites by their characteristic displacement of the bowel gas pattern on abdominal films and by the absence of shifting dullness. Although sonography and CT can accurately localize abdominal fluid collections, differentiation of ascites from pseudocysts sometimes may not be possible. Therefore, fine needle aspiration of the localized CSF collections under sonographic or CT guidance should be performed to increase the diagnostic yield.
If infection is present, the pseudocyst wall should be excised and the peritoneal shunting catheter removed. The formation of a CSF pseudocyst is a poor prognostic sign for the usefulness of the peritoneal cavity for shunting but previous abdominal pseudocyst formation and peritonitis are not contraindications to subsequent peritoneal shunting. However, in some reported cases, the CSF had to be diverted to other cavities because of either recurrence of the cysts or failure of the peritoneum to absorb fluid. Culture of the tip of the peritoneal catheter was reported to be more sensitive than culture of the CSF.
References: Chung JJ, Yu JS, Kim JH, et al. Intraabdominal complications secondary to ventriculoperitoneal shunts: CT findings and review of the literature. *Am J Roentgenol* 2009;193(5):1311–1317.
Wallace AN, McConathy J, Menias CO, et al. Imaging evaluation of CSF shunts. *Am J Roentgenol* 2014;202(1):38–53.

23 **Answer C.** Interstitial, or hydrocephalic edema, occurs in the setting of increased intraventricular pressures, which cause rupture of the ventricular ependymal lining. This allows transependymal migration of CSF into the extracellular space, most commonly the periventricular white matter. Fluid composition is identical to CSF. Various causes of interstitial edema include obstructing masses, meningitis, subarachnoid hemorrhage, and normal pressure hydrocephalus. In contrast, ependymitis granularis refers to small triangular areas of abnormal signal around the anterolateral frontal horns. This normal anatomic variant results from regionally decreased myelin, increased extracellular fluid, or focal breakdown of the ependymal lining with gliosis. On CT, the combination of ventriculomegaly and increased periventricular hypodensity is suggestive of the diagnosis of interstitial edema. MRI is a more sensitive imaging modality for the detection of transependymal flow of CSF, showing hypointensity on T1-weighted imaging and periventricular hyperintensity on T2-weighted imaging/FLAIR.
In symptomatic patients, decompression with resection of the obstructing lesion (noncommunicating hydrocephalus) or ventriculostomy catheter placement (communicating hydrocephalus) allows normalization of ventricular pressures. In turn, this enables normal antegrade resorption of interstitial fluid across the ependymal lining and back into the ventricular system. Without intervention, the findings ultimately progress to cerebral atrophy and gliosis.
Reference: Ho ML, Rojas R, Eisenberg RL. Cerebral edema. *Am J Roentgenol* 2012;199(3): W258–W273.

24 **Answer A.** Flattening of the posterior globes reflects the transmission of elevated perioptic CSF pressure on the compressible posterior sclera. Studies have found it to be one of the most specific indicators of increased intracranial pressure. Low cerebellar tonsils is a finding seen with intracranial hypotension. An empty sella can be seen with increased intracranial pressure but is nonspecific and not the most common finding. Chronically shunted patients with stiff ventricles may not show significant change in ventricular size.
References: Brodsky MC, Vaphiades M. Magnetic resonance imaging in pseudotumor cerebri. *Ophthalmology* 1998;105(9):1686–1693.
Passi N, Degnan AJ, Levy LM. MR imaging of papilledema and visual pathways: effects of increased intracranial pressure and pathophysiologic mechanisms. *Am J Neuroradiol* 2013;34(5):919–924.

25 Answer C. The temporal horns of the lateral ventricles dilate sooner than the frontal horns, which may be because they are less resistant to pressure or because of CSF flow dynamics. Papilledema occurs with increased intracranial pressure and is not always present in hydrocephalus. Sutural splaying only occurs with unfused sutures. Venous expansion occurs with intracranial hypotension.

References: Heinz ER, Ward A, Drayer BP, et al. Distinction between obstructive and atrophic dilatation of ventricles in children. *J Comput Assist Tomogr* 1980;4(3):320–325.
Hosoya T, Yamaguchi K, Adachi M, et al. Dilatation of the temporal horn in subarachnoid haemorrhage. *Neuroradiology* 1992;34(3):207–209.
Naidich TP, Epstein F, Lin JP, et al. Evaluation of pediatric hydrocephalus by computed tomography. *Radiology* 1976;119:337–345.

26 Answer C. The frontal radiograph demonstrates a cholecystectomy clip in the right upper quadrant and absence of a splenic shadow in the left upper quadrant. The lateral radiograph demonstrates multiple vertebral endplate anomalies in a "Lincoln log" configuration. This constellation of findings are often found in sickle cell disease.

Sickle cell anemia (SCA) is a hemolytic anemia characterized by abnormally shaped (sickled) red blood cells (RBCs), which are removed from the circulation and destroyed at increased rates, leading to anemia. Of greater clinical importance, the sickled RBCs cause vascular occlusion, which leads to tissue ischemia and infarction.

The spleen possesses a slow, tortuous microcirculation that renders it susceptible to congestion, sludging, and polymerization. The end result of this process is splenic infarction, which progresses over time to functional autosplenectomy. The infarcted spleen is replaced by fibrosis, with calcium and hemosiderin deposition. By 5 years of age, 94% of patients with SCA are asplenic, which is likely the case with this patient.

Cholelithiasis is one of the common complications of SCA. The treatment of cholelithiasis in patients with SCA is cholecystectomy. Gallstones are usually pigment stones that result from chronic hemolysis leading to increased bilirubin production. A frequency ranging from 5% to 55% has been reported, but an overall 70% of patients with SCA will develop gallstones at one stage of their life.

In the spine, infarction may appear as a central, square-shaped endplate depression, resulting from microvascular endplate occlusion and subsequent overgrowth of the surrounding portions of the endplate. This appearance is seen in approximately 10% of patients, but it is essentially pathognomonic for SCA and has been called the Lincoln log or H-shaped vertebra deformity.

Neurofibromatosis I, von-Hippel-Lindau disease, and tuberous sclerosis do not typically affect the gallbladder and spleen. In addition, Lincoln log vertebral bodies are not seen in these conditions.

References: Fortman BJ, Kuszyk BS, Urban BA, et al. Neurofibromatosis type 1: a diagnostic mimicker at CT. *Radiographics* 2001;21(3):601–612.
Leung RS, Biswas SV, Duncan M, et al. Imaging features of von Hippel-Lindau disease. *Radiographics* 2008;28(1):65–79.
Lonergan GJ, Cline DB, Abbondanzo SL. Sickle cell anemia. *Radiographics* 2001;21(4):971–994.
Umeoka S, Koyama T, Miki Y, et al. Pictorial review of tuberous sclerosis in various organs. *Radiographics* 2008;28(7):e32.

27 Answer D. The new chest radiograph demonstrates bibasilar opacities. The opacity on the right looks like an infiltrate, although it is difficult to tell whether the opacity at the left base is atelectasis or an infiltrate. These findings are not typical of a viral etiology, which usually presents with hyperinflation and peribronchial thickening. In a patient with these findings and the given clinical history, acute chest syndrome (ACS) must be suspected.

Acute chest syndrome (ACS) describes an acute pulmonary illness, characterized by a new pulmonary consolidation and some combination of fever, chest pain, and signs of pulmonary compromise such as cough, dyspnea, and tachypnea. The cause of ACS is not fully understood, and there have been many causative agents identified, including infection and fat emboli; frequently, the underlying cause is not discovered in individual patients. ACS may progress to acute respiratory distress syndrome and death.

The severity of the clinical symptoms distinguishes ACS from the clinically milder pneumonia. Because ACS may be caused by pneumonia, the two entities may constitute a continuum.
ACS is the second leading cause of hospitalization in patients with SCA, after painful crises. It accounts for 25% of deaths in patients with SCA and is currently the single leading cause of death in SCA. Children with sickle cell are more prone than adults to develop ACS (50% of all children with sickle cell disease will experience at least one episode of ACS), but adults with sickle cell have a higher mortality rate (4.3%) than do children.
The radiographic finding necessary for the diagnosis of ACS is a single area or multiple areas of pulmonary consolidation. However, 30% to 60% of patients have no initial radiographic abnormality, often because they are admitted for another reason (usually for pain crises), and subsequently develop ACS. Abnormal chest radiographs show middle and lower lobe airspace disease more commonly than upper lobe disease. Pleural effusions are frequent and do not help differentiate infectious from noninfectious causes of ACS. The majority (70%) of patients with ACS are hypoxic (oxygen saturation <90%, as measured by pulse oximetry).
Treatment consists of hydration, transfusion, supplemental oxygen, and analgesia. Incentive inspirometry to improve atelectasis, antibiotic therapy for suspected infection, and steroids may also be used. Mechanical ventilation was needed in 13% of patients in one study. In severe cases, extracorporeal membrane oxygenation (ECMO) has been used successfully. The mean hospital stay is 7 days for adults and 4 days for children.
References: Donnelly LF. *Pediatric imaging the fundamentals*. Philadelphia, PA: Elsevier/Saunders, 2009.
Lonergan GJ, Cline DB, Abbondanzo SL. Sickle cell anemia. *Radiographics* 2001;21(4):971–994.

28 Answer A. Stroke, atrophy, and cognitive impairment are major consequences of sickle cell anemia (SCA). Approximately 25% of all patients with SCA will have a neurologic complication over their lifetime; 11% of these complications will occur by age 20 years. Many children experience "silent infarction" (defined as absence of clinical symptoms with MR imaging findings of infarct). Silent infarction is twice as common as clinical infarction and may occur in up to 22% of children by 12 years of age.
Because of the considerable lifelong cognitive and functional impairments that result from stroke, efforts have been directed toward identifying patients at risk for stroke to institute preventive therapy. Transcranial Doppler ultrasonography (US) has emerged as a valuable tool for assessing large cerebral artery flow dynamics. Studies show that elevated velocities in the distal internal carotid artery and proximal middle cerebral artery correlate with an increased risk of stroke. Increased velocity in these vessels has been shown to correlate with areas of MR imaging abnormality and vessel narrowing at both conventional and MR angiography. Preventive therapy (usually maintenance transfusions on a monthly basis) is now offered to these patients. Screening transcranial Doppler US should begin by the age of 3 years.
Reports of uncommon colonic abnormalities in sickle cell anemia include conditions such as acute necrotizing colitis in adults, pseudomembranous colitis (PMC) in a child, ischemic colitis, and life-threatening toxic megacolon. Pathogenesis of these inflammatory complications seems also to be due to intestinal ischemic microvascular occlusion. A barium enema is contraindicated for imaging of these intestinal lesions, if associated with an acute abdomen because of a high risk of perforation. Contrast-enhanced CT with oral water-soluble contrast is the imaging tool of choice and may show long segmental intestinal wall thickening, which is irregular and shaggy, compared to a symmetrical homogeneous pattern which is seen in Crohn disease. Also, CT exams in these patients may show the famous "accordion sign," which represents trapped contrast between thickened edematous colonic haustral folds.
An I-123 MIBG scan would be helpful to see if a tumor is MIBG avid as in cases of tumors of neural crest origin such as neuroblastomas, which often originate in the adrenal region. There is no

association of sickle cell anemia and the development of such tumors. In addition, there is no known association between sickle cell disease and the subsequent development of vesicoureteral reflux, so a VCUG would not be of benefit in this patient.

References: Agha M, Eid AF, Sallam M. Sickle cell anemia: imaging from head to toe. *Egyptian J Radiol Nucl Med* 2013;44(3):547–561. Lonergan GJ, Cline DB, Abbondanzo SL. Sickle cell anemia. *Radiographics* 2001;21(4):971–994.

29 Answer C. Juvenile idiopathic arthritis (JIA) includes all forms of arthritis that develop before the age of 16 years, persist for at least 6 weeks, and have no identifiable cause. JIA is the most common rheumatic disease in children, with a reported prevalence of 16 to 150 per 100,000 children. JIA is a clinical diagnosis with varied manifestations and is influenced by genetic and environmental factors. In the past, imaging evaluation for known or suspected JIA had relied primarily on radiography. However, radiographic findings such as bone erosions, joint space narrowing from cartilage destruction, and growth disturbances are irreversible findings that occur late in the course of disease. The development of improved therapeutic agents whose use can prevent joint destruction, especially when treatment is initiated early, highlights the importance of early (preradiographic) detection of inflammation. The potentially serious side effects of these newer therapeutic agents in the pediatric population underscore the importance of accurately assessing disease activity, disease progression, and treatment response. As a result, management of JIA has evolved to include greater utilization of advanced imaging techniques such as contrast-enhanced magnetic resonance (MR) imaging and Doppler ultrasonography (US). Both of these modalities can help in detecting inflammatory lesions before permanent joint destruction occurs and can monitor disease progression and treatment response to more effectively guide therapy.

Unlike the systematic protocols for monitoring adult patients with rheumatoid arthritis, there are no defined imaging protocols for JIA. The timing and utilization of imaging in JIA must be tailored to the individual patient, with consideration given to the strengths and weaknesses of each available modality in evaluating the joints in question and directing therapeutic decision making.

Preerosive signs of inflammation such as synovitis and osteitis are undetectable on radiographs. Radiographic findings in early-stage JIA are often nonspecific. The most commonly encountered radiographic findings include soft tissue swelling, joint effusion, and osteopenia. Osteopenia is usually periarticular in the early stages of disease secondary to joint inflammation, whereas in advanced-stage JIA, it can be diffuse due to decreased physical activity or steroid administration.

Because of its multiplanar capability and excellent bone and soft tissue contrast resolution, MR imaging is ideal for imaging patients with JIA. MR imaging allows comprehensive evaluation of the synovium, articular cartilage, growth cartilage, bone marrow, cortical bone, and soft tissues. In early JIA, MR imaging can help detect synovitis before it is apparent at physical examination, a potentially important prognostic indicator. MR imaging is the only imaging modality that can demonstrate bone marrow edema, although its prognostic significance in JIA has not been clearly defined. In adult rheumatoid arthritis, bone marrow edema is a predictor of future erosions. Therefore, the presence of bone marrow edema in the setting of JIA is considered a preerosive abnormality and an indication for initiating therapy to prevent permanent joint damage. MR imaging has been shown to help detect more than twice as many bone erosions in the wrist as either US or radiography and more than twice as many cases of sacroiliitis as radiography in a pediatric population. It can also help identify radiographically occult extra-articular inflammatory lesions such as tenosynovitis and enthesitis. MR imaging does not utilize ionizing radiation, which is an important consideration in the pediatric population. However, when a joint is being evaluated with MR imaging, correlative radiographs should be obtained to document findings and for future reference during treatment monitoring.

The TMJ can be involved in any of the JIA subtypes and is affected in 17% to 87% of the patient population. Given the morphology and complex anatomy of the TMJ, this joint is at especially high risk for growth disturbances when affected by inflammatory arthritis, and long-term involvement may

result in both poor aesthetic and functional outcomes. It is well documented that clinical symptoms, such as pain, may not be present even in the setting of severe erosive TMJ disease, and subjective symptoms may lead to underestimation of the degree of early inflammation.
Reference: Sheybani EF, Khanna G, White AJ, et al. Imaging of juvenile idiopathic arthritis: a multimodality approach. *Radiographics* 2013;33(5):1253–1273.

30 Answer C. Histiocytic disorders are a group of diseases derived from macrophages and dendritic cells. Langerhans cell histiocytosis (LCH) is the most common dendritic cell disorder and is named because of its similarity to the Langerhans cells found in the skin and mucosa. However, it was later discovered that the abnormal cells in LCH are actually derived from myeloid dendritic cells that exhibit the same antigens (CD1a, S100, and CD207) and exhibit the same unique intracytoplasmic organelles as in Langerhans cells. These intracytoplasmic organelles, known as Birbeck granules, appear racquet shaped at electron microscopy and help differentiate LCH from other histiocytic disorders and xanthogranulomatous diseases. The proliferation and accumulation of LCH cells in various organs results in the clinical disease.
LCH is divided into three groups on the basis of the number of lesions and systems involved. The unifocal (localized) form is seen in approximately 70% of LCH cases, is limited to a single bone or a few bones, and may involve the lung. Patients usually present between 5 and 15 years of age. The multifocal unisystem (chronic recurring) form comprises approximately 20% of cases and involves multiple bones as well as the reticuloendothelial system (liver, spleen, lymph nodes, and skin). It often is accompanied by diabetes insipidus when the pituitary gland is involved. Patients with this form of disease present earlier than those with unifocal disease, typically between 1 and 5 years of age. The multifocal multisystem (fulminant) form constitutes approximately 10% of LCH cases and often is fatal. It typically is diagnosed in the first 2 years of life and is characterized by disseminated involvement of the reticuloendothelial system, anemia, and thrombocytopenia.
The clinical manifestation of LCH depends on its severity and the number of organs involved and ranges from self-limited to fatal disease (in cases where disease has disseminated to multiple systems). Diagnosis of LCH is made by corroborating clinical features, histopathology, immunohistochemistry, and radiologic findings.
The CNS is involved in approximately 16% of LCH cases. If the facial bones or anterior or middle cranial fossa are affected, the incidence of CNS involvement is higher, affecting up to 25% of patients with LCH. The most common clinical CNS manifestation of LCH is diabetes insipidus secondary to infiltration of the posterior pituitary gland, which results in decreased secretion of antidiuretic hormone. T1-weighted MR imaging demonstrates loss of the normal posterior pituitary bright spot. Approximately 70% of patients will also show thickening of the pituitary stalk, a finding best appreciated on contrast-enhanced MR images.
Bone lesions are the most common radiographic manifestation of LCH and occur in approximately 80% of patients. Although any bone can be affected, LCH has a predilection for the flat bones. The skull is the most common flat bone involved, followed by the mandible, ribs, pelvis, and spine.
The vertebral body is the most commonly affected part of the spine in LCH. Early lesions appear lytic at radiography and computed tomography (CT). MR imaging demonstrates decreased T1 signal intensity and increased T2 signal intensity, with areas of enhancement. As the disease progresses, the early lytic lesions can result in symmetric uniform collapse of the vertebral body with preservation of the intervertebral disk spaces. The flattened vertebral body has been termed “vertebra plana” and may result in pain and substantial neurologic defects. Spinal deformities are rare. Although vertebra plana can have additional causes in children, such as leukemia, metastatic neuroblastoma, aneurysmal bone cyst, or Ewing sarcoma, the most common cause in children is LCH.
In addition, lung involvement occurs in approximately 10% of LCH cases. It is much more common in adults and is almost always associated with smoking. At CT, LCH is characterized by centrilobular

micronodules with a predominantly bilateral symmetric upper- to midlung distribution. The costophrenic angles are usually spared. As the disease progresses, cysts develop and can eventually become the major imaging finding. Cysts vary in size but usually are less than 1 cm. A confluence of cysts may result in bullous formation, which then predisposes the patient to recurrent spontaneous pneumothorax.

Reference: Zaveri J, La Q, Yarmish G, et al. More than just Langerhans cell histiocytosis: a radiologic review of histiocytic disorders. *Radiographics* 2014;34(7):2008–2024.

INDEX

C

D

E

F

N

O

P

R

S

T

U

V

W

X